The Neurobiology of Decision Making under Risk

Mkael Symmonds

Wellcome Trust Centre for Neuroimaging
Institute of Neurology
University College London

Thesis submitted for the degree of

DOCTOR OF PHILOSOPHY
of
UNIVERSITY COLLEGE LONDON

August 2011

Declaration

I, Mkael Symmonds, confirm that the work presented in this thesis is my own. Where information has been derived from other sources, I confirm that this has been indicated in the thesis.

August 1st 2011

Abstract

Risk is a highly salient psychological decision variable, and sensitivity to risk is an evolutionarily ancient attribute. In this thesis I address the neurobiological foundation of risk assessment, and show that behaviour is driven by an underlying distributed neural representation of different elements of risk in the brain. In particular, I show using fMRI (in Chapter 4) and MEG (in Chapter 8) that variance (dispersion) and skewness (asymmetry) of gambles evokes anatomically separable neural responses in a parietal, prefrontal and insula cortical network. I discuss possible theoretical neurobiological mechanisms by which preferences could be imbued to choice, and show that subjective tastes for risk, in terms of behavioural sensitivity to each of these risk dimensions, influences the encoding of risk and subsequent anticipatory responses.

In Chapter 5, I show that a representation of prospective outcomes several trials into the future is supported by a dissociated encoding of the statistical information of future states in medial prefrontal cortex; furthermore that this encoding is contingent upon overarching goals or constraints.

In Chapter 6, I demonstrate that economic choice is highly susceptible to exogenous biological influences, namely the effect of metabolic state, whilst in Chapter 7 I provide evidence that the encoding of risk is not affected by dopaminergic disruption, suggesting that dopamine might mediate effects on risk-taking via its role in reward feedback representation.

In summary, the studies in this thesis elaborate the neural mechanisms underlying how humans make both single-shot and sequential decisions under risk, central elements in decision-making scenarios ranging from foraging to financial investment. This demonstrates that phylogenetically ancient circuitry subserving valuation and reward decompose choice into their salient statistical features, enabling the sophisticated representation of the future and its alternatives.

Acknowledgements

This thesis was carried out at the Wellcome Trust Centre for Neuroimaging, Institute of Neurology. I have been fortunate to work for four years in such a wonderful environment with so many exceptional colleagues and now close friends. Excellent science arises from collaborative effort, and the opportunities for fruitful dialogue and endeavour have been second to none. All work presented herein was funded by a Wellcome Trust Programme Grant to my principal supervisor, Ray Dolan. I am indebted to him for all his support, for motivating and guiding me through the sometimes turbulent course of research, and for giving me the latitude to pursue diverse ideas throughout my time at the lab.

I am also very grateful for all the advice given by Karl Friston, my second supervisor, who has provided much inspiration. Considerable thanks also to Peter Bossaerts, whose talks were the nidus of many of my ideas. He has been a close and vital collaborator on substantial parts of this thesis, patiently educating me in economics and gently giving essential advice over the last few years. There have been so many other vital collaborators; Julian Emmanuel and Rachel Batterham, for educating me in the intricacies of metabolic research and without whose help I could not have carried out the feeding study; Dominik Bach, for helping me pursue the 'known unknowns'; Elizabeth Fagan, who worked closely with me during her Masters project on dopamine and risk; Gareth Barnes, for being an MEG guru; Rosalyn Moran, who it has been a privilege to know and share ideas with, and who has given critical help at numerous junctures; Nick Wright, for his always stalwart support as co-conspirator for many of the studies in this thesis, and most importantly as a loyal friend who I have been very lucky to meet.

My time at the FIL has been replete with enriching and entertaining interactions with so many others. My time would have been greatly impoverished without getting to know Steve Fleming and Tamara Shiner. It's been excellent and enjoyable to work with Klaus Wunderlich, Antoinette Nicolle, Rimona Weil, Valerie Voon, Ivo Vlaev, and Marc Guitart. Sinead Mullally has been a superb neighbour and provided a constant source of conversation and tea. I'll fondly miss my other second-floor companions past and present for all the camaraderie.

Several others at the FIL were fundamental in assisting me throughout my thesis, and I give special thanks to David Bradbury, Jan Glassman, Eric Featherstone, Will Penny and Peter Aston for innumerable assistances.

There are two individuals to whom I dedicate this work. To Molly, our faithful dog, who reluctantly tolerated occasional late dinners for the sake of neuroscience. Finally, most important of all, my wonderful wife Libby, for her love, unconditional support and encouragement, and without whom none of this would have been possible.

Contributions

The work in this thesis is entirely my own unless otherwise indicated. I devised, designed, executed, analysed and wrote all components presented. All parts have been improved with much advice from Prof Ray Dolan, my principal supervisor. Substantial parts of this thesis have been read and commented on by Profs Karl Friston and Peter Bossaerts.

Ideas in Chapter 4 were formulated with great assistance from Nick Wright and Dominik Bach. The analytic methods used in Chapter 5 rested on significant contribution from Peter Bossaerts. Setting up and carrying out the work Chapter 6 was carried out at University College Hospital in collaboration with Julian Emmanuel and Rachel Batterham, who performed the hormonal assays therein. Chapter 7 was partly based on data collected by Elizabeth Fagan during an MSc project, who I supervised in conjunction with Ray Dolan. Gareth Barnes and Rosalyn Moran advised and provided MEG analysis routines used in Chapter 8.

Publications

Chapter 4 forms a publication in press (Symmonds et al., 2011). Chapter 5 has been published as (Symmonds et al., 2010a). Chapter 6 has been published as (Symmonds et al., 2010b). Chapter 2 forms the basis for a book chapter (Symmonds and Dolan, 2011). Chapters 7 & 8 are currently in preparation for submission.

The paradigm in Chapter 4 has been further utilised and adapted for work with Nick Wright (in submission) amongst others. I have also been involved in several close and ongoing collaborations, with resulting data published as (Weil et al., 2010; Nicolle et al., 2011; Voon et al., 2011; Wright et al., 2011).

Contents

Declaration 2
Abstract 3
Acknowledgements 4
Contributions 6
Publications 7
Contents 8
Chapter 1 15
Introduction and overview 15
1.1 What is 'risk', and why is it important? 15
1.2 Investigating decision making under risk 17
1.2.1 Dimensions of Risk 17
1.2.2 Prospective decision making under risk 18
1.2.3 Physiological and pharmacological influences 18
1.2.4 Competing economic and psychological theories of risk evaluation 19
1.2.5 Neurobiology of decision making under risk: aims of the studies 19
1.3 Outline of the thesis 21
Chapter 2 22
Background & Literature Review 22
2.1 Introduction 22
2.1.1 The neuroscience of decision making 23
2.1.2 The nature of preferences 24
2.2 Concepts of choice and preference 25
2.2.1 Revealed preferences or behavioural biases? 25
2.2.2 Competing valuation systems 26
2.2.3 Searching for a hedonimeter 27
2.2.4 The randomness of choice 29
2.2.5 Different types of value? 30

2.2.6 Dynamic changes in preference 31
2.2.7 The role of neuroscientific evidence 32
2.3 Risk 33
2.3.1 Introduction 33
2.3.2 Classical economic theory 34
2.3.3 Behavioural economics and utility theories 38
2.3.4 Finance and mean-risk theories 40
2.3.5 Psychology: risk and affect 41
2.3.6 Methods of evaluating decision making under risk 42
2.4 What are the potential neural mechanisms by which preferences could be expressed? 43
2.4.1 Regionally-specific encoding of intrinsic value 44
2.4.2 A change in neural sensitivity within a brain region 46
2.4.3 Distributed encoding of value by neurotransmitters 49
2.4.4 Change in neural activity coupled to action 52
2.4.5 Change in regional connectivity and modulation of preference 54
2.5 Conclusion 55
Chapter 3 57
Methods 57
3.1 Introduction 57
3.2 Decision theory and behavioural modelling 57
3.2.1 Decision theory 57
3.2.2 Behavioural modelling 59
3.3 Functional magnetic resonance imaging 64
3.3.1 Introduction 64
3.3.2 Principles of MRI 65
3.3.3 Constructing an MR image 70
3.3.4 Functional MRI 72

3.3.5 Data analysis 78
3.4 Magnetoencephalography 83
3.4.1 Introduction 83
3.4.2 Principles of MEG 85
3.4.3 Data analysis 90
Chapter 4 93
Deconstructing neural responses to risk 93
4.1 Introduction 93
4.2 Methods 94
4.2.1 Task 94
4.2.2 Independent manipulation of variance and skewness 95
4.2.3 Behavioural modelling 97
4.2.4 FMRI 101
4.3 Results 102
4.3.1 Behaviour 102
4.3.2 Functional imaging 108
4.4 Discussion 117
4.4.1 Risk and risk preferences 118
4.4.2 Neural encoding of risk 118
4.4.3 Summary 121
Chapter 5 122
Prospective decision making under risk 122
5.1 Introduction 122
5.2 Methods 123
5.2.1 Behavioural Experiment 123
5.2.2 Functional MRI 135
5.3 Results 136
5.3.1 Behavioural 136

5.3.2 Functional imaging 141
5.4 Discussion 149
5.4.1 Representing outcome distributions in prospective decisions 149
5.4.2 Accounting for future choices 151
5.4.3 Prospective evaluation of strategies - conclusion 153
Chapter 6 155
The effect of metabolic state on decision making under risk 155
6.1 Introduction 155
6.1.1 Risk preference and reference points 155
6.1.2 Neural regulation of food intake 155
6.1.3 Risk sensitive foraging theory 156
6.1.4 Aims and hypotheses 157
6.2 Methods 159
6.2.1 Participants 159
6.2.2 Study protocol 160
6.2.3 Paradigm 162
6.2.4 Behavioural analysis 164
6.2.5 Decision-making model 165
6.3 Results 165
6.3.1 Metabolic state measures 165
6.3.2 Effect on risk-sensitive choice 168
6.3.3 Decision-making model 171
6.4 Discussion 172
6.4.1 Effects of a change in metabolic state on risk preference 172
6.4.2 Immediate effects of eating on risk preference 173
6.4.3 Effects of extreme metabolic states 174
6.4.4 Conclusion 174
Chapter 7 175

Effects of dopamine on decision making under risk 175
7.1 Introduction 175
7.1.1 Neuromodulators and decision making under risk 175
7.1.2 Aims 177
7.2 Methods 178
7.2.1 Setup 178
7.2.2 Paradigms 178
7.2.3 Aims and hypotheses 180
7.2.4 Payment 181
7.2.5 Psychological questionnaires 181
7.2.6 Behavioural modelling 182
7.3 Results 182
7.3.1 Behaviour 182
7.3.2 Behavioural modelling 185
7.4 Discussion 188
7.4.1 Risk sensitivity 188
7.4.2 Effects of L-dopa 189
7.4.3 Risk versus reward learning 190
7.4.4 Dopamine receptors 191
7.4.5 Genetic heterogeneity 191
7.4.6 Role of other neurotransmitters 192
7.4.7 Conclusion 192
Chapter 8 193
The chronometry of risk processing 193
8.1 Introduction 193
8.2 Materials and Methods 195
8.2.1 Participants 195
8.2.2 Task 195

8.2.3 Independent manipulation of variance and skewness 195
8.2.4 Behavioural modelling 196
8.2.5 MEG 198
8.3 Results 201
8.3.1 Behaviour 201
8.3.2 MEG source level analysis 202
8.4 Discussion 210
8.5 Conclusion 213
Chapter 9 215
General Discussion 215
9.1 Evidence for summary statistic models 215
9.1.1 Overview and contributions 215
9.1.2 Behaviour 216
9.1.3 Neural encoding of summary statistics 217
9.1.4 Choice 218
9.1.5 Future directions 219
9.2 Tracking of risk in sequential decision making 220
9.2.1 Overview and contributions 220
9.2.2 Continuation value models of choice 221
9.2.3 Chosen versus evaluated risk 222
9.2.4 Target level 222
9.2.5 Future directions 223
9.3 Integration of risk with risk-preference 224
9.3.1 Overview and contributions 224
9.3.2 The effect of risk preference on risk encoding 224
9.3.3 The role of the insula 225
9.3.4 Searching for a hedonimeter 226
9.3.5 Future directions 227

9.4 Modulating risk preference 227
9.4.1 Overview and contributions 227
9.4.2 Physiological state 228
9.4.3 Neuromodulatory influences on risk 228
9.4.4 Future directions 229
9.5 Conclusion 229
Bibliography 231
Appendix A 256
Appendix B 257
Appendix C1 260
Appendix C2 266
Appendix D 272

Chapter 1

INTRODUCTION AND OVERVIEW

1.1 WHAT IS 'RISK', AND WHY IS IT IMPORTANT?

Stochasticity is a fundamental property of natural environments, and maintenance of adequate nutrition and energy stores in the face of this environmental variability is critical for survival and reproduction. It is therefore unsurprising that sensitivity to environmental uncertainty or variation in resources reflects a phylogenetically conserved adaptation, evident in a pervasive sensitivity to risk across species (Real et al., 1982; Barnard and Brown, 1985; Wunderle et al., 1987; Croy and Hughes, 1991; Bateson and Kacelnik, 1997).

Risk in this sense is a property of the outside world, describing a fundamental indeterminism in possible future outcomes[1]. Foraging animals, or humans in a modern economy, can modulate their exposure to risk by making appropriate choices. An assessment of alternative actions is central to decision-making, requiring a weighing up of each potential outcome arising from different choices, and the chance of each outcome occurring. Thus, decision-making under risk entails the evaluation of a probability distribution over outcomes, including a judgement of the intrinsic value of each of these outcomes to an individual decision-maker.

For example, imagine you are considering purchasing one of two property investments for £100k (**Figure 1.1**). Property A has a predicted market value in 5 years time of either £115k (with a 70% chance), £100k (15% chance), or £30k (15% chance). How much is this property worth? Or property B, whose worth is £170k (with a 15% chance), 100k (15% chance), or £85k (70% chance). Which property is preferred? If we considered only the expected value (average or mean value of the properties) then we should be indifferent as

[1] This is in contrast to internally generated uncertainty about the state of the world, reflecting imprecision in perception, lack of knowledge about the relative chance of possible future events (also called ambiguity), or prior hypotheses about these probabilities. These types of uncertainty are closely related and often intertwined in real-world decisions.

both are worth exactly £100k. However, in the examples outlined the price one is willing to pay also depends upon an individual's taste for risk (i.e. their risk-preference).

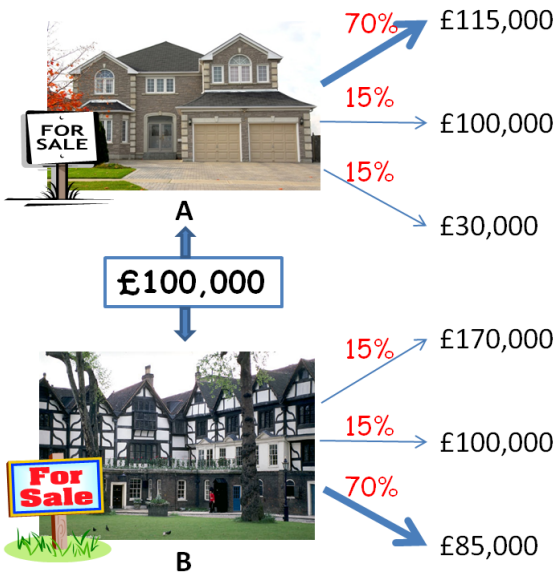

Figure 1.1 A "risky" decision. Deciding between an investment in one of two properties, with a chance of making a profit or a loss.

Risk-sensitivity is integral to psychological descriptions of human personality and decision-making (Kahneman and Tversky, 1979; Loewenstein, 2001), while economic models attempt to provide a quantitative framework for behaviour under risk (Sharpe, 1964; Rothschild and Stiglitz, 1971). Borrowing from these ideas, in ecology, risk-sensitive foraging theory describes an integration of risk and reward in decision making, a formulation echoing financial analysis (Markowitz, 1952; Sharpe, 1964; Stephens, 1981).

Recent financial crises highlight the consequences for society of inappropriate risk evaluation. There is understandable interest in psychological and economic fields in elucidating the mechanisms of, and influences upon, decision-making under risk, albeit from different perspectives and with different motivations. There are clear practical implications in understanding this process: financial advisors seek to measure risk-attitudes before recommending appropriately tailored investment strategies to clients (Bluethgen et al., 2008); analysts utilise diverse models of behaviour based upon specific economic tenets to predict individual or group choice; marketing managers and policy makers increasingly leverage descriptive insights from behavioural economics and psychology aiming to systematically influence behaviour (Thaler and Sunstein, 2008a).

Risk is also a key computational variable. Knowledge of risk or uncertainty allows deviations from expected outcomes (i.e. prediction error) to be appropriately weighted in learning and estimation (Preuschoff et al., 2008). Detection of environmental change requires a comparison of sampled outcomes to a predicted distribution of outcomes; if consistent no new learning or exploration needs to occur, but if these representations fail to match this indicates that the parameters of the world have shifted (and, for example, the learning rate needs to be increased (Behrens et al., 2007)).

From a clinical perspective, aberrant risk-taking with potentially devastating sequelae is a feature of neurological and psychiatric disorders (e.g. frontal lobe injury, Parkinson's disease, addiction) (Gallagher et al., 2007), and can be pharmacologically induced (e.g. by alcohol, amphetamines, dopamine agonists) (Zeeb et al., 2009). An understanding of the neurophysiological machinery underlying risky decisions would provide a cogent proximate description of risk evaluation. A coherent framework based upon neurobiological foundations may enable a quantitative assessment of decision making deficits, allow arbitration between competing decision theories, and reveal systematic biological influences on behaviour.

1.2 INVESTIGATING DECISION MAKING UNDER RISK

1.2.1 DIMENSIONS OF RISK

Risk is psychologically multi-faceted and, in the example of a decision between house purchases, could relate to the spread of outcomes (e.g. measured as variance) or an asymmetry between better or worse than average outcomes (e.g. measured as skewness). A like or dislike of variance dictates that both houses are equally valued (both sets of outcomes have equal variance). A preference for one of the houses indicates an additional preference for either negatively skewed (house A – small chance of a poor outcome), or positively skewed (house B – small chance of a good outcome) distributions.

In **Chapter 4**, I present a decision-making paradigm designed to dissociate these separate dimensions of risk, and to dissociate distinct neural mechanisms contributing to the evaluation of different aspects of an outcome distribution, as well as determining how these representations are integrated with an individuals' risk-preference. Directly building upon

these findings of the functional anatomy of decision making under risk, **Chapter 8** employs magnetoencephalography (MEG) to map out the precise timing of these same decision processes.

1.2.2 PROSPECTIVE DECISION MAKING UNDER RISK

Many everyday situations require agents to prospectively generate a chain of actions (a path through a decision-tree). This also leads to a distribution of outcomes, again engendering uncertainty or risk. Such sequential decisions are a prime focus in ecology, where animals forage to ensure intake exceeds minimal need constraints (Stephens et al., 2007), and in finance where traders reap bonuses by exceeding a target return from sequential transactions (Panageas and Westerfield, 2009). Common to these examples is that the distribution of possible outcomes (energy, money) differs for each available series of choices. For sequential decisions this representation of a distribution of outcomes may pertain to events sometime in the future, and also be conditioned upon a whole series of anticipated actions of the decision-maker.

In **Chapter 5**, I present a sequential decision-making paradigm designed to address how expected risks (i.e. the distribution of outcomes) are tracked prospectively when formulating a chain of decisions, and how this representation is integrated with the need to reach an overarching goal.

1.2.3 PHYSIOLOGICAL AND PHARMACOLOGICAL INFLUENCES

In addition, anticipated distributions of outcomes (the risk) can be altered by shifts in external or internal parameters (such as a change in financial target, or a change in metabolic state). Thus, an integration is required between these exogenous variables and the process of evaluating outcomes in order for organisms to choose appropriately. In **Chapter 6**, I focus on changes in behaviour induced by physiological changes in metabolic state, aiming to map out the influence of hunger and satiety on the evaluation of economic decision making variables.

An important, and widely reported finding, is that specific neuromodulatory neurotransmitters play a key role in decision making and learning. In particular, dopamine has an integral role in reward processing, and aberrant dopamine signalling, either because of disease processes (i.e. Parkinson's disease) or when exogenously manipulated, can lead to deficits on tasks involving risk. In **Chapter 7**, I examine the effects of levodopa

administration on the evaluation of risk, using the carefully controlled paradigms developed in previous chapters to assay specific effects on the appraisal of reward distributions.

1.2.4 COMPETING ECONOMIC AND PSYCHOLOGICAL THEORIES OF RISK EVALUATION

There are two dominant theories of risk-evaluation, which we discuss more fully in **Chapter 2**. (see e.g. Weber and Johnson for a review (Weber and Johnson, 2008)). In brief, Expected Utility Theory in microeconomics, originally proposed by Bernoulli, and later axiomatized by Von Neumann and Morgenstern (Von Neumann and Morgenstern, 1944), proposes that a decision-makers' subjective values for each possible outcome are determined by an implicit utility function. Here, 'utilities' are weighted by the probability of each outcome and risk-preference emerges as a by-product of this framework (Pratt, 1964). Alternative theories in finance (Markowitz, 1952; Sharpe, 1964), psychology (Coombs and Huang, 1970), and ecology (Stephens, 1981) propose that outcome distributions are decomposed into "summary statistics"[2] (e.g. mean, variance, skewness), with risk-preference directly generated by preference for each component. More recent economic and psychological theories (such as Prospect Theory (Kahneman and Tversky, 1979; Tversky and Kahneman, 1992), or Scalar Utility Theory (Marsh and Kacelnik, 2002)), fall into one of these two camps. It turns out that observation of behaviour alone cannot distinguish Expected Utility (EU) from summary statistic models, since both make identical choice predictions, as any utility function can be approximated by preferences for summary statistics using a polynomial (Taylor series) expansion (Scott and Horvath, 1980; Müller and Machina, 1987; D'Acremont and Bossaerts, 2008).

1.2.5 NEUROBIOLOGY OF DECISION MAKING UNDER RISK: AIMS OF THE STUDIES

Neuroscientific evidence can play a key role in distinguishing between these competing decision theories. Expected utility and related theories ascribe risk no special role as a separate cognitive variable. A decision-maker who obeys a specific set of axioms of rational choice, and who behaves as if he is maximising an implicit non-linear utility function will

[2] Normally, summary statistics refer to quantities that summarise effects in hierarchical statistical models. Here, we use summary statistics to refer to the sufficient statistics of a probability distribution that summarise its form. These are generally taken to be the first few moments of a distribution (e.g., the mean, variance, skew and kurtosis).

necessarily be observed to manifest a taste for risk. This does not require an explicit computation of risk (or any proxy for risk), and this is in sharp contrast to mean-risk models. Any evidence for a neural representation of risk during decision making is supportive of the latter process. Thus, one aim of the studies in this thesis (specifically in **Chapter 4, Chapter 5, and Chapter 8**) exploit choice-generated neural data in adjudicating between different models and theoretical camps.

The use of parametric predictor variables to model neural responses to complex stimuli with several dimensions is well established (Buchel et al., 1998; Wood et al., 2008), and the correlation of neural data with dynamically changing internal variables of a computational model has been implemented in several studies of valuation (O'Doherty et al., 2004; Samejima et al., 2005); for review see (Corrado and Doya, 2007). We discuss this approach in **Chapter 2**.

Several previous neuroimaging studies have focused on representations of variance (Preuschoff et al., 2006; Tobler et al., 2007; Christopoulos et al., 2009; Tobler et al., 2009), which reflects only a first-order approximation of risk (Rothschild and Stiglitz, 1971) and ignores the influence of positive and negative skewness on risk perception, as in my example where variance between choices is equivalent (Garrett and Sobel, 1999). Hence, by using model-based fMRI analysis (O'Doherty et al., 2007) I aimed to determine directly whether the brain encodes the summary statistics (variance and skewness) of a decision.

Chapter 5 tackles the more complex question of how planned choices, and the resulting anticipated distribution of outcomes (i.e. predicted risk), is tracked several trials ahead and how this representation takes account of available strategies and externally imposed targets. Again, decision strategies can be formulated as a series of mathematical models, and both behavioural and neural data can be utilised to ask which model(s) best explain choice and concurrent neural activity (Symmonds et al., 2010a).

Chapters 6 and 7 go on to investigate the impact of physiological and pharmacological manipulations on the decision making process, and specifically how they influence the evaluation of risk. Here, I again utilise decision models to test competing hypotheses, as well as using model parameters to quantify these induced effects.

1.3 OUTLINE OF THE THESIS

Chapter 2 presents an overview of the literature on the neurobiology of preference, and of decision making under risk. In **Chapter 3** I outline the behavioural modelling and neuroimaging methods used in this thesis. Building on this conceptual outline, I then detail the specifics of the techniques employed in each subsequent chapter.

The empirical studies presented in **Chapters 4-8** all explore the central theme of decision making under risk, and are broadly divided into three types. **Chapters 4 and 5** use functional magnetic resonance imaging (fMRI) to delineate the neural circuitry involved in processing risk both in single-shot and in sequential decisions. **Chapter 4** in particular sets the scene for the subsequent investigations, as here I test a variety of behavioural models which recur throughout all chapters of the thesis. **Chapters 6 and 7** investigate behavioural perturbations in risk evaluation by experimentally controlled manipulations of physiology (both metabolic and neuromodulatory). **Chapter 8** uses magnetoencephalography (MEG) to map out the chronometry of decision making under risk in the brain.

Core to all these studies is the use of economically-inspired models of behaviour to delineate decision making and choice, and a framework borrowed from financial economics to describe risk in terms of probability distributions of outcomes. This in turn enables a dissociation of different risk dimensions, particularly pertinent in the novel experimental design of studies in **Chapter 4 and 8**. By independently manipulating risk dimensions, I dissociate different regions of the brain interested in specific aspects of risky outcomes, and also use this to dissociate the objective assessment of risk (i.e. risk perception, in the neurobiological sense akin to sensory perception), from the integration of this statistical information with subjective attitudes towards risk (i.e. personal preferences).

Finally, **Chapter 9** draws together the findings from these experiments, returning to the themes discussed in **Chapter 2** to highlight the mechanistic implications for understanding the biology of risk processing and to consider the future directions and important unanswered questions in the field.

Chapter 2

BACKGROUND & LITERATURE REVIEW

2.1 INTRODUCTION

Choice conjures the idea of a volitional or directed selection of desirable actions, motivated by internal likes and dislikes. Unsurprisingly, the conundrums raised by choice are centre stage in philosophical and scientific debate since antiquity (MacPherson, 1968; Aristotle, 1998). Choice is generally envisaged as a conscious selection of alternatives, under an assumption that individuals possess 'preferences', or a predilection to make certain types of choice in specific situations. This realisation is often thought to reflect the expression of either acquired or 'hard-wired' drives that are expressed in a biological substrate. Thus, an individual with a preference for chocolate over lemon is considered to possess an internal machinery capable of representing this enhanced valuation of chocolate relative to lemon, a valuation that provides the basis for a consistent and rational selection between these two goods.

Traditional economic thinking relates preferences to a statement about well-being. An agent who expresses a particular choice is considered to be maximising their own subjective 'utility' or welfare. Every decision or choice is considered an expression of preference and in the 'revealed preference' framework (Samuelson, 1938), choice and preference are synonymous. While revealed choices are ultimately the dependent variable for classical economics, understanding the neurobiology of preferences necessitates that we entertain a range of mechanisms by which human choices are generated, expressed and influenced.

2.1.1 THE NEUROSCIENCE OF DECISION MAKING

The neuroscience of choice and preference dates back to the 19th century, with the emergence of the idea of functional specialisation as a fundamental organisational principle of the brain. While phrenologists attributed behavioural characteristics to the contours of the scalp (Gall and Spurzheim, 1818), the observation of specific and consistent behavioural deficits following localised brain damage led to the development of neurology as a medical speciality (Broca, 1865; Jackson, 1873). The tradition of inferring function from structural and electrophysiological perturbations has remained powerful, enabling a mapping of both primary sensory and motor systems (Penfield and Boldrey, 1937), complex cognitive processes such as language (Head, 1920; Ojemann, 1978), memory (Scoville and Milner, 1957), and more recently a mapping of areas important in decision making, strategy selection and learning (Shallice and Burgess, 1991; Bechara et al., 1994).

The early 20th century heralded the birth of behavioural psychology, pioneered by the classic findings of Pavlov, Skinner, Tolman, Hull and others (Schultz and Schultz, 2007). This tradition provided insights into core processes mediating learning and choice, but was restricted in scope by the primitive methods available to study concurrent neurobiological activity during decision making. In the 1960's Olds and colleagues produced a startling finding that stimulation of specific brain loci in animals imbued behaviour with apparent hedonic value. For example, self-stimulation experiments in rats showed they were disposed to compulsively press a lever to the exclusion of other hedonic behavioural options. Thus, a dramatic form of preference could be driven by electrical stimulation of the rats' subcortical dopaminergic structures (Olds and Milner, 1954).

A refinement in neuroscientific techniques in the 1980's saw the emergence of single-unit recording methodologies. These revealed that activity of individual neurons in early visual areas could predict trial-by-trial choices of an animal in a random-dot motion discrimination experiments (Parker and Newsome, 1998). Such an approach provided the first direct link between neural activity at a single unit level and the expression of choice behaviour. Subsequent studies have asked more sophisticated questions about the construction of value and choice in an economic framework. A key example is a report showing that a region of parietal cortex

called LIP, expressed activity that correlated with the reward magnitude and probability (expected value) associated with an upcoming action (Platt and Glimcher, 1999).

The development of neuroimaging techniques, in particular functional magnetic resonance imaging (fMRI), has meant questions related to choice and preference can now be addressed non-invasively in humans. Early neuroimaging studies of financial decision making dissected out regions involved in processing monetary gain and loss (Thut et al., 1997; Elliott et al., 2000), as well as brain activation related to anticipation versus receipt of reward (Breiter et al., 2001). More sophisticated studies have borrowed economically-inspired models of behaviour to seek out a brain representation of key decision variables. Notable examples include a demonstration that brain activity tracks a Pascalian idea of a value representation constructed from a combination of amount and probability (Knutson et al., 2005; Dreher et al., 2006), to financial and ecological concepts of risk and uncertainty (Preuschoff et al., 2006; Christopoulos et al., 2009; Mohr et al., 2010a), and the idea that anticipated temporal delay reduces the value of rewards (Kable and Glimcher, 2007; Pine et al., 2009).

2.1.2 THE NATURE OF PREFERENCES

Preferences can be thought of as biologically determined traits (Eysenck, 1990; Ebstein, 2006), but in reality they are dynamic and flexible, and indeed often inconsistent. The idea of preference is broad and diverse, encompassing a liking for different goods, a favouring of reward over punishment through to preferences for specific components of a decision ('decision variables'). The latter can encompass risk preference, impulsivity (the preference for delayed versus immediate goods) and social preferences ('other-regarding' preferences, altruism and fairness). Whether such preferences are convenient theoretical artefacts for classifying individual choice or whether they relate to intrinsic biological processes and inter-individual differences is the subject of intense and wide-ranging programmes of research. This breadth is evident in a facility to draw on human and animal psychology, neurobiology, economics, ecology and computational science, though a source of confusion can be each discipline's different terminology, theory, experimental technique and hypothetical assumptions that colour the literature. There are many excellent reviews and recent descriptions of these conceptual edifices, along with attempts to bridge between them (Glimcher and Rustichini, 2004; Kenning and Plassmann, 2005; Sanfey et al., 2006; Berns et al., 2007; Doya, 2008). The aim here, and

throughout this thesis, is to discuss preferences from a biological perspective, acknowledging that this strays outside a traditional boundary of what some would regard as preference.

In this review, I first survey examples of preference and choice that raise questions as to their biological implementation. I then discuss how strict economically-inspired definitions of preference might need to be loosened, or expanded, when probing the biological systems that drive choice behaviour. Finally, I examine plausible mechanisms for a neural instantiation of preference and discuss how preference can be modulated by physiological, pharmacological or direct neural manipulation. These latter concepts then form the springboard for the subsequent experimental investigations described herein.

2.2 CONCEPTS OF CHOICE AND PREFERENCE

2.2.1 REVEALED PREFERENCES OR BEHAVIOURAL BIASES?

'Revealed preference' is often assumed to imply that an individual *wants* the chosen outcome, but there are many scenarios where this is not necessarily the case. For example, the status quo bias (Samuelson and Zeckhauser, 1988), where individuals show a predilection to stick with a previously selected option would not necessarily be thought of as an expression of an internal desire. Instead, it is more parsimonious to think of it as reflecting a biological intrinsic default response mode which needs to be overcome, usually requiring an expenditure of effort to recruit an alternative motor action program. Overcoming this default has been demonstrated to evoke enhanced activity in the subthalamic nucleus (Fleming et al., 2010a), paralleling earlier findings from single-unit recordings where 'incorrect' actions (saccadic eye movements in monkeys in a simple instrumental task) have been attributed to baseline (pre-stimulus) neuronal activity encoding a default motor action program (Lauwereyns et al., 2002). These examples highlight a recurring dichotomy that different types of choice may be generated by entirely disparate mechanisms despite the end result (the apparent 'revealed preference') being indistinguishable. Strictly speaking the status quo bias *is* a preference to stay with the default rather than change, despite clearly not being driven by any desire to attain an internal goal or 'utility maximize'. This example illustrates a necessity to invoke ideas beyond the typical remit of an economic definition of preference to fully understand the biological generators of choice.

2.2.2 COMPETING VALUATION SYSTEMS

There are important examples where choices do not accord with internal wants. An addict may perform an action (e.g. taking drugs or alcohol) in the present despite expressing a desire to avoid doing this very action on a prior occasion. Explanations exist that fit in with a classical concept of preference, such as state-dependent utility (Karni et al., 1983), where due to physiologically-driven craving, at the point of consumption the addictive substance it truly is valued more than it is disliked. Alternative explanations include the idea that choices alter depending upon the particular choice set available to the decision maker (Koszegi and Rabin, 2007). However, we know that relapses are frequently triggered by environmental cues (e.g. seeing drug-related paraphernalia, watching others drinking alcohol, or the roguery of advertising) and this suggests an alternative possibility of a mistake, lapse or default action. Rather than being a momentary failure to execute a desired action, addicts seem to pursue a sequence of deliberate and complex actions to attain a goal that seems is simultaneously craved but not wanted.

Young children and animals are notoriously impulsive, being unable to delay gratification of desire (Mischel et al., 1989). From an economic perspective they can be considered to express a high temporal discount rate (delayed reward is worth less than immediate reward, so 1 marshmallow now is preferred to waiting minutes for 2 marshmallows). However, the drives directing such behaviours do not always fall neatly in line with an economic model. In reverse-reward experiments, participants are simultaneously shown 2 options of different numerical magnitude (e.g. 5 versus 2 raisins). Whichever set of items is selected, the opposite set is actually received. So for a chimpanzee to obtain 5 raisins from the experimenter, they must select the smaller set of 2 raisins. Both primates (Boysen and Berntson, 1995) and preschool children (Carlson et al., 2005) are notoriously poor at learning to pick the smaller option, despite being visibly upset when they fail to get the larger reward.

Where is the preference in the above? Is it for the chosen, or the unchosen option that chimps and children are distressed at not getting? The effect is not a failure in understanding the correct contingency or an inability to appreciate number. In fact when edible items are replaced with inedible items, performance significantly improves (Boysen and Berntson, 1995; Schmitt and Fischer, 2011). Instead, the magnetic pull of a large pile of food interferes with the ability to

preferentially select the smaller option. Similar examples from the animal literature include Hershenberger's experiments (Hershberger, 1986), demonstrating that while chicks readily acquire an instrumental approach response to obtain food, they are totally unable to learn a reversed 'move away' response to obtain the same outcome. These difficulties are thought to reflect conflict between Pavlovian (i.e. conditioned) and instrumental ('goal-directed') responses. This speaks to the more general idea of multiple valuation systems that are under different degrees of control and amenable to different types of overt and covert influences.

2.2.3 SEARCHING FOR A HEDONIMETER

In contrast to the idea of multiple valuation systems is the concept of a unitary representation of value, corresponding to a classical idea of 'utility'. Utility theory is based on a set of axioms or rules about consistent behaviour, and generates strong constraints upon allowable choice. However, there are multiple examples of behavioural biases that contradict the assumptions of utility theory, for example the Allais paradox (**Figure 2.1**). Implicit in utility models of behaviour is the idea that value is an integrated measure, constructed from different influences on choice and the product of interactions between internal preference and external information about a decision.

First decision				Second decision			
Gamble A		Gamble B		Gamble C		Gamble D	
Outcome	Probability	Outcome	Probability	Outcome	Probability	Outcome	Probability
10000	1	10000	0.89	0	0.89	0	0.9
		0	0.01	10000	0.11		
		50000	0.1			50000	0.1

First decision				Second decision			
Gamble A		Gamble B		Gamble C		Gamble D	
Outcome	Probability	Outcome	Probability	Outcome	Probability	Outcome	Probability
10000	0.89	10000	0.89	0	0.89	0	0.89
10000	0.11	0	0.01	10000	0.11	0	0.01
		50000	0.1			50000	0.1

Figure 2.1. The Allais paradox. Allais' paradox illustrates one violation of expected utility theory. Top - when given a choice between Gamble A and Gamble B, the modal preference is A>B. In a second decision between Gamble C and Gamble D, the modal preference is D>C. Bottom – the fact that this violates expected utility can be seen if the gamble outcomes are decomposed into a common consequence (the outcomes in the first row with 0.89 probability), and the remaining state-outcomes. If the outcomes common to A,B and C,D are ignored, gambles A/C and gambles B/D are identical. However most individuals reverse their preference between the first and the second decision. This either implies that probabilities cannot be linearly decomposed, or that the values of outcomes from a given gamble are not independent.

However, there is no biological necessity for there to be a single area, an internal homunculus or hedonimeter (Edgeworth, 1881) tracking or constructing implicit value. While sectors of orbitofrontal cortex (OFC) have emerged as leading candidate regions for representing value, OFC lacks direct access to motor output networks and shares reciprocal connections with many other cortical and subcortical regions (e.g. the interconnected posterior parietal, cingulate and insular cortex and striatum) strongly associated with valuation (Cavada and Goldman-Rakic, 1989; Sesack et al., 1989; Shi and Cassell, 1998; Haber, 2003). Indeed, some neurobiological theories echo the revealed preference idea that value *is* choice, positing that valuable states of the world are simply states that fulfil prior expectations of actions, these expectations having been engendered by evolution to confer adaptive survival (Friston, 2010).

2.2.4 THE RANDOMNESS OF CHOICE

A major conundrum when thinking about neurobiological mechanisms in decision making is the fact that choices are often noisy or stochastic. While 'preference' to a traditional economist implies a consistent ordering of choices, real choices show a high variability, being probabilistic rather than deterministic (Herrnstein, 1974). This is accounted for in computational behavioural modelling by the addition of a stochastic choice generating function (e.g. logit-softmax or probit choice models). In practice, noise could arise prior to the valuation process, for example in primary or associative sensory cortex encoding stimulus properties as is evident in situations of sensory uncertainty (Knill and Pouget, 2004). Cortical neuronal firing rates are inherently stochastic, with one root of this randomness being variability in synaptic vesicular release (Korn et al., 1993; Faisal et al., 2008). Variability in spike trains often, but not always, conform to a Poisson process (Tolhurst et al., 1983; Maimon and Assad, 2009). Models of noisy evidence accumulation during the formation of a decision can thus account for a considerable degree of stochasticity seen in choice (Resulaj et al., 2009).

In contrast to the idea that variability in behaviour solely reflects noise in sensorimotor neurons, data from monkeys performing an depth-discrimination task ('near' or 'far' random dot stereogram stimuli presented as a noisy stimulus) show that choice-related neuronal activity in disparity-sensitive neurons in area V2 during can be temporally decoupled from performance effects of sensory uncertainty on behaviour (Nienborg and Cumming, 2009). While stimulus information in the first few hundred milliseconds of presentation predicts behaviour, neuronal activity predictive of choice in these sensory neurons arises later. Moreover, this choice-related activity reflects a difference in sensitivity ('gain') for near and far stimuli, a change modulated by reward size. For large rewards, performance is better, but the correlation between V2 neuronal activity and choice is worse (i.e. a better coupling between stimulus-encoding properties of these neurons and behaviour with large rewards at stake). This strongly suggests that 'top-down' expectations influence a coupling between stimulus and choice in early sensory regions. In a similar vein, modulations in the degree of correlation between neuronal firing within areas also vary the stochasticity of a neural ensemble (Shadlen and Newsome, 1998).

Economists have dealt with this issue by proposing different models of stochastic preference. These models loosely map on to the many neurobiological loci where noise is generated. The valuation process itself could be prone to random error, akin to 'random utility' models from

economics, where noise is injected into the utility function (Hey and Orme, 1994). I instantiate this noisy valuation method for the behavioural modelling in this thesis (see **Chapter 3** for a discussion). Alternatively, motor selection itself could be variable (the analogous 'trembling hand' models of choice (Harless and Camerer, 1994), where you know what you *want* to choose but imprecision in your executed actions leads to 'mistakes'). Individual preferences themselves could be stochastically sampled from an underlying generative function (Loomes and Sugden, 1995). Other possibilities include the idea that potential outcomes from all possible choices influence the decision process. While choice is usually envisaged as a selection of an optimal action in accordance with one's own priors and preferences, there is good evidence that suboptimal outcomes (i.e. potentially irrelevant alternatives) impact on decisions. These irrelevant outcomes contribute to classic paradoxes of choice (Birnbaum, 2008), such as the impact of regret (Loomes and Sugden, 1982). Weighting of alternative unchosen outcomes also forms a key component in multiattribute decision theories (Roe et al., 2001; Stewart et al., 2003), I also find evidence of this in **Chapter 5**, where individuals make dynamically inconsistent strategic decisions. Indeed counterfactual outcomes are represented in prefrontal cortex (Ursu and Carter, 2005) while fictive errors in economic learning tasks are seen in striatum (Lohrenz et al., 2007). Choice variability could arise, in part, from a differential weighting of these suboptimal outcomes.

Thus, a range of plausible neurobiological mechanisms could contribute to variability in choice at a whole-organism level; noise at different levels of the decision process is not discrete. There is a dearth of evidence exploring the genesis of choice variability in humans. However the mapping of such processes onto economic theories of stochastic preference could provide a fruitful source of testable hypotheses to better understand the whims and vagaries of choice, and moment-by-moment fluctuations in preference.

2.2.5 DIFFERENT TYPES OF VALUE?

If indeed there are multiple brain areas tracking value, this means that multiple valuation systems may be susceptible to distinct influences and potentially come into conflict. This raises deeper questions about what is actually meant by value and preference. The addiction example highlights a disparity between temporary cravings and long-term desires, a consideration that led Berridge and colleagues (Berridge, 1996) to propose a distinction between 'wanting' and 'liking'. While 'liking' corresponds to hedonic pleasure (i.e. the experience of reward), 'wanting' is more aligned with appetitive salience and motivation (i.e. anticipated reward). An extended account of this parsing of choice behaviour involves a

pharmacological division between these two components, with 'wanting' dependent upon the dopaminergic system and 'liking' on an endogenous opiod system. This in turn highlights another biological level within which preference can be generated – rather than being regionally encoded, some aspects of preferences might be a property of a distributed pharmacological neuromodulatory influence. I explore and experimentally test this idea (specifically the influence of dopamine) in **Chapter 7**.

While providing a compelling heuristic, it turns out that a distinction between 'wanting' and 'liking' is not entirely clear cut. Tindell (Tindell et al., 2009) has shown that salt-deprived rats can acquire preferences (i.e. instrumental choices) for previously disliked salt-giving levers in the absence of any new training or experience of the now beneficial salty outcome. This indicates that systems controlling preference can also integrate information about physiological state, in the absence of information about hedonic pleasure or 'liking', although physiological state may well have immediate access to a value-signalling system (as opposed to complex goals) given its' central role in shaping adaptive fitness. Indeed, supporting this idea, in **Chapter 6** I present evidence that physiological state can bias preference in the economic domain.

2.2.6 DYNAMIC CHANGES IN PREFERENCE

A final consideration about preferences is their lability. Behaviour often shows response shifts to exogenous and endogenous variables, from the typically economic (price, resource availability) to the biological and psychological (physiological state, arousal, emotion). Preference also changes over time, both in response to changes in environmental conditions (e.g. accumulation of wealth, reproductive success) and sources of unobserved heterogeneity (e.g. drifting of preferences over time). For biological success, it makes sense that preferences are amenable to 'top-down' cognitive influences. For example, it may be appropriate in times of financial crisis to make a 'risk-averse' choice and stick with a steady reliable source of income, while in more optimistic times 'risk-seeking' or entrepreneurial choices may be of greater long-term benefit (see **Chapter 5** for an experimental test of decision making under an externally imposed constraint).

Many preferences are phylogenetically ancient. *Drosophila* flies can choose between competing cues to avoid punishment, a function supported by their dopaminergic system (Zhang et al., 2007). There is also a pervasive sensitivity to risk not only in humans (Kahneman and Tversky, 1979), but also in distantly related species including birds and fish

(Real et al., 1982; Wunderle et al., 1987; Croy and Hughes, 1991; Bateson and Kacelnik, 1997). These 'evolved' preferences suggest biological hard-wiring. Indeed, many of these species lack an highly developed prefrontal cortex, yet manifest preferences that are dynamically altered in response to complicated strategic motives. Flexible preferences mean that even if a specific neural substrate is responsible for a general tendency to emit distinct behaviours, these regions necessarily need to receive information both from a hierarchy of 'higher' (e.g. maintaining a strategy) and 'lower-level' inputs (e.g. physiological or emotional state).

These behavioural switches link more broadly to the idea of 'exploratory' behaviour. A hesitancy to explore is used as a biological marker of trait anxiety in animal models (Hogg, 1996). Can we call exploration a preference? A 'preference' to explore the unknown bucks the natural trend to stay with known rewarding actions ('exploitation'), and can lead to a different selection of actions (choices) depending on circumstance, a process poorly-captured in many economic models. Computationally, this explore-exploit dilemma is critical in learning theory, and there is evidence that exploratory behaviour is instantiated in rostral anterior prefrontal cortex (Daw et al., 2006) and anterior cingulate cortex (ACC) (Procyk et al., 2000). Thus an 'exploratory' preference could reflect the function of a very different kind of neural process, more related to task-switching and behavioural flexibility (Ragozzino, 2007), perhaps an example of a top-down process that modulates classical preferences rather than a biological predilection in itself.

2.2.7 THE ROLE OF NEUROSCIENTIFIC EVIDENCE

On the one hand, choice and preference can be considered the only relevant end-product of a 'black-box' process (Gul and Pesendorfer, 2008). This is perfectly reasonable as an approach to decision making as economic models are designed solely to predict choice, not to imply biological mechanisms. However, neuroscientists are primarily interested in mechanistic 'proximate' questions - it is not sufficient to observe how cars move if you want to understand the internal workings of a combustion engine. The aims of neuroscience include understanding the biological underpinnings of behaviour and beyond this a biophysically-motivated model of choice. This in turn can yield insights about disease processes, reveal neural targets that determine pathological behaviour, and even potentially 'improve' an individuals' decision-making. As framed by Marr (Marr, 1982), to address these questions one needs to specify computational goals, their algorithmic basis, as well as the biological hardware that implements these processes.

2.3 RISK

2.3.1 INTRODUCTION

Risk is a paradigmatic example of a decision variable. Risk has many components – in lay terms a decision is 'risky' if it is uncertain, has a small chance of success, if the potential loss is large, or if there are extreme losses or gains relative to the status quo. Thus the perception of risk captures elements of both the probabilities and magnitudes of possible outcomes. The quantification of risk is key to modern economics, and how individuals treat risk – their risk preferences – dictates a large range of choices. This thesis focuses on decision making under risk as a means to understand the neurobiological mechanisms underpinning decision making.

Using risk as an example is informative for several reasons. Firstly, risk is a well-explored concept in economics, from which ideas in psychology and ecology have derived. It can be objectively quantified in a straightforward manner based on an economic framework, and preferences for risk can be measured in monetary terms. Financial risk is also simple to manipulate, and money is a motivating secondary reinforcer that can elicit attentive and real (*incentive compatible*) behaviour in human experimental participants. Parallels can be drawn with sensory variables – many of the early advances in sensory neuroscience were based on the visual system, with its precisely quantifiable stimuli possessing different stimulus attributes or dimensions, and the robust and simple manner in which psychophysical responses could be elicited.

We can therefore use risk to understand neural processing of abstract decision variables. Conversely, neuroscientific enquiry into risk processing can offer insights for economic theory. There exist well-defined alternative explanations for the construction of risk preference in economics and finance (and psychology and ecology). Many of the predictions of these theories pertain to choice, the ultimate measurable variable, but all can be accurate enough in their choice predictions such that the theories are rendered indistinguishable. However, as discussed above, neuroscientific evidence can evince the underpinnings of behaviour, and potentially map neural circuitry onto the elements or building blocks of these disparate theoretical structures. This therefore can provide evidence in favour of specific mechanisms for constructing decisions.

2.3.2 CLASSICAL ECONOMIC THEORY

A description of how much a gamble was worth became necessary at the start of the modern financial era, when investors wished to calculate the value of their prospective property and trade investments.

In the mid-17th century, Blaise Pascal proposed that the value of a lottery X with *n* potential outcomes should be quantified by its expectation (average outcome).

$$EV(X) = \sum_{i=1}^{n} p_i(x_i) \cdot x_i \qquad \textbf{(2.1)}$$

While 'rational', this does not explain why most people would prefer a certain amount of money to taking a risk on a lottery with equal expected value. This problem was illustrated by the St Petersburg Paradox. Imagine the following game. A coin is flipped – if it lands heads, the game stops and the winnings are £1. If tails, the coin is flipped again. A heads on the second toss stops the game but this time with winnings of £2, whilst tails permits a further throw. The game continues until a heads is thrown, at which point the winnings are 2^{N-1}, where *N* is the number of coin tosses. The probability distribution of outcomes is shown in **Figure 2.2**. How much should a decision-maker pay to play such a game? According to Pascal's logic, this lottery is literally invaluable:

$$EV(X) = \frac{1}{2} \cdot 1 + \frac{1}{4} \cdot 2 + \frac{1}{8} \cdot 4 + \ldots = \frac{1}{2} + \frac{1}{2} + \frac{1}{2} + \cdots = \infty \qquad \textbf{(2.2)}$$

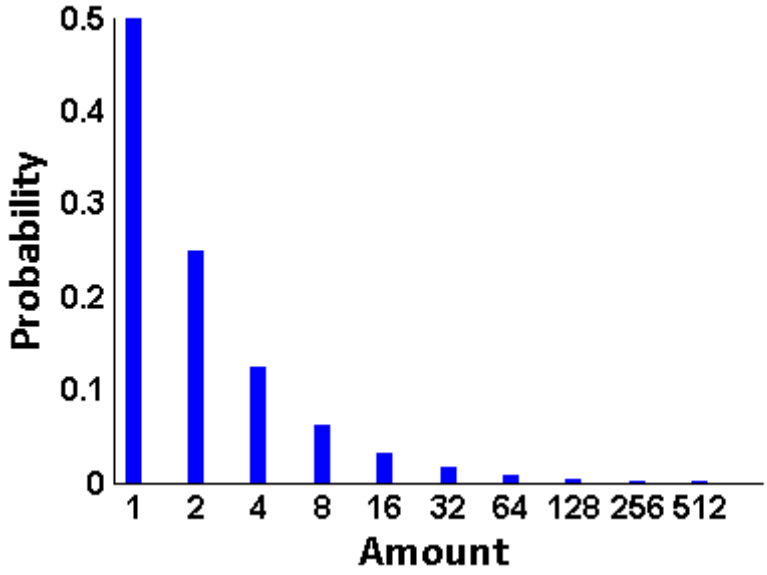

Figure 2.2. Outcome distribution for the St Petersburg paradox. A fair coin is tossed N times until a "head" is thrown, at which point the game ends and the winnings are 2^{N-1}. This highly positively skewed distribution has infinite expected value.

Daniel Bernoulli advanced a solution to this 'paradox', suggesting that individuals transform the outcomes from a lottery into subjective values (*expected utility – EU*) according to an implicit concave 'utility function'.

$$EU(X) = \sum_{i=1}^{n} p_i(x_i) \cdot u(x_i) \qquad \textbf{(2.3)}$$

A logarithmic transformation of objective amounts to subjective values (i.e $.u(x) = log_2(x)$) yields an expected utility for the St Petersberg paradox of:

$$EU(X) = \sum_{i=1}^{\infty} \frac{1}{2^i} \cdot log_2(2^{i-1}) = 1 \qquad \textbf{(2.4)}$$

This translates in to a more realistic monetary equivalent value of $2^{EU(X)}$=£2[3].

[3] A flaw in Bernoulli's solution can be seen if we exponentiate possible winnings: i.e. winnings are now $\exp(2^{N-1})$. This again yields an infinite sum of series, and by a similar logic any non-linear transformation of utility will be susceptible to this trick. A decision maker only prepared to pay a finite amount to play these games must ignore probabilities below some threshold (or magnitudes above a threshold).

More generally, a lottery is worth less than its expected value for an individual with a concave utility function, by Jensen's inequality (**Figure 2.3**). In other words, there is a *risk premium* to pay for accepting such a gamble. Bernoulli's marginally decreasing utility captures the intuitive concept that a £1 gain from £100 to £101 does not *feel* as valuable as an increment from £1 to £2. This has close parallels with Weber's 'law' in psychophysics, where sensitivity to a sensory increment scales with the absolute magnitude, leading to diminishing marginal sensitivity.

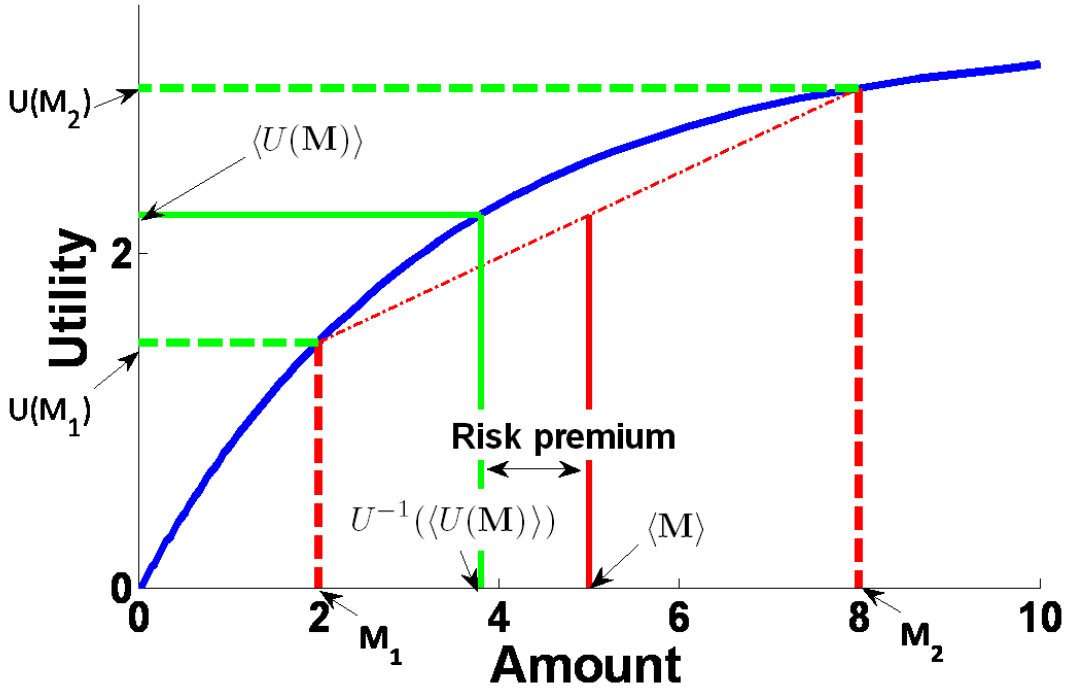

Figure 2.3. Illustration of a concave utility function. For a 2 outcome lottery M = [M_1,M_2; ½, ½], the expected value of the lottery $\langle M \rangle = [M_1 + M_2]/2$. . For a concave utility function, the expected utility of the lottery $= \langle U(M) \rangle = [U(M_1) + U(M_2)]/2$. This translates into an equivalent amount of $U^{-1}(EU) < \langle M \rangle$. This is true for all concave functions and any probability mixture of amounts, by Jensen's inequality. This difference is the risk premium of the lottery – how much extra an individual would have to be paid to yield indifference between the lottery and a sure amount with matched expected value.

The power of Expected Utility Theory was firmly established by von Neumann and Morgenstern (Von Neumann and Morgenstern, 1944), who derived the same mathematical form from axiomatic first principles. An individual who possesses preferences for all possible lotteries (*completeness*), consistently rank orders these lotteries (*transitivity*), can construct new lotteries of intermediate value from a mixture of existing gambles (*continuity*), and who does not change their preference ordering of 2 lotteries in the presence of a new outcome common to both (*independence*), will prefer lottery 1 (*L1*) to lottery 2 (*L2*) if and only if

EU(*L1*)≥EU(*L2*), as defined by **equation (2.3)**. Completeness and transitivity ensure that the axes in **Figure 2.3** are invariant and can be given a scale, while continuity ensures that probability mixtures of outcomes can be mapped between the x and y axes. Independence means that this mapping is linear in probabilities.

There are several points to note about the concept of utility functions in Expected Utility Theory. Firstly, they are unique up to a linear monotone transformation – in other words, utility is ordinal, but the specific utilities themselves do not have an implicit meaning. Utility of a gamble for different individuals can only be compared under the assumption that they are using the same utility function to construct value, as a transformation of utility values (by addition of a constant, or a scaling) does not alter the relative ordering of these numbers. Secondly, in expected utility theory, probabilities and amounts are defined independently. This is called *probabilistic sophistication* (Machina, 2005). Thirdly, risk is a by-product of the process of transforming objective into subjective value, rather than a variable in itself. Indeed, the shape of the utility function defines risk, in the sense that the same distribution of outcomes will yield very different risk premia dependent upon the form of the utility function.

Absolute risk aversion (ARA) can be defined in the EUT framework by the Arrow-Pratt measure (Pratt, 1964):

$$ARA(x) = -\frac{u''(x)}{u'(x)} \qquad \textbf{(2.5)}$$

where u is an individual's utility function. ARA scales an individual's risk premia, and is usually assumed to be a decreasing function of wealth (x). In other words, the richer you are, the more likely you are to pay a fixed amount to play a given gamble. Relative risk aversion is:

$$RRA(x) = -x \cdot \frac{u''(x)}{u'(x)} \qquad \textbf{(2.6)}$$

In this thesis (see **Chapters 4-8**), when modelling classical expected utility, I use the isoelastic function $U(x) = x^{1-\rho}/1-\rho$, which exhibits constant relative risk aversion and is widely used in economics because of its attractive mathematical property that the relative utility of a risky vs risk-free asset is independent of initial wealth levels. In practice, this

scale-free utility function is inaccurate (Rabin, 2000), but serves its purpose in the conditions I consider in this thesis where wealth does not appreciably change. I save further discussion of reference-dependence and scaling for **Chapter 5**.

2.3.3 BEHAVIOURAL ECONOMICS AND UTILITY THEORIES

Since its inception, EUT has come under attack from behavioural theorists because of its normative approach. Many famous violations of EUT have been demonstrated, including the Allais paradox (see above), the Ellsberg paradox (Ellsberg, 1961), and a host of other discrepancies highlighted by the heuristics and biases program (Tversky and Kahneman, 1974), and the concept of bounded rationality (Simon, 1982; Gigerenzer and Goldstein, 1996). These ideas have been hugely influential, both spawning new fields of research in behavioural economics, ecology, and evolutionary psychology, and pervasive in society (Levitt and Dubner, 2006; Thaler and Sunstein, 2008b). Here I discuss Prospect Theory, which directly addresses decision making under risk, and which I have used as a benchmarch utility function in **Chapters 4 and 5**.

2.3.3.1 ***Prospect theories***

Kahneman and Tversky outlined several key behavioural findings which they sought to capture in a new, all-encompassing choice theory (Kahneman and Tversky, 1979). The basic formulation is identical to EUT, with outcomes specified as amounts and probabilities. Prospect theory (PT) then diverges in several ways. One proposition is that individuals overweight events with small probabilities. This has received considerable empirical support (Gonzalez and Wu, 1999), and can explain the Allais paradox. A second cornerstone is that losses have more impact than equivalent monetary gains. This is important in explaining the framing effect where choices for the same gamble differ depending on whether it is presented as either a potential gain or a potential loss (Gonzalez et al., 2005). This also explains the reflection effect where preference reversal are seen for choices between a gambles with positive outcomes and a matched sure amount, versus equivalently setup choices where all outcomes are translated into the negative domain (Fagley, 1993). In classical expected utility theory the utility function is concave (or convex) everywhere which proscribes such a reversal. However actual experimental comparisons of the weight attributed to losses and gains are sparse and the picture is inconsistent (Hershey and Schoemaker, 1980; Schneider and Lopes, 1986; Budescu and Weiss, 1987). The third

component of Prospect Theory is that risk preference can differ between losses and gains, which can also explain the reflection and framing effects,

Another feature is that outcomes are evaluated with respect to a reference point rather than zero wealth. Thus outcomes falling below the reference point are treated as losses. This reference point was originally and is most commonly suggested to be the status quo (Kahneman and Tversky, 1984; Tversky and Kahneman, 1991; Schneider, 1992), although in practice the reference point could be any individual (Köszegi and Rabin, 2006) or even multiple (Lopes and Oden, 1999) anchors. A last difference is that Kahneman and Tversky suggested an editing procedure, whereby some choice options are ruled out at the outset of the decision process. This is necessary to prevent violations of stochastic dominance (where a quirk of probability weighting means that for gambles with very rare outcomes the theory can lead to a prediction of a more risky choice even when this option is the least valuable and there is a clear alternative winning option under all eventualities).

This theory redefined the interaction between psychologists and economists, presenting well thought out experimental hypotheses and evidence that systematically took on the tenets of neoclassical microeconomic theory. Despite this, there are many difficulties with this approach. Perhaps foremost is that the editing procedure is nebulously defined. A later formulation, Cumulative Prospect Theory (CPT) (Tversky and Kahneman, 1992), improved the theory by specifying that probabilities are weighted in a rank-dependent way (similar to Quiggin (1982)), where the weighting is a function of the cumulative probability of an event rather than its absolute probability. This leads to greater generalisability and avoids situations of stochastic dominance violation. I use CPT in **Chapter 4**, which contains a mathematical exposition.

A second and more general problem with the theory is its broad parameterisation. If individuals possess independent risk preferences, weighting functions, loss aversion, and reference points, this means that 6 parameters are required to describe behaviour. It also means that the unrestricted version of PT can predict virtually any pattern of behaviour, for instance the finding that individuals in learning situations often underweight rather than overweight small probabilities (Camerer, 2000). This is much more complex than the models it was designed to replace, and also leads to some practical problems with behavioural fitting as parameters are not necessarily independent. For example, choices for mixed gambles can be explained both in terms of different risk-preferences for relative gains and losses, as well as by loss aversion.

A third, and perhaps more pervasive issue, is that PT remains a description of behaviour under particular circumstances rather than explaining or specifying a mechanistic formulation of choice. Although various neurobiological investigations have addressed the instantiation of Prospect Theory in the brain (De Martino et al., 2006; Tom et al., 2007; Hsu et al., 2009), and have been successful in demonstrating that the brain does not behave according to EUT predictions, these focus on specific elements of PT under specific manipulations (framing effect, binary mixed gambles, and win-lose gambles). PT thus remains an extension of EUT (Harrison and Rutström, 2009), applicable and very powerful in specific scenarios (e.g. probability extremes). For more complex decisions, with multiple alternatives or a distribution of outcomes, and in particular in learning situations where a model of the world needs to be updated following receipt of new information, PT (and EUT) becomes less useful as a realistic bottom-up computational model (D'Acremont and Bossaerts, 2008).

2.3.4 FINANCE AND MEAN-RISK THEORIES

EUT and Prospect theory propose that decision-makers' subjective values for each possible outcome are determined by an implicit utility function, with 'utilities' weighted by the probability of each outcome and risk-preference emerging as a by-product of this framework (Pratt, 1964). Alternative theories in finance (Markowitz, 1952; Sharpe, 1964), psychology (Coombs and Huang, 1970), and ecology (Stephens, 1981) propose that outcome distributions are decomposed into "summary statistics" (e.g. mean, variance, skewness), with risk-preference directly generated by preference for each component. These models are a central focus of this thesis, and I describe their implementation in detail in subsequent chapters.

Mean-risk theories have advantages over EUT-type models. Firstly, they generalise to any outcome distribution. Secondly, complex outcomes with multiple probabilities and outcomes can be simplified into a few descriptive parameters, which is computationally attractive, useful for learning, and neurobiologically appealing. Moreover, they can capture many features of the behavioural models such as Prospect Theory, as relative gains and losses (compared to an average outcome), and overweighting or underweighting of probability extremes can also fall out of mean-risk models. They have disadvantages – specifically that they are not probabilistically sophisticated, so that information about some outcomes can be lost in summarisation, in other words some outcomes assume more importance than others

due to their contribution to the overall shape of the distribution. A lack of probabilistic sophistication is no bar in itself, and indeed CPT itself does not preserve the distinction between probabilities and amounts.

It turns out that observation of behaviour alone cannot distinguish Expected Utility from summary statistic models. Both can make identical choice predictions, as any utility function can be approximated by preferences for summary statistics using a polynomial expansion (Scott and Horvath, 1980; Müller and Machina, 1987; D'Acremont and Bossaerts, 2008). To illustrate, for any utility function, $y = U(x)$, a Taylor expansion of the outcomes in gamble x about an arbitrary mean outcome amount μ gives:

$$U(x) = U(\mu) + U'(\mu) \cdot (x - \mu) + \frac{U''(\mu)}{2} \cdot (x - \mu)^2 + \frac{U'''(\mu)}{3!} \cdot (x - \mu)^3 + \cdots \quad \textbf{(2.7)}$$

Taking the expectation (average) of both sides:

$$\mathrm{E}[U(x)] = U(\mu) + \frac{U''(\mu)}{2} \cdot \mathrm{E}[(x - \mu)^2] + \frac{U'''(\mu)}{3!} \cdot \mathrm{E}[(x - \mu)^3] + \cdots \quad \textbf{(2.8)}$$

which has the form of a mean-variance-skewness model, with variance and skewness preference determined by the (local) curvature of an individual's utility function (and visa versa).

This raises the critical importance of exploiting choice generated neural data in adjudicating between these models. Several studies have focused on variance (Preuschoff et al., 2006; Tobler et al., 2007; Christopoulos et al., 2009; Tobler et al., 2009), which reflects a first-order approximation of risk (Rothschild and Stiglitz, 1971) but ignores the influence of positive and negative skewness on risk perception, as in the example in **Chapter 1** where variance between choices is equivalent (Garrett and Sobel, 1999).

One key aim in this thesis was to use model-based fMRI analysis (O'Doherty et al., 2007) to determine directly whether the brain encodes the summary statistics (variance and skewness) of a decision.

2.3.5 PSYCHOLOGY: RISK AND AFFECT

Finally, there has been an alternative psychological tradition that focuses on risk sensitivity as a product of affective state (Loewenstein, 2001). The central proposal is that the

contribution of emotions to decision making is often neglected in traditional theories. This is despite clear evidence that, for example, emotional state influences risk taking (Isen and Patrick, 1983; Isen and Geva, 1987). A similar biological position has been advocated by Damasio and colleagues as the somatic marker hypothesis (Damasio et al., 1996).

The strong hypothesis that decisions are a *consequence* of the affective assessment of bodily states is clearly neurobiologically implausible, and much of the evidence for this theory is based upon the Iowa Gambling task which has inherent difficulties in interpretation (see **Chapter 7** for a further discussion). However, the notion that emotions are important in decision making under risk is resonant, and I would argue that rather than a separate stream of influence, emotions are both a product and contributor to valuation. The sensation and anticipation of 'loss' is potently emotional, and has been incorporated in regret theory (Loomes and Sugden, 1982), however 'loss' is simply a categorical definition of one particular consequence of a risky decision. A fuller conceptualisation accounting for the relative ('emotional') weight of different outcomes converges with the economic ideas expressed above – measuring preferences could be construed as a proxy for measuring the affective assessment of different stimulus dimensions, in as far as they impact on choice.

Similarly, the idea that emotions exploit a privileged subconscious pathway (Bechara et al., 2000) reflects the idea of multiple valuation processes discussed in the previous section. The pertinent questions then becomes not *if* emotion is important in decision making under risk, but *how* risky decisions are assessed and executed by the brain, and *where* different influences (emotional or otherwise) might take effect.

2.3.6 METHODS OF EVALUATING DECISION MAKING UNDER RISK

Multiple methods have been employed to assess decision making under risk. Qualitative methods have involved questionnaires – very useful in assessing responses to 'real-world' decision scenarios across domains, however difficult to quantify in economic terms. Not only are the values attributed to such outcomes tricky to ascertain, but also one usually does not know the priors that individuals bring to bear in answering such questions, nor the validity of responses. For this reason experimental economics has concentrated on eliciting choices for lotteries.

A variety of methods risk-preference elicitation methods exist (Harrison and Rutström, 2008), including direct elicitation of certainty equivalents with the Becker-DeGroot-

Marschak procedure (Becker et al., 1964), a multiple price list design (Holt and Laury, 2002), and a multiple paired lottery choice task (Hey and Orme, 1994). In the studies in this thesis, I have used either a paired lottery design, or the simpler two-alternative forced choice between a lottery and a sure amount of money. The principal difference between the paradigms developed herein and preceeding studies is that the lotteries used possess multiple rather than binary outcomes. The advantage of a comparison between a lottery and a fixed sure amount is that neural responses to individually presented risks can be isolated.

A variety of other risk assessment methods have been used in psychological paradigms, including the Iowa Gambling Task (Bechara et al., 1997), and the Balloon Analogue Risk Task (Lejuez et al., 2002). These have the problem that risks are unknown or ambiguous, thus the tasks require learning and feedback. Other tasks present explicit risks, such as Rogers' Cambridge Gamble Task (Rogers et al., 1999), and Game of Dice task (Brand et al., 2005). These are similar to the pie-chart tasks used in this thesis. The advantage of the latter is that multiple outcome lotteries can be presented in a visually straightforward way.

Having examined both controversies and difficulties in understanding the biology of choice and preference, and subsequently discussing behavioural approaches to risk, I next focus on how preferences in general, and specifically attitudes to risk, might be implemented in the brain.

2.4 WHAT ARE THE POTENTIAL NEURAL MECHANISMS BY WHICH PREFERENCES COULD BE EXPRESSED?

What are the plausible mechanisms by which preferences are expressed in the brain? The most obvious is a direct neural instantiation of an hedonimeter (Edgeworth, 1881), a regionally specific encoding of intrinsic value. A more subtle question is to ask how 'preference' is reflected within a single neural region. Alternatively, preferences may be determined by concentrations of neurotransmitters, a whole-brain property at the synaptic level. Preferences might be expressed at different time-points in the process of decision making, thus we can ask whether preferences are generated in early valuation or later motor response systems. Finally, rather than individual regions or systems in the brain being critical for generating preferences, one can consider whether modulations in the interaction or communication within a network of regions holds the key to understanding inter-individual variability in choice.

2.4.1 REGIONALLY-SPECIFIC ENCODING OF INTRINSIC VALUE

Gottfried et al measured fMRI data during an appetitive olfactory conditioning paradigm, where arbitrary picture stimuli were paired with pleasant smells of different foods (Gottfried et al., 2003). Following learning, one of the olfactory stimuli was selectively devalued by consuming the associated food to satiety. This enabled a distinction between stimulus-bound neural responses predicting simply the type of odour (i.e. a 'flavour' response) from responses that differentiated between valued versus devalued cues (i.e. an anticipated hedonic response that could reflect preference). While a network of regions in OFC, amygdala, piriform cortex and midbrain were activated during presentation of odours, only subregions of amygdala and OFC exhibited responses that paralleled the effects of selective satiety, showing decreased activation for sated compared to unsated odour cues.

Of course this is not a causal demonstration of neural activity tied to preference, but exemplifies one of the earliest usages of neuroimaging to identify regions conforming to the internal representation of a decision variable. In this case, the fact that the OFC activation for the same physical stimulus changed in a manner that correlated with a behavioural manipulation of preference highlighted the OFC as a candidate region instantiating the expression of preferences. In the same study other regions, for example insula cortex and striatum, decreased their activity for the sated stimulus, but increased their activity for the alternative control stimulus. This observation highlights that an interpretation of findings is constrained by the purported models being tested. If, for example, one hypothesises that the brain forms a relative ranking of value, rather than representing value on a cardinal scale, then the insula would fit this description. A rigorous specification of choice models can help marshal divergent findings and this is the essential advantage of model-based approaches, whether neuroeconomic or biophysically inspired.

Converging evidence for over a decade has identified the OFC as encoding reward value. Single neuron recordings have shown a correlation in firing of OFC neurons with preferences in monkeys (Tremblay and Schultz, 1999). Neuroimaging studies show that OFC responses are neither valence-specific, manifesting responses to both rewards and punishments (O'Doherty et al., 2001a), nor domain-specific showing responses to food and other primary reinforcers (Small et al., 2001), money (Elliott et al., 2000) and social value (Rushworth et al., 2007). These responses also appropriately scale with increasing amounts of anticipated value (Elliott et al., 2003), and actual behavioural preference (Plassmann et al., 2007b).

Recent findings from direct neuronal recordings in monkeys show that a proportion of OFC neurons adapt to condition, manifesting similar ranges of response under different scales of outcome (Padoa-Schioppa, 2009). This suggests that the OFC not only responds to changes in value, but also integrates value with contextual and other goal-orientated information. In different paradigms, OFC also encodes differences in stimulus value (FitzGerald et al., 2009b), choice value (Boorman et al., 2009) and counterfactual outcomes (Coricelli et al., 2005). These components are all important for the generation of choice. Nevertheless finding a region that maintains a stable, ordered, and scaled representation of value is not the same as finding the seat of preferences in the brain. OFC and similar regions could be representing value for other reasons, for instance maintaining a representation of anticipated versus received rewards contingent on choice for learning purposes, or being an arbiter in providing control of behavioural responses by gating influences from other valuation regions. For instance, value-sensitive responses to reward feedback have been found in primary somatosensory (Pleger et al., 2008) and visual (Weil et al., 2010) cortices in perceptual learning paradigms. Even if OFC performs computations of differences in value, perhaps being the generator of probabilistic choices for abstract value-based decisions rather than decisions based on comparisons of direct sensory evidence, it appears to be only one component of a network of value-sensitive regions. Moreover, it is plausible that 'preference' or intrinsic value is imbued to decision values prior to this information arriving in OFC.

Multiple candidate regions that have been reported to express value-related responses include posterior parietal cortex (PPC) (Platt and Glimcher, 1999; Iyer et al., 2010), posterior cingulate cortex (PCC) (McCoy and Platt, 2005), insula (Yacubian et al., 2006), nucleus accumbens/ventral striatum (Elliott et al., 2003; Knutson et al., 2005), the ventral tegmental (VTA) and substantia nigra (SN) areas of midbrain (Tobler et al., 2005). Other value-sensitive brain regions such as ACC appear to encode negatively-valenced components, such as cost or effort (Walton et al., 2003).

The range of findings support one hypothesis – that OFC and similar regions encode the (non-linear) sum of value-sensitive inputs in an excitatory manner that in turn positively correlate with desired stimuli and actions. Equally possible is that decrements in activity in a region could influence choice (perhaps by a reduction in tonic inhibition of action), as is evident in basal ganglia circuitry (Mink, 2003). In other words, even if there were a regionally specific encoding of preference, this does not mean that value necessarily corresponds to increases in neuronal activity. It is also possible that disparate pools of

neurons within a region could exhibit very different relationships with stimuli or behaviour, either individually influencing a target region or interacting within a region (e.g. by lateral inhibition, Blakemore and Tobin, 1972). Single-cell recording studies in orbitofrontal cortex yield this mixed picture, revealing distinct populations of adjacent neurons that are value sensitive, some expressing increases and others decreases in firing rate with increments in subjective value (Kennerley et al., 2009).

2.4.2 A CHANGE IN NEURAL SENSITIVITY WITHIN A BRAIN REGION

'Preference' describes a tendency to select a particular kind of action. The 'sweet-toothed' choose sugary rather than savory foods; a 'risk-seeking' person chooses uncertain options; an 'impulsive' child fails to temper desire for immediate gratification while an 'altruistic' individual takes account of others' welfare. Whilst these disparate tendencies may share common neural representations of value, economic models point to overall value as constructed from intrinsic subcomponents.

One can represent this process as $\boldsymbol{Choice} = f(\boldsymbol{Value}) = f(\boldsymbol{\mu}, \boldsymbol{\vartheta})$, where $\boldsymbol{\mu}$ are the stimulus properties or biological primitives relevant to behavior, and $\boldsymbol{\vartheta}$ represents the parameters that govern how an individual treats or processes these properties. $\boldsymbol{\mu}$ can relate to primary sensory properties of the stimulus (form, taste, smell etc), but equally can be a function of these sensory properties (i.e. $\boldsymbol{\mu} = g(\boldsymbol{Stimulus})$). For example, this could be a transformation of visual information presented in a gamble into decision variables such as magnitude and risk, or a non-linear weighting of more abstract stimulus feature such as reward probability. This framework partitions the decision making process into four sub-components, each represented in the brain. Choice pertains to action, the end-product of a motoric network. Value relates to affective or hedonic anticipation or impact of those actions (as I discuss above), but $\boldsymbol{\mu}$ and $\boldsymbol{\vartheta}$ pertain to underlying decision variables. While $\boldsymbol{\mu}$ is a function of the stimulus properties themselves and invariant with respect to behavioural predilections, $\boldsymbol{\vartheta}$ describes how individuals treat each of these underlying properties (e.g. whether magnitude has a positive or negative impact on value). Thus, a search for the neural instantiation of preferences can be seen as a search for a representation of these underlying $\boldsymbol{\vartheta}$ parameters.

One means of identification of such candidate areas would be to segregate areas representing $\boldsymbol{\mu}$ (potentially processing these decision variables) from areas encoding $\boldsymbol{\vartheta}$ (behavioural preference toward these decision variables). Lesion studies implicate both factors – for

example the finding that patients with damage to their ventromedial prefrontal cortex (VMPFC) are less averse to uncertainty than healthy counterparts (Hsu et al., 2005; Shiv et al., 2005) could be interpreted as the emergence of normative economic behaviour (a change in $\boldsymbol{\vartheta}$) or simply reflect a lack of sensitivity to this stimulus variable because of an inability to process uncertainty (no representation of $\boldsymbol{\mu}$). There have been a large cohort of studies demonstrating neural sensitivity to decision-relevant stimulus properties ($\boldsymbol{\mu}$), ranging from sensory attributes (O'Doherty et al., 2001b) and reward identity (Chib et al., 2009), to abstract decision variables such as financial magnitude of reward (Elliott et al., 2000), probability (Hsu et al., 2009), expected value (Knutson et al., 2005), valence (Delgado et al., 2000), and risk (Preuschoff et al., 2006).

Figure 2.4. Example of a study examining stimulus variable encoding. Correlation of ventral striatal activity with anticipated expected value and uncertainty in a binary-outcome decision making task (adapted from Preuschoff et al., 2006).

Other studies have attempted to identify regions correlating directly with preferences (ϑ). Structural studies have reported that prefrontal grey matter volume is inversely correlated with impulsivity (Bjork et al., 2009), and right prefrontal cortex lesions promote riskier choice (Clark et al., 2003). Alternatively, functional observations include findings that activation in striatal (Tom et al., 2007) and prefrontal (Gianotti et al., 2009) regions correlates with loss and risk aversion, while lateral and medial OFC correlate positively and negatively with risk aversion respectively (Tobler et al., 2007).

When making a decision, brain areas governing preference need to interact with circuitry involved in valuation, a process I summarise above as $f(\boldsymbol{\mu}, \boldsymbol{\vartheta})$. This influence could occur at an early stage of processing, during encoding of stimulus properties themselves. Both inferior frontal gyrus (IFG) and adjacent lateral prefrontal cortex express differential

responses to high and low risk, with greater responses for high than low risk in risk-seekers, but an opposite response in risk-averse individuals (Christopoulos et al., 2009; Tobler et al., 2009). This expression of risk-sensitivity would be expected from areas extracting or constructing the subjective value of risk, making this cortical zone a good candidate locus for integration of different aspects of financial value with intrinsic economic preferences.

This interaction between an observed behavioural preference and a regional expression of neural activity in response to a stimulus, context or decision trial has also been applied in studies of intertemporal and interpersonal ('social') choice. The effect of delay on behaviour (preference for impulsive choice) is mirrored by the effect of delay on neural responses in ventral striatum, medial prefrontal and posterior cingulate cortex (Kable and Glimcher, 2007). In this task, striatal responses demonstrate an integration of two types of economic preference, for both magnitude (marginally decreasing utility) and delay (Pine et al., 2009).

Invetigations of moral judgements and social preferences implicate prefrontal and insular cortices (Koenigs et al., 2007; Hsu et al., 2008). For example, the Ultimatum Game is a stylized economic paradigm of social interaction used to investigate the neural basis of social preference. Here, a 'proposer' might offer a fair 50:50 split of a £10 kitty to a 'responder'– the crucial element is that the 'responder' can elect to accept the offer, in which both parties receive the split as proposed, or reject the offer, in which case both parties get nothing. While the 'rational' response in a one-shot anonymised version of this task is to accept any offer amount, even in these circumstances of no reciprocity or reputation-formation real-life responders typically reject offers of up to 30% of the kitty (Camerer, 2003). This punishes the proposer for an inequitable split despite a personal financial cost incurred by the responder, hence indexing the responder's trade-off between self- and other-regarding preferences. Here, the stimulus variable of interest ($\boldsymbol{\mu}$) is inequity itself, an objective measure of fairness. How such inequity influences the responder's choice to accept or reject is proposed to depend upon their 'inequity-aversion' (ϑ) (Edgeworth, 1881; Fehr and Schmidt, 1999).

One can employ a version of Ultimatum Game where participants think they are responding to human proposers, but where offers are actually experimentally controlled (Wright et al., 2011). This enables a manipulation of inequity (i.e. the objective stimulus property $\boldsymbol{\mu}$), which was found to linearly correlate with activity in posterior insula. Crucially in this study, a bias in subjective appreciation of fairness was induced by altering the context of the decision – responders believed that offers were made by three socially different groups of subjects,

offering fairer or less fair splits of the kitty. Identical offers from these different social groups induced differential neural responses to inequity in mid-insula, responses that paralleled a behavioural bias in choice. A different network of regions in precuneus, left prefrontal and temproparietal cortex reflected endogenous inequity-aversion across subjects (i.e. independent of the contextual manipulation), illustrating that even within the context of a specific task, preferences for the same stimulus feature can be expressed in different regions and modulated in a distinct manner.

2.4.3 DISTRIBUTED ENCODING OF VALUE BY NEUROTRANSMITTERS

Midbrain dopaminergic neurons in the ventral tegmental area (VTA) and substantia nigra (SN) modulate their firing rate in response to rewarding stimuli (Tobler et al., 2005). Although dopamine was originally hypothesised to be a qualitative and quantitative hedonic signal (Yokel and Wise, 1978; Wise and Rompré, 1989), an aliquot of dopamine is not an intrinsic biological measure of utility, nor is dopamine release universally related to preference. A clear example is seen in genetically engineered rats with no endogenous dopamine synthesis but who still express relative preference for different types of reward (Cannon and Palmiter, 2003). However, dopamine does appear to play a central role in cost-benefit analysis (Phillips et al., 2007). This effect appears to be modality-specific and dictated by the precise dopaminergic projection target, as dopamine depletion in ventral striatum reduces propensity for physical effort (Salamone et al., 2007), but not for time delay (Wakabayashi et al., 2004). By contrast systemic dopaminergic modulation does influence inter-temporal decision making (Wade et al., 2000), an influence localised to orbital prefrontal cortex (and striatum) (Kheramin et al., 2004; Pine et al., 2010). However, there appear to be multiple dopamine-sensitive decision regions, as for example D1 blockade in ACC also reduces preference for expending effort for rats (Schweimer and Hauber, 2006).

Critically, dopamine neurons respond to surprising rewards (Schultz et al., 1997), revealing a central role in associative learning. Although non-discriminative between reward types, dopaminergic firing in VTA does appear to reflect subjective (action) value with integrated responses to both delay and reward amount (Roesch et al., 2007). Dopaminergic neurons send diffuse projections to striatum (nigrostriatal pathway) and prefrontal cortex (mesocortical pathway) and thereby transmit a hedonic value or teaching signal to a variety of brain regions, for learning, stimulus evaluation, and directed action. Increasing striatal dopamine for instance does not elicit reward craving by itself, even in addicts, but does change a cocaine addicts' sensitivity to environmentally salient cues (Volkow et al., 2008).

Single-unit recording studies have shown that the tonic firing rates of dopaminergic midbrain neurons scale with reward uncertainty in risk-based decision-making tasks in primates (Fiorillo et al., 2003), although the interpretation of this finding is subject to dispute (Fiorillo et al., 2005; Niv et al., 2005). These nuclei also receive inputs from areas such as the habenula (Matsumoto and Hikosaka, 2007), which responds to negatively-valenced stimuli and feedback (Ullsperger and Von Cramon, 2003). Hence, the VTA/SN could act as a hub to compare predicted action values and obtained outcomes. It is therefore possible that certain preferences could be engendered at this early stage, perhaps by differential responses to outcomes and interindividual variability in the effect of precision of predictions on dopaminergic output.

Figure 2.5 Midbrain dopaminergic neurons show a phasic and sustained response to probabilistic reward. A. Population histogram of dopaminergic neuron firing showing a phasic response to cue and feedback. B. The sustained response exhibits a quadratic relationship with reward probability (i.e. consistent with a variance or risk signal). C. This sustained response also scales with spread when reward amounts rather than probabilities are manipulated. (Adapted from Fiorillo et al., 2003)

There are substantial hormonal influences on behaviour. For example, circulating hormones such as leptin and ghrelin act as satiety and hunger signals, reporting the status of body

energy reserves (e.g. adipose tissue), energy requirements, and acute nutrient intake to hypothalamic and midbrain targets in the central nervous system that regulate feeding behavior (Korotkova et al., 2003). They also act on brain regions (in particular dopaminoceptive areas) implicated in human decision-making (Krügel et al., 2003; Hommel et al., 2006). Metabolic state itself may thus directly affect the neural expression of preference, an hypothesis I test in **Chapter 6**.

Other neurochemical systems are implicated in preference, with both serotonergic depletion (Denk et al., 2005) and NMDA antagonism (Floresco et al., 2007) promoting impulsivity. Several neuromodulatory transmitters are purported to play a specific role in risky decision-making, including noradrenaline, serotonin, and dopamine (Rogers et al., 2004; Zeeb et al., 2009). Clinically, Parkinson's disease, where nigro-striatal dopamine pathways are impoverished, can lead to disorders of decision-making (Cools et al., 2003). Dopamine agonists, used to treat this disorder, can cause pathological gambling behaviour as a side-effect of therapy (Gallagher et al., 2007). Additionally, manipulation of dopamine levels in rats disrupts decision-making under uncertainty in foraging tasks. Thus, administration of amphetamine (which augments dopamine release) increases preference for a risky choice, while the effects of amphetamine can be abolished by dopamine receptor blockade (St Onge and Floresco, 2008).

Finally, genetic polymorphisms affecting receptor function or expression are a suggested conduit for value and preference. For example, DRD4 polymorphisms modulate the incentive value of alcohol in alcoholics (MacKillop et al., 2007), while genetic polymorphisms affecting DRD2 receptor expression alter neuronal responses to food reward (Felsted et al., 2010). Although attributing specific whole-organism behavioural phenotypes or neural responses to genetic polymorphisms is highly contentious with results often contradictory and inconclusive (Hariri et al., 2002; Schinka et al., 2002; Munafo et al., 2003; Kreek et al., 2005), nevertheless it is conceivable that alterations in receptor function in specific neural regions could bias valuation and action-selection process thereby engendering behavioural predilections.

2.4.4 CHANGE IN NEURAL ACTIVITY COUPLED TO ACTION

Action is supported by multiple brain regions and networks. Saccadic eye movements are driven by the frontal eye fields via superior colliculus , while limb movements are guided by motor efferents from Betz cells in primary motor cortex projecting to spinal anterior horn cells. Motor cortex receives inputs from thalamus, which in turn receives afferents from multiple areas including the supplementary motor area in premotor cortex, basal-ganglia and cerebellum (Houk and Wise, 1995), and interparietal sulcus, an associative region of cortex containing neurons with sensory receptive fields (Shadlen and Newsome, 1996).

Figure 2.6 Risk-related activity in inferior frontal gyrus correlates with risk preference and with choice. A. Inferior frontal gyrus correlates with risk. B. The response to high and low risk changes direction as an individual's risk aversion increases. C. The correlation with risk depends both on the level of risk and on the choice that an individual makes. (Adapted from Christopoulos et al., 2009)

This division between action and perception is evident in multiple neural processes. Interestingly, preferences for actions can be dissociated from preferences for stimuli, which echoes an idea that actions can in themselves create or establish preferences (Ariely and

Norton, 2008; Sharot et al., 2009a). For instance, OFC is predominantly associated with (learned) valuation of (reinforcing) stimuli, but there is evidence of a distinct process in ACC (which projects anatomically to premotor regions) of value encoding for reinforced actions, and ACC sulcus may be required for learning of action values (Kennerley et al., 2006). Similar regions in ACC have also been shown to encode decision uncertainty (Behrens et al., 2007), and the ACC gyrus is involved is learning social values (Rushworth et al., 2007). Thus, it is possible that interactions between subregions of cingulate cortex might imbue taste for uncertainty or social preferences by differentially weighting action values represented in ACC.

ACC is also necessary for an appraisal of the energetic cost versus benefits of actions, and a preference to expend effort to achieve a goal. Take a situation where rats are required to make a decision between two alternatives, either to climb over a barrier to obtain a large food reward, or to expend low effort but receive a smaller food reward. ACC lesions alter the modal preference for expending effort to reap reward (Walton et al., 2003), an effect specific for energetic actions but not for non-effortful costs, such as a delay in obtaining reward (with the converse true for OFC) (Rudebeck et al., 2006).

Neuroimaging studies have identified areas differentially responding to selected actions (e.g. the selection of risky vs safe options in a gambling task). Christopoulos *et al* have parsed a risk-sensitive network into (right) IFG, a region whose activity promotes safe choices, from ventral striatum and ACC, engendering risky choice (Christopoulos et al., 2009) (**Figure 2.6**). Direct disruption of activity in this right lateral prefrontal region by repetitive transcranial magnetic stimulation biases choice towards risk-seeking (Knoch et al., 2006b), while transcrianial anodal direct current stimulation, inducing activation in this area, promotes safer choice (Fecteau et al., 2007). In the domain of intertemporal choice, McClure *et al* have suggested an interaction between subcortical and cortical areas push and pull choices towards impulsivity or patience (McClure et al., 2004).

More recently, studies have examined the interaction between preference and choice-related activity. Superior and inferior frontal gyrus and OFC express greater or less activity prior to a risky choice in a manner that positively correlates with risk aversion (Engelmann and Tamir, 2009b). A similar pattern is seen in PPC (Weber and Huettel, 2008b), which has polysynaptic links to basal ganglia and premotor regions (Tanne-Gariepy et al., 2002) and direct connections with insula (Cavada and Goldman-Rakic, 1989). These choice-related activations also relate to psychological measures such as harm avoidance in both ventral striatum

(Matthews et al., 2004), and insula (Paulus et al., 2003b). In itself, this does not distinguish between modulation of stimulus evaluation and action selection, as risk-seekers will always tend to select a preferred riskier option if the expected values of options are matched. However, this parallels the interaction between brain areas governing preference and circuitry involved in valuation (i.e. $f(\boldsymbol{\mu}, \boldsymbol{\vartheta})$). Rather than envisaging this influence at valuation or stimulus encoding, hypothesizing a modulation of choice-related activity by preference postulates a direct effect of preference on regional activity coupled with motor output, without a distillation through a prefrontal or subcortical hedonometer. In other words, some preferences could originate within the motor network, where biases arise during a translation of sensory inputs into specific actions.

2.4.5 CHANGE IN REGIONAL CONNECTIVITY AND MODULATION OF PREFERENCE

The brain is a non-linear dynamical system, with dense interconnections between and within brain areas. There has been an increasing realisation that connectivity between regions is a key component of a functional neural architecture – this connectivity generates macroscopic synchronisation of neuronal pools (i.e. oscillatory activity) (Sporns et al., 2000), and supports metastable representations that change and switch at a behavioural timescale (Oullier and Kelso, 2006). This connectivity itself could be the source of preferences in the brain – if parietal cortex or striatum quantifies specific decision variables, prefrontal cortex integrates this information with context and incentive salience, and premotor cortex plans actions, perhaps the true instantiation of preference lies in the strength of connections and mutual influence between these regions.

Changes in behaviour and associated neural responses in medial prefrontal cortex and striatum following knowledge acquisition have been shown to be mediated by functional connections from dorsolateral prefrontal cortex (DLPFC) (Li et al., 2011). Right DLPFC is also implicated in rejection of fair offers in the Ultimatum Game (Wright et al., 2011), and disrupting this region by transcranial magnetic stimuluation induces a reversible increased tendency to accept normatively 'unfair' offers (Knoch et al., 2006a). Dorsomedial prefrontal cortex (DMPFC) has been separately shown to express connectivity (correlation between time-series of inferred neuronal activity) with anterior insula and DLPFC during a risky decision making task, with the relative strength of these functional connections dependent upon individual strategic preferences (Venkatraman et al., 2009). Similarly, an interconnected network of DLPFC, IFG and VMPFC have been mapped out by functional connectivity analyses to highlight how DLPFC mediates restraint in choices about food (Hare

et al., 2009). These studies indicate a network of regions involved in decision making whose interactions, rather than intrinsic activity, dictate preference and choice.

2.5 CONCLUSION

The process of decision making can thus be broken down into constituent parts, each supported by different neurobiological mechanisms. Preferences generated at each step are instantiated at a regional or network level, and controlled by multiple competing mechanisms. Consequently, there are multiple potential sites at which preferences can be endogenously or exogenously influenced. At one end of the spectrum is a demonstration that in vivo stimulation single neurons in early sensory visual cortex can bias motion discrimination decisions in monkeys (Salzman et al., 1990). At the other end, aberrant decision making with altered behavioural preference is a feature of brain injury (Clark et al., 2008), Parkinson's disease, (Gallagher et al., 2007), and can even be pharmacologically induced (e.g. by alcohol, amphetamines, and dopamine agonists) (Zeeb et al., 2009).

A coherent framework based upon neurobiological foundations allows arbitration between competing decision theories, and also reveals the sources of systematic biological influences on behaviour. Neurobiological evidence thus furnishes process-based theories of choice (i.e. theories that describe choices as the product of a series of distinct computations in functionally or anatomically separable networks), and yields new hypotheses beyond the bounds of traditional economic dictum.

The various conceptual approaches to choice and preference, demonstrations of disparate influences on decision making, and interactions between several different types of value, speak to different questions and levels of understanding of choice processes. For a biological model, we need to define the types of valuation system we are considering, the network or areas involved in the associated computational processing and the synaptic physiology that might underlie the process. In the same way that axiomatic economic models place well-defined constraints upon rational choice, biological parameters also place constraints on the plausible mechanisms that mediate the generation of actions and the preferences they express.

In the following chapters, I explore the neurobiological encoding of risk as a paradigmatic example of an economic variable, examining the anatomical network of areas involved in

representation of risk as a stimulus variable. I manipulate endogenous physiological state as well as exogenously administrating dopamine to delineate the extent and direction of these behavioural influences. Finally, I also identify where risk preferences are integrated with this information to direct choice and when these effects are expressed.

Chapter 3

METHODS

3.1 INTRODUCTION

In this chapter, I provide an overview of the methods used in the experiments in this thesis. I initially discuss decision theory and computational modelling of behaviour. Economic modelling of choice forms a cornerstone of each of the studies, and here I discuss the underlying principles and the statistical methods used both for fitting these models to data and for model comparison. The subsequent sections review the theory and practice of functional magnetic resonance imaging and magneto-encephalography, the two neuroimaging modalities used herein.

3.2 DECISION THEORY AND BEHAVIOURAL MODELLING

3.2.1 DECISION THEORY

Decision theory describes a broad formal framework for describing and quantifying questions about behavior in diverse environments, and reflects a wide range of theoretical and experimental traditions (e.g. Wald, 1950; Savage, 1951; Edwards, 1961; Green and Swets, 1974; Slovic et al., 1977; Sutton and Barto, 1998; Houston and McNamara, 2001; Bellman, 2003; MacKay, 2003; Gold and Shadlen, 2007). Decision theory is a critical tool for analysis of psychological data and its neural substrate, allowing mechanistic questions, hypotheses, and predictions to be posed by alternative models.

Decision theory encompasses many different types of problem, including learning and prediction (e.g. reinforcement learning (Sutton and Barto, 1998)), detection and classification (e.g. signal detection theory (Green and Swets, 1974)), exploration and exploitation, valuation and choice (e.g. microeconomic theory (Savage, 1951)). In this thesis, I concentrate on the latter, as the experiments endeavour to minimise effects of learning,

perceptual uncertainty, lack of knowledge, and ambiguity, focusing on how humans evaluate explicitly presented risks.

There are many different aspects to valuation and choice, and as discussed previously (see **Chapter 2**), including risky and intertemporal choice, dynamic and sequential decision making, and model-free versus model-based algorithms. Generally decisions under uncertainty are characterised by three components. Firstly, any action with uncertain outcomes can be described in terms of the different potential outcomes, or states of the world that might arise. The chance of these different outcomes can be described as a probability distribution or likelihood function over these states. Secondly, each of these states has potential value or cost, and the description of the value of potential outcomes is called the loss or cost function. Thirdly, most relevant in situations of learning and exploration, prior knowledge or assumptions can be integrated with new information to update beliefs about the probability of different states of the world occurring. To optimally combine knowledge of probability and cost entails maximisation of expected utility, as discussed in **Chapter 2**. Prior knowledge can be integrated in an optimal manner using Bayes theory. Approximations of expected utility can be employed to simplify the computational situation – rather than representing all possible states of the world and the full probability distribution, an estimate of value can be reached, for example either by summarising the probability distribution (Parzen, 1962), pruning states to the core essentials (a strategy used by game-playing chess or backgammon computers) (Tesauro, 1992), or using past estimates to infer future value as in reinforcement learning (Sutton and Barto, 1998).

In this thesis I borrow ideas and models in microeconomics and finance, in particular the concept of the construction of a utility measure for judging alternative actions, and for trading off risk and reward. One of the central questions addressed by experimental and behavioural economics is *which* utility function people use to construct decisions. These ideas have in turn heavily influenced thinking in ecology and engineering. Optimal control theory is founded upon the idea of maximising expected return of future states (Todorov, 2006), risk analysis incorporates uncertainty measures into the loss function (Bedford and Cooke, 2001), and foraging theory equates utility with reproductive fitness (Stephens et al., 2007).

3.2.2 BEHAVIOURAL MODELLING

In essence, all behavioural models attempt to predict aspects of behaviour as a function of sensory input. For the models implemented in this thesis, the relevant behavioural variable is choice, although one could alternatively desire to fit movements, reaction times, errors, or physiological measures. As discussed in the previous chapter, one can represent this process as $\boldsymbol{Choice} = f(\boldsymbol{Value}) = f(\boldsymbol{\mu}, \boldsymbol{\vartheta})$, where choice is a function of both stimulus properties $\boldsymbol{\mu}$ and individual parameters governing a person's behavioural attitudes $\boldsymbol{\vartheta}$. In other words, models are probability distributions over choices, conditioned on external variables. Neurobiological models attempt to map these functions and variables onto specific neural processes, either at a cellular (biophysical modeling) or systems (behavioural or network modeling) level. If a model describes data well, then one can explore how internal components of the model map onto processes in specific neural regions. Moreover, one can ask not only if the model predicts choice, but also if the expected profile of neural activity matches the model components. The use of parametric modulators to model the neural response to complex stimuli with several dimensions is well established (Buchel et al., 1998; Wood et al., 2008), and the correlation of neural data with dynamically changing internal variables of a computational model has been implemented in several studies of the neural valuation system (O'Doherty et al., 2004; Samejima et al., 2005); for review see Corrado and Doya (2007).

3.2.2.1 *Generative models of choice*

One of the first elements in constructing a behavioural choice model is to decide on the form of the value function. I use value function models derived from economic theory, as described in the previous chapters, and in more detail subsequently when I consider different models in turn. In addition, value functions need to be combined with a generative model of choice. In other words, one needs to describe how stimulus values are translated into discrete choices.

This translation could be deterministic (i.e. a rule where option A is always chosen over option B if its value is greater). Such normative choice rules form the basis of axiomatic foundations of economic theory. In practice, they do not describe behaviour well, and one normally needs to model stochastic preference. The commonest way of doing this is by translating value differences through a sigmoidal function (**Figure 3.1**).

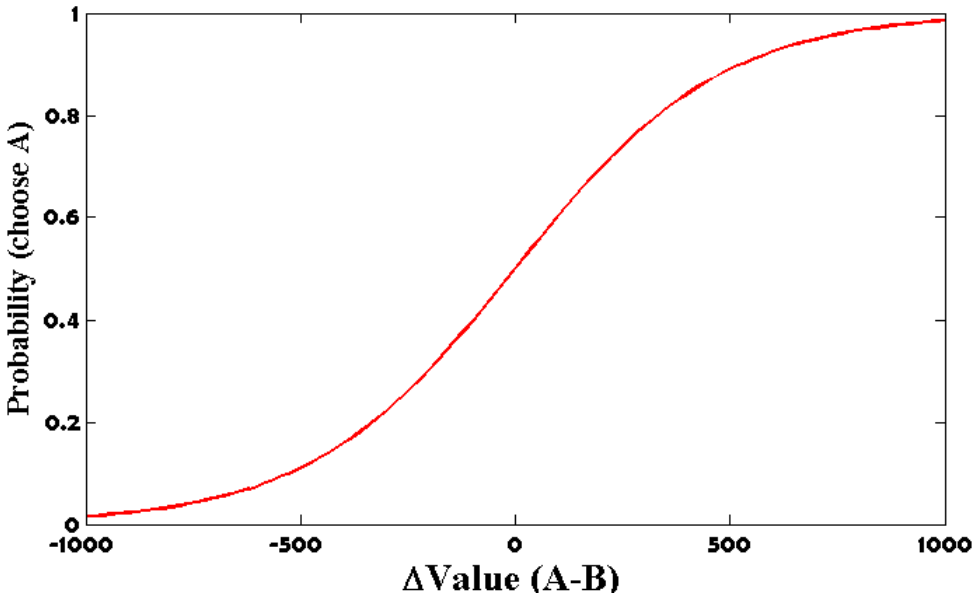

Figure 3.1 Logistic sigmoid. A logistic function, $1/1 + e^{-\beta\Delta V}$, transforms the value or utility of different options into a choice probability.

Thus when the values of options are far apart, the probability of choosing the higher valued option is close to certain, whereas when values are closely matched, choices are less predictable.

There are several advantages of modelling stochastic choice in such a way. Firstly, this captures behaviour better than a deterministic function. Secondly, this parallels implicit neural noise at various levels of the system (see **Chapter 2**). This noise can be envisaged as error at the valuation stage – this error distribution being either Gaussian or the more peaked double-exponential (Gumbell) form. These error distributions correspond to probit (cumulative normal) or logit responses at the choice level respectively. For multinomial choice, these can be extended to multinomial probit or logit (softmax) forms. Whilst in perceptual decision making, a probit response function is often used, for value-based decision making the logit function is more often employed (Sutton and Barto, 1998). This is both the tradition in reinforcement learning, but also serves the useful purpose of being better able to capture aberrant choices that deviate greatly from expected (the double-exponential distribution has fatter tails). A third advantage of modelling stochastic choice is that the resulting prediction is probabilistic (i.e. the probability or likelihood of choosing option A on each trial). This is very useful when using maximum likelihood (ML) techniques to estimate best-fitting parameters, as discussed below.

3.2.2.2 ***Model estimation and parameter inference***

There are two common ways of estimating best-fitting model parameters. These are broadly divided into classical and Bayesian approaches, or approaches that have minimal distributional assumptions (although not necessarily entirely non-parametric), and those that require a specification of a likelihood function.

3.2.2.2.1 LEAST SQUARES MINIMISATION AND RELATED APPROACHES

The first approach is least-squares minimisation (LSM). Widely used for linear regression, LSM minimises the squared-residual error between data and prediction. It is versatile and straightforward, and does not require *a priori* assumptions about the error distribution. Minimising the squared-error (rather than an alternative error term such as absolute error magnitude) means that an analytical solution can be derived (by calculus or matrix algebra). It can be used to summarise data (sum-of-squares error), and describe model fits (proportion of variance accounted for, r^2).

However, LSM does not necessarily yield unbiased or accurate estimates of best fitting parameters, and relies on assumptions of normality. Asymptotically, it can converge to the optimal solution but this is not generally true. LSM can be extended to multidimensional datasets, and knowledge about the precision of data points can be incorporated to improve fitted estimates, such as in robust or weighted LSM. It can be easily used to fit binary choice data without requiring a model of noise. It is also very valuable in cases where the underlying distribution is complex or unknown, or if sequential observations are not independent of one another. I use a closely related method (the method of simulated moments) in **Chapter 5** to fit multinomial choice data. I save a detailed exposition of the specific method for this chapter.

3.2.2.2.2 MAXIMUM LIKELIHOOD (ML) ESTIMATION

Maximum likelihood estimation (MLE), originally developed by Fisher (Aldrich, 1997), is one of the most standard approaches used in statistics. It is optimal in the asymptotic case with large samples, providing unbiased and efficient best-fitting parameter estimates. Parameters obtained by LSM approximate ML estimators and MLE is at the heart of inference, statistical testing, and model comparison. I use MLE extensively to fit models described in this thesis, in **Chapters 4, 6, 7, and 8**, and provide an overview of the method here.

To identify the specific parameter vector ϑ that is most likely to have generated the data sample in vector $\mathbf{y} = (y_1, y_2,\ldots,y_N)$ under the assumptions of model **M**, one needs to first mathematically formulate $f(\boldsymbol{y}|\boldsymbol{\theta}, \boldsymbol{M})$, the probability density function (pdf) specifying the chance of observing any **y** given ϑ and **M** (e.g. see **Figure 3.2**A). We discussed possible forms of these generative models of the data above and in the preceding chapter.

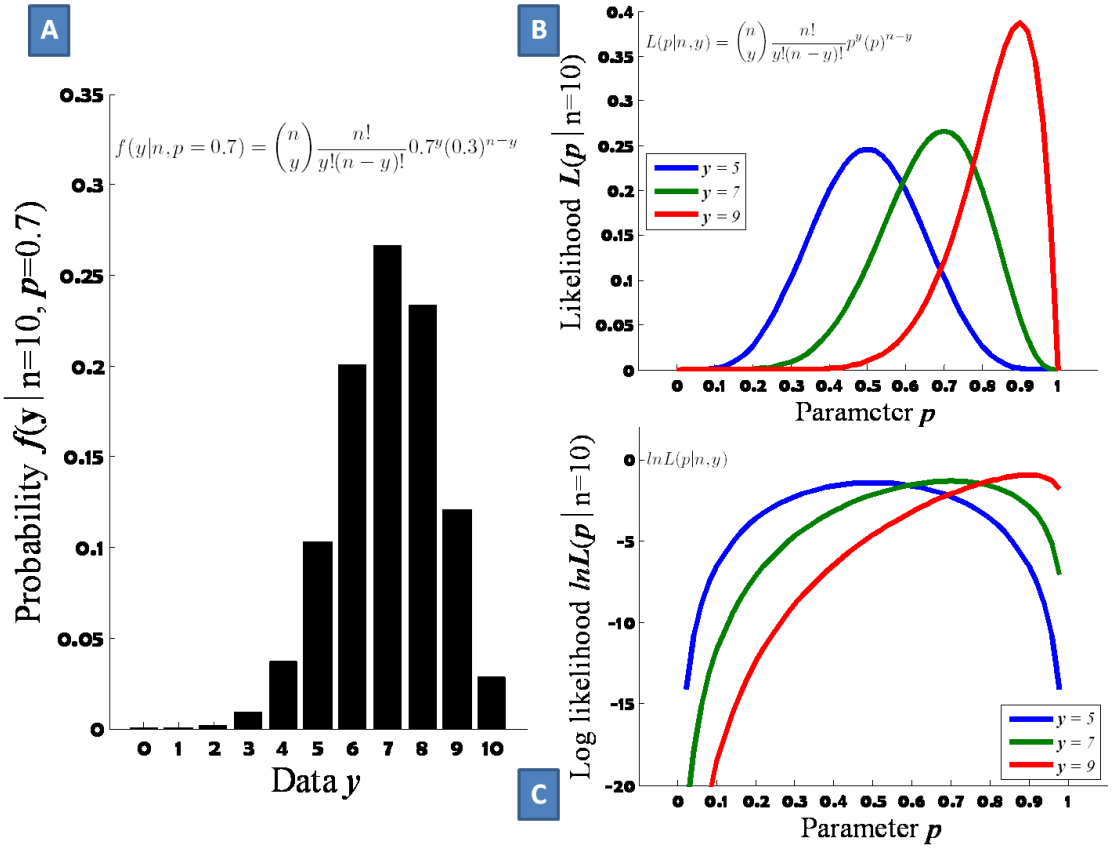

Figure 3.2 Illustration of probabilistic data from the binomial problem. The binomial distribution (A) describes the chance of y successes from n trials, with a success probability of p. B shows the likelihood distribution over p after observing 5, 7, or 9 successes. C shows the log-likelihood functions for the same y's. (Based on Myung, 2003).

The actual converse (inverse) problem to be solved is to calculate the likelihood of any ϑ given an observed set of data **y**, $L(\boldsymbol{\theta}|\boldsymbol{y}, \boldsymbol{M})$. Rather than a distribution over possible values of the data, L describes a distribution over possible values of the model parameters (e.g. see **Figure 3.2**B), hence the likelihood function has one dimension for each parameter. We can specify this likelihood on a point-by-point basis, since for any given observation y_1:

$$L(\boldsymbol{\theta}|\boldsymbol{y} = \boldsymbol{y}_1, \boldsymbol{M}) = f_1(\boldsymbol{y}_1|\boldsymbol{\theta}, \boldsymbol{M}) \qquad \textbf{(3.1)}$$

thus for binary choice data (i.e. $\mathbf{y}_i \in [0,1]$), with independent and identically distributed (i.i.d.) observations:

$$L(\boldsymbol{\theta}|\boldsymbol{y},\boldsymbol{M}) = \prod_{n=1}^{N} f_n(\boldsymbol{y_n}|\boldsymbol{\theta},\boldsymbol{M}) \quad \textbf{(3.2)}$$

$$\ln L(\boldsymbol{\theta}|\boldsymbol{y},\boldsymbol{M}) = \ln \prod_{n=1}^{N} f_n(\boldsymbol{y_n}|\boldsymbol{\theta},\boldsymbol{M}) = \sum_{n=1}^{N} \ln f_n(\boldsymbol{y_n}|\boldsymbol{\theta},\boldsymbol{M}) \quad \textbf{(3.3)}$$

thus:

$$\ln L(\boldsymbol{\theta}|\boldsymbol{y},\boldsymbol{M}) = \sum_{n=1}^{N} y_n \ln f_n(\boldsymbol{y_n} = 1|\boldsymbol{\theta},\boldsymbol{M}) + (1 - y_n) \ln f_n(\boldsymbol{y_n} = 0|\boldsymbol{\theta},\boldsymbol{M}) \quad \textbf{(3.4)}$$

As seen above, one usually maximises the log-likelihood (see **Figure 3.2C**), which is monotonically related to the likelihood, as it is computationally easier to deal with sums of log-probabilities than products of probabilities. While for some problems an analytical solution is possible (as it is for the illustrated binomial problem), for the complex non-linear models considered in this thesis we use numerical techniques. These come in a variety of forms, most commonly either gradient-ascent algorithms or, as we use here, non-linear optimisation which does not require derivatives to be taken and which can cope with step-changes in the likelihood surface.

Optimisation algorithms do not guarantee convergence to a global maximum; local maxima are often problematic. As there is no general solution to this, here I typically initialise the algorithm with a range of starting parameters, choosing the iteration with the highest likelihood value. At the maximum likelihood value, one can read out the maximum likelihood parameter estimates to make further inference.

3.2.2.3 ***Model comparison***

Alternative hypotheses about behaviour, and its underlying mechanisms, can thus be mathematically expressed as models. Model parameters can be optimised to best describe behaviour, but how can different hypotheses be compared? One can simply compare a set of models' maximum likelihood estimates or residual values, which will indicate which model best fits the current data. However, this does not take into account model parsimony or

complexity. An over-parameterised model will inevitably fit the data well but may be a poor out-of-sample predictor compared to a simpler model.

There are a number of ways of accounting for model complexity, including the Akaike and Bayesian information criteria (Akaike, 1974; Schwarz, 1978). These take into account model fit and model complexity (based on the number of parameters) to give a modified likelihood. I describe these further as they are used in subsequent chapters. They approximate the full Bayesian solution, which accounts for model complexity and the covariance between model parameters (in other words, one parameter may be more powerful in explaining the data than another, or parameters may not behave independently in likelihood-space).

These modified likelihood values can be compared to work out the best-fitting model. Fixed-effects analyses assume one best-fitting model for the population, which I implement here. An alternative random effects analysis allows for different best-fitting models across individuals.

3.3 FUNCTIONAL MAGNETIC RESONANCE IMAGING

3.3.1 INTRODUCTION

Functional magnetic resonance imaging (fMRI) is a powerful, non-invasive method that can be employed to indirectly measure neural activity during cognitive processing *in vivo* in the human brain. fMRI assays local cerebral blood flow changes over a timescale of seconds, made feasible by the rapid, spatially localised, neurovascular coupling between blood flow and regional neuronal activity. The precise mechanics governing the generation of fMRI signals is still being elucidated, and the potential applications continue to be extended (Logothetis, 2008). The undoubted power and replicability of fMRI has been underscored by its wide use in cognitive psychology and the consistency between fMRI findings and known neurophysiological ground truths from decades of research into cortical processes.

One of the main roles of fMRI has been to provide evidence of functional localisation of specific cognitive processes, although more recent uses have included the modelling of interacting networks of regions (functional integration – e.g. see Penny, Stephan et al (2004a)). Below, I discuss first the theoretical basis for MRI, before describing the specifics of fMRI data acquisition, processing and statistical analysis.

3.3.2 PRINCIPLES OF MRI

3.3.2.1 *Nuclear magnetic resonance and relaxation*

Nuclear magnetic resonance (NMR) is a property of atomic nuclei, induced in the presence of a magnetic field. Nucleons (protons and neutrons) possess a quantum attribute called 'spin', and atomic nuclei with unpaired nucleons have a non-zero net spin and consequently can act as magnetic dipoles. In particular, the hydrogen nucleus contains a single proton and is the most abundant element in living organisms, thus measuring the magnetic properties of compartmentalised hydrogen nuclei provides a means for anatomical topological mapping according to the specific make-up (i.e. the density of mobile hydrogen nuclei – *proton density*) of biological tissues.

In the presence of a static magnetic field, $\mathbf{B_0}$, proton dipoles align in either a parallel or antiparallel configuration. A fractional excess of protons in the lower energy parallel configuration (about 1 in 100000 for 1.5T), imposes a bulk magnetic moment, $\mathbf{M_0}$, on the sample. These dipoles also precess around the external field's axis (**Figure 3.3**) at a specific angular frequency ($\boldsymbol{\omega}$), given by the Larmor relationship:

$$\boldsymbol{\omega} = -\boldsymbol{\gamma}\mathrm{B} \qquad \textbf{(3.5)}$$

γ is the isotope-specific gyromagnetic ratio and **B** is the magnetic field strength in Tesla (T). This is also the proton's resonant frequency, with energetic absorption (**E**) given by Planck's equation, $\boldsymbol{E} = h\boldsymbol{\omega}/2\pi$, where h is Planck's constant (6.626×10^{-34} Js).

Applying a radiofrequency (RF) pulse perpendicular to $\mathbf{B_0}$ produces an oscillatory field $\mathbf{B_1}$, causing resonant absorption of energy in protons with matching Larmor frequencies.

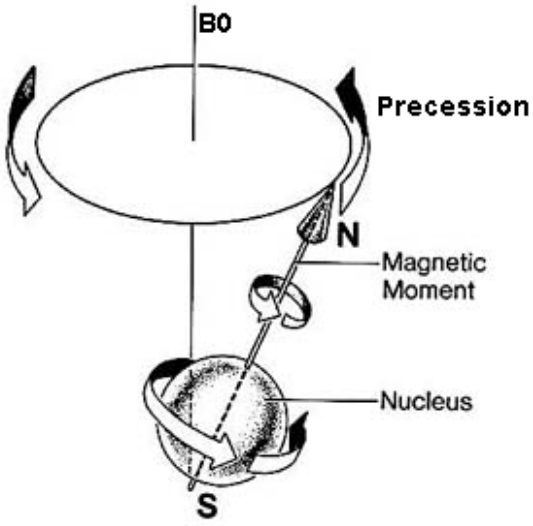

Figure 3.3 Precession of a nuclear magnetic dipole around an external B0 field.

Subsequent spin-state transitions from low to high energy levels synchronises precession (*phase coherence*) and creates a bulk rotating transverse magnetization moment ($\mathbf{M_{xy}}$), perpendicular to $\mathbf{B_0}$. Concurrently, the longitudinal magnetization moment ($\mathbf{M_z}$) is reduced as more protons align in an antiparallel (higher energy) configuration. This tilts the net magnetization vector from alignment with the $\mathbf{B_0}$ z-axis into the transverse xy plane. The degree of tilt is called the flip angle, and an RF pulse sufficient in amplitude and duration can flip the magnetization vector sideways (a 90° flip angle) or into reverse (a 180° flip angle).

On cessation of the RF pulse, as the nuclei gradual return to equilibrium (*relaxation*) and precession continues in the transverse plane, energy is emitted as an oscillating electromagnetic field, which can induce current flow in a receiver RF coil. Detecting this current flow forms the basis for MRI signal acquisition (Bloch et al., 1946). Relaxation occurs in two ways – longitudinal (T1) and transverse (T2) relaxation.

3.3.2.1.1 T1 RELAXATION

T1 relaxation refers to the reestablishment of $\mathbf{M_z}$ as protons release energy and their spins regain equilibrium along $\mathbf{B_0}$. T1 is the time constant of the longitudinal relaxation rate (**Figure 3.4**):

$$\boldsymbol{M_{z(t)} = M_{(0)}\left(1 - e^{-t/T1}\right)} \qquad \textbf{(3.6)}$$

T1 is governed by intrinsic material properties, and differences in T1 constants between tissue types can be utilised to provide contrast in T1-weighted imaging.

3.3.2.1.2 T2 AND T2 RELAXATION*

T2 relaxation refers to the gradual loss of phase coherence with and decay of $\mathbf{M_{xy}}$. This decay is determined by two phenomena. Quantum spin-spin interactions induce random field variations between protons desynchronising the precession phase. This rate of transverse magnetisation decay is described by the time constant T2:

$$\boldsymbol{M_{xy(t)} = M_{xy(0)}e^{-t/T2}} \qquad \textbf{(3.7)}$$

Further, local external field inhomogeneities cause an increased rate of phase decoherence (a predominant effect). This more rapid loss of transverse magnetization is governed by the time constant T2*, where:

$$\frac{1}{T2^*} = \frac{1}{T2} + \frac{1}{T2^{inh}} \qquad \textbf{(3.8)}$$

$1/T_{inh}$ is the relaxation rate due to the magnetic field inhomogeneities.

A damped oscillatory RF signal measured immediately after the RF pulse is switched off (*free induction decay*) results from T2* effects (**Figure 3.4**):

$$\boldsymbol{M_{xy(t)} = M_{xy(0)}e^{-t/T2^*}cos(\omega t)} \qquad \textbf{(3.9)}$$

Fluid has a long T1 and T2, in contrast to the shorter T1 and T2 from tissues with cellular structure. This is mainly dictated by proton binding, as mobile protons in fluid retain energy for a longer duration.

3.3.2.2 *Image contrast*

Image contrast between different tissue types is generated by measuring the decaying signal following an RF pulse at a specific time. Tissue differences in T1, T2 and T2* are reflected in different signal constitutions from different tissues at a given time-point (because of these varying rates of decay).

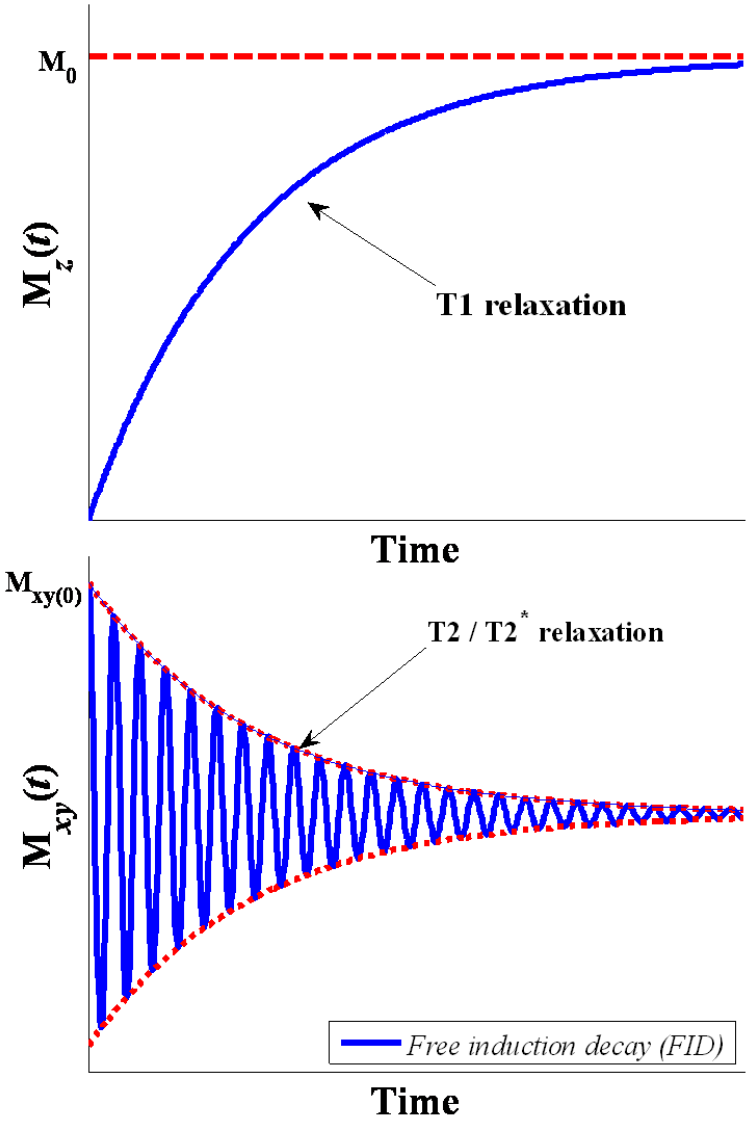

Figure 3.4 Relaxation processes. T1, T2, and T2* are the time constants of the exponential changes in magnetization over time following and RF pulse. The T2* constant dictates the envelope of free induction decay (FID).

A train of RF pulses is sent during image acquisition. The time interval between each pulse is the TR (*repetition time*). For a gradient echo (GE) scan, the MR signal is collected a short time following each 90° RF pulse at the TE (*echo time*). The image signal intensity (S) thus depends upon the TR, TE and the number of proton spins within the tissue sample:

$$S \propto \rho \left(1 - e^{-TR/T1}\right) e^{-TE/T2^*} \qquad \textbf{(3.10)}$$

where ρ is the proton spin density.

Spin echo (SE) sequences include an additional 180° pulse to remove local field inhomogeneity effects (therefore isolating the T2 contribution).

Thus at a specific TR, different tissue types will generate different signal intensities (**Figure 3.5**).

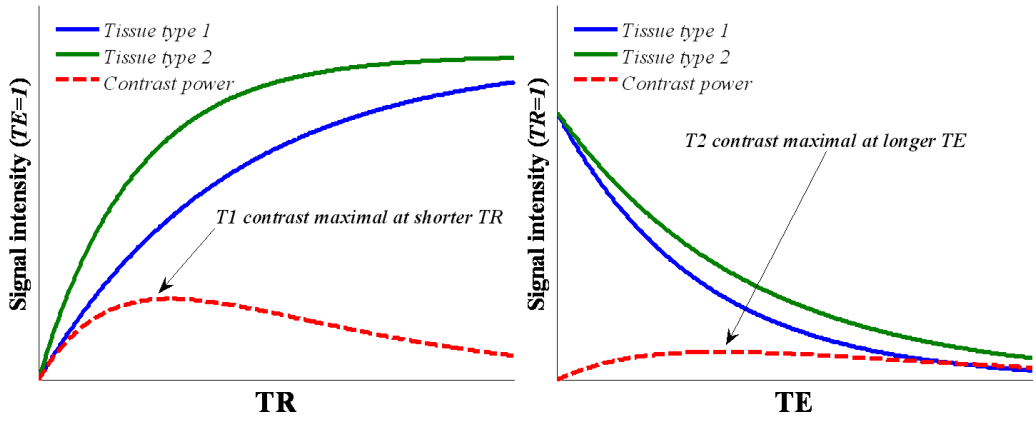

Figure 3.5 Contrast power for T1 and T2. Contrast power is dictated by the difference in signal intensity over time for T1 and T2 relaxation processes. T1 is enhanced by a shorter TR, T2 enhanced by a longer TE.

A short TR and TE enhances T1 contrast, while a long TR and TE enhances contrasts dependent on T2 (SE sequences) or T2* (GE sequences). A long TR/short TE isolates the proton spin-dependent signal (*proton density weighting*).

3.3.3 CONSTRUCTING AN MR IMAGE

3.3.3.1 *Spatial encoding*

To construct an MR image from these received RF signals, the MR signal needs to be imbued with spatial information (*spatial encoding*). This utilises a 3D array of external magnets to generate fields (*gradient fields*) in the z (slice-selective), y (read-out or frequency encoding) and x (phase encoding) directions (Lauterbur, 1973), which are switched on with each RF pulse. The strength of these gradient fields vary in a linear manner across the volume of interest, thus entraining linear variation in (hydrogen nucleus) proton spin-precessions across the volume, according to the Lamor relationship (3.5). A narrow-bandwidth RF pulse will therefore excite corresponding protons precessing at a specific spatial location. Spatial resolution (*slice thickness*) is determined by the RF pulse bandwidth and slice-selective gradient strength.

While the slice-selective gradient is applied simultaneous with each RF pulse, the frequency-encoding gradient is applied during signal measurement, and the phase-encoding gradient applied between RF pulse onset and measurement. The phase-encoding gradient shifts the phase of photon precession, and both frequency and phase information can be recovered from the emitted signal by Fourier transform to specify the position in the transverse plane. Phase and frequency encoding can be repeated multiple times during each TR interval to collect data from each xy location (‘*k space’,* or the frequency-phase map), for a slice at a specific z location. A 3D array of gradient fields thus allows a partitioning of a volume of interest into cubed elements (*voxels*).

3.3.3.2 *Echo-planar imaging*

Conventional MRI records one phase-encoded line of k space for each TR. Echo-planar imaging (EPI) (Mansfield, 1977) affords faster data acquisition, as an entire image volume is acquired following a single RF excitation pulse by collecting the complete k-space dataset within the short time that free induction decay is detectable. A series of refocusing ‘echoes’ are produced by gradient reversals (i.e. 180° RF pulses in the phase and frequency gradient coils) which resynchronise proton precession and allow collection of further signal. These echoes can be adapted to give T2 or T2* contrast, and rapidly changing the frequency y-gradients allows the sampling of a trajectory through k-space.

EPI allows for sampling of an entire volume of interest at sub-centimetre spatial resolution in a rapid timescale (Stehling et al., 1991) commensurate with cognitive processes (typically 2-4s TR). Fast acquisition is also desirable because the BOLD effect may be confounded by signal instabilities originating from cardiac and respiratory cycles or head motion.

The rapid signal changes in gradient coils are the main technical limitation to EPI, and also can cause side effects at high field strengths, such as the generation of eddy currents in neural tissue which can lead to peripheral nerve stimulation. In addition, artefacts can occur due to magnetic field inhomogeneities or induced eddy currents. These are particularly evident in the phase-encoding direction (*Nyquist ghosts*), which can be minimised by various correction techniques (Bruder et al., 1992; Buonocore and Gao, 1997). Susceptibility artefacts can also occur, especially at air-bone interfaces, which can cause distortions or signal dropout. This can be a particular issue for collection of data from neural tissue abutting, or in the same slice as the sinuses (such as the orbitofrontal cortex), which can be ameliorated by tilting the direction of the transverse plane during acquisition (Deichmann et al., 2003).

3.3.3.3 ***Image optimization***

Image quality is determined by the signal-to-noise ratio (SNR), given by:

$$SNR = \frac{FOV_x \cdot FOV_y \cdot \Delta z}{N_x} \sqrt{\frac{NEX}{N_y \cdot BW}} \qquad \textbf{(3.11)}$$

where FOV_x and FOV_y are the fields of view in the x and y axis respectively, Δz is slice thickness, N_x and N_y are the x and y dimensions of each voxel, NEX is the number of phase encoding excitations (i.e. number of samples per TR over which to average), and BW is the receiving bandwidth. Thus, SNR can be improved by reducing the slice thickness, a tighter voxel sampling or sharper receiving bandwidth, or averaging over repeated measurements.

3.3.4 FUNCTIONAL MRI

Neuronal activation is tightly coupled to local cerebral haemodynamics. 90% of the brain's energy supply arises from the aerobic metabolism of glucose, which consumes 20% of bodily oxygen intake (Siesjo, 1978). Brain activity, coupled to glucose metabolism (Sokoloff, 1977), is proportional to the oxygen consumption rate ($CMRO_2$), and in turn closely related to cerebral blood flow (CBF). MRI can be adapted to detect magnetic field changes induced by the differing paramagnetic properties of oxygenated and deoxygenated haemoglobin, described as the blood oxygenation level dependent (BOLD) signal.

3.3.4.1 *The Blood oxygen level-dependent (BOLD) signal*

Increases in neural activity results in an initial increase in oxygen consumption due to increased metabolic demand. This increases the local intravascular deoxyhaemoglobin to oxyhaemoglobin concentration ratio (Vanzetta et al., 2005). Local CBF increases after a few seconds, with a proportionate rise in glucose consumption. This leads to a relative oversupply of oxyhaemoglobin delivery (Fox and Raichle, 1986), also the increased CBF causes local venodilatation and an increase in blood volume (CBV) (Buxton et al., 1998). fMRI is sensitised to detect these BOLD signal changes.

3.3.4.1.1 OXYGEN LIMITATION EFFECTS

Measured brain oxygen consumption depends on blood flow and the oxygen concentration gradient, which by Fick's principle gives:

$$CMRO_2 = CBF \cdot 4[Hb] \cdot (Y_a - Y_v) \qquad \textbf{(3.12)}$$

$[Hb]$ is the total haemoglobin concentration; Y_a and Y_v are arterial and venous oxygen saturations ($Y_a - Y_v \propto OEF$, where OEF is the oxygen extraction fraction).

Large shifts in CBF are in fact accompanied by only modest changes in $CMRO_2$, originally thought to indicate significant anaerobic glucose metabolism in the brain (Fellows et al., 1993). The subsequent oxygen limitation model (Buxton and Frank, 1997) attributed this mismatch to

inefficient capillary oxygen extraction at high blood flow rates (i.e. $\Delta OEF \neq \Delta CMRO_2$). This explains the increase in CBF during neuronal activation, concurrent decrease in oxygen extraction (Hoge et al., 1999), therefore overall increase in blood venous oxygenation (arterial oxygenation remains constant) which can be detected in the BOLD signal.

3.3.4.1.2 MRI CHARACTERISTICS

Deoxyhaemoglobin is paramagnetic due to unbound iron-containing haem groups, as opposed to isomagnetic oxyhaemoglobin (Pauling and Coryell, 1936), therefore induces magnetic susceptibility differences between venous blood and surrounding tissue, leading to small magnetic field distortions. These distortions alter T2 and T2* relaxation of mobile water-bound protons, reducing the equivalent MR signal (Thulborn et al., 1982). Critically, this can be measured as BOLD contrast in gradient echo EPI sequences, initially demonstrated in animals (Ogawa et al., 1990), and subsequently shown in humans (Bandettini et al., 1992; Ogawa et al., 1992). There are both intra- and extravascular contributions to the BOLD signal, with approximately 60% of the BOLD signal arising from the intravascular space at 1.5 Tesla (T) field strengths (Boxerman et al., 1995).

Increased metabolic demand following neuronal activation changes blood oxygenation in a characteristic manner (the *haemodynamic response function* (HRF)) (Heeger and Ress, 2002; Buxton et al., 2004).

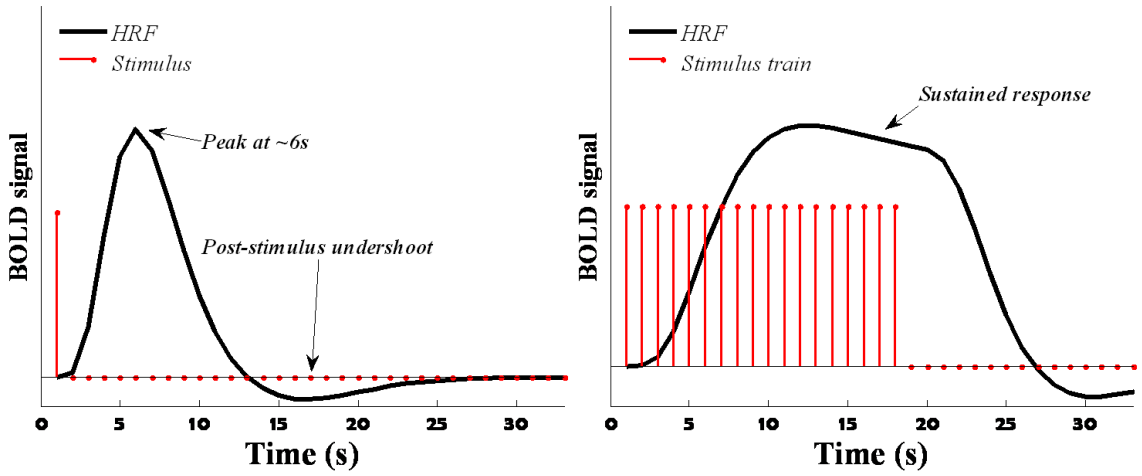

Figure 3.6 The haemodynamic response function. On left: plot of the HRF (modelled as the sum of 2 gamma functions) following a single stimulus (modelled as delta function), as instituted in SPM. The peak is at 6s post stimulus and there is a post-stimulus undershoot. On right: response to a train of stimuli or boxcar of 18s modelled as the convolution of the HRF with the stimulus function, leading to a sustained response.

Classically, neuronal activity leads initially a transient dip in the HRF, attributed to an increase in deoxyhaemoglobin, before a rise in CBF, decrease in deoxy- to oxyhaemoglobin ratio, and an increase in the BOLD signal, which peaks approximately 6 seconds following activity onset. There is usually a post-stimulus undershoot lasting several more seconds, suggested to be due to a transient mismatch in CBF and CBV due to elasticity of the venous compartment (Buxton et al., 1998). The magnitude of the BOLD response corresponds to a 1-3% signal change in occipital cortex following visual stimulation, and the HRF temporal kernel dictates the temporal resolution of fMRI.

3.3.4.1.3 NEUROPHYSIOLOGY

The BOLD signal is thought to be linearly proportional to summed average local neuronal activity over time (Boynton et al., 1996; Buckner, 1998; Heeger et al., 2000). Assuming temporal summation means that predicted haemodynamic responses can be modelled by a linear convolution of stimulus input with the HRF kernel (**Figure 3.6**). At very short inter-stimulus intervals, this assumption can break down (Friston et al., 1998a; Birn et al., 2001), due to saturation in the neuronal or haemodynamic response.

Simultaneous microelectrode intracortical recordings of neural and fMRI signals following visual stimulation in monkeys has delineated the relative contribution of local field potentials (LFPs, correlated with input synaptic activity) and multi-unit activity (MUA, correlated with output spiking) to the BOLD response (Logothetis et al., 2001).

While both have influence, the MUA-attributed signal is transient as opposed to sustained LFPs, suggesting that the fMRI-detectable signal reflects input, rather than efferent spiking output, from a region (Logothetis, 2008). While MUA and LFPs are often coupled, under certain conditions this is not the case – for example synchronised subthreshold synaptic activity may cause a haemodynamic response without neuronal efferent spiking enhancement (Mathiesen et al., 1998). Moreover, additional effects such as neuronal response noise (asynchronous activity) may influence metabolic demand and also contribute to the measured signal (Heeger and Ress, 2002). It is also unclear how BOLD relates to the differences between input inhibitory versus excitatory modulation, nor is there consensus as to how signal decrements below baseline should be interpreted (Harel et al., 2002; Shmuel et al., 2006; Schridde et al., 2008).

Figure 3.7 Correlation of BOLD signal with LFPs and MUA. A. Mean LFP (red), MUA (black) and total (green) neural response (averaged across all frequencies), and BOLD signal (blue). There is significantly higher LFP activation for both the transient and the sustained portion of the response, suggesting that this is the main contributor to the BOLD signal. Error bars show 1 s.d. B. Distribution of r2 values for LFP-BOLD and MUA-BOLD correlation. Values were significantly higher for LFP than MUA, again suggesting that LFPs are the principal determinant of the BOLD response. Note that the relationship is frequency dependent, with high frequency signals above ~16Hz showing a strong positive correlation with BOLD (r2>0.5), but low frequency signals being uncorrelated or negatively correlated. (Adapted from Logothetis et al., 2001).

3.3.4.1.4 BOLD SENSITIVITY

The sensitivity of the BOLD signal is determined by the relative T2*-dependent signal values from active and resting conditions, measured at a specific TE. Optimal BOLD contrast occurs when TE ≈ baseline T2*.

BOLD sensitivity is also affected by voxel size, the TR, and the static field strength $\mathbf{B_0}$. Larger voxels will increase signal-to-noise but also reduce T2* differences. Short TRs increase the sampling rate and resolution of the HRF, but increase flow-dependent artefacts (although this can be counteracted to an extent (Duyn et al., 1994; Glover et al., 1996). Greater $\mathbf{B_0}$ increases signal-to-noise and shortens the optimal sampling time, but also causes more susceptibility-induced artefacts.

3.3.4.2 ***FMRI acquisition***

3.3.4.2.1 EXPERIMENTAL DESIGN

FMRI utilises the relatively high temporal and spatial resolution of EPI to delineate changes in brain activity in response to cognitive tasks or conditions. Multiple designs can be employed to analyse the statistical contribution of one or many experimentally controlled factors (and their interactions) to regional neural activation, with factorial and parametric (regression) designs commonplace. Early fMRI designs were epoched, or divided into separate blocks of stimulation, with an optimal epoch interval at approximately 16s to match the temporal profile of the HRF and minimise the effect of noise (by the matched filter theorem) (Friston, 2004).

The advent of rapid event-related designs (Burock et al., 1998) has allowed the delineation of trial-by-trial changes in brain activation. This has considerable advantages for complex cognitive paradigms, as trial order can be randomised and individual trials can be parameterised, meaning that the internal components of computational decision models can be tested against neural data, as is the case in the studies presented in this thesis. Typical classifications such as categorical or parametric (pertaining to levels of a specific factor or a sample level drawn from a continuous distribution) can be subsumed by the all-purpose general linear model (GLM), discussed below.

3.3.4.2.2 DESIGN EFFICIENCY

BOLD detection power and estimation efficiency depends upon the interstimulus interval (*stimulus onset asynchrony* – SOA) distribution. While event-related designs have improved power to characterise the HRF (*estimation efficiency*), they have a reduced ability to detect activation in comparison with epoched designs. Efficiency and detection power can be maximised by matching the sampling of experimental factors (Birn et al., 2002) and sampling the HRF in a distributed manner (*jittering*) by ensuring that the SOA is not an integer multiple of the TR (Henson, 2007). Selecting an appropriate distribution for stimulus onsets also increases power, as event-related designs that mimic epochs with clustered presentations of stimulus levels are more optimal.

3.3.5 DATA ANALYSIS

3.3.5.1 *Introduction*

The statistical analysis techniques used for neuroimaging in this thesis are instantiated with Statistical Parametric Mapping (SPM) software (versions SPM5 and SPM8, Wellcome Trust Centre for Neuroimaging, London, www.fil.ion.ucl.ac.uk/spm) . This uses a mass univariate approach to model activity on a voxel-by-voxel basis, as a linear combination of experimental variables in a GLM (Friston et al., 1995a).

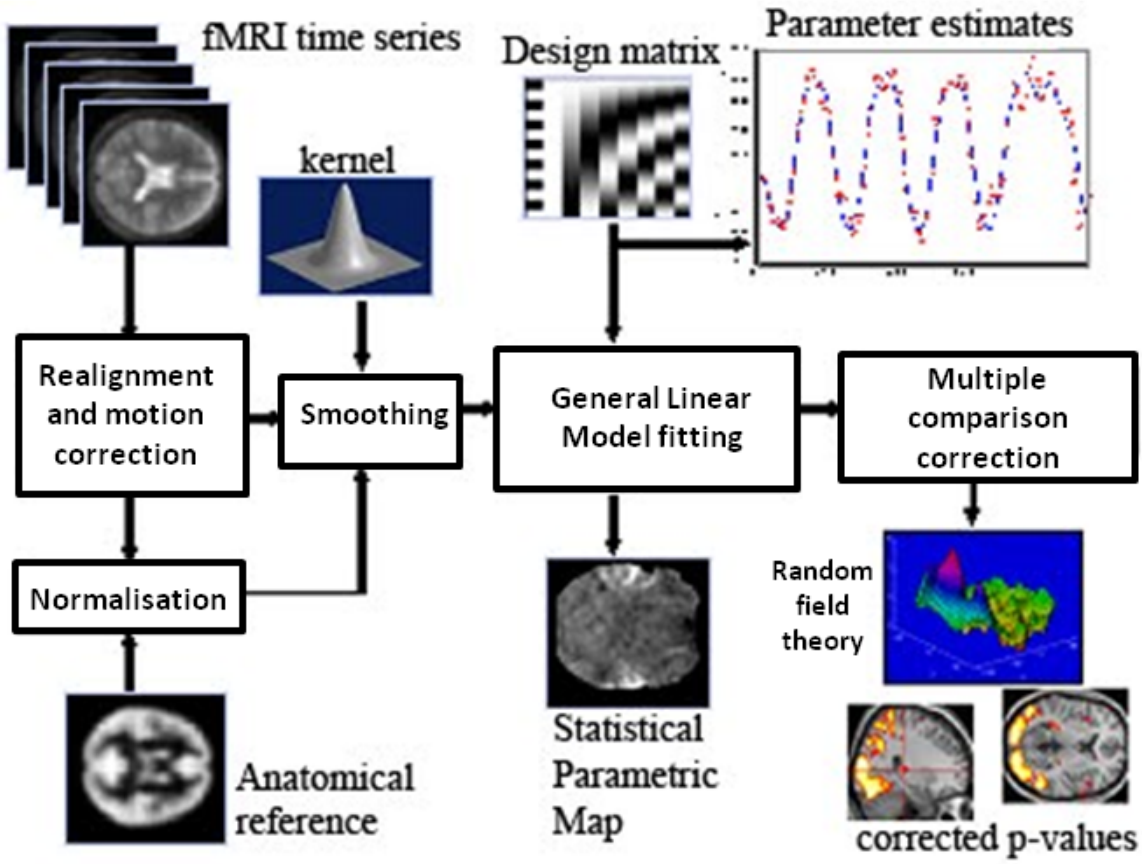

Figure 3.8 Processing pathway in SPM. Box diagram of the sequential steps involved in processing and analysing voxel-based neuroimaging data.

Initially, data is preprocessed, both to filter noise and critically to place all data into the same standardized anatomical format for subsequent statistical model estimation and inference.

3.3.5.2 ***Spatial preprocessing***

fMRI images initially require a series of spatial preprocessing steps to render them suitable for statistical analysis. This processing pathway is illustrated below, and we describe each step therein. In addition, the first few acquired volumes in a data series (*dummy volumes*) are discarded to allow time for scanner T1-equilibration effects.

3.3.5.2.1 REALIGNMENT AND UNWARPING

Unavoidable head motion during image acquisition causes anatomical misalignment, which can be rectified by realigning the image time series using a 6-parameter rigid-body transformation to translate and rotate all images into the same orientation and position as the first image in the series. Additional movement-dependent noise arising from movements during the acquisition of a single volume (Grootoonk et al., 2000), and movement-by-inhomogenetity interactions arise due to tiny non-uniformities in $\mathbf{B_0}$ causing location-dependent changes in the BOLD signal.

There are two common ways of dealing with this residual unwanted variance, both employed in the studies in this thesis. One can include the estimated movement parameters in the GLM design matrix as covariates of no-interest. Unwarping (Hutton et al., 2002) is a model-based method, where additional fieldmap images of the magnetic field and inhomogeneities are collected, and subsequently used to predict movement-by-inhomogeneity interactions which can be inverted to recover the original anatomy.

3.3.5.2.2 NORMALISATION AND CO-REGISTRATION

Standardisation of statistical results and anatomical inferences between subjects and across studies requires the mapping of all acquired MR images to a universal anatomical template reference. Initially EPI functional images are co-registered with the T1-weighted structural image, by minimising the between-image statistical divergence (mutual information). This includes both a linear and non-linear transformation (Friston et al., 1995b). Voxels are then segregated (*segmented*) into grey and white matter maps using non-linear deformation fields to map voxels onto template tissue probability maps (Klein et al., 2009). Subsequently, normalisation matches these images to a standard template to ensure spatial homology.

Studies in this thesis use the Montreal Neurological Institute template (Collins et al., 1995), as instituted in SPM.

3.3.5.2.3 SMOOTHING

A smoothing filter is then applied to data, which improves the signal-to-noise ratio and ensures that the error terms meet necessary statistical normality assumptions for subsequent inference using random field theory. A Gaussian convolution kernel is used in SPM, measuring approximately 2-3 times the voxel size (i.e. 6-8 mm) at full-width half-maximum (FWHM). Smoothing also ensures spatial averaging, which also compensates for minor interindividual differences in functional anatomy.

3.3.5.3 ***Statistical modelling***

3.3.5.3.1 THE GENERAL LINEAR MODEL

A GLM is a statistical model where a data matrix **Y** is estimated as a linear mixture of predictors (*explanatory variables*) in a *design matrix* **X**, and a residual error matrix **ε**, where errors are assumed to be independent and identically distributed (i.e. multivariate normally distributed, or *spherical*):

$$\boldsymbol{Y} = \boldsymbol{X}\beta + \varepsilon \qquad \textbf{(3.13)}$$

β is a vector of parameter estimates which specifies the best-fitting linear mixture of columns (*regressors*) in **X**, given by:

$$\hat{\beta} = ((\boldsymbol{X}^T\boldsymbol{X})^{-1}\boldsymbol{X}^T)\boldsymbol{Y} \qquad \textbf{(3.14)}$$

These parameter estimates are estimated in practice in SPM using restricted maximum likelihood (*ReML*).

The GLM approach subsumes many common statistical models, such as multiple regression, t- and F-tests, analysis of variance (ANOVA) and covariance (ANCOVA), and multivariate analysis of variance (MANOVA) and covariance (MANCOVA), all of which are special instances of a GLM. The GLM can also be expanded to deal with non-linear couplings between **Y** and **X** (generalised linear models) (Nelder and Wedderburn, 1972). In this thesis, we use

the mass univariate approach where **Y** is one column corresponding to a individual voxel's timeseries, and **X** models the experimentally imposed conditions as well as measured covariates of interest and confounds (e.g. movement regressors).

There are several issues specific to modelling of fMRI data that need to be accounted for in constructing the statistical model. Low-frequency noise can derive both from the MRI instrumentation, scanner drift and other sources such as head motion, cardiorespiratory effects and global fluctuations in the BOLD signal. These can also be accounted for by introducing low-frequency drift terms into the design matrix. In addition, the assumption of sphericity is usually violated, as error terms are non-independent (temporally autocorrelated) (Woolrich et al., 2001). A pre-whitening correction is performed in SPM, where the temporal autocorrelation structure of the data is first estimated, before being filtered from the data and model to render the residuals uncorrelated.

The effects of interest (i.e. an experimentally controlled sequence of events) in the design matrix **X** pertain to predicted neural activity (e.g. transient increases in neuronal activity for specific conditions), which needs to be convolved with a model of the HRF to form predictions about the BOLD signal in **Y** (e.g. see **Figure 3.6**).

3.3.5.3.2 INFERENCE

3.3.5.3.2.1 Contrasts

Inference is made on parameter estimates by calculating the significance of the effect sizes β. Parameter estimates can be utilised in various ways. Differences in parameter estimates can describe the difference in the effect of experimentally controlled categorical conditions on neural activation in a voxel. A linear combination of parameter estimates can describe a functional (e.g. linear or quadratic) relationship between levels of a categorical variable and the data. Alternatively, if a specific column of **X** (e.g. $\mathbf{X_1}$) corresponds to a parametric regressor, then the corresponding parameter estimate β_1 pertains to the slope of the linear relationship between the predictor $\mathbf{X_1}$ and the data at that voxel **Y** (i.e. a linear regression). Combinations of parameter estimates are termed *contrasts*, with the simplest contrast vector testing only one explanatory variable (one column in **X**). **X** includes a constant column (i.e. the intercept), which models an implicit baseline (the mean BOLD signal).

The (one-tailed) significance of a contrast can be calculated from the t-statistic:

$$T = \frac{c'\hat{\beta}}{\sqrt{Var(c'\hat{\beta})}} \quad \textbf{(3.15)}$$

where c' is the contrast vector, and the denominator is the standard error.

Combinations of contrasts can also be specified as a matrix of contrast weights (an F-test), for example if one wanted to infer the significance of a one-way ANOVA model with 3 levels, where one simultaneously asks if *any* of the levels 1, 2 or 3 of the experimental factor correlate with changes in the data.

3.3.5.3.2.2 Hypothesis testing and multiple comparisons

A statistical parametric map comprises many thousands of individual tests, of which some would be expected to be significant by chance. This expected false-positive error rate can be a-priori specified as a statistical threshold (e.g. a p=0.05 significance level sets a 5% error rate per test). To appropriately control for error across the entire family of tests performed, a family-wise error (FWE) correction can be used, for example the Bonferroni correction which modifies the threshold (α) to achieve a desired false-positive rate (p_{FWE}) according to the number of statistical tests (n) performed:

$$p_{FWE} = 1 - (1 - \alpha)^n \approx n\alpha \quad \textbf{(3.16)}$$

$$\alpha = \frac{p_{FWE}}{n} \quad \textbf{(3.17)}$$

This is a conservative estimation which excessively penalises spatially correlated neuroimaging data, where neighbouring voxels are more likely than chance to yield the same statistical result (because of intrinsic functional topography as well as the smoothing step). To increase power, an a priori region of interest (ROI) can be specified (which limits the number of voxels under active consideration, therefore the severity of the FWE correction). Alternatively, an independent contrast can validly be used to highlight regions recruited in a task for subsequent use as an ROI (although one must be careful to avoid ascribing erroneously high significance to a pre-identified identified voxel with repeated statistical testing (Poldrack and Mumford, 2009; Vul et al., 2009).

Gaussian random field theory (Siegmund and Worsley, 1995; Worsley et al., 1996) can be used instead of Bonferroni correction to obtain a more appropriate correction. This

calculates the number of independent observations, or resolution elements (*resels*) in a volume, according to the statistical smoothness of the SPM, and then determines the expected number of clusters of activation above a given threshold (*Euler characteristic*). This determines the appropriate correction to produce a given FWE-corrected rate, but assumes that the residuals are distributed in accordance with a Gaussian random field (hence a smoothing step is statistically required).

Inference can be made either at the most spatially precise voxel-level (i.e. is there a significant effect at a specific voxel?), or alternatively at the cluster level (i.e. is the number of activated voxels in a particular contiguous cluster greater than would be expected by chance?). Cluster-level inference is often appropriate for spatially extended activations that one desires to localise to an anatomical region (rather than a specific x,y,z coordinate), but also requires the specification of a cluster-defining threshold (i.e. at the voxel level to isolate islands of supra-threshold activity). In practice, the underlying statistical assumptions are valid to at least a cluster-defining threshold of $p \approx 0.05$ (Friston et al., 1996), which is employed in this thesis.

3.3.5.3.2.3 Group inference

For inference at the between-subject (2nd) level, a hierarchical procedure is used where within-subject (1st level) contrast estimates are used as a response variable **Y** in a further 2nd level GLM analysis (Penny et al., 2003). Assuming that 1st level parameter estimates are drawn from a normal distribution in the population, this hierarchical method constitutes a random effects analysis accounting for between-subject variability. A full mixed effects analysis would simultaneously account for within- and between-subject variance, however in practice if individual subjects' design matrices are similar, the variances of subjects' estimates will also be similar, and a hierarchical random-effects approach closely approximates this full approach.

3.4 MAGNETOENCEPHALOGRAPHY

3.4.1 INTRODUCTION

Magnetoencephalography (MEG) is a neuroimaging technique that employs very sensitive magnetic flux detectors to measure the magnetic fields produced by changing electrical

activity in the brain (Cohen, 1968). The principle advantage of electrophysiological methods over fMRI in studying brain function is the very high temporal resolution afforded, at a millisecond timescale commensurate with synaptic processes (**Figure 3.9**).

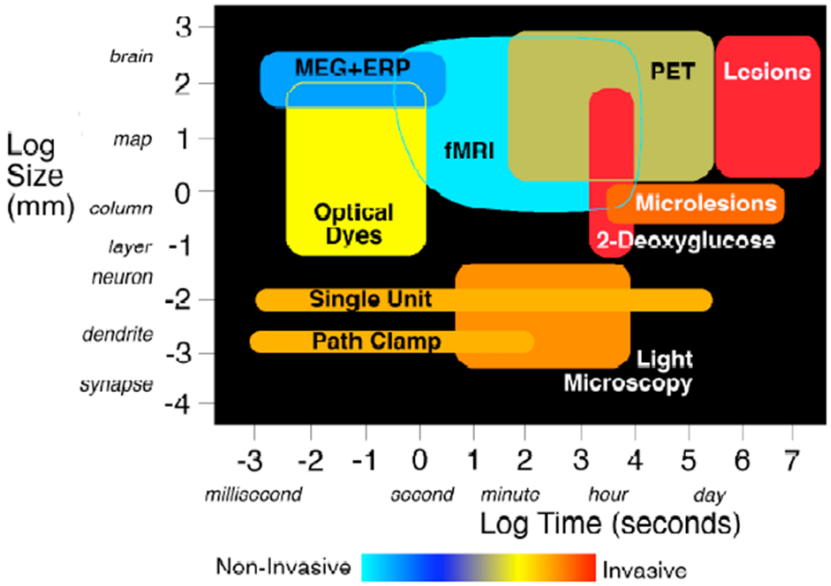

Figure 3.9. Illustration of the spatio-temporal resolution and invasiveness of different neuro-investigative methods. Adapted from (Churchland and Sejnowski, 1992) MEG=magneto-encephalography; ERP=evoked response potentials; fMRI=functional magnetic resonance imaging; PET=positron emission tomography.

The principles of MEG are founded on those developed for electroencephalography (EEG) analysis, a technique used for many decades (Shipton, 1975), which measures electrical activity recorded from scalp sensors. The prime advantage of MEG over EEG is that electrical fields can be heavily distorted by changes in conductance between brain, dura, skull and scalp, while magnetic fields are influenced much less. This renders it possible to accurately localise (with certain restrictions) intracortical activity with relatively high fidelity. Thus inferences can be made about the generators of neural activity rather than consequent field changes at the scalp. MEG is most sensitive to tangential currents in cortical generators with limited ability to delineate subcortical activity, however especially when used in conjunction with anatomical prior knowledge from fMRI, is an extremely powerful tool to investigate the temporal sequence of cognitive processing in the brain (as I use it in **Chapter 8**).

3.4.2 PRINCIPLES OF MEG

3.4.2.1 *Cellular electrophysiology*

Neurons are dynamic generators of electrical activity, mediated by the flow of ions down concentration gradients (i.e. current) between extra- and intracellular compartments through membrane-bound channels. Multiple different ion channels yield different conductance mechanisms, with different temporal properties and contributions to the electrical signal. Rapid depolarisation is mediated by voltage-gated sodium and potassium channels, while several ligand-gated channels (as well as passive 'leak' conductances) giving slower timecourses of current change. Action potentials are generated by the synchronised opening and closing of many ion channels, leading to a propagating wave of electrical depolarisation through a dendritic tree. At the post-synaptic membrane, the excitatory or inhibitory influence of the afferent neuron depends upon the direction of transmembrane current flow, in turn dictated by the selective stimulation of ion channels. Excitatory post-synaptic potentials (EPSPs) are generated by inward cationic flow leading to an *active source* at the synapse, while inhibitory post-synaptic potentials (IPSPs) are caused by inward anionic or outward cationic flow leading to an *active sink*.

These active sources/sinks are compensated by opposite passive current flows elsewhere across the neuronal membrane (there is no accumulation of charge in the volume). These sink-source configurations lead to an electromagnetic field propagating through the cellular medium. If dendrites are aligned parallel (as in pyramidal cortical neurons), the summed effect of longitudinal current flows generate an orthogonal magnetic field (i.e. a magnetic dipole) (**Figure 3.10**). Critically, only magnetic fields which have a vector component perpendicular to the scalp will be detectable by extrinsic sensors. This means that the generating currents need to be orientated parallel to the head surface. In other words, MEG is maximally sensitive to dendrites in the sulcal walls rather than in cortical gyri (**Figure 3.11**).

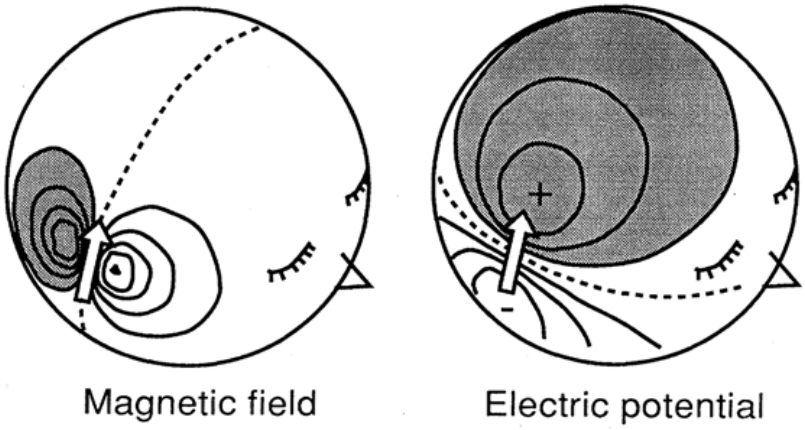

Figure 3.10 Magnetic field and electrical potential signals from a dipole. The orientation of the two fields are at right-angles. (Adapted from Hämäläinen et al., 1993).

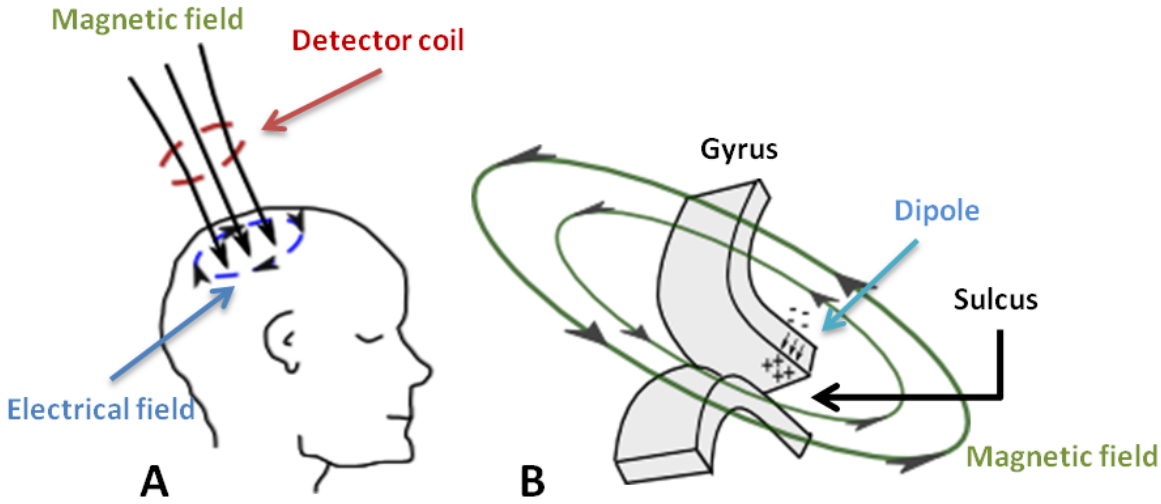

Figure 3.11 Magnetic and electrical fields from a dipole II. A. Perpendicular magnetric fields are detected by the MEG gradiometer detector coils. B. Dipoles in the sulcal walls generate these perpendicular magnetic fields. While some gyral dipoles will contribute to the magnetic signal because the head is not a perfect sphere, the maximal signal arises from the sulci.

3.4.2.2 *Biophysics*

Current strength diminishes with increasing distance from a synapse according to an inverse square law, and an individual PSP generates a current strength of approximately 20 fA m. The dipole strength needed to explain measured magnetic fluxes at the scalp is approximately 10 nA m, therefore one can estimate that 1 x 10^6 synapses are active during a typical PSP (Hämäläinen et al., 1993). In reality, this number is somewhat higher as this

corresponds to the detectable PSP with appropriate dipolar orientation. This corresponds to an approximate 40 mm^2 cortical area at minimum, which thus sets the limit of spatial resolution of MEG (Chapman et al., 1984).

The physics of electromagnetic fields are governed by Maxwell's equations, which describe how electric currents and charges produce electrical and magnetic fields. They can be used to solve the forward problem, which is how to calculate the magnetic field at point $\boldsymbol{r}$ ($\mathbf{B}(\boldsymbol{r})$) outside the head from a distribution of current (*current density*, $\mathbf{J}(\boldsymbol{r})$) in the cortex, since:

$$\mathbf{B}(r) = \frac{\mu_0}{4\pi} \int \frac{\boldsymbol{J}(r') \times \boldsymbol{R}}{\boldsymbol{R}^3} \qquad \textbf{(3.18)}$$

where r and r' are the positions outside and inside the volume respectively, and $\boldsymbol{R}$ is the displacement vector between the points.

Although intracerebral anatomy causes some electromagnetic field inhomogeneities (for example, with conductance higher along the orientation of nerve fibre tracts), the brain can reasonably be viewed as a homogenous volume conductor. To account for the different conducting compartments of the head, the volume can be treated as a combination of these homogeneous conductors corresponding to brain, skull and scalp. Moreover, to make the forward model more realistically approximate the cortical surface, the boundary element method can be used (Barnard et al., 1967; Ferguson and Stroink, 1997), which approximates a complex surface as a tessellation of triangles rather than assuming a spherically uniform volume.

The relative sensitivity of a given detector to electromagnetic signals generated within a spatial volume is called the lead field. This projection from current dipoles within the brain to a set of magnetometers outside the brain completes the forward model.

While the forward biophysical model is complex but tractable, the inverse problem where one attempts to estimate the source locations from the external field is theoretically intractable, as a potentially infinite number of current densities inside the head can produce the same external magnetic field. Solutions to the inverse problem thus require putting appropriate anatomical and functional constraints on the data, as discussed below.

3.4.2.3 *Instrumentation and measurement*

The neuromagnetic fields of the brain are typically in the order of 50-500 fT (10^{-15} Tesla), 100 million times weaker than the earth's magnetic field. To detect such small fields requires the use of superconducting quantum interference devices (SQUIDs). SQUIDs are based on superconducting loops containing a Josephson junction (Josephson, 1962), which is a thin non-conducting barrier, which can pass a tunnelling current. Phase coherence is a quantum mechanical property of superconductors, and any induced current in the superconducting loops due to changes in magnetic flux will lead to a compensatory current flowing across the Josephson junction, governed by:

$$I = I_c \sin\theta \qquad \textbf{(3.19)}$$

$$\frac{\partial\theta}{\partial t} = \frac{2\pi V}{\Phi_0} \qquad \textbf{(3.20)}$$

where I_c is the critical current for the junction, ϑ is the phase-difference across the junction, V is the voltage and φ_0 is the magnetic flux quantum constant ($\Phi_0 = h/2e = $ 2.07 fWb).

To maintain superconductance, the SQUIDs need to be housed in a reservoir containing liquid helium, and the necessity for close proximity of the detectors to the head means that adequate thermal insulation for the equipment is essential.

Significant sources of noise apart from the earth's magnetic field include within-subject electric fields generated by heart or muscle, motion-induced artefacts due to paramagnetic material on or within the subject such as dental bridges, or stimulus-locked artefact such as rhythmic movement or eyeblinks. External changing fields also cause disruption, for example from electrical equipment, including power supply frequencies, lifts, stimulus equipment, and nearby MRI scanners. Apart from direct frequency interference, radio-frequency fields can alter the SQUID gain, and vibrations can cause degraded performance. To a great extent, external sources of magnetic noise can be nullified by appropriate electromagnetic shielding – the MEG at the Wellcome Trust centre for Neuroimaging, where the study in **Chapter 8** was carried out, houses the MEG gradiometers in a purpose-built ferromagnetically-shielded room. In addition, the gradiometers which pick up the voltage in the SQUIDs include compensation coils such that they are sensitive only to local changes in magnetic flux, rather than external homogeneous fields.

Initial neuromagnetometers were single-channel detectors (Romani et al., 1982). Subsequently, multichannel arrays of magnetometers were developed, to sample the field around the head in a parallel manner to an electroencephalogram (EEG). A spacing of 30-40mm is sufficient to avoid aliasing effects due to insufficient spatial resolution, and in **Chapter 8** we use an MEG with 274 gradiometers.

3.4.2.4 *Relationship of fMRI and MEG*

Although both fMRI and MEG assess neural activity, they have differential sensitivity to certain neuronal effects. Most obviously are their respective temporal and spatial resolutions – while fMRI is limited by the timescale of neurovascular coupling, and therefore has at best power to resolve events at ~3s intervals, MEG can sample at the millisecond timescale. Conversely, fMRI has a spatial resolution at the 3-4mm scale (limited by the smoothing kernel), while MEG is constrained by the proximity of the head sensors to a 10-fold less spatial grain.

More subtle differences exist between MEG and fMRI. BOLD is thought to reflect presynaptic input firing (Logothetis et al., 2001), and is most sensitive to excitation. MEG, on the other hand, reflects combined EPSPs and IPSPs. Moreover, MEG can detect oscillatory neuronal activity, to which fMRI may be blind. Indeed, as was seen in **Figure 3.7**, there exist strong positive correlations between BOLD signal and high frequency oscillatory power, with far less correlative strength in the alpha and beta bands (8-32 Hz), and a negative correlation with low frequencies (Logothetis et al., 2001).

Similarly, MEG is very sensitive to cortical processes, but much less useful at detecting subcortical activity. For some subcortical structures (e.g. thalamus), the typically closed nature of the neuronal architecture means that theoretically external flux changes will be minimal (i.e. there are some brain regions that are essentially invisible to MEG). Conversely, fMRI has been proved excellent at resolving activity in a variety of subcortical structures. Thus MEG and fMRI are broadly complimentary modalities, both proxies for underlying neural activity but sensitive to different aspects of neuronal architecture and kinetics. By utilising both, as in this thesis, one can dissect both the anatomy and temporal structure of functional networks underlying cognitive processes.

3.4.3 DATA ANALYSIS

3.4.3.1 *Preprocessing*

Initially the timeseries data are epoched to delineate a time-window of interest. The data is then usually bandpass filtered, for example between 0.1 and 100 Hz, to remove drift and improve signal-to-noise ratio (most responses of interest are expressed at frequencies of up to 50Hz. To aid analysis, the data are also downsampled (e.g. to twice the maximal filtered frequency).

Artefact detection is important to ensure clean data. One major source of these is eyeblinks, which contain frequency components within the domain of interest and therefore are not eliminated by filtering. Fortunately, the power of eyeblink responses tends to be an order of magnitude larger than the cortical signal, therefore a pragmatic threshold for trial rejection is an order of magnitude greater than the root mean square (RMS) trial power. Alternatively, robust averaging techniques can be used where trials are weighted by their variance, or specialised detection algorithms can be trained to feature-detect artefactual responses. An additional step is baseline correction, to adjust for trial by trial variability in the starting point of the measured response. To an extent, a low pass filter will also help standardise the baseline (by removing low frequency DC drift). Finally, the data also may require smoothing, to compensate for intersubject variability in the spatiotemporal location of responses and ensure overlap in group level analysis.

3.4.3.2 *Sensor-level analysis*

Data can be analysed either at the level of the sensors (the measured flux changes in the gradiometer array), or at the level of posited sources (the intracortical generators of the magnetic flux changes). These data can either be considered in the time domain, or, as is particularly pertinent for changing oscillatory activity in recurrent neural networks, in the frequency domain.

3.4.3.2.1 TIME DOMAIN

Time domain processing first locks epochs locked to a specific time point. This yields averaged evoked responses in response to stimuli (e.g. visual or somatosensory evoked responses), or preparatory stimuli (e.g. prior to a motor response). Alternatively, for a

specific time window of interest, data can be averaged over time to yield a 2D spatial map of the relevant response magnitude.

3.4.3.2.2 TIME-FREQUENCY ANALYSIS

Alternatively, the data can be further processed with time-frequency decomposition, to produce information regarding changes in power in different frequency bands over time. This decomposition is equivalent to a Fourier transform of the data, although in practice a variety of methods are used, such as wavelet decomposition (Morlet et al., 1982). Once converted, the 4D-dataset (time, frequency, spatial location (x,y)) can be averaged, either to highlight a specific time or frequency band. This makes the statistical analysis of the data tractable.

3.4.3.3 ***Source localisation***

3.4.3.3.1 INVERSE PROBLEM

The inverse problem describes the estimation of sources inside the brain for magnetic fields detected by the MEG magnetometers. Though formally an ill-posed problem, there are several means of estimating a solution.

One can use a probabilistic generative model to give the likelihood of a current dipole at any spatial location given the data. Generally, if the forward model can be described as $\theta(\boldsymbol{b}|\boldsymbol{x})$ (i.e. the probability of a given magnetic field **b** given a current distribution parameterised as **x,** including assumptions about the error distribution), then the probability density of **x** ($p(x)$) is given by Bayes' theorem:

$$p(x) \propto \psi(x) \int \theta(b|x)\, db \qquad \textbf{(3.21)}$$

where ψ(x) is the prior probability density.

The maximum likelihood estimator for **x** can be found by the same modelling methods described above for decision theory, for example by LSM or a numerical algorithm depending on the form of the forward model. The solution is commonly called the *equivalent current dipole* (ECD) (Tuomisto et al., 1983).

The principal extra assumption when modelling multiple simultaneous dipole generators is that the position (and orientation) of these dipoles will remain the same while their amplitude will vary over time (Scherg, 1990). The number of estimated dipoles can either be a priori specified, or estimated from the data (Mosher et al., 1992).

The alternative to the ECD technique is to use an 'imaging solution' to the inverse problem, where the entire volume is modelled as a set of densely-spaced dipoles, with fixed locations and orientations given by cortical anatomy. The observation model is then a linear combination of the lead fields, the solution of which can be estimated by, for example, the *minimum norm* technique. This estimates the current distribution $\boldsymbol{J}$ with the minimum overall amplitude sufficient to explain the data. More recently, alternative Bayesian methods of source reconstruction have been developed, for example the *multiple sparse prior* (MSP) technique which imposes constraints upon the topology of source space and has been shown to be superior to the minimum norm method (Friston et al., 2008). We use MSP source reconstruction in **Chapter 8.** Further refinements include using anatomical or functional priors derived from (f)MRI in the probabilistic model.

3.4.3.4 *Statistical inference*

Statistical inference for MEG proceeds in a similar fashion to that for fMRI. One can utilise the same methods in SPM software, including setting up a statistical model of data in a GLM, and employing random field theory to correct for multiple comparisons across N-dimensional spaces. The principles and practice of statistical analysis are therefore identical to that for fMRI data, except that rather than only making inferences about signal amplitude in 3D space, there are multiple dimensions in which the data can be considered (sensor vs source space, time vs time-frequency). I therefore will not reiterate the steps here and refer the reader to the above discussion (see section 3.3.5.3).

Chapter 4

DECONSTRUCTING NEURAL RESPONSES TO RISK

4.1 INTRODUCTION

When foraging animals, or humans in a modern economy, make a decision they must evaluate potential outcomes of a choice and the chance of each outcome occurring. As discussed in **Chapter 1,** risk is a multi-dimensional property of a distribution of potential outcomes, subsuming both the uncertainty or range of potential outcomes, but also the shape of this distribution.

To dissociate different components of risk, which I quantify here in terms of dispersion (variance) and asymmetry of outcomes (skewness), I designed a novel decision-making task that controlled the distribution of outcomes and ensured that variance and skewness of a set of lotteries were manipulated independently by design (see **4.2.2**). Hence, as variance and skewness of gambles were orthogonal factors ($r^2 = 5 \times 10^{-6}$), I could test whether neural activity evoked by variance could be distinguished from that evoked by skewness. In brief, in my task participants chose between a 'gamble' (a lottery with a number of potential outcomes) or a 'sure' option (a fixed amount of money). I predicted distinct preferences for both variance and skewness (possibly with different preferences for positive versus negative skewness).

I hypothesised that variance and positive/negative skewness would have a distinct representation within dorsomedial prefrontal cortex (DMPFC), anterior insula, posterior parietal cortex (PPC), and ventral striatum, given previous findings of risk-related activations in these areas (for a meta-analysis see Mohr et al (Mohr et al., 2010a)). A related aim was to establish the locus of integration of such summary statistics with an individuals' subjective taste for risk. In effect I aimed to map a final common pathway mediating an integration of objective (task-based) and subjective (individual disposition to risk) decision variables prior to behavioural output.

4.2 METHODS

The study was approved by the Institute of Neurology (University College London) Ethics Committee. 24 subjects (mean age: 24; age range: 19-34; male: 12) participated in the experiment. 1 (female) subject was excluded because they used a fixed strategy (always chose sure amount), hence behavioural preferences could not be estimated. I provided a 5-minute practice tutorial to demonstrate the paradigm. Stimuli were presented and responses recorded using Cogent presentation software (Wellcome Trust Centre for Neuroimaging, London) written in MATLAB (version 6.5, MathWork, Natick, MA). Imaging data were analysed using Statistical Parametic Mapping software (SPM8; Wellcome Trust Centre for Neuroimaging, UK). Visual cues were projected onto a screen, visible via an angled mirror mounted on the MRI head coil. Choices were indicated by pressing a button box with the right index finger.

4.2.1 TASK

I designed a decision-making task where the variance and skewness of a set of lotteries could be independently experimentally manipulated (**Figure 4.1A**). Hence, I could ensure that variance and skewness of gambles were orthogonal factors, thus could test whether neural activity evoked by variance could be distinguished from that evoked by skewness. Participants were required to choose between taking a 'sure' (fixed) amount of money or electing to 'gamble' (choosing to play a lottery with a number of potential outcomes). Gambles were represented as pie-charts, where variance and skewness of outcomes varied over a range, with expected value kept constant. I predicted distinct preferences for both variance and skewness (possibly with different preferences for positive versus negative skewness).

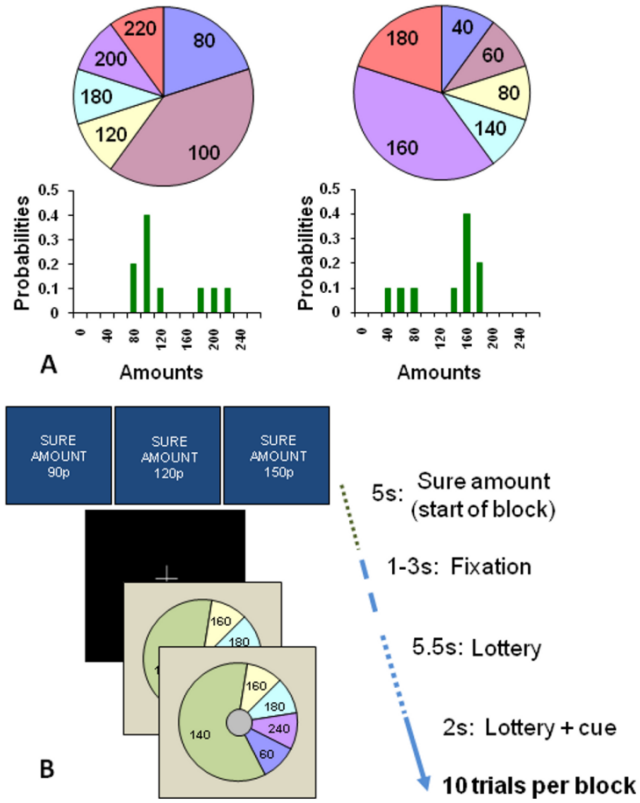

Figure 4.1 Task. A. I represented gambles on-screen as pie-charts, divided into different segments showing possible outcomes from the lottery. The numbers written in each segment showed the monetary value of each outcome (in pence) and the angle subtended by each segment indicated the probability of each outcome occurring. A positively skewed gamble (left), has a small chance of a better than average outcome (the tail is to the right). Conversely, a negatively skewed gamble (right) has a small chance of a worse than average outcome (the tail of the distribution is to the left). Both example gambles have equal variance and expected value. B. The task consisted of trials, grouped into experimental blocks of ten. For each trial, a pie chart was shown and after 5.5 seconds, a cue to respond appeared on screen (for 2 seconds). Subjects indicated by a button press while the cue was on-screen if they wanted to gamble on the lottery, or alternatively select a fixed, sure amount of money. To commence a block, the sure amount was written on the screen (3 levels – 90p, 120p, 150p). At the end of each block, one trial from the block was randomly selected and played out for real. If subjects had elected to gamble, I resolved the lottery by an on-screen graphic of a red ball spinning around the outside of the pie which stopped at a randomly selected position. 180 trials were presented in total (60 stimuli at each of 3 sure levels).

4.2.2 INDEPENDENT MANIPULATION OF VARIANCE AND SKEWNESS

I constructed a stimulus set of 60 lotteries where variance and skewness were independent and varied over a range (**Appendix A**, **Figure 4.2**). For every level of variance (10 levels), I independently varied skewness (6 levels, 3 positively skewed, 3 negatively skewed). Expected value of the lotteries was kept constant (between £1.26 and £1.34), while variance ranged from 0.1 to 0.7 £^{2}, and (standardised) skewness ranged from -1 to 1. Stimuli were constrained to have between 3 and 9 outcomes (segments of the pie chart), with outcome

probabilities varying in minimum 0.1 increments between 0 and 1 to mitigate against probability distortion effects at small probabilities. These restrictions allow the generation of a space of possible lotteries varying in skewness and variance. I pre-specified the desired levels of variance and skewness and selected lotteries to give as orthogonal a stimulus set as possible. The lotteries were also resampled to ensure variance and skewness were decorrelated from the number of segments in each presented pie chart gamble (variance r^2 = 0.01; skewness r^2 = 0.0004). Where 2 lotteries were equidistant from the desired array of points, a lottery was selected at random. Using multiple outcomes is critical, as for binary gambles, it is impossible to independently manipulate statistical moments across a range of values.

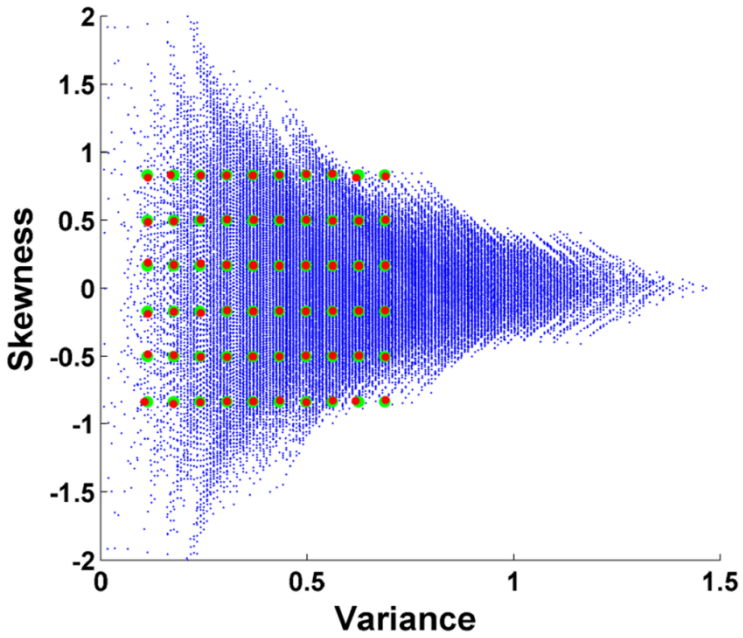

Figure 4.2 Construction of stimulus set. Figure of stimulus set construction, plotted as variance against skewness of lottery outcomes. Blue dots represent all possible gambles, constructed with EV = £1.26-£1.34, according to stimulus set constraints. Green dots represent desired array of stimuli, and red dots are the actual selected stimuli (n=60) for use in experiment, with independent manipulation of variance and skewness.

To commence a block, the sure amount was written on the screen (3 levels – 90p, 120p, 150p). At the end of each block, one trial from the block was randomly selected and played out for real. If subjects had elected to gamble, I resolved the lottery by an on-screen graphic of a red ball spinning around the outside of the pie until it stopped at a randomly selected position. This procedure was also tested in practice trials, to demonstrate the idea that the size of each segment of the pie chart represented the chance of that outcome occurring. Resolving one trial per block helped maintain subjects' task engagement during and thus maximise sensitivity to detect evoked responses to the experimentally-manipulated stimulus dimensions. Importantly, one does not expect any shifts in individual behavioural preferences to change the evoked response to the objective features of the gamble stimuli themselves. In addition, any changes in behaviour can only count against (i.e. reduce the sensitivity of) an analysis of correlations between trial-by-trial choice, individual preference, and neural activity. 180 trials were presented in total (60 stimuli for each of the 3 sure levels). Monetary earnings ranged between £16.10 and £24.30 (mean £19.40).

4.2.3 BEHAVIOURAL MODELLING

4.2.3.1 *Mean-risk models*

For a given lottery with N potential outcomes *(m_1, m_2,… m_N)*, with probabilities $p = p_1, p_2, \ldots p_n$, the statistical moments (expected value (EV), variance (Var), standardised skewness (Skw)) of the outcome distribution are defined as follows:

$$EV = \sum_{n=1}^{N} m_n p_n \qquad \textbf{(4.1)}$$

$$Var = \sum_{n=1}^{N} (m_n - EV)^2 p_n \qquad \textbf{(4.2)}$$

$$Skw = \frac{\sum_{n=1}^{N} (m_n - EV)^3 p_n}{Var^{3/2}} \qquad \textbf{(4.3)}$$

I analysed choice data by fitting a linear mean-variance-skewness model (**MVS**) where individuals are allowed to express different preferences for variance and skewness, and compared this to a set of reduced models and a standard power utility model commonly used to model standard expected utility (Camerer, 2003). The reduced models included a model based on mean difference (**M**) alone (where subjects only take account of the difference

between the sure amount and the expected value of the gamble in selecting actions), a mean-variance model (**MV**), and a mean-skewness (**MS**) model.

I then define the subjective value, or utility (U) of each lottery for the models:

Mean model (**M**)

$$U = EV \quad \textbf{(4.4)}$$

Mean-variance model (**MV**)

$$U = EV + \rho Var \quad \textbf{(4.5)}$$

Mean-skewness model (**MS**)

$$U = EV + \lambda Skw \quad \textbf{(4.6)}$$

Mean-variance-skewness model (**MVS**)

$$U = EV + \rho Var + \lambda Skw \quad \textbf{(4.7)}$$

ρ and λ are free parameters reflecting preference for variance and skewness respectively.

I also tested a further set of models, where subjects were allowed to express a preference separately for positive and negatively skewed gambles. These models are specified as:

Mean-variance-positive skewness (**MVpS**):

$$U = EV + \rho Var + \lambda_p Skw^+ \quad \textbf{(4.8)}$$

Mean-variance-negative skewness (**MVnS**):

$$U = EV + \rho Var + \lambda_n Skw^- \quad \textbf{(4.9)}$$

Mean-positive skewness-negative skewness model (**MpSnS**):

$$U = EV + \lambda_p Skw^+ + \lambda_n Skw^- \quad \textbf{(4.10)}$$

Mean-variance-positive skewness-negative skewness model (**MVpSnS**):

$$U = EV + \rho Var + \lambda_p Skw^+ + \lambda_n Skw^- \quad \textbf{(4.11)}$$

Where Skw^+ indictates $Skw \geq 0$ and Skw^- indicates $Skw < 0$, and λ_p and λ_n reflect preferences for positive and negative skewness respectively.

4.2.3.2 *Expected Utility models*

Expected utility model (**EUT**)

$$U = \sum_{n=0}^{N} \frac{{m_n}^{1-\kappa}\, p_n}{1-\kappa} \qquad \textbf{(4.12)}$$

κ reflects the concavity of the utility (power) function, hence the degree of risk-aversion.

A loss aversion (**LA**) model, which weights the utility of amounts below the expected value of the lottery by a loss aversion parameter (λ):

$$U = \sum_{n=0}^{N} I \cdot \frac{(m_n - EV)^{1-\kappa}\, p_n}{1-\kappa} - (1-I) \cdot \frac{|m_n - EV|^{1-\kappa}\, p_n}{1-\kappa} \qquad \textbf{(4.13)}$$

Where I is an indicator variable (I = 1 when (m_n-EV)≥0, and I = 0 when (m_n-EV)<0).

I also tested a probability weighting (**PW**) model, where probabilities are transformed according to a one-parameter probability weighting function (Prelec, 1998):

$$U = \sum_{n=0}^{N} \frac{{m_n}^{1-\kappa}\, g(p_n)}{1-\kappa} \qquad \text{where} \quad g(p_n) = e^{-(-\ln p_n)^{\alpha}} \qquad \textbf{(4.14)}$$

I finally tested a cumulative prospect theory (**CPT**) model (Tversky and Kahneman, 1992). For a given lottery with N potential outcomes, we redefine outcomes relative to a reference point R, such that the outcomes are $m_{-T}, m_{-T+1}, m_{-T+2} \ldots, R, \ldots m_{N-2}, m_{N-1}, m_N$, with probabilities $p = p_{-T}, p_{-T+1}, p_{-T+2} \ldots, p_R, \ldots p_{N-2}, p_{N-1}, p_N$. Overall utility $U = U^- + U^R + U^+$, is given as:

For $m > R$:

$$U^+ = g(p_N)u(m_N) + \sum_{k=1}^{N} \left[g\left(\sum_{j=0}^{k} p_{N-j}\right) - g\left(\sum_{j=0}^{k-1} p_{N-j}\right) \right] u(m_{N-k}) \qquad \textbf{(4.15)}$$

For $m < R$:

$$U^- = g(p_{-T})u(m_{-T}) + \sum_{k=1}^{T} \left[g\left(\sum_{j=0}^{k} p_{-T+j}\right) - g\left(\sum_{j=0}^{k-1} p_{-T+j}\right) \right] u(m_{-T+k}) \qquad \textbf{(4.16)}$$

For $m = R$:

$$U^R = 0 \qquad \textbf{(4.17)}$$

where:

$$u(m_i) = \begin{cases} \dfrac{-\lambda(R - m_i)^{\kappa}}{1 - \kappa} & m_i < R \\ \dfrac{(m_i - R)^{\omega}}{1 - \omega} & m_i \geq R \end{cases} \quad \textbf{(4.18)}$$

$$g(p_i) = \begin{cases} e^{-(-\ln p_i)^{\alpha}} & m_i < R \\ e^{-(-\ln p_i)^{\delta}} & m_i \geq R \end{cases} \quad \textbf{(4.19)}$$

This is a rank-dependent model where small probability extreme outcomes are overweighted ($\alpha \in [0, 1],\ \delta \in [0, 1]$), and outcomes below the reference point have more influence than relative gains (here $\lambda \in (1,\ 5)$). Rather than using the status quo as the reference point, I used a non-zero reference point of £1.20. This enables the model to overweight small probability events at both extremes of the distribution, a parallel to skewness sensitivity.

4.2.3.3 ***Heuristics***

A max-min (**MaxMin**) model where only the maximum and minimum amounts in a given lottery are used to construct a (weighted) expected value:

$$U = \frac{\max\limits_{1 \leq n \leq N} m_n \cdot p_{\max m_n} + \min\limits_{1 \leq n \leq N} m_n \cdot p_{\min m_n}}{p_{\max m_n} + p_{\min m_n}} \quad \textbf{(4.20)}$$

An alpha max-min model (**AMaxMin**), where these maximum and minimum possible amounts are weighted by an additional parameter alpha:

$$U = \frac{\alpha \left(\max\limits_{1 \leq n \leq N} m_n \cdot p_{\max m_n} \right) + (1 - \alpha) \left(\min\limits_{1 \leq n \leq N} m_n \cdot p_{\min m_n} \right)}{p_{\max m_n} + p_{\min m_n}} \quad \textbf{(4.21)}$$

α = 0 reflects a 'loss minimising' heuristic, α = 1 reflects a 'gain maximising' heuristic.

For completeness I also tested versions of these models coupled to a power utility transformation of amounts (**MaxMinp**, and **AMaxMinp**). Lastly I tested an heuristic where individuals attend only to the segment with maximum probability **(MaxP**):

$$U = m_{\max\limits_{1 \leq n \leq N} p_n} \quad \textbf{(4.22)}$$

4.2.3.4 *Action selection*

The models compare the utility of the lottery with the value of the sure amount (S) to generate a trial-by-trial probability of choosing the lottery over the sure amount, using a logistic/softmax function which allows for noise in action selection (by free parameter β).

$$P_{choose\ gamble} = \frac{1}{1 + e^{(U-S)/\beta}} \quad \textbf{(4.23)}$$

I estimated best-fitting model parameters using maximum likelihood analysis, with optimisation implemented with a non-linear Nelder-Mead simplex search algorithm in Matlab (Matlab, Natwick, USA) and compared models using Group Bayes Factors, with the Akaike Information Criterion (AIC) (Akaike, 1974) and Bayesian Information Criterion (BIC) (Schwarz, 1978) providing an approximation to the model evidence and penalising model complexity (Penny et al., 2004b).

4.2.4 FMRI

4.2.4.1 *Scanning parameters and preprocessing*

I acquired gradient echo T2*-weighted echo-planar images (EPI) with blood-oxygen-level-dependent (BOLD) contrast, on a 3 Tesla head scanner (Magnetom Allegra, Siemens Medical). Imaging parameters were: 42 oblique transverse slices; slice thickness, 2 mm; gap between slices, 1 mm, repetition time TR=3.1s; echo time TE=25ms; field of view FOV=192×192 mm^2, matrix size 128 x 64 (RO x PE). I employed an EPI sequence that optimized for BOLD sensitivity in the OFC using a combination of an increased spatial resolution in the read-out direction and a reduced echo time (Weiskopf et al., 2007). Together with the oblique orientation of the slice acquisition, this can compensate and recover for potential signal loss in OFC. During the same experimental session, a T1-weighted image was obtained for anatomical reference. To correct for geometric distortions induced in the EPIs at high field strength, I collected fieldmaps based on dual echo-time images (TE1 = 10 ms, TE2 = 12.46ms), and processed these using the SPM8 fieldmap toolbox (Hutton et al., 2002) to produce a voxel displacement map indicating the field distortions. Images were realigned with the first volume, normalized to a standard EPI template, and smoothed using an 8mm full-width at half-maximum Gaussian kernel. Unwarping was carried out using the routine in SPM8, correcting for distortions in each acquired image by combining the measured fieldmaps with estimated susceptibility-induced changes due to motion.

4.2.4.2 *Statistical analysis*

Data were analyzed with a general linear model (GLM), with BOLD responses to each stimulus modelled as a box-car of duration 7.5s (duration of stimulus presentation), time-locked to stimulus presentation and convolved with a hemodynamic response function. I constructed regressors to identify parametric responses to variance and skewness, which modulated the height of the box-car. Each of three runs was modelled separately. Trials were split into positively and negatively skewed lotteries, with regressors indicating variance, skewness, and choice (gamble or sure). Sure amount screens, stimulus onsets, keypresses, and resolution of gambles at the end of each block were also modelled to factor out BOLD activity unrelated to variables of interest. I also included subject-specific realignment parameters from the image preprocessing to account for motion-related artifacts in the images that were not eliminated in rigid-body motion correction. Regression parameter estimates of linear contrasts were estimated and entered into t-tests using random-effects analysis to provide group statistics. Contrasts of parameter estimates reflect selective activations due to the experimental effects. These contrasts or selective activations were then used in subsequent (between-subject) tests at the second level. I was largely concerned with detecting activations using one sample T-tests to show that the contrast was significantly greater than zero over subjects. However, I also used these contrasts to look for correlations between subject-specific preferences and physiological responses (selective activations). I used a cluster-defining voxel-wise threshold of $p<0.01$, reporting whole-brain significant clusters family-wise error (FWE) corrected for multiple comparisons at $p<0.05$, or significant voxels within a priori regions of interest (small-volume FWE-corrected at $p<0.05$). Regions of interest based on previous studies comprise anterior insula/inferior frontal gyrus, ventral striatum and dorsomedial prefrontal cortex (Preuschoff et al., 2006; Christopoulos et al., 2009; Tobler et al., 2009; Mohr et al., 2010a). Percent signal change within a cluster is estimated with RFXplot (Gläscher, 2009). Figures show second-level SPM-T images thresholded at $p<0.005$ (uncorrected for display purposes only), superimposed upon a canonical image. Stereotactic coordinates are reported in MNI space (Mazziotta, 2001).

4.3 RESULTS

4.3.1 BEHAVIOUR

Subjects (n = 23) distributed their choices between gamble and sure options throughout the course of the experiment (mean percentage of gamble choices = 53%, std. 14%). The sure option changed over the course of the experiment enabling us to decorrelate choice from the statistical features of interest. Additionally, as I focused on deconstructing risk (i.e. the

distribution of outcomes), the expected value of the gamble remained constant throughout (between £1.26-£1.34). When the sure amount was greater, subjects therefore opted to gamble less often (mean percentage of gamble choices per sure amount level - 90p: 85%, std. 13%; 120p: 58%, std. 20%; 150p: 18%, std 14%). There were few error (missed) trials (4 +/- 0.5%), which are excluded from analyses. The mean correlation between choice and variance was -0.009 (std 0.079) and the mean correlation between choice and skewness was 0.0035 (std 0.087).

4.3.1.1 ***Behavioural modelling***

I independently manipulated variance and skewness, and predicted that individuals' preferences would be sensitive to both summary statistics. As described, I compared a mean-variance-skewness model (**MVS**) where individuals are allowed to express preferences for both variance and skewness, to a set of alternative decision models.

4.3.1.1.1 MODEL FITS

As predicted, a mean-variance-skewness (**MVS**) model provided a significantly better fit to the behavioural data than the 4 main alternative models (summed AIC: **M**: 4139; **MV**: 3599 **MS**: 3993 **MVS**: 3431 **EUT**: 3760; Group Bayes Factors (log-GBF relative to worst performing **M** model): **M**: 0; **MV**: 540 **MS**: 145 **MVS**: 708 **EUT**: 378 (Kass and Raftery, 1995; Raftery, 1995; Penny et al., 2004b); **MVS** model posterior probability>0.99 (very strong evidence in favour of **MVS**) (**Figure 4.3A**). Similar results were obtained using the Bayesian Information Criterion (BIC) (Schwarz, 1978), an approach which penalises model complexity more severely than the AIC (log-GBF relative to **M** model calculated from BIC: **M**: 0; **MV**: 466; **MS**: 72; **MVS**: 561; **EUT**: 305). Here, I paid subjects for 18/180 trials during the entire experiment, motivated by a need to keep individuals engaged with the task. While paying for multiple trials has the potential to blunt risk-sensitivity, the fact that the risk-sensitive models were clearly superior to the risk-neutral (**M**) model demonstrates that risk-sensitivity was preserved, and suggests that participants assessed and treated each gamble individually.

Given the intuition that positive and negative skewness exert separate influences on behaviour, I also tested whether models with separate parameters for positively and negatively skewed gambles (i.e. one extra parameter than the **MVS** model) fit participants' choices better than the three-parameter **MVS** model, and also whether models with preferences for variance and either positive or negative skewness fitted choice as well as the full **MVS** model. Again, the **MVS** model proved superior to these other models (**Figure 4.4**).

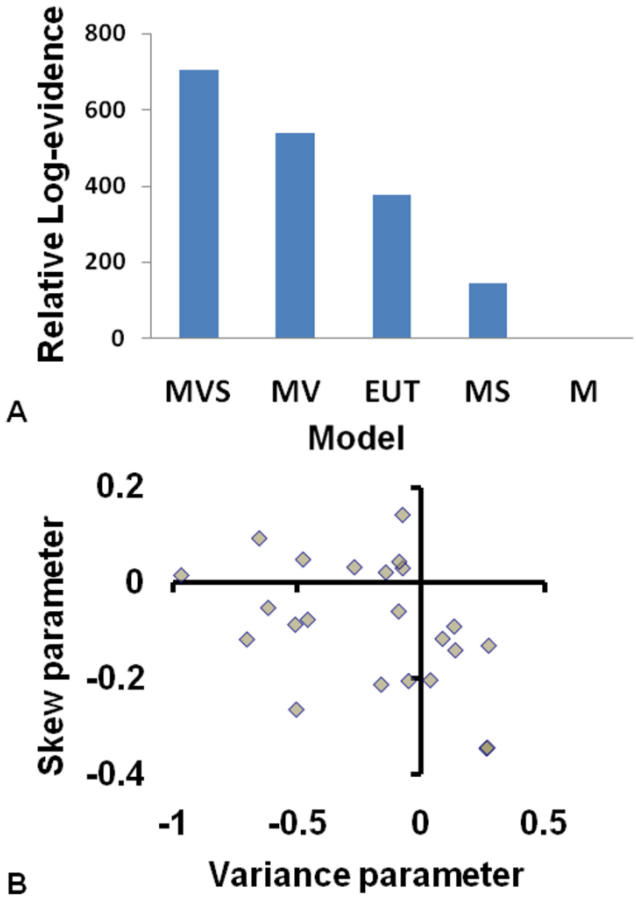

Figure 4.3 Behavioural modelling. A. Relative log-evidence for each of 5 models: mean only (M), mean-variance (MV), mean-skewness (MS), mean-variance-skewness (MVS) and power utility (EUT). Relative log-evidence (log-Group Bayes Factor) calculated as summed difference in log-evidence for each model relative to worst performing M model, across subjects. Model evidence is approximated by the Akaike information criterion (AIC), calculated as AIC = 2.k – 2.ln(L), where L is the maximum likelihood estimate of the model and k is the number of free parameters. A higher score indicates a better model fit (higher model likelihood). There was strong evidence in favour of the MVS model in a fixed effects analysis of Group Bayes Factors (model posterior probability >0.99 in favour of MVS). B. Parameter estimates from the MVS model reveal a range of preferences for variance (negative coefficent reflects variance aversion), and skewness (negative coefficient reflects aversion to positive versus negative skewness).

4.3.1.1.2 PROBABILITY DISTORTION AND LOSS AVERSION EFFECTS

Although I mitigated severe probability distortion by constraining the gambles such that the smallest probability used was 0.1, it nevertheless is possible that behaviour attributed to skewness preference could be caused by probability weighting effects. To outrule this possibility, I fit an additional model with probability weighting to the behavioural data, using the same specification as Hsu and colleagues (Hsu et al, 2009), with power utility and a 1-parameter (Prelec) probability weighting function. Although this outperformed a power utility model without probability weighting, it was vastly inferior to the mean-variance-

skewness model (probability weighting model AIC: 3674, log Group Bayes factor **MVS** vs probability weighting = 243). I also fit a loss aversion (**LA**), and full cumulative prospect theory (**CPT**) model, with the reference point set at the £1.20 sure amount rather than the status quo of £0. This allows for potential overweighting of small probability outcomes at both extremes of the distribution, similar to skewness preference. The **MVS** model outperformed the **CPT** and **LA** models (log Group Bayes factor **MVS** vs **CPT**: 236; **MVS** vs **LA**: 131; **Figure 4.4**).

4.3.1.1.3 HEURISTIC MODELS

I also examined whether individuals are using a heuristic, such as attending to the smallest/largest outcome or some weighting of the two by comparing a series of models of different possible heuristics (see Methods). None of these models explained the data well and all were inferior to both the MV and MVS models (**Figure 4.5**). This provides strong evidence that subjects use the entire lottery distribution to guide choice rather than reducing the process to a simpler heuristic.

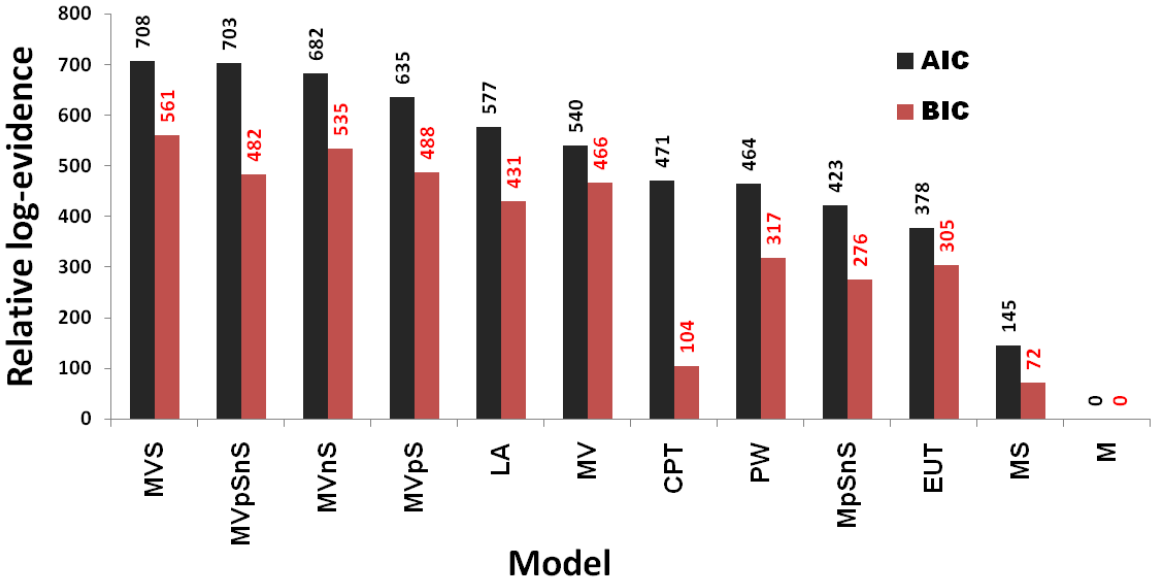

Figure 4.4 Comparison of mean-risk and expected utility models including: mean only (M), mean-variance (MV), mean-skewness (MS), mean-variance-skewness (MVS), power utility (EUT), mean-variance-positive skewness (MVpS), mean-variance-negative skewness (MVnS), mean-positve skewness-negative skewness (MpSnS), mean-variance-positive skewness-negative skewness (MVpSnS), loss aversion (LA), probability weighting (PW) and cumulative prospect theory (CPT). Relative log-evidence, with model evidence approximated by either AIC or BIC to penalise for model complexity, calculated against worst performing M model, across subjects, and are given above each model. A higher relative log-evidence indicates a better model fit (higher model likelihood).

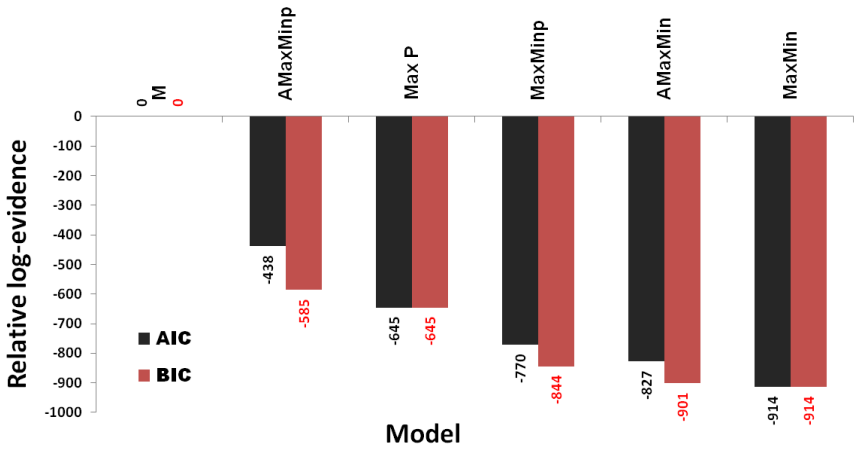

Figure 4.5 Comparison of heuristic models. The heuristic models (AMaxMinp, MaxP, MaxMinp, AMaxMin, MaxMin) proved inferior to the mean model in a comparison of relative log evidence (more negative number indicates a worse model fit).

4.3.1.1.4 PARAMETER ESTIMATES FOR RISK PREFERENCES

I next used the winning **MVS** model to provide subject-specific preferences for variance and skewness. Parameter estimates from the **MVS** model showed that 16/23 subjects were averse to variance (average variance preference: -0.20; s.e.m. 0.07), and 15/23 were averse to positive skewness (average skewness preference: -0.09; s.e.m. 0.03) (**Figure 4.3B**). β (temperature) values for the logistic function were low, indicating that choices were well partitioned by the linear model (average beta = 0.14; s.e.m. 0.01). Some subjects had strong skewness preference but were insensitive to variance, other subjects were indifferent to skewness. 8/23 showed a negative variance and skewness parameter, which corresponds to a (locally) sigmoid utility function. There was a weak negative correlation between variance and skew-preference (r^2 = 0.17; p = 0.05). No individuals in the sample were both variance and positive-skew-seeking. The **MVS** model was at least as good as the **MV** and **MS** alternatives in the majority of individual cases, outperforming the **MS** model in 19/23 subjects and the **MV** model in 17/23 subjects.

4.3.1.1.5 CHANGES IN PREFERENCE OVER TIME

It is possible that subjects might switch their behavioural preferences from preferring positive to preferring negative skewness over the course of the experiment. I checked this possibility by separately fitting the MVS model per subject to the first and second half of the data. I found no evidence that individuals reverse their preference for skewness during the

experiment, with 15 subjects starting and finishing with preference for negative skewness, 5 subjects starting and finishing with preference for positive skewness, and only 3 subjects reversing preference from negative to positive skew seeking (20/23 subjects with no switch in preference, binomial test = n.s.). I explored this question further, and tested if there was any systematic shift in preference at all. There was no significant change in the estimated variance preference parameters from the 1st to the 2nd half of the session across subjects (paired t-test, p = .75). However there was a change in skew-preference (paired t-test, p = 0.005). Consequently, for the imaging analysis, I use individuals' average behavioural preferences estimated across the experimental session. Note that any change in preference over time will count against the analysis by introducing noise into the data, rendering it less likely to detect a significant result, and also mean that I may underestimate the true effect size of some reported correlations.

4.3.2 FUNCTIONAL IMAGING

4.3.2.1 *Responses to variance and skewness*

Having established that a **MVS** model best explained participants' choice behaviour, I next asked whether statistical components of this model have a distinct neural representation. In line with the predictions, brain activity in right posterior parietal cortex (PPC) (peak MNI coord: 32, -60, 50; p = 0.003, cluster extent = 1318 voxels) showed a significant correlation with lottery variance on each trial, irrespective of choice (**Figure 4.6A&B**, **Table 4.1**). No brain activity negatively correlating with variance survived family-wise error-correction.

In contrast to a segregated representation of variance, I observed a distributed encoding of skewness. Using the pair of regressors representing stimulus-evoked BOLD activity modulated by the degree (magnitude) of lottery skewness, for positive and negatively skewed trials respectively, I tested both whether there were regions encoding the full range of skewness on a linear scale, and whether there were regions whose activation depended solely on the degree of positive or negative skewness. No single area linearly correlated with the full range of skewness (i.e. both increasing activation for greater positive skewness, and decreasing activation for greater negative skewness), which I assessed using a conjunction between activity for positive and negative skewness (at p<0.01 voxelwise threshold). Instead, I found dissociable cortical and subcortical regions correlating with positive and negative skewness respectively. As positive skewness increased (a small chance of a better than average outcome) so too did BOLD signal in ventral striatum (peak voxel MNI coord: -10, 4, -14; p = 0.033 (small volume corrected), cluster extent =228 voxels), and right anterior insula extending into inferior frontal gyrus (IFG) (on right: peak voxel MNI coord: 30,16,-14;

p = 0.021 (small volume corrected), cluster extent = 234 voxels; on left: peak voxel MNI coord: -40,24,-16; p = 0.017 (small volume corrected), cluster extent = 67 voxels.) (**Figure 4.6C-F**, Table **4.1**), a priori regions of interest where risk-related activity has been seen in previous studies (Schultz et al., 2008). In contrast, negative skewness correlated with activity in medial prefrontal cortex (peak voxel MNI coord: 4, 44, 36; p< 0.001, cluster extent =1673 voxels)(**Figure 4.6G&H, Table 4.1**). There were no areas surviving correction that correlated with decreasing positive or decreasing negative skewness (i.e. greater BOLD signal for less skewed lotteries). Ventral striatum, insula, and prefrontal cortex expressed dissociated responses to positive and negative skewness (**Figure 4.6D,F,H**). No areas correlating with increasing magnitude of skewness irrespective of sign (i.e. more active for skewed than symmetrical lotteries, irrespective of whether the outliers were better or worse than the average) survived correction.

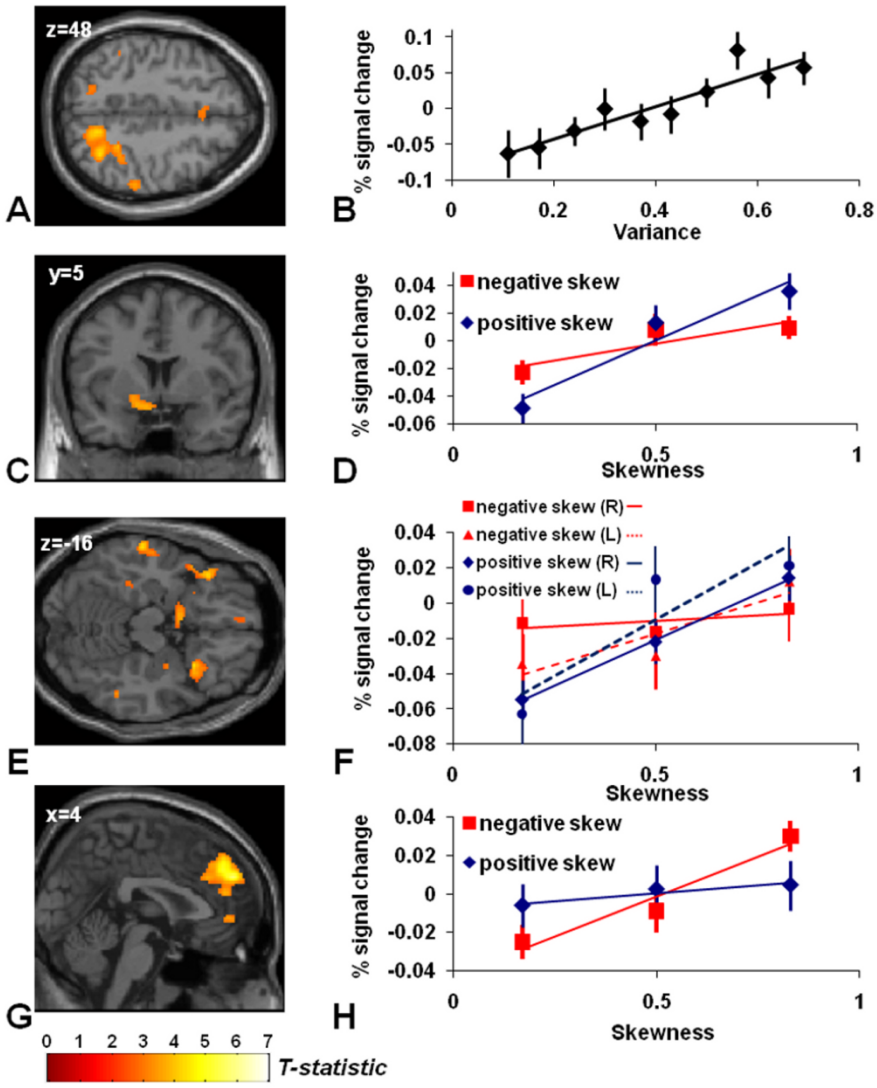

Figure 4.6 Responses to summary statistics. Figure shows second-level SPM-T images thresholded at p<0.005, superimposed upon a canonical image. A. Linear correlation between PPC activity and variance (peak coord: 32, -60, 50; p = 0.003, whole-brain corrected). B. Estimated percent signal change, averaged activity over all voxels within PPC cluster. C. Correlation between increasing positive skewness and BOLD signal in ventral striatum (peak coord: -10, 4, -14; p = 0.033, small volume corrected). D. Estimated percent signal change, averaged activity over all voxels within ventral striatum cluster, for positive and negative skewed gambles. E. There was also positive correlation seen in bilateral anterior insula (peak coords: right - 30,16,-14, p = 0.021; left - -40,24,-16, p=0.017; small volume corrected). F. Estimated percent signal change for positive and negatively skewed gambles, averaged activity over all voxels within right and left anterior insula clusters (plotted separately). G. Correlation between increasing negative skewness and BOLD signal in DMPFC (peak coord: 4, 44, 36; p< 0.001, whole-brain corrected). H. Estimated percent signal change, averaged activity over all voxels within ventral striatum cluster. Error bars on correlation plots show standard error. All statistical inference performed in SPM (reported in the main text and supplementary tables), thus separate correlation strength and effect size not re-calculated from plotted correlations, with relationships shown for illustrative purposes.

Area	L/R	MNI coordinates			Z score	P value	Cluster Extent
		x	y	z			
A. Response to Variance							
Posterior Parietal Cortex	R	32	-60	50	3.71	0.003†	1318
		28	-46	46	3.66		
		16	-62	48	3.59		
B. Response to Positive Skewness							
Anterior insula / inferior frontal gyrus	R	30	16	-14	3.59	0.021††	117
Anterior insula / inferior frontal gyrus	L	-40	24	-16	3.59	0.017††	67
Ventral Striatum	L	-10	4	-14	3.36	0.033††	228
		-16	8	-8	3.20	0.050††	
C. Response to Negative Skewness							
Dorsal medial prefrontal cortex / medial frontal gyrus	R	4	44	36	4.76	<0.001†	1673
	L	-8	32	34	3.93		
		-2	48	18	3.38		

Table 4.1 Response to Risk Dimensions. A. Anatomical locations of regions positively correlating with the lottery variance on each trial. B. Anatomical locations of regions correlating with increasing positive skewness on each trial. C. Anatomical locations of regions correlating with increasing negative skewness on each trial. I report significant clusters surviving correction at p≤0.05 († = cluster-level family-wise error whole-brain corrected p-value), or significant voxels at p≤0.05 within regions of interest (†† = voxel-level family-wise error region-of-interest corrected p-value). Peak voxel MNI coordinates within significant clusters are given, with corresponding voxel-level Z scores. I define anatomical ROIs by 2cm-diameter spheres centred upon MNI coordinates for anterior insula, ventral striatum, and anterior cingulate/dorso-medial prefrontal cortex, where risk-related activation has previously been reported.

4.3.2.2 *Regional encoding of utility*

Given that the **MVS** model specifies value as a linear mixture of variance and skewness, I would expect that regions expressing activity correlating with gamble utility would also be expected to show a partial correlation with both variance and skewness. Conversely, the fact that I do not see common regions correlating with variance and skewness argues against a unitary representation of lottery value. However, this may be due to reduced detection power in an additive mixture of random variables, thus I also tested directly for a representation of value. I ran separate GLMs to identify regions correlating with the trial-by-trial utility of the lottery (stimulus value; **MVS** model), the difference in utility of lottery vs. sure amount (relative stimulus value), and utility of the chosen - utility of the unchosen option (relative action value). No areas correlated with stimulus value, even within regions of interest (variance and skew-sensitive areas, or prefrontal cortex) at an uncorrected

($p<0.001$) threshold. For relative stimulus value, I observed a 5-voxel cluster at uncorrected significance ($p<0.001$, voxel-level) in right ventromedial OFC. Relative action values were reflected in robust activation in a network of regions comprising bilateral precentral sulcus extending into supplementary motor area, and bilateral inferior parietal lobe ($p<0.001$, corrected). As might be expected, these regions form a typical motor/motor preparatory network (Cunnington et al., 2002).

4.3.2.3 *Integration with variance and skewness preferences*

I considered whether regions encoding the statistics of lottery outcomes also integrated this information with individuals' tastes for risk. These variance or skewness-encoding regions could express different sensitivities to these statistics depending upon an individual's risk preferences, as discussed in **Chapter 2**. Thus I tested whether areas expressing variance and skewness-related activity altered in sensitivity (correlation effect size) to these statistics in a manner that correlated with subjects' preferences, as estimated from the **MVS** model. I identified a significant interaction between BOLD activation for positive skewness and subject-specific skew-preference (peak voxel MNI coord: -36, 24, -16; $p = 0.007$, cluster extent = 80 voxels) in anterior insula. Thus the greater the activation reflecting skewness in this area the stronger the behavioural preference for positive over negative skewness (**Figure 4.7**). There was no significant correlation surviving correction between behavioural preference and skewness-evoked activation in other regions. By contrast, the posterior parietal area correlating with variance did not express any differential activation that co-varied with subject-specific variance preference (masked for voxels expressing variance-related activation, no significant voxels at mask threshold 0.05 uncorrected). Note that these (very) significant correlations between skew preference and activations over subjects were completely orthogonal to the statistical tests for the activations per se (both within and between subjects). The fact that these two orthogonal (skewness related and preference related) effects co-localise lends further validity to the assertion that this insular region responds selectively to skewness.

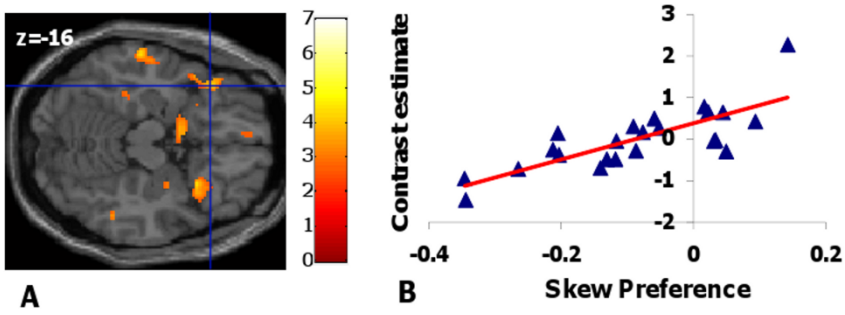

Figure 4.7 Correlation of skew-evoked activity with individual preferences. A. Within the anterior insula regions showing a correlation in signal with positive skewness, the left anterior insula shows a significant positive correlation with individual skew-preference (peak coord: -36, 24, -16; p = 0.007, small-volume corrected). B. Plot of behavioural model (MVS) skewness parameter estimate against neural contrast estimate for positive-skew related activity.

Area	L/R	MNI coordinates			Z score	P value	Cluster Extent
		x	y	z			
Anterior insula / inferior frontal gyrus	L	-36	24	-16	4.36	0.007	80
Anterior insula / inferior frontal gyrus / BA45	L	-56	18	6	4.09	0.018	38

Table 4.2 Correlation of skew-related activity with skew-preference. 2nd-level analysis of anatomical locations of regions where the strength of the skewness response correlated with subject-specific skew-preferences (estimated from MVS model). I restrict the analysis to, and perform family-wise error correction for multiple comparisons within all voxels sensitive to skewness (identified at p<0.01 uncorrected). Voxels reported at p<0.05 corrected.

4.3.2.4 *Choice-related activation*

Information about the summary statistics of a decision informs individuals' choices, hence to identify areas showing a coupling with action (i.e. reflecting gamble or sure choices), I next asked whether activation specifically within regions responsive to variance and skewness correlated with choice. There was a significant effect of choice within variance-sensitive posterior parietal cortex (gamble>sure choice; peak voxel MNI coord: 26, -60, 54; p = 0.008, cluster extent = 547 voxels, small volume-corrected for variance-related areas of activity)

(Figure 4.8), in skew-sensitive ventral striatum (peak voxel MNI coord: -8, 4, -10; p = 0.016, small volume-corrected for skewness-related areas of activity) and medial prefrontal region (peak voxel MNI coord: 6,44,18; p = 0.049, small-volume corrected for skewness-related areas of activity) (**Table 4.3**). In addition to these areas, across the whole-brain, a network of regions showed greater BOLD signal for gamble than sure choices (**Table 4.4**), including ventral striatum, prefrontal, occipital and bilateral posterior parietal cortex. No areas showed the opposite pattern (sure>gamble signal).

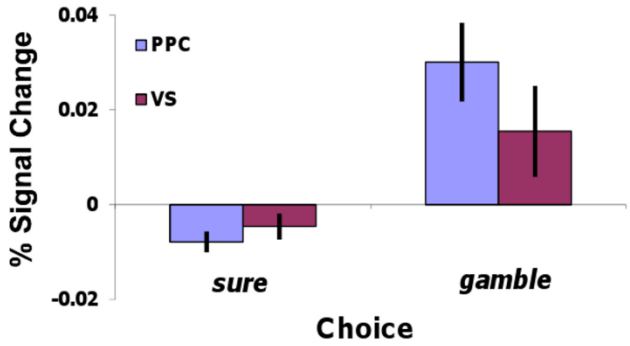

Figure 4.8 Choice-related activity. Both ventral striatum and posterior parietal cortex (PPC) show significantly greater BOLD signal for gamble versus sure choices (ventral striatum peak coord: -8, 4, -10; p = 0.016, small-volume corrected; PPC peak coord: 26, -60, 54; p = 0.008, small-volume corrected).

Area	L/R	MNI coordinates			Z score	P value	Cluster Extent
		x	y	z			
Posterior parietal cortex (variance-sensitive voxels)	R	26	-60	54	4.03	0.008	547
		30	-68	30	3.97	0.010	
		18	-62	30	3.70	0.023	
Ventral Striatum (skew-sensitive voxels)	L	-8	4	-10	3.11	0.016	39
		-16	4	-15	2.83	0.033	
Medial Prefrontal cortex (skew-sensitive voxels)	R	6	44	18	3.53	0.049	525

Table 4.3 Choice-related activity I. BOLD signal correlating with choice within variance- and skew-sensitive regions of interest. We report significant voxels at p<0.05, family-wise error corrected for regions of interest.

Area	L/R	MNI coordinates			Z score	P value	Cluster Extent
		x	y	z			
Ventral Striatum	L	-6	8	-4	4.59	<0.001	2614
Ventral Striatum	R	18	22	-2	4.40		
Middle Frontal Gyrus	R	20	40	-14	4.43		
Occipital Lobe/BA17	L	-14	-94	-8	4.34	<0.001	1742
Occipital Lobe		-26	-84	-8	4.30		
Occipital Lobe/BA18		-8	-78	-4	4.02		
Superior Parietal Lobe	L	-12	-70	40	4.20	0.001	785
Superior Parietal Lobe		-20	-60	52	3.42		
Precuneus		-16	-60	26	3.03		
Superior Parietal Lobe	R	26	-60	54	4.03	<0.001	1248
Parietal Lobe/Precuneus		20	-62	32	4.02		
Parietal Lobe/Mid-occipital gyrus		30	-68	30	3.97		

Table 4.4 Choice-related activity II: Anatomical locations of regions expressing greater BOLD signal for gamble versus sure choices. We report significant clusters surviving correction at p<0.05 (cluster-level family-wise error corrected). Peak voxel MNI coordinates within significant clusters are given, with corresponding voxel-level Z scores.

If activation correlating with choice within risk-sensitive regions influences action selection, a strong expectation is that this choice-coupled neural activity should also be modulated by individual risk-preferences. This provides an alternative mechanism for risk-preferences to influence decisions, rather than only by altering neural sensitivity to the stimulus dimensions of variance and skewness., as I highlighted in **Chapter 2**. For example, in regions sensitive to variance one might predict an enhanced correlation of BOLD signal with choice (gamble>sure) in more variance-averse individuals. Within the variance-sensitive posterior parietal cortex region, I observed just such an effect (peak voxel MNI coord: 36, -58, 42; p=0.035, cluster extent =656 voxels). Thus, for subjects with strong variance aversion there was greater activation for a gamble choice than a sure choice (**Figure 4.9A&B**). Clusters in right supplementary motor area (SMA), posterior cingulate, and occipital lobe also showed a similar relationship (**Table 4.5**). Performing the same analysis for skewness revealed that left anterior insula and right mid-insula express a positive correlation between choice and skew-preference (peak voxel MNI coord: -24, 22, -6; p = 0.033, small-volume corrected, cluster extent = 666 voxels) (**Figure 4.9C&D**, **Table 4.6**). Moreover, the same right insula region showing an interaction between choice activity and skew-preference also showed a

positive correlation with variance-preference (at voxel MNI coord: 46, -4, -14; p=0.040 small volume corrected for skew-sensitive voxels), suggesting that right anterior insula activity integrates both variance- and skew-preferences to influence choice.

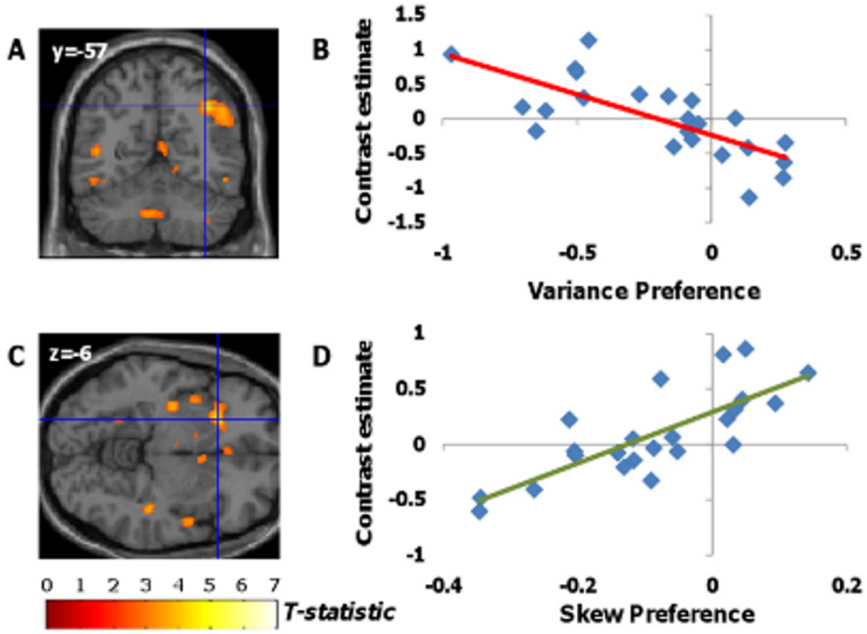

Figure 4.9 Coupling of choice and neural activity in PPC and anterior insula depends upon subject-specific risk-preferences. A. Correlation between PPC activity for choice (gamble>sure) and individual variance-aversion (peak coord: 36, -58, 42; p=0.035, whole-brain corrected). B. Contrast estimate (for gamble>sure choice), from peak coordinate (indicated by cross-hairs), correlated with behavioural variance preference parameter, with greater activity for gamble vs sure choices in variance-averse individuals, but greater activity for sure vs gamble choices in variance-seeking individuals. C. Correlation between anterior insula activity for choice (gamble>sure) and individual skew-preference (peak coord: 36, -58, 42; p=0.035, small-volume corrected). D. Contrast estimate (for gamble>sure choice), from peak coordinate (indicated by cross-hairs), correlated with behavioural skewness-preference parameter, with greater activity for gamble vs sure choices in positive skew-seeking individuals. Within this cluster, there was also a significant correlation between variance-seeking and choice-related activity (at coord: 46, -4, -14; p=0.040, small volume corrected for skew-sensitive voxels).

Area	L/R	MNI coordinates			Z score	P value	Cluster Extent
		x	y	z			
Superior Frontal Gyrus / Supplementary Motor Area	R	6	20	58	4.10	0.014	790
		6	34	38	3.28		
		8	24	36	3.73		
Posterior Cingulate / BA29	L	-2	-38	20	3.76	0.026	699
Occipital Lobe / Lingual Gyrus	R	20	-72	0	3.43		
Occipital Lobe - Cuneus	R	12	-70	6	3.36		
Posterior Parietal Cortex / BA40	R	38	-58	42	3.67	0.035	656
	R	48	-58	40	3.14		
	R	30	-66	34	3.13		
Anterior insula / inferior frontal gyrus	R	46	-4	-14	3.31	0.040†	57

Table 4.5 Interaction between choice and variance-preference. Regions where neural response to choice (gamble>sure) correlated with individual variance-preference. I report significant clusters at p<0.05 family-wise error whole-brain corrected. Peak voxel MNI coordinates within significant clusters are given, with corresponding voxel-level Z scores.

Area	L/R	MNI coordinates			Z score	P value	Cluster Extent
		x	y	z			
Anterior Insula / Inferior Frontal Gyrus	L	-24	22	-6	3.78	0.033	666
		-10	12	-12	3.29		
		-38	4	-4	3.11		
Insula / Superior Temporal Gyrus	R	54	-4	-12	3.60	0.039	643
		52	2	-2	3.59		
		46	-8	-14	3.53		

Table 4.6 Interaction between choice and skew-preference. Regions where neural response to choice (gamble>sure) correlated with individual skew preference. I report significant clusters at p<0.05 family-wise error corrected within regions of interest. Peak voxel MNI coordinates within significant clusters are given, with corresponding voxel-level Z scores.

4.4 DISCUSSION

This study demonstrates that during choice individuals have behaviourally distinct tastes for both the spread of possible outcomes (variance), and also the shape and asymmetry of the

outcome distribution (skewness). Moreover, the finding that these different risk dimensions have a distinct neural representation provides strong evidence that the brain adopts a 'summary statistic' approach to outcome evaluation (Rangel et al., 2008b).

4.4.1 RISK AND RISK PREFERENCES

Risk has typically been approximated by variance in previous studies (McCoy and Platt, 2005; Preuschoff et al., 2006; Tobler et al., 2007; Christopoulos et al., 2009; Tobler et al., 2009). This measure neglects other psychologically salient features, such as choices yielding a small chance of either a much better (positive skewness) or much worse (negative skewness) than average outcome (Coombs and Bowen, 1971; Harvey and Siddique, 2000; Jullien and Salanie, 2000). In contrast to alternative risk-measures focusing only on the chance of a poor outcome (e.g. downside risk (Bawa, 1975), probable loss (Fishburn, 1984)) I found that participants are influenced by both negative and positive skewness in addition to variance.

Skewness-preference permits individuals to express simultaneously a desire to gamble in a casino ('risk-seeking') and buy insurance ('risk-aversion') (Garrett and Sobel, 1999), which cannot be explained by a sensitivity to variance alone, and has been invoked to explain behaviour inconsistent with classical theory (e.g. gambling on a long-shot at the races, or buying a ticket for the National Lottery) (Golec and Tamarkin, 1998; Wang et al., 2006). Thus, I quantify a dimension not captured by variance, showing that the overall shape of a distribution of outcomes significantly drives choices and that 'risk-preference' is not a unitary measure.

On average, I find relative negative skew preference and variance aversion in the sample of participants. Here I systematically examine these separate influences by experimental design, both showing that the overall shape of the outcome distribution drives choice and independently evokes neural activity. Together this supports the idea that 'risk-preference' is not a unitary measure, either of behaviour or in terms of activity it is likely to evoke in the brain.

4.4.2 NEURAL ENCODING OF RISK

4.4.2.1 *Variance*

In line with the behavioural finding of sensitivity to different elements of risk, I also find a distributed representation of risk dimensions in the brain. Variance is linearly encoded in

posterior parietal cortex (PPC), consistent with single unit data and fMRI studies showing enhanced activity in PPC during risky decision-making (Platt and Glimcher, 1999; Huettel et al., 2005; Mohr et al., 2010a). Parietal cortex represents numerical range (Piazza et al., 2007) and expresses an interaction between number and space (Hubbard et al., 2005), which suggests that variance representation in PPC reflects an intuitively spatial evocation of the spread of an outcome distribution. This may well explain the absence of PPC activity in studies where risk is varied by altering the probability of a win, rather than presenting a range of possible outcome amounts (Preuschoff et al., 2006). While it is possible that PPC expresses an effect consequent upon psychological effects of increasing risk, such as enhanced attention (Behrmann et al., 2004), I find this effect is specific for variance rather than skewness, despite both influencing risk perception.

4.4.2.2 *Skewness*

The finding of skewness-related activity in prefrontal cortex, insula, and striatum, in effect encoding a stimulus dimension entirely independent of variance, emphasises that risk is not synonymous with variance alone. Anterior insula and dorso-medial prefrontal cortex (DMPFC) have consistently been implicated in the detection and evaluation of risk, probability, uncertainty and volatility (Critchley et al., 2001; Kuhnen and Knutson, 2005; Preuschoff et al., 2006; Behrens et al., 2007; Knutson and Bossaerts, 2007; Tobler et al., 2007; Bach et al., 2009; Christopoulos et al., 2009; Engelmann and Tamir, 2009a; Smith et al., 2009; St Onge and Floresco, 2009; Tobler et al., 2009; Bossaerts, 2010; Mohr et al., 2010b; Xue et al., 2010), and ventral striatum manifests immediate and delayed, linear and non-linear responses to probability (Preuschoff et al., 2006; Hsu et al., 2009) and a positive correlation with reward magnitude (Knutson et al., 2005; Tobler et al., 2007; Yacubian et al., 2007). Hence, previous observations on the neural basis of risk may have tapped into a combination of risk elements, while here I dissociate responses to variance and skewness.

I identify neural responses to positive skewness in ventral striatum, anterior insula, and IFG, but to negative skewness in DMPFC. This distinction parallels related findings that DMPFC encodes the probability of loss (Smith et al., 2009; Xue et al., 2010), and suggests that DMPFC may encode features of below-average outcomes in contrast to ventral striatum tracking of better than average outcomes. This finding can also explain why risk-correlation has not been reported in ventral striatum in studies where skewness has been controlled (Christopoulos et al., 2009; Tobler et al., 2009). The finding of separable anatomic regions correlating with positive and negative skewness does not predict that subjects would have distinct attitudes toward positive and negative skewness. While this is a plausible prediction I found no evidence for a separate expression of preference in these regions. The skewness

parameter from the **MVS** model reflects how much subjects value positive relative to negative skewness in a gamble. Given that I can approximate subjects' behaviour with a single skew parameter, it is equally likely that skew-preference arises from an interaction between brain areas. In order for the **MVpSnS** model to win (in terms of predicting choice), the participants would need to have very different sensitivities for positive and negative skewness, or express skewness intransitivities such as liking symmetric above any skewed gamble. It is possible that within a larger behavioural sample I would have sufficient data to demonstrate such different sensitivities for positive and negative skewness.

4.4.2.3 *Integration with risk preferences*

4.4.2.3.1 *CHANGE IN REGIONAL SENSITIVITY TO RISK*

Medial PFC and striatum are reciprocally connected (Sesack et al., 1989; Croxson et al., 2005), project to prefrontal and pre-motor areas involved in action planning and execution (Haber, 2003), as well as to insular cortex (Guldin and Markowitsch, 1983; Shi and Cassell, 1998). These connections can meditate information transmission between areas translating different features of the outcome distribution into summary statistics, and areas integrating this information with context and individual risk-preferences. This distributed network for risk evaluation echoes, for example, distributed neural processing in vision, where discrete visual dimensions (colour, motion, form), are processed in segregated networks (Courtney and Ungerleider, 1997).

Anterior insula and IFG activity is modulated by individual taste for risk, expressing greater activity for positively skewed gambles in individuals who prefer positive skewness, and showing a correlation with choice also dependent upon individual skewness and variance-preference. This suggests that anterior insula and IFG perform a risk-valuation and subsequently promote or inhibit risk-taking, consistent with previous observations (Christopoulos et al., 2009; Engelmann and Tamir, 2009a; Xue et al., 2010). I also observed greater loading for skewness than variance in anterior insula, generated by a wide range of skewness-preference in my participants, as opposed to previous studies where skewness was fixed (Christopoulos et al., 2009; Tobler et al., 2009). I also decorrelated choice from risk, whereas previous studies may have detected risk anticipation contingent on choice rather than the process of quantifying decision statistics (Kuhnen and Knutson, 2005; Preuschoff et al., 2006; Christopoulos et al., 2009; Tobler et al., 2009; Xue et al., 2010). Anticipation of chosen risk could recruit insula activity, explaining consistent reports of (risk-attitude dependent) activity in this region.

4.4.2.3.2 *MODULATION OF CHOICE-RELATED ACTIVATION*

PPC and ventral striatum activity also correlated with choice, with activation in PPC dependent upon the degree of variance-aversion, corroborating previous findings (Weber and Huettel, 2008a). Striatum responded to both positive skewness and gamble choice, although subjects mostly avoided positively skewed gambles. One possibility here is that striatum could encode statistical properties of a gamble and independently engender action following integration of risk-preferences and statistical information. Note that variance preferences are also significant in driving choice, hence could also influence striatal activity. Alternatively, striatum could exert a negative influence on the choice to gamble. The pattern of activity I observed would be expected in a region inhibiting risky choice, as the strongest coupling occurs in individuals who are most variance-averse. This region overlaps the medial intraparietal area, integral to motor intention (Grefkes et al., 2004; Andersen and Cui, 2009), thus parietal cortex might promote safe choices via polysynaptic links to basal ganglia and premotor regions (Tanne-Gariepy et al., 2002; Clower et al., 2005). The PPC has direct connections with insula (Cavada and Goldman-Rakic, 1989), thus may also directly pass quantitative information about variance to anterior insula for integration with other statistics and an emotional response.

4.4.3 SUMMARY

In this study, I considered two plausible ways in which individual preferences could modulate neural activity. I first find preferences modulating stimulus-evoked activity, with individuals with stronger preference for skewness demonstrating increased insula sensitivity to skewness. Secondly, I show variance and skewness preferences modulate action-related neural activation, as individuals with stronger preferences have greater coupling between neural activity and choice within risk-sensitive regions. Overall, this provides evidence that preferences modulate both stimulus-evoked and choice-related activity.

Chapter 5

PROSPECTIVE DECISION MAKING UNDER RISK

5.1 INTRODUCTION

In **Chapter 4**, I provided behavioural and neural evidence to support the idea that key components of an outcome distribution, such as variance and skewness, are explicitly encoded in the brain. However, this study and previous experiments focus on immediate returns from single choices (Knutson et al., 2005; Abler et al., 2006; Yacubian et al., 2006; Elliott et al., 2008; De Martino et al., 2009) leaving a relative dearth of knowledge about sequential choice. Many everyday situations require agents to generate a chain of actions (a path through a decision-tree), leading to a distribution of outcomes, which engenders uncertainty. This is a focus in ecology, where animals forage to ensure intake exceeds minimal need constraints (Stephens et al., 2007), and in finance where traders reap bonuses by exceeding a target return from sequential tranactions (Panageas and Westerfield, 2009). Common to these examples is that the distribution of possible outcomes (energy, money) differs for each available series of choices.

Selecting serial actions from a set of strategies thus requires integration of immediate decisions with overarching goals, and poses two separate problems. Firstly, do humans evaluate the distribution of outcomes when planning choice? Secondly, do individuals assume 'optimal' future choices when making sequential decisions? These are closely linked in the decision process, as the anticipated distribution of outcomes will depend upon (i.e. be contingent upon) anticipated future choices.

In game theory and classical dynamic programming, decision-makers' strategies under every contingency are described by a set of actions which maximize subjective value ('utility'). In sequential choice these utilities are called *continuation values*, as action-values are contingent upon following a future strategy. Thus, in assigning continuation values, decision-

makers must make assumptions about the type of future choices they will make. Standard dynamic programming constrains decision-makers to invoke only optimal choices in the future (optimal continuation value: OCV). Critically, an optimal strategy can be planned in advance, implying that "online" updating is irrelevant or irrational (dynamically inconsistent) in the absence of new information (Dekel et al., 1998; Epstein and Schneider, 2003). An OCV decision-maker, when presented with decision 1 followed by decision 2, makes the same set of choices even if the order is reversed (as long as no new information is presented until after choices are made).

However, decision-makers can assign utilities to options assuming that they might *not* take the optimal choice in the future. This might occur if choices became unexpectedly constrained, when planned strategies would no longer be available. All available strategies (rather than just the pre-planned 'optimal' strategy) are taken into account before each choice, for example by assuming that future choices are distributed randomly (average continuation value: ACV). This entails that strategies are dynamically re-evaluated and action-values recalculated depending on which strategies are available. This scenario allows for dynamic inconsistency, where future choices can depend upon the order in which options are presented.

Here, I tested different models of strategy valuation and planning, simultaneously acquiring neural data (using fMRI). I hypothesised that neural activity evoked in single-shot decision paradigms would also support decision variables mediating sequential choice.

5.2 METHODS

5.2.1 BEHAVIOURAL EXPERIMENT

The study was approved by the Institute of Neurology (University College London) Ethics Committee. 17 subjects (age range 22-36; 7 male) participated; one dropped out from scanning because of claustrophobia and was excluded from analysis. Monetary earnings were between £18 and £28, including a fixed £10 participation fee. Stimuli were presented on a standard PC using Cogent presentation software (Wellcome Trust Centre for Neuroimaging, London) run in MATLAB (version 6.5, MathWork, Natick, MA). Choices were made by keypress selections on the computer keyboard of a standard personal computer.

5.2.1.1 ***Task***

I implemented a simple computerized sequential gambling task, where subjects were required to make serial choices between a sure or risky alternative (**Figure 5.1**).

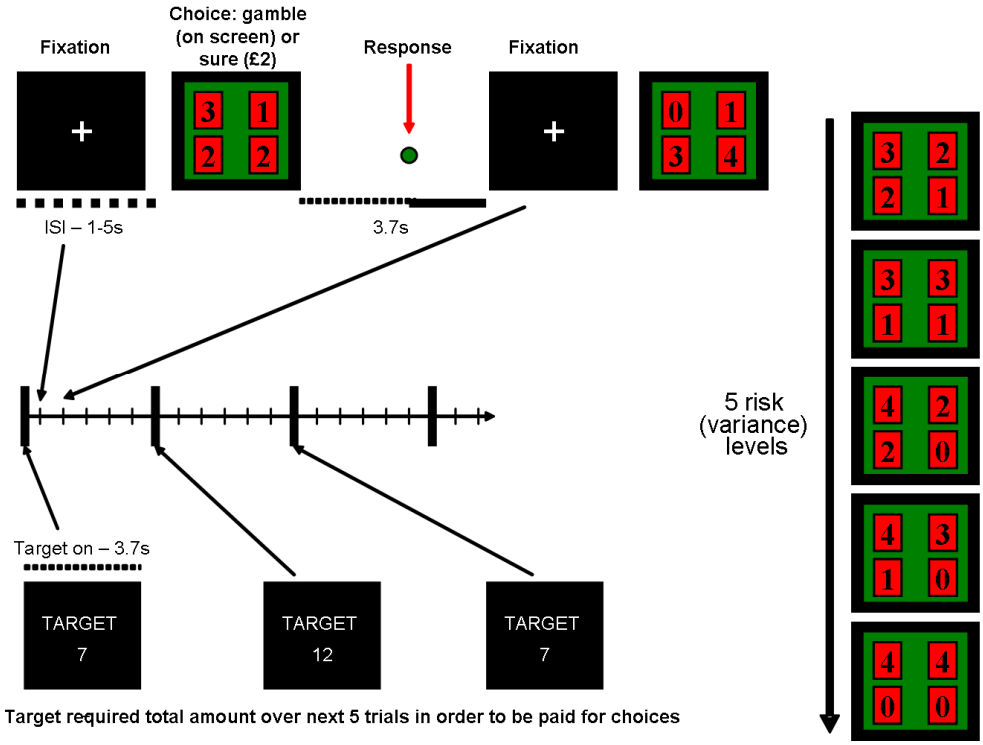

Figure 5.1 Task structure and timings. Trials were grouped into blocks of five. To commence each block, a financial target appeared on the screen for 3.7s (Four levels for behavioural experiment outside scanner – 5, 9, 11, 13; Two levels inside scanner – 7, 12). A fixation cross was shown at the beginning of each trial for 1-5s (jittered). A lottery then appeared on the screen, and subjects had up to 3.7s to indicate by button press their choice (gamble or £2 for sure). Lotteries were represented by four red cards, with numbers (0, 1, 2, 3, or 4) indicating monetary values in pounds, each with a probability of 0.25 of being selected. A computerised random number generator was used for selection; subjects were shown the selected trial and block outcomes. Total earnings were the summed total return from the 10 selected trials.

Lotteries were shown as 4-card arrays. Subjects chose to gamble, or alternatively select a fixed, sure amount of £2 on each of 5 trials in a block. Card numbers (0, 1, 2, 3, 4), indicate monetary values (£). I used 5 different card combinations, generating 5 lotteries with equal and matched expected value of £2, but with different variance. Five lotteries were offered in each block and the sure amount was fixed throughout. On each block, the same 5 lotteries were presented once, using a randomised order of presentation, necessary if one is to detect dynamically

inconsistent choices. Subjects were paid based upon 10 randomly selected individual trials, contingent upon reaching the target amount in the block.

I imposed different financial targets per block, to alter the distribution of outcomes. Note that the outcome or value of each block is quantitatively determined by the target level, in that rewards were withheld if the target level was not attained. This has a profound effect on valuation and allowed us to manipulate the outcome distribution in a simple experimental way. No feedback on trial-by-trial outcomes was given. Eliminating feedback enabled us to distinguish whether individuals adhere to a predetermined strategy, irrespective of the particular sequence in which the options are presented (consistent with classical dynamic programming models where choices are made based upon the optimal continuation value), or if they continuously re-evaluate, taking into account a range of available strategies on each trial.

I provided instructions with a 15 minute verbal tutorial and a practice run of 5 blocks (with full feedback, but only for the practice session), to ensure that subjects understood the paradigm. Subjects were told that 10 trials would be randomly selected at the end of the experiment from all sessions (inside and outside scanner) where all trials had an equal chance of being picked. For selected trials, if the required target had been reached in that block, the outcome of that trial would be paid out (i.e. 10 *trials* are chosen to determine pay, contingent on whether the target was reached at the end of each *block*). This would be £2 if they had picked the certain fixed amount or whatever the outcome of the lottery (determined by a random selection of one of the four cards), if they had chosen to gamble. If the target had not been reached, then no money would be won from the trial irrespective of choice.

5.2.1.2 ***Analysis***

I initially categorised trials by two factors, current target level and the variance (risk) of lottery presented. These data were assessed by analysis-of-variance (ANOVA) and multiple regression implemented in SPSS (SPSS for Windows, Rel. 12.0.1. 2001. Chicago: SPSS Inc.).

I then analysed choices by block. There are $2^5 = 32$ possible combinations of choices in each block, and I refer to each of these combinations or trajectories of choices, as a strategy *s*, (s = 1…S), where S indexes the total possible number of choice combinations (S = 32 on trial 1, S =

16 on trial 2 etc.). The frequency with which each strategy was chosen was compared to simulated strategy choice frequencies by χ^2-test.

I fit stochastic choice, prospective (continuation value) utility models to behaviour with the method of simulated moments (McFadden, 1989), comparing non-nested models with Hansen's statistic (Hansen, 1982). This estimation is based on comparing observed frequencies of choices with simulated frequencies, derived from an underlying structural model. Free parameters were optimised with a non-linear simplex search algorithm in MATLAB 7.0. I selected the best-fitting model and assessed relative model performances by a comparison of criterion values on an individual subject basis.

5.2.1.3 ***Behavioural modelling***

The behavioural models have two components - a model of valuation and a model of how future choices are incorporated. These models specify how strategies are compared, and which strategies impact upon the value of the current choice (to gamble or not to gamble).

On the first trial in a block, there are 16 possible strategies given a choice to gamble, and 16 possible strategies given a choice of the sure amount. This reflects the fact that there are five ordered binary choices between a lottery and a certain payout, so 32 (2^5) possible sets of choices are available in any given block. Each of these strategies has its own outcome distribution. Note that the set of available strategies reduces as sequential choices are made, such that by the fifth trial in a block only two possible alternative strategies are available (to gamble or opt for the sure outcome). In other words, the set of possible strategies at any given trial is contingent upon previous choices in the block, and the order in which the gamble options have been presented.

5.2.1.3.1 VALUATION MODEL

I implemented a mean-variance-skewness model, assigning values (utilities), $V_{s,t}^{h}$, to available ***strategies*** *s = 1...S*, on each ***trial*** *t = 1…T,* for every ***target level*** *h = 1...H*. The set of strategies evaluated are contingent upon previous choices in each ***block*** *m = 1...M*. For example, on ***trial*** *t=4,* there will be four possible available strategies to evaluate, given a certain sequence of simulated or actual choices for ***trials t =****1,2,3.* Each of these strategies will generate their own distribution of possible numerical outcomes. The probability distribution of outcomes for each strategy will alter dependent upon ***target level*** *h*.

Let $\mathrm{B}_{s,t}^{h}$ comprise the set of discrete outcomes given strategy *s* on trial *t,* where $\mathrm{B}_{s,t}^{h}(j)$ indexes the *j*th outcome from this set, and $P_j\left(\boldsymbol{B}_{s,t}^{h}(j)\right)$ indicates the probability of the *j*th outcome.

With this formulation, strategy value on trial *t* is specified as:

$$V_{s,t}^{h} = \mathrm{E}\left(\mathrm{B}_{s,t}^{h}\right) - \rho \cdot Var\left(\mathrm{B}_{s,t}^{h}\right) + \lambda \cdot Skw(\mathrm{B}_{s,t}^{h}) \qquad \textbf{(5.1)}$$

$\mathrm{E}\left(\mathrm{B}_{s,t}^{h}\right)$ denotes the expected (mean) value of the distribution of outcomes from strategy *s*:

$$\mathrm{E}\left(\mathrm{B}_{s,t}^{h}\right) = \sum_{j} P_j\left(\boldsymbol{B}_{s,t}^{h}(j)\right) \cdot \mathrm{B}_{s,t}^{h}(j) \qquad \textbf{(5.2)}$$

$Var\left(\mathrm{B}_{s,t}^{h}\right)$ denotes the variance of the outcome distribution:

$$Var\left(\mathrm{B}_{s,t}^{h}\right) = \sum_{j} P_j\left(\boldsymbol{B}_{s,t}^{h}(j)\right) \cdot \left[\boldsymbol{B}_{s,t}^{h}(j) - \mathrm{E}\left(\mathrm{B}_{s,t}^{h}\right)\right]^2 \qquad \textbf{(5.3)}$$

and $Skw\left(\mathrm{B}_{s,t}^{h}\right)$ denotes the (unstandardised) skewness of the outcome distribution:

$$Skw\left(\mathrm{B}_{s,t}^{h}\right) = \sum_{j} P_j\left(\boldsymbol{B}_{s,t}^{h}(j)\right) \cdot \left[\boldsymbol{B}_{s,t}^{h}(j) - \mathrm{E}\left(\mathrm{B}_{s,t}^{h}\right)\right]^3 \qquad \textbf{(5.4)}$$

As in **Chapter 4**, ρ is a coefficient reflecting aversion to variance in outcomes and λ reflects the degree of positive skew seeking behaviour.

The main results focus on the mean-variance-skewness valuation model. For completeness, I also tested alternative utility models paralleling those in **Chapter 4**, although it is important to note that here these models are not directly statistically comparable as they are non-nested with a different number of parameters.

An expected utility model (EUT) was specified as:

$$V_{s,t}^{h} = \sum_{j} P_j\left(\boldsymbol{B}_{s,t}^{h}(j)\right) \cdot \frac{\left[\boldsymbol{B}_{s,t}^{h}(j)\right]^{1-\rho}}{1-\rho} \qquad \textbf{(5.5)}$$

ρ reflects the curvature of the power utility function, and hence risk aversion.

Prospectic utility (PT) was specified as :

$$V_{s,t}^{h} = \sum_{j} P_j\left(\boldsymbol{B}_{s,t}^{h}(j)\right) \cdot \Delta_{\boldsymbol{B}_{s,t}^{h}(j)\geq R} \frac{\left|\boldsymbol{B}_{s,t}^{h}(j) - R\right|^{1-\rho}}{1-\rho} \qquad \textbf{(5.6)}$$

Where $\Delta_{\{A\}c}$ is a step function (=1 if A is true, = -1 if A is false), *R* is the reference point (I set *R* = 10, the summed expected value of the five lottery proposals within a block), and ρ reflects the curvature of the utility function. In this simplified version of prospect theory, I have no probability weighting and risk seeking for losses is of the same level as risk aversion for gains.

Here I did not implement more complex variants of prospect theory with differential weighting of relative losses and gains, or other variants of decision models, as MVS model incorporates aspects of this behaviour while being much easier to fit (because it is linear in its arguments).

5.2.1.3.2 CONTINUATION VALUE MODELS

To simulate choice**,** the continuation value models perform a tree-search of all possible choice (action) and outcome (state) combinations from current ***trial*** *t* to the end of each simulated ***block***. This search is contingent on (i.e. constrained by) previous choices. I recalculate the value of available strategies on each ***trial***, and as the ***block*** proceeds, the number of possible strategies available reduces such that by ***trial*** *t*, there will be 2^{6-t} possible strategies remaining.

For a given target, several strategies can lead to similar distributions of outcomes. However, strategies will differ in their outcomes depending upon the target level. Moreover, a critical feature for all these decision rules is that subjects' previous choices within a block determine the remaining available strategies to be evaluated. These models assume that the full space of possible actions and outcomes is known. I make this simplifying assumption in order to

render model estimation tractable (i.e. specifically I do not incorporate uncertainty about future options). This is not unreasonable, given that the task has a simple repeating structure with the same five lotteries being presented on each block throughout practice, behavioural, and scanning sessions.

5.2.1.3.2.1 Optimal continuation value (OCV)

Agents pre-determine a specific policy, representing the outcome distribution from their optimal strategy on each trial (i.e. a prospective decision-maker making choices consistent with a classical dynamic programming model). Thus, OCV prescribes the choices for a prospective decision-maker who acts in accordance with classical dynamic programming principles, and is oblivious to the order in which options are presented.

I assign action values (Q) to the binary options (gamble (specified as Q^1) or sure (specified as Q^0)), calculated on every trial, as the decision-maker progresses through the decision tree. These two action values are then compared to determine a simulated choice.

$$Q^0 = V^h_{\bar{s},t} \;\; where \;\; \bar{s} = \underset{s}{\text{argmax}}\{V^h_{s,t} \big| \text{sure choice}\} \qquad \textbf{(5.7)}$$

$$Q^1 = V^h_{\bar{s},t} \;\; where \;\; \bar{s} = \underset{s}{\text{argmax}}\{V^h_{s,t} \big| \text{gamble choice}\} \qquad \textbf{(5.8)}$$

s indexes the possible continuation trajectories (available strategies), or branches of the decision tree. Note that the OCV will remain the same on every trial within a block when a subject adheres to the strategy selected at block outset. In the case of a deviation from an optimal trajectory, the next best (utility maximising) strategy is taken from the remaining options available. Importantly, in the case of these deviations, the OCV model prescribes that appropriate correction is taken based on always trying to follow the utility-maximising strategy.

5.2.1.3.2.2 Average continuation value (ACV)

This model entails that agents calculate the average value or utility of each of the two alternative choices on each trial (i.e. choosing to gamble or take the sure amount), rather than forecasting with respect to optimal continuation trajectories. This model does not require that agents have an explicit plan of future choices, and is akin to a model where the current choice is made under an assumption that choices are made randomly for the rest of

the block. Every possible strategy impacts upon current continuation values. As such, the decision maker can be thought of as myopic.

$$Q^0 = \frac{1}{S}\sum_{s=1}^{S}\left\{V_{s,t}^h \middle| \text{sure choice}\right\} \quad \textbf{(5.9)}$$

$$Q^1 = \frac{1}{S}\sum_{s=1}^{S}\left\{V_{s,t}^h \middle| \text{gamble choice}\right\} \quad \textbf{(5.10)}$$

5.2.1.3.2.3 Sure continuation value (SCV)

This model assumes agents weigh up the current choice against a benchmark of taking the sure option for the remainder of the block. This implements a simple heuristic where the choice to gamble or take the sure amount is made given a fixed benchmark.

$$Q^0 = V_{\bar{s},t}^h \ \ where$$
$$\bar{s} = \left\{V_{s,t}^h \middle| \text{sure choice for trial} = t, \ldots, 5\right\} \quad \textbf{(5.11)}$$

$$Q^0 = V_{\bar{s},t}^h \ \ where$$
$$\bar{s} = \left\{V_{s,t}^h \middle| \text{gamble choice for trial } t, \text{ sure choice for trial} = t+1, \ldots, 5\right\} \quad \textbf{(5.12)}$$

where *t* indexes the current trial in the block.

5.2.1.3.3 NUMERICAL EXAMPLE

I provide a simple numerical example of how these models work in practice (**Figure 5.2**). Imagine you are faced with a 2-stage sequential decision between a gamble (g) and a sure amount (s) of money fixed at £2. The first decision (decision X) is whether to accept a 50:50 gamble giving either £4 or £1. The second decision (decision Y) is whether to accept a gamble giving a 75:25 percent chance of winning £3 or £0, or again opting for a sure amount of £2. There are 4 possible strategies to consider (ss, sg, gs, gg combinations, which I refer to as strategies A, B, C, D), each giving a different distribution of outcomes. In these models, these distributions are evaluated according to a utility function (U), to give 4 separate numbers, or utilities, one per strategy.

I now assign numbers to these utilities for illustrative purposes: U(ss) = 10; U(sg) = 8; U(gs) = 4; U(gg) = 7. Imagine now having to choose a current action. If you were an 'optimal' decision maker you would compare the highest utilities given each choice (in this case U(ss) for a sure choice, U(gg) for a gamble choice). As U(ss)>U(sg)>U(gg)>U(gs), you prefer to make a sure choice on the current trial. For the next decision, you again make a sure choice, now comparing U(ss) = 10 vs U(sg) = 8. Thus, you have selected strategy A. What if you are a decision-maker conforming to an average continuation value model? In this case, you weigh up the average utility of outcomes from each current choice (i.e. you compare (U(ss) + U(sg))/2 = 9 to (U(gs) + U(gg))/2 = 5.5). In this example, you also prefer to make a sure choice (as U(s, ·) > U(g, ·)). For the subsequent decision, you compare U(ss) = 10 and U(sg) = 8, and again make a sure choice, following strategy A.

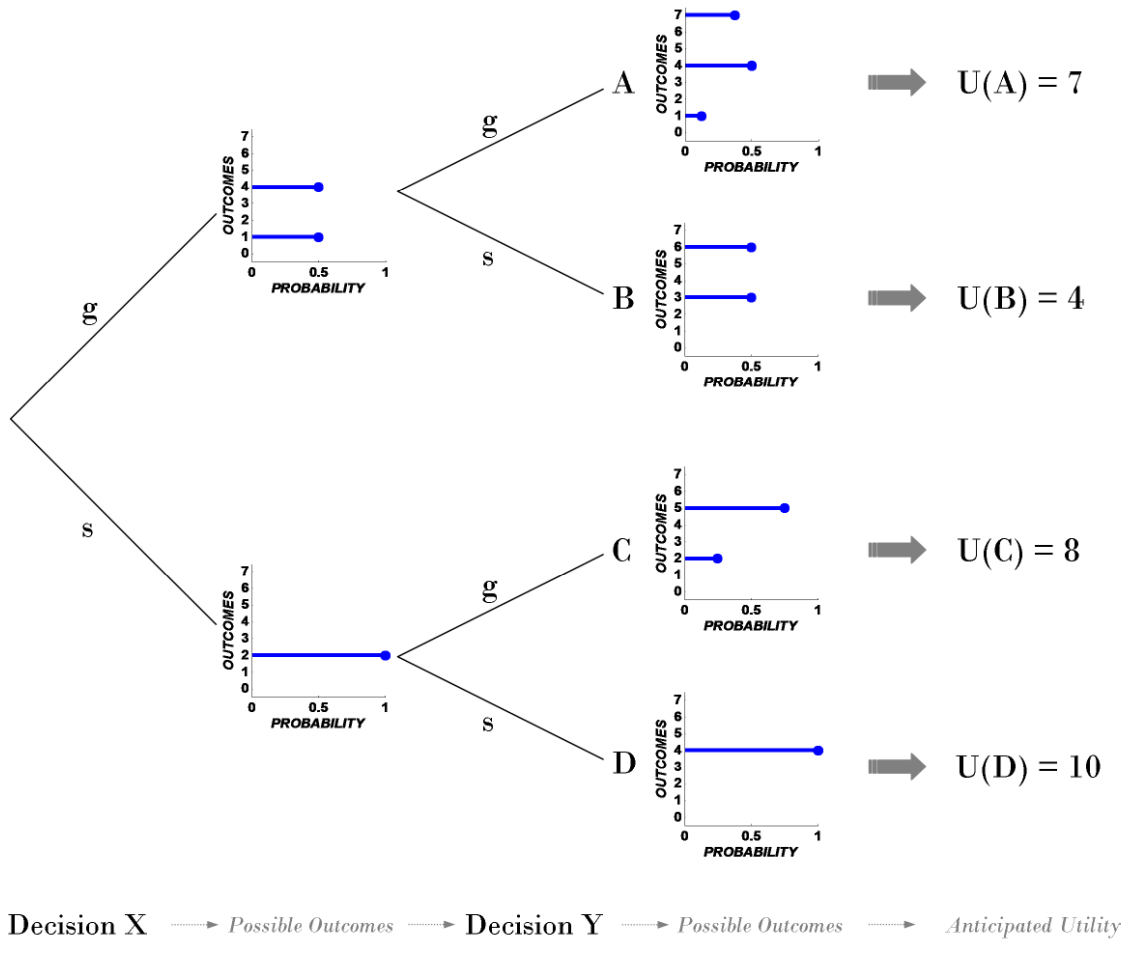

Figure 5.2 A two-stage decision example I. Numerical example of a two-stage decision.

Now let us consider a situation where the order of decisions is reversed (**Figure 5.3**). There remain 4 strategies, but their order has changed such that we have: U(ss) = 10; U(sg) = 4;

U(gs) = 8; U(gg) = 7. If you are an optimal continuation value decision maker you choose the sure option as U(ss)>U(sg)>U(gg)>U(gs), followed by another sure option (as U(ss)>U(sg)). The order has no effect upon the ranking of the strategies and you make a dynamically consistent choice by following strategy A again. If you are an average continuation value decision maker you will compare (U(ss) + U(sg))/2 = 7 to (U(gs) + U(gg))/2 = 7.5, and pick the gamble choice initially. On the next decision, you make a sure choice, as U(gs)>U(gg), such that now you follow strategy B, and have made a dynamically inconsistent choice as the order in which the options are presented has affected choices.

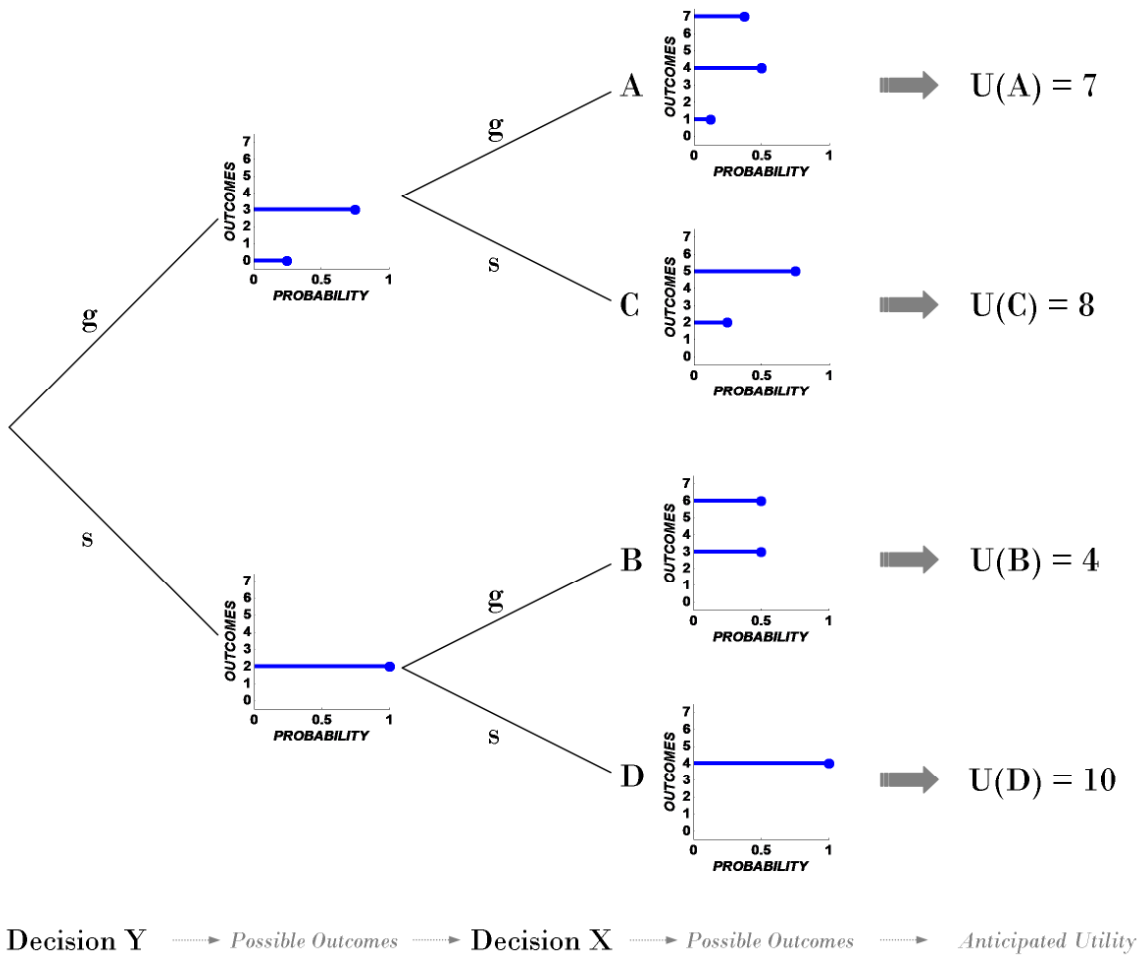

Figure 5.3 A two-stage decision example II. Numerical example of a two-stage decision in reversed presentation order.

A sure continuation value decision maker would make a consistent choice in this example, where the 'sure, sure' strategy A has the highest utility, but also can make dynamically

inconsistent choices if this is not the case. The actions actually selected (and whether they will be dynamically consistent) will depend in practice upon the specific utilities assigned to the available choices by the decision-maker.

Note that in these models, order-independence (dynamic consistency) only holds if there is no new information arriving, which is the case in this experiment in which no trial-by-trial feedback is given. Also that these models reflect different methods of valuation and planning (i.e. an anticipated selection of choices), rather than testing execution of a pre-formed plan (i.e. self-consistency).

5.2.1.3.4 ACTION SELECTION

I account for randomness in choice by the addition of noise at action selection (modelled by a logistic choice function (see **Chapter 2** and **Chapter 4**). In other words, I add simulation-specific noise ε, on each valuation. Choice is then determined as:

$$\begin{cases} If\ P_{choose\ gamble} - \varepsilon > 0 \implies choose\ gamble \\ If\ P_{choose\ gamble} - \varepsilon \leq 0 \implies choose\ sure \end{cases} \quad \textbf{(5.13)}$$

In fact, subjects do not choose neatly in accordance with either logit or probit (i.e. Gaussian) noise, the two most commonly used functions, as these require that suboptimal choices are chosen in proportion to how far their values are away from the optimum. Generally, subjects are less diversified in their exploration of alternative strategies than predicted by either logit or probit, although their aberrant choices can deviate widely from the optimum. However, this is better approximated by a logistic function, where noise follows the Gumbell or double exponential distribution,, than a probit function where noise is normally distributed, as the former has fatter tails and therefore can accommodate more deviant choices. Within this model-space, by always using the same noise distribution, I can compare relative fitting behaviour. Any deviation from this noise model will count against our ability to discriminate neural activity correlating with these model components.

5.2.1.3.5 MODEL ESTIMATION

I based the model estimation on a comparison of the observed frequencies of block-by-block choices (i.e. strategies) with simulated frequencies, derived from each of the underlying structural models outlined above. The models generate a choice per trial per simulated block

(using the probabilistic action selection rule), from which I calculate the simulated frequencies (φ) with which each strategy is chosen. I ran 1200 simulated blocks per model, across all 6 target levels, with a randomised trial order per block. These simulated frequencies are then compared to actual observed choices (*z*), using the method of simulated moments (McFadden, 1989). *z(i)* is a vector of choices over available strategies on block *i*, with its elements taking the value 1 for the chosen strategy, and 0 otherwise.

$$y_i = z(i) - \varphi \qquad \textbf{(5.14)}$$

$$D = \min_{\vartheta} \left[\frac{1}{N}\sum_{i=1}^{N} y_i\right]' \Omega^{-1} \left[\frac{1}{N}\sum_{i=1}^{N} y_i\right] \qquad \textbf{(5.15)}$$

Where y_i is a vector of observations from one block *i* (observed – simulated frequencies), Ω is a weighting matrix, and *D*, the criterion function, is the weighted sum-of-squares difference between the observed and simulated frequencies across all blocks (*i* = 1, …, N). Optimisation of *D* (which finds the best fitting set of parameters θ), is carried out in a two-step procedure. Initial unweighted estimates are derived with Ω = **I** (identity matrix). A weighted optimisation is then performed. To estimate the precision of the observations, I calculate the covariance matrix (Ω) of the differences between simulated and observed frequencies that come out of an unweighted optimisation.

$$\Omega = \frac{1}{N}\sum_{i=1}^{N}\left[y_i - \frac{1}{N}\sum_{i=1}^{N} y_i\right]\left[y_i - \frac{1}{N}\sum_{i=1}^{N} y_i\right]' \qquad \textbf{(5.16)}$$

In order to make Ω invertible, it is necessary to aggregate unchosen strategies, otherwise the weighting matrix is rank-deficient. The estimated precision is then the inverse of this covariance matrix (Ω^{-1}). I weight observations according to this precision in performing the weighted optimisation to calculate an unbiased estimator. This method of moments criterion function *D* is not differentiable in the parameters (there are step changes in the value of the function as the parameters vary), hence this necessitates the use of a non-linear method to optimize the parameters with respect to the criterion function *D* (by using the Nelder-Mead simplex algorithm implemented in Matlab). I use the method of simulated moments to optimize the models because the problem of multinomial sequential choice is high-dimensional and computationally difficult to integrate. This means that we cannot easily use Bayesian methods to get a measure such as the Bayesian information criterion. In these

circumstances, the method of simulated moments provides a robust way of optimizing models, and the criterion function acts as a likelihood estimate that allows comparison of the model-space.

The optimized criterion value *D* is a direct measure of the residual sum of squared error of each model. *D* (multiplied by the number of observations) is χ^2-distributed (Hansen's J statistic) (Hansen, 1982). Relative model likelihoods calculated from χ^2 statistics are not comparable for non-nested models. However, to the extent that the number of parameters are equal (for a given utility and noisy choice model), criterion values can be directly compared. Hence inverse criterion values (D^{-1}), reflecting relative goodness-of-fit, were directly compared for best fitting models on an individual subject basis.

5.2.2 FUNCTIONAL MRI

All subjects had previously completed the behavioural experiment, and understood that the task structure and presented lotteries were identical. I used two target levels during scanning (7 and 12). Visual cues were projected onto a screen, visible via an angled mirror mounted on the MRI head coil. Choices were indicated by pressing a button box with the right index finger, and responses recorded using Cogent presentation software.

5.2.2.1 *FMRI - scanning parameters and preprocessing*

The general procedure and imaging sequence was identical to **Chapter 4**. The imaging parameters were: 48 oblique transverse slices; slice thickness, 2 mm; gap between slices, 1 mm, repetition time TR=3.1s; echo time TE=30ms; field of view FOV=192×192 mm^2.

I employed a slightly different model of neural responses to **Chapter 4**. To capture all variance of interest (i.e. the modulation of neural response preceding each choice), δ functions were placed half-way between the onset of the presentation screen and the subsequent keypress response, and I include first order temporal derivatives to ensure that coupled neural activity within a +/-2s window should be captured by the canonical HRF (Friston et al., 1998b). This also avoids the need to constrain the model by making predictions concerning the timing of the neural responses to the different regressors.

The contrasts of interest purely concern responses parametrically modulated by specific stimulus dimensions, reflecting activity independent of the regressors modeling non-specific responses to stimulus presentation. Covariates of no interest comprised the onsets of the target screens and subject-specific realignment parameters from the image preprocessing to account for motion-related artifacts in the images that were not eliminated in rigid-body motion correction. BOLD data from blocks in which a response had been missed were factored out by explicitly including a regressor for these error trials. All data were analysed using Statistical Parametic Mapping software (SPM5; Wellcome Trust Centre for Neuroimaging, UK). Trial-type specific beta values of linear contrasts were estimated, and these were entered into t-tests using random-effects analysis to provide group statistics.

I report results with small volume correction for regions of interest dictated by prior studies at $p<0.05$ (svc: a 6mm radius sphere centered upon a priori coordinates) and at a threshold of $p\leq0.001$ uncorrected (unc).

5.3 RESULTS

5.3.1 BEHAVIOURAL

5.3.1.1 *Trial-by-trial choices*

I first analysed subjects' choices in terms of a decision to gamble or opt for the sure amount, on a trial-by-trial basis, across all sessions (inside and outside scanner). I observed a linear relationship between risk (variance) of an individual gamble, and the percentage of time that subjects chose the gamble over the sure alternative (**Figure 5.4**). A repeated-measures analysis of variance demonstrated a significant main effect of both riskiness of each gamble, $F(2.86,42.95) = 2.88$, $P = 0.049$, (Greenhouse-Geisser corrected degrees of freedom, $\varepsilon = 0.72$; Mauchly's test for sphericity: $\chi^2(9) = 19.49$, $p<0.05$), and target level, $F(5,75)= 16.32$, $P < 0.001$ (within-subjects contrasts; negative linear effect of risk – $F(1,15) = 9.64$, $P = 0.007$, $r = 0.63$; linear effect of target – $F(1,15) = 42.37$, $P < 0.001$, $r = 0.86$; Fig. 2). There was also a significant interaction between risk and target level, $F(20,300) = 2.72$, $P < 0.001$), such that at higher target levels the slope of the linear relationship was reduced. There was no tendency for subjects to be more risk seeking at the beginning or end of the blocks, with neither a linear or quadratic effect of time-point within a block on the probability of choosing to gamble (risk x target level x time ANOVA; linear contrast: beta = -0.023, $r^2 = 0.001$, $p = 0.679$, quadratic contrast: $p = 0.42$).

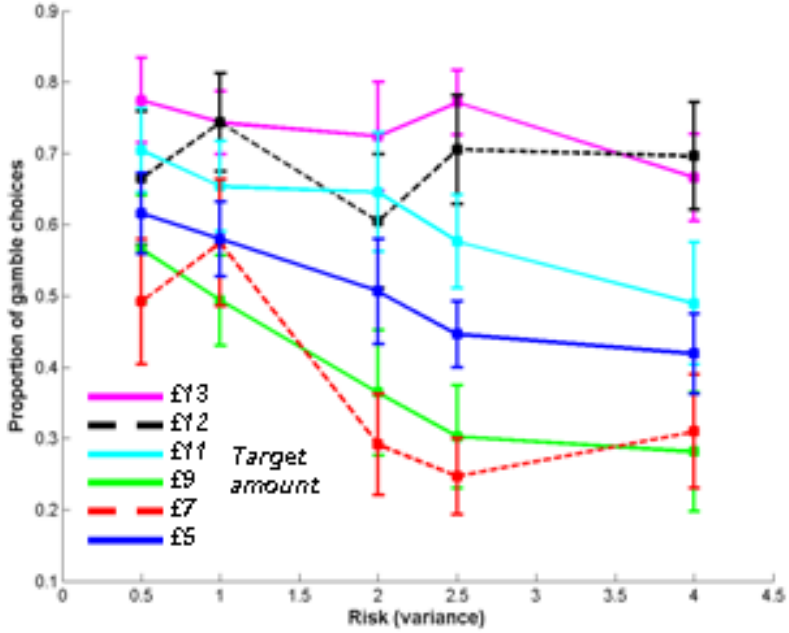

Figure 5.4 Analysis of trial-by-trial choices. Graph showing the proportion of time that the gamble option was selected overall, for each of the five presented lotteries (Abscissa is the variance of each individual lottery in [pounds]^2). Data plotted for both choices in the behavioural experiment outside the scanner (solid lines: using target amounts £5, £9, £11, £13) and choice made inside the scanner (dashed lines: using target amounts £7, £12). Error bars show standard error (n=16). The proportion of gamble choices linearly decreased with increasing risk of each lottery, demonstrating increasing risk aversion (p = 0.049). There was also a significant linear interaction between the risk of each presented lottery and the target level (p = 0.007).

5.3.1.2 *Analysis of choices by block*

Descriptively, subjects switched strategy in a systematic manner as the target level changed (**Figure 5.5**). For low target, subjects tended to choose strategies involving fewer lottery gambles. However, for higher targets, as the chance of getting nothing increased, subjects chose strategies involving more lottery gambles, thereby increasing expected return. There was considerable heterogeneity in strategy selection, particularly for medium target levels. Analysing group data across all subjects demonstrated that choices were structured (χ^2 test against random choice, d.f. = 155, $p<0.001$).

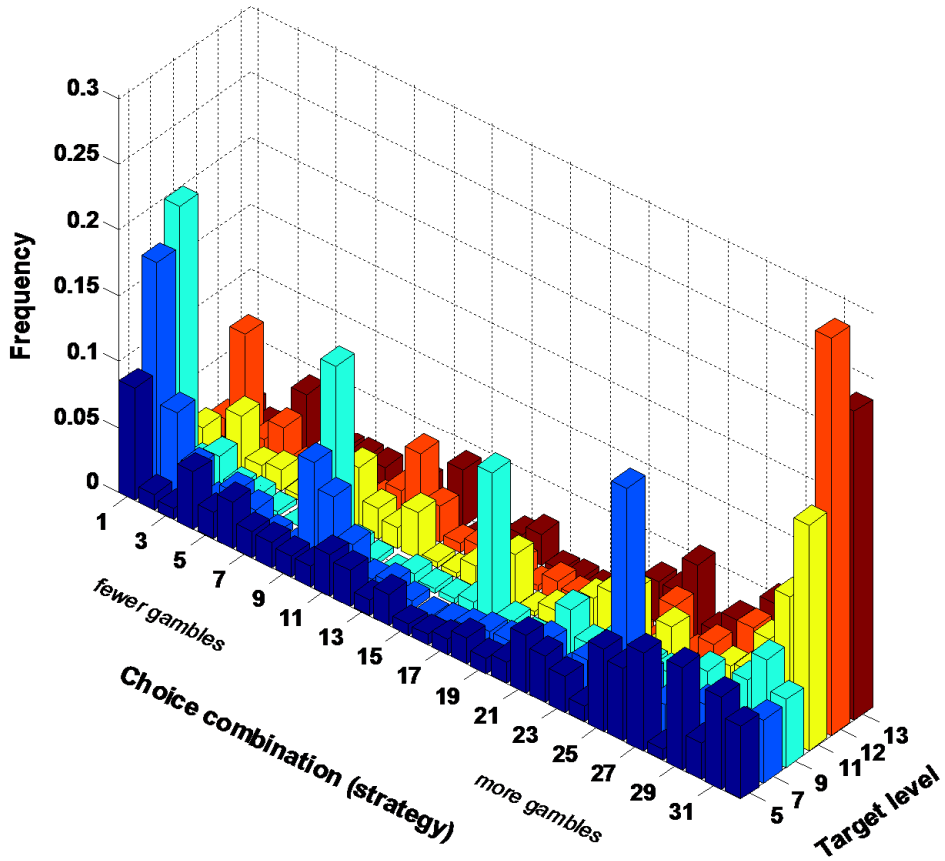

Figure 5.5 Choice Strategies for Different Target Levels. Bar plot of frequencies with which different choice combinations (i.e. strategies) were chosen, for each of the 6 target levels employed. Choice strategy on x axis, numbered from 1 to 32 according to the 2^5=32 possible combinations of five sequential binary choices to gamble or not gamble. Choice strategies sorted by increasing number of times a gamble is chosen (i.e. combination 1 where all choices opt for sure amount, combination 32 where all choices opt for the gamble). 6 target levels on y axis. Choice frequency (i.e. number of blocks in which the specific choice combination occurred, divided by total number of blocks) on z axis. Blockwise data is aggregated across all 16 subjects for illustration. Model fitting was performed on a subject-by-subject basis.

5.3.1.3 *Model results*

A comparison of each of the continuation value decision making models is illustrated in Figure 5.6**A**. An ACV model obtained the lowest optimised weighted criterion value (ACV: mean *D* = 6.3, s.e.m. 1.5; OCV: mean *D* = 11.9, s.e.m. 3.0; SCV: mean *D* = 29.5, s.e.m. 7.4). I also compared models to random choice (where all strategies are selected with equal frequency) to give an absolute measure of accuracy. A random model obtains a mean criterion value of 78.3. The average distance (i.e. summed least-squares error) between the array of observed frequencies and the array of model-simulated frequencies is 6.3 for ACV and 78.3 for the random model. Therefore, the summed least-squares error for ACV is 92% less than is the case for the random model. According to the ACV model, all 16 subjects were averse to variance (variance coefficient = 0.21, std. 0.03), and were positive skew-seeking (skewness coefficient = 1.2×10^{-3}, std. 0.6×10^{-3}). The value of the sigma parameter (temperature parameter of the softmax/logistic function used to account for noisy choice) were low (average sigma = 0.31, std. 0.62). This indicates that the valuation model performs well at explaining choice without modelling a large degree of additional randomness in action selection. It is important to note that although on average the ACV model was superior, there was heterogeneity in the best-fitting model on a subject-by-subject basis (**Figure 5.6B**). The ACV model was superior to the SCV model in 13/16 subjects (Figure 5.6**C**). Both parametric and non-parametric tests of the criterion value statistics at the group level revealed that ACV obtained a significantly better fit than SCV (paired t-test: p = 0.001; binomial test: p = 0.002), but was indistinguishable from OCV on these behavioural data alone (paired t-test, p = 0.294; binomial test, p = 0.402).

Continuation value models coupled with alternative utility models (PT and EUT) did not perform as well as the MVS utility model (Figure 5.7), therefore for subsequent analysis I use the latter.

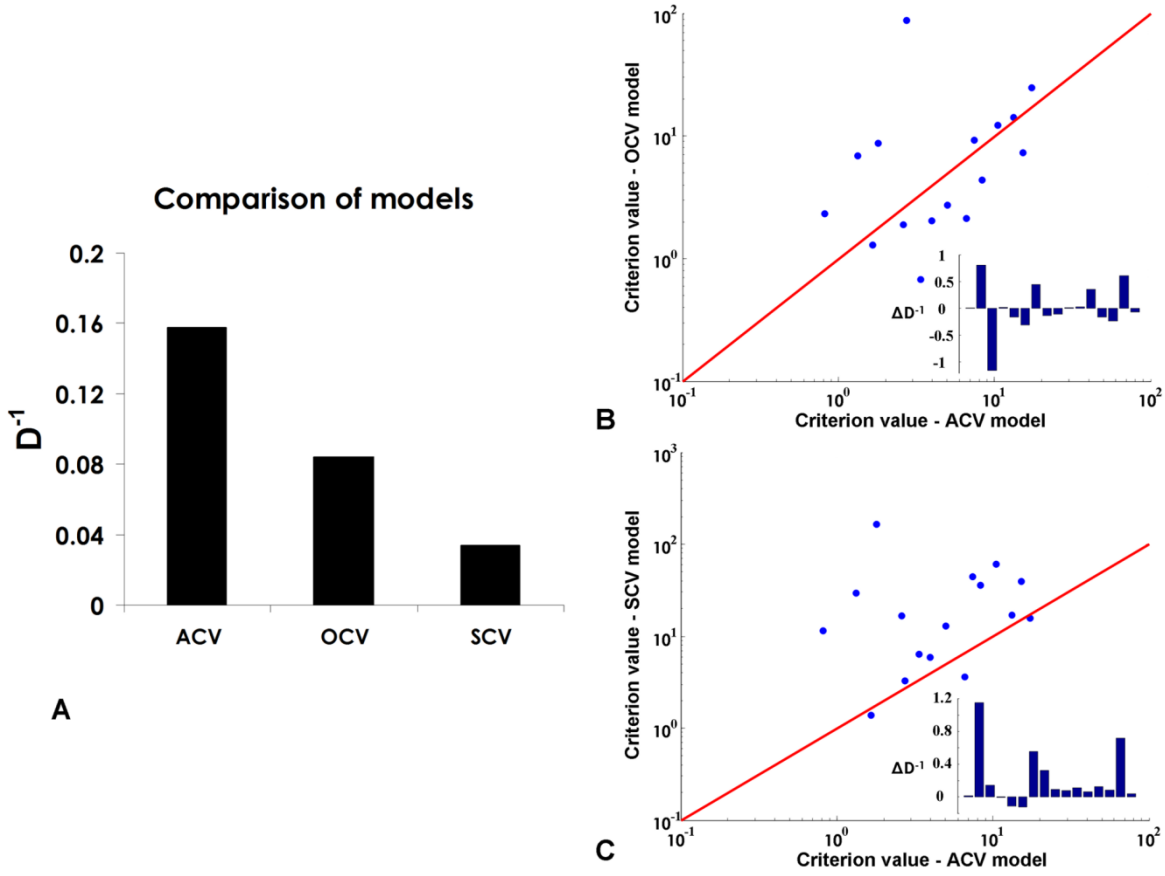

Figure 5.6 Comparison of Models. A. There were 3 types of continuation value model, indicating different decision-making processes – optimal, where only the relative optimal outcomes (of gambling or not gambling on each trial) are evaluated, average, where the relative average of possible outcomes are evaluated (so all possible choice trajectories considered), and sure, where the choice to gamble is evaluated with respect to the alternative of taking the sure option for the remainder of the block. To illustrate the relative superiority of the different models, I plot the inverse of the average criterion function ((mean D)$^{-1}$, where D is the criterion value (the distance between simulated and actual choice frequencies)). Larger values for D^{-1} indicate a better model fit. B&C. For each subject (n=16), the criterion value, D, from the mean-variance skewness, average continuation value model, is compared to the optimal continuation value and sure continuation value models. Points above the red line indicate that the mean variance skewness model with average continuation value provides the better fit. Values are plotted on logarithmic axis for illustration; the red line indicates equality between models. The ACV model and OCV model are comparable in their behavioural fits across subjects. The ACV model outperforms the SCV model for most subjects (4C). I also plot the residual values (differences) in D^{-1} per subject in the bottom corner.

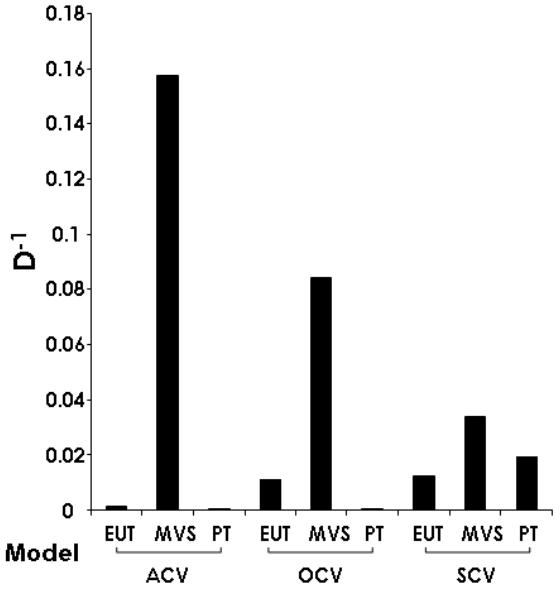

Figure 5.7 Model comparison of 3 utility models. EUT – expected utility, MVS – mean-variance-skewness, PT – prospect theory-type. ACV – average continuation value, OCV – optimal continuation value, SCV – sure continuation value. To illustrate relative model fits, I plot the inverse of the average criterion function (mean D)$^{-1}$, where D is the criterion value (the distance between simulated and actual choice frequencies)). Larger values for D^{-1} indicate a better model fit.

5.3.2 FUNCTIONAL IMAGING

I analysed fMRI data initially using the average continuation value model. I parametrically modulated the magnitude of the neural response on every trial with four regressors indicating target level (high or low), expected value, variance and skewness of the expected (i.e.choice-contingent) outcome distribution respectively. I first include the target level to account for evoked activity differences solely due to changes in effort or concentration evoked by a difference between a low and high target, and activity due to explicit tracking of the target or context. In addition, this removes correlations between the regressors induced by the fact that at high targets, the expected value is naturally always low and the skewness is always positive (high chance of failing to reach target and receiving nothing).

I then performed a directed stepwise linear regression to analyse the contribution of each variable in turn to the BOLD signal, by sequentially orthogonalising regressors. Thus, I first

account for as much neural activity as possible with the expected value regressor, and then explain residual activity with the variance regressor, and finally explain activity with the skewness regressor. Any residual activity correlating with skewness is therefore independent of expected value and variance. In addition, orthogonalisation is necessary because correlations remain between the statistical moments even having accounted for gross differences due to the target level (correlation coefficients: expected value vs variance, 0.57; expected value vs skewness, 0.50; variance vs skewness, 0.01). It is important to note that including the target regressor changes the inference about activity tracking the predicted outcome statistics – I analyse activity tracking the conditional moments (i.e. expected value, variance, and skewness changes with respect to the current target level), rather than the raw unconditional statistics. This analysis conditional on current target is similar to previous studies investigating the tracking of value in different frames or conditions (De Martino et al., 2006; Elliott et al., 2008; Plassmann et al., 2008; De Martino et al., 2009), and asks if expected outcomes are encoded relative to context. These statistics are also conditional upon choice, unlike **Chapter 4** where I endeavoured by experimental design to examine stimulus-bound responses to risk independent of choice.

One key idea here, and elsewhere in this thesis, is the principle of using neurophysiological data to arbitrate between models of decision making that are difficult to distinguish using choice data alone. If future trials were not considered at all (i.e. participants were oblivious to the task structure, and the need to attain a target), and instead if each lottery is compared to the sure amount in isolation (i.e. a single-shot evaluation akin to that discussed in **Chapter 4)**, one would not expect to observe neural signals correlating with expected value or skewness (since all gambles were symmetric and had the same expected value) i.e. the null hypothesis. This hypothesis in itself is fairly trivial to refute using just behavioural data, as clearly the participants' choices are sensitive to the target level. On the other hand, if individuals anticipate future outcomes in a strategic manner (using either of the two most likely strategies according to choice data, of OCV where a specific set of choices are weighted, or ACV where all possible future choices are weighted), the presence of such correlated signals can be interpreted as providing evidence that such strategies are taken into account and that the observed pattern of neural response tracks the anticipated distribution of outcomes (specifically in brain regions previously implicated in representing statistical moments of choice in single choice paradigms). I aim to discriminate specifically between OCV and ACV models using neural data, given that these models were indistinguishable solely from the behavioural analysis of sequential choice. I use the fact that these models predict different anticipated outcome distributions on a trial-by-trial basis, together with

fine-grained neural signal changes (as opposed to categorical choice data), to give additional power to arbitrate between these models.

5.3.2.1 *Average continuation value model*

Fluctuations in expected value for each choice correlated with activity in right medial orbitofrontal cortex (mOFC) (MNI co-ordinates: 6, 50, -14; t=4.16, p=0.032, svc) and nucleus accumbens (MNI co-ordinate: right nucleus accumbens: 4, 10, -6; t=3.74, p=0.036, svc). Note, this regressor is linearly independent of that tracking the target level (Figure 5.8**B**, **Table 5.1**). The target regressor itself correlated with activity in areas including right middle frontal gyrus (MNI coordinate 46, -2, 54, t=5.76, p<0.001 unc), anterior cingulate cortex (MNI coordinate 6, 44, 14; t=5.08, p<0.001 unc), and paracentral lobule/supplementary motor area (MNI coordinate -6, -24, 56; t=4.66, p<0.001 unc) (Figure 5.8**B**, **Table 5.2**). I also tested the alternative ACV model that did not explicitly model the target separately (i.e. we ask if there is BOLD signal that correlates with the unconditional statistics of the outcome distribution, not adapted to target level). In this model, no brain activity positively correlated with the overall expected value of a choice, even at a liberal threshold of p<0.005 uncorrected significance.

I next examined neural activity accountable by changes in the average variance of possible future outcomes given each choice, having accounted for activity attributable to target and expected value. The orthogonalised component of variance-related activity correlated with BOLD in anterior insula (right anterior insula, MNI coordinates: 40, 20, -6; t = 3.64, p = 0.028 svc ;left anterior insula, MNI coordinate -38, 20, 4; t =3.84, p=0.001 unc), also right putamen (MNI coordinate 26,28,-8; t = 6.42, p<0.001, unc), and right ACC (MNI coordinate 8, 44, 16; p<0.001 unc) (**Figure 5.8C, Table 5.3**).

Having accounted for neural activity due to target, expected value, and variance of anticipated outcomes, I next sought to explain residual activity in terms of the (orthogonalised component of) skewness of the expected outcome distribution, observing correlated activity in medial frontal pole, left superior parietal cortex and postcentral gyrus, and left inferior frontal gyrus (p<0.001 unc) (**Figure 5.8D, Table 5.4**).

As an additional analysis, I estimated a separate general linear model where I modelled neural responses covarying with subject-specific expected utility on a trial by-trial-basis, calculated according to the behavioural parameters estimated from subjects' parameters

from the ACV model. As might be expected, the largest cluster of significant activity correlating with expected utility was found in medial prefrontal cortex (peak voxel MNI coordinate: -8, 56, -2; t = 3.87; extent = 66 voxels; **Table 5.5**).

5.3.2.2 *Optimal continuation value model*

Given that the OCV model was statistically indistinguishable from ACV on the behavioural data alone, I implemented an analysis based upon predictions from the alternative OCV model for each subject, to investigate whether neural activity correlated with the internal parameters of this model. In essence we are asking whether brain activity can adjudicate between models. I formulated the fMRI design matrix in an identical manner, and found no significant activity in a priori regions of interest correlating with the regressors tracking the outcome distribution, at a threshold of $p<0.001$ unc significance. For completeness, I tested the alternative OCV model not explicitly modelling the target separately and also found no brain activity correlated with the overall expected value of a choice (at $p<0.005$ unc). This suggests that neural activity in brain regions previously associated with economic decision making is better captured by an ACV model, with online trial-by-trial updating rather than the OCV model with a fixed pre-set strategy.

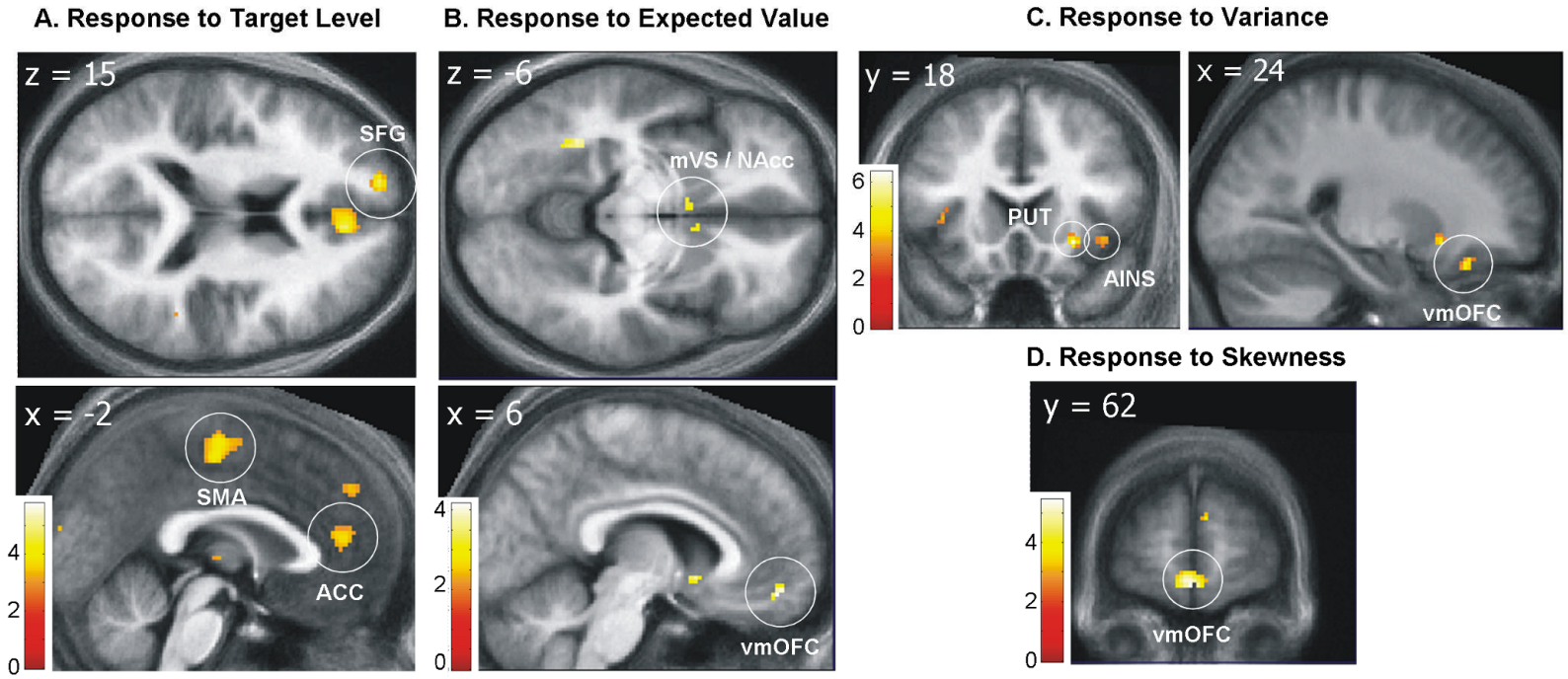

Figure 5.8 Responses to Target Value, Expected Value, Variance, and Skewness. A. Main effect of target level. SMA – supplementary motor area; ACC – anterior cingulated cortex; SFG – superior frontal gyrus. B. Main effect of parametric response to expected value given by ACV model. mVS/NAcc – medial ventral striatum/nucleus accumbens, VmOFC – ventromedial orbitofrontal cortex. C. Parametric response to expected variance (risk) of each choice. PUT – putamen. AINS – anterior insula. D. Parametric response increasing with (positive) skewness in medial frontal pole. SPMt thresholded at p<0.005 superimposed upon a canonical structural template. Colour bars show t value scales for voxel colourmaps.

Area	L/R	MNI coordinates			T value	Extent (voxels)
		x	y	z		
mid-orbital gyrus - ventromedial orbitofrontal cortex	R	6	50	-14	4.16	22
fusiform gyrus	L	-36	-46	-8	3.84	25
ventral striatum - nucleus accumbens	R	4	10	-6	3.74	13
superior medial gyrus	L	-10	58	0	3.58	9

Table 5.1 Response to Expected Value: Anatomical locations of regions correlating with the expected value on each trial, having accounted for mean changes in activity due to the target level. Data are thresholded at p<0.005, uncorrected. I report areas reaching a peak voxel-level significance p≤0.001 and cluster size of >5 voxels only.

Area	L/R	MNI coordinates			T value	Extent
		x	y	z		
middle frontal gyrus, BA6	R	46	-2	54	5.76	12
anterior cingulate cortex	R	6	44	14	5.08	41
middle occipital gyrus	L	-28	-84	36	4.75	9
superior frontal gyrus	L	-16	60	16	4.67	8
paracentral lobule/ supplementary motor area, BA6	L	-6	-24	56	4.66	67
	L	-2	-16	58	4.27	
precentral gyrus	L	-32	-30	60	4.50	22
postcentral gyrs	L	-44	-20	58	4.28	38
middle occipital gyrus	R	32	-86	24	4.23	9

Table 5.2 Response to Target Level: Anatomical locations of regions correlating with the target level. I report areas reaching a peak voxel-level significance p≤0.001 and cluster size of >5 voxels.

Area	L/R	MNI coordinates			T value	Extent
		x	y	z		
Putamen	R	26	18	-8	6.42	23
middle frontal gyrus	R	42	46	0	4.91	94
inferior frontal gyrus	R	42	42	-10	3.15	
superior orbital gyrus	R	24	30	-18	4.87	29
inferior parietal lobe	L	-62	-46	38	4.52	25
inferior temporal gyrus	R	52	-58	-20	4.17	10
ventral striatum	L	-8	-2	-8	4.00	14
postcentral gyrus, BA6	R	62	0	30	3.97	16
anterior cingulate cortex	R	8	44	6	3.92	34
anterior insula	L	-38	20	4	3.84	29
anterior insula	R	40	20	-8	3.64	33
middle frontal gyrus	L	-44	48	6	3.61	12
inferior frontal gyrus / anterior insula	R	30	26	-8	3.61	9

Table 5.3 Response to Variance: Anatomical locations of regions correlating with the expected variance on each trial, having accounted for mean changes in activity due to the target level and expected value. Data are thresholded at p<=0.005, uncorrected. I report areas reaching a peak voxel-level significance p≤0.001 and cluster size of >5 voxels only.

Area	L/R	MNI coordinates			T value	Extent
		x	y	z		
postcentral gyrus, BA 1	L	-30	-44	62	5.44	175
superior parietal lobe, BA2	L	-20	-54	62	3.93	
mid-orbital gyrus, medial orbitofrontal cortex	L	-2	62	-12	5.27	80
inferior frontal gyrus	L	-46	24	-10	4.82	20
medial temporal pole	L	-26	18	-22	4.08	8
	R	40	14	-36	4.51	52
superior frontal gyrus	L	-14	14	46	4.33	6
middle temporal gyrus	L	-66	-40	-10	4.13	19
precentral gyrus, BA 6	R	18	-20	64	4.10	100

Table 5.4 Response to Skewness: Regions correlating with the expected skewness on each trial, having accounted for mean changes in activity due to the target level, expected value, and variance. Data are thresholded at $p<0.005$, uncorrected. I report areas reaching a peak voxel-level significance $p\leq0.001$ and cluster size of >5 voxels only.

Area	L/R	MNI coordinates			T value	Extent
		x	y	z		
corpus callosum / mid-cingulate gyrus	R	4	2	24	4.18	27
primary somatosensory cortex	R	22	-26	46	4.04	8
prmary motor cortex	L	-12	12	62	4.02	41
medial prefrontal cortex	L	-8	56	-2	3.87	66
	R	2	62	-12	3.83	
Thalamus	L	-20	-20	16	3.83	13
Thalamus	L	-22	-12	16	3.76	7
pre-supplementary motor area	L	-22	22	34	3.67	24
anterior insula	L	-52	20	0	3.65	10

Table 5.5 Response to Integrated Utility: Anatomical locations of regions correlating with the overall utility of choice on each trial. I report areas reaching a peak voxel-level significance p≤0.001 and cluster size of >5 voxels only.

5.4 DISCUSSION

5.4.1 REPRESENTING OUTCOME DISTRIBUTIONS IN PROSPECTIVE DECISIONS

In this study, I first asked how humans evaluate outcome distributions from different strategies in a sequential choice task. Using a mean-variance-skewness model, I find the subjects in this task are variance-averse and positive-skew-seeking. Positive skew-seeking manifests when participants excessively opt for the sure rather than risky option even with low targets (where the chance of failing to reach the target is small). This implies an attraction of small chances of above-average outcomes, and dislike of small-probability below-average outcomes.

As discussed in **Chapter 4,** previous investigations of risky decisions have segregated (chosen) risk and value-related activity in regions such as cingulate and insula cortices (risk) and ventral striatal and medial orbitofrontal areas (valuation) (Kuhnen and Knutson, 2005;

Lee, 2005; Huettel et al., 2006; Rangel et al., 2008a). Finding separable areas of brain activity parametrically varying with the anticipated mean, variance and skewness of chosen actions again supports predictions from an MVS model, although unlike **Chapter 4** here I cannot independently vary these statistics (hence some of the expected value related activity I observe in ventral striatum, for example, could also be tracking positive skewness, although conversely the observed skewness-related activity *cannot* reflect a tracking of expected value).

5.4.1.1 ***Target level***

The analysis includes a regressor accounting for the target (high/low), controlling for target-induced changes in attention, concentration, or effort, and means that OFC responses track the moments of the outcome distribution conditional upon target level. In effect, the mOFC BOLD signal tracks relative rather than absolute changes in expected value (as I did not see similar activity without controlling for target level). This suggests adaptive value-encoding, similar to findings from direct neuronal recordings in monkeys where a proportion of OFC neurons adapt to condition, manifesting similar ranges of response under different scales of outcomes (Padoa-Schioppa and Assad, 2008; Padoa-Schioppa, 2009; Kobayashi and de Carvalho, 2010). This adaptation potentially can overcome the limited dynamic range of neuronal signalling, implying that responses to expected value are integrated with information about the target in generating action values.

5.4.1.2 ***Skewness***

The skewness response identified comprises superior parietal and medial prefrontal cortex (a region overlapping with findings from **Chapter 4**), also shown to reflect subjective value in tasks with stochastic outcomes (Peters and Buchel, 2009). It is unlikely that this simply reflects cognitive demand or planning, as I see a parametric response even having separately accounted for the target level. I detect a signal reflecting expected utility of each choice (incorporating the target, relative expected value, and risk), calculated as the subject-specific combination of these statistical moments, also in medial prefrontal cortex. This locus of activity overlaps with areas where activity correlates with subjective utility (Daw et al., 2006). However, computations for sequential decision making, where outcomes are stochastic and forecast several trials into the future, are represented in a more anterior location to that found when decision utilities represent deterministic outcomes from single-shot choices (Plassmann et al., 2007a).

5.4.2 ACCOUNTING FOR FUTURE CHOICES

5.4.2.1 *Dynamic consistency*

The second question related to how individuals account for their possible future choices when selecting actions. Behaviourally, I found individuals re-evaluate on each trial (ACV) rather than comparing choices to the risk-free alternative (SCV). Furthermore, neural activity distinguished between behaviourally equivalent OCV and ACV models, with correlations of key variables from the latter rather than the former. However, classical dynamic programming models are based upon OCV, where decision-makers assume a specific optimal series of future planned choices. These models insist upon dynamic consistency (choices are independent of the order in which options are presented), and have been used to describe choice in computational (Sutton and Barto, 1998), ecological (Houston et al., 1988) and economic (Samuelson, 1969) settings. ACV implies that potential outcomes from a number of strategies influence current choice in the decision-making process (as ACV decision-makers assume future choices are made randomly).

5.4.2.2 *Optimal strategic decision making*

The likelihood that decision makers represent or weight outcomes of alternative strategies relates to the possibility that future actions may deviate from an optimal trajectory. This can be either intentional (due to exploration or future constraints on available choices) or by accident (lapses or mistakes). In reality, we are unlikely to follow a predetermined path in our strategic decisions. If we ignored alternative outcomes altogether, then deviations from an optimal strategy would lead to unpredicted and possibly far worse outcomes than originally envisaged. Indeed, there is good evidence that weighting of even potentially irrelevant alternative outcomes plays a role in paradoxes of choice (Allais, 1953; Loomes and Sugden, 1982; Birnbaum, 2008), with counterfactual outcomes being represented in prefrontal cortex (Ursu and Carter, 2005) and striatum (Lohrenz et al., 2007). An alternative reason why an 'average plan' rather than an optimal strategy might be employed is because of additional mental effort required in planning future actions. Predicted outcomes could instead be sampled from the whole range of possible alternatives to build up an average picture of what might transpire given current choice. It is possible that the ACV strategy in fact represents the Bayes optimal policy under constraints of bounded rationality. In other words, if there was a bound or limit to the depth of the decision tree that could be processed,

ACV might capture this limitation better than OCV. ACV far outperforms random choice, which would be an alternative best heuristic if decision-makers were completely ignorant of future options. Instead, ACV explicitly models the assumption that all future options are known, but that despite this the decision-maker does not have a specific plan of their future choices.

5.4.2.3 *Weighting alternative outcomes*

Although using a fixed strategy model is possible in the task, it is likely to dramatically fail in situations where an individual errs or if some planned alternatives are no longer available. An ACV decision-maker considering all possible future outcomes is myopic (i.e. does not deterministically plan choices in advance). However, such a decision-maker can mitigate future errors or constraints by weighting all possible action-outcome combinations, enabling recovery from error by selecting the best set of remaining choices without needing to assume a fixed strategy. In other words, it makes sense dynamic programming should account for a decision-maker's awareness that deviations from a specific policy may occur in the future. One method of implementing this is to optimise the average continuation value. ACV can also partly capture decision processes where a proportion of (but not necessarily all) possible outcomes in a decision-tree are considered – in other words, a mixture between ACV and OCV models. Thus a more informed version of the ACV model might weight strategies according to the proportion of time that they are expected to be chosen either according to previous experience (i.e. a learning model), or based on a rational expectations model similar to quantal response equilibria (QRE) models of choice (McKelvey and Palfrey, 1998) (the asymptotic case where subjects are assumed to make trial-by-trial choices knowing their overall response and error distribution).

I therefore further tested a QRE model, implementing this by calculating for each subject their response distribution from actual trial-by-trial choices for the whole experiment. I then used this response distribution to calculate decision weights for each choice. The new QRE continuation value model then used these decision weights rather than either a uniform distribution (ACV) or deterministic choice (OCV).

The results from this new model gave an average optimized criterion value of 6.6 (compared to the ACV model value of 6.3). On a subject by subject comparison, the new model gave a lower (better) criterion value in 7 subjects, worse in 7 subjects, and almost equivalent in 2 subjects.

Thus, the new 'weighted-average' continuation value model was virtually equivalent to the old average continuation value model on direct comparison for the group. In most subjects (12/16), the new model gave criterion values between those obtained for the ACV and OCV models, consistent with the expectation that this model is a hybrid between these two models. For 4 subjects the least-squares error (i.e. criterion function) was less than for all other models. Most often, the results were broadly similar to the ACV model. Also, the estimated parameters of this weighted average model were very similar to those estimated by the old ACV model (new model, average variance parameter = 0.22; average skewness parameter = 1.26×10^{-3}), probably due to the average model approximating the weighted average model. The similarity between the QRE and ACV models suggests that the ACV model well approximates the evaluation process by assuming equal weighting of all strategies. It is an important avenue for future work to distinguish if certain strategies are indeed more heavily weighted, and if this weighting distribution is implicit or learnt.

5.4.3 PROSPECTIVE EVALUATION OF STRATEGIES - CONCLUSION

I necessarily test the joint hypothesis (that both MVS and ACV models are true), because the continuation value models are coupled to a valuation model. Thus while the neural data support ACV over OCV contingent upon MVS, it is possible that this could be bettered by a combination with an alternative utility model. I cannot draw direct statistical comparisons between utility models in the current framework (as the models are non-nested with different numbers of parameters), and these further model variants remain to be tested in future work. It is possible that I do not see neural responses corresponding to an OCV model even in individuals who actually do follow this strategy purely because there is no requirement for a trial-by-trial tracking of the outcome distribution if you have pre-planned a trajectory of choices. However, the fact that we see responses corresponding to the ACV model suggests, that at least in some subjects, these average continuation values are being continuously tracked and re-evaluated.

The design assumes a fixed best-fitting strategy across subjects, and cannot rule out variation in strategies both between and within-subjects (i.e. switching strategies through the experimental session). However, such heterogeneity would have the effect of obscuring the ability to differentiate between models. Rather than conforming to standard models of sequential decision-making, these data suggest that a set of possible strategies are neurally represented and drive choices. More generally, these findings indicate that strategic

outcomes are evaluated by similar neural metrics as in single-shot choice, where a behavioural preference for higher-order features of outcome distributions is mirrored by neural sensitivity to expected value, variance and skewness.

Chapter 6

THE EFFECT OF METABOLIC STATE ON DECISION MAKING UNDER RISK

6.1 INTRODUCTION

6.1.1 RISK PREFERENCE AND REFERENCE POINTS

Prospect Theory, one of the most influential descriptive theories of decision-making under risk, emphasises that risk-attitude in humans is reference-dependent (Kahneman and Tversky, 1979). When choosing between options yielding gains, humans are on average risk-averse (i.e. avoiding options with a higher uncertainty or variance), while when choosing between options yielding losses below a reference point, humans make riskier choices. This finding is paralleled by observations in animals, where a pervasive sensitivity to risk is systematically influenced by a metabolic reference point (Real et al., 1982; Barnard and Brown, 1985; Wunderle et al., 1987; Croy and Hughes, 1991; Kacelnik and Bateson, 1996). For example, animals become more risk-seeking following a reduction in energy levels by fasting, or increase in basal energy requirements through change in ambient temperature (Caraco, 1981; Caraco et al., 1990).

6.1.2 NEURAL REGULATION OF FOOD INTAKE

Circulating hormones report the status of body energy reserves (e.g. adipose tissue), energy requirements, and acute nutrient intake to targets in the central nervous system that regulate feeding behaviour. Much early work focused on the homeostatic pathway influencing the hypothalamus (Morton et al., 2006; Lenard and Berthoud, 2008), however more recently there has been an increasing realisation that these signals can act directly on

brainstem, limbic and prefrontal regions (via the so-called 'non-homeostatic' pathway), including brain regions implicated in human decision-making (Grill and Kaplan, 2002; Krügel et al., 2003; Hommel et al., 2006; Figlewicz et al., 2007; Chaudhri et al., 2008). There is therefore a potential for changes in metabolic state, and induced changes in hormone levels, to directly influence decisions in the economic domain.

Here, I sought to characterise whether changes in metabolic state systematically influence human risk-attitude in financial decisions. Do we observe consistent changes in risk-preference in the economic domain after feeding (i.e. a transfer of effect from the metabolic to the cognitive domain)? Hormones including oxytocin and testosterone levels have been shown to have an influence on economic behaviour (Kosfeld et al., 2005; Apicella et al., 2008). However, physiological state-dependent influences play no part in traditional economic theory, in contrast to ecological theory with its emphasis on a dependence of foraging behaviour on metabolic state (Houston and McNamara, 1999).

6.1.3 RISK SENSITIVE FORAGING THEORY

Stephens suggested that when an animal chooses between two foraging options giving normally-distributed energetic returns with equal means but different variance, an organism aiming to maximise 'fitness' (i.e. survival probability) prefers safer (lower variance) options when above a metabolic reference point (e.g. energetic requirement over the day) but riskier (higher variance) options when below a metabolic reference point (Stephens, 1981). Alternative models predict that risk-preference will dynamically adjust depending upon metabolic state, energy reserves, and intake rate (Houston and McNamara, 1982; McNamara, 1992). If energy intake rate is below a reference point, this induces greater risk-seeking. Above a reference point, there is a change toward greater risk-aversion. The metabolic reference point is often taken in ecology as the intake rate required to reach a survival threshold, but in principle can be any homeostatic marker. These models also predict that baseline risk-attitude will depend upon baseline energy reserves, with increased baseline risk-aversion as energy reserves exceed a threshold. Finally, at repletion, marginal changes in energy are not predicted to have significant impact on ecological fitness, and organisms will become insensitive to risk (risk-neutral). This relationship between energy intake, energy reserves, and attitude toward risk closely mirrors Prospect

Theory's account of the relationship between risk-attitude for money, economic reference points, and the effect of changes in wealth (see **Figure 6.1** for illustration). Indeed, a direct link between these conceptual frameworks from psychology and ecology is suggested by observations that human monetary decisions under risk are systematically influenced by an 'earnings budget' (i.e. an experimental manipulation of the reference point) (Pietras et al., 2008).

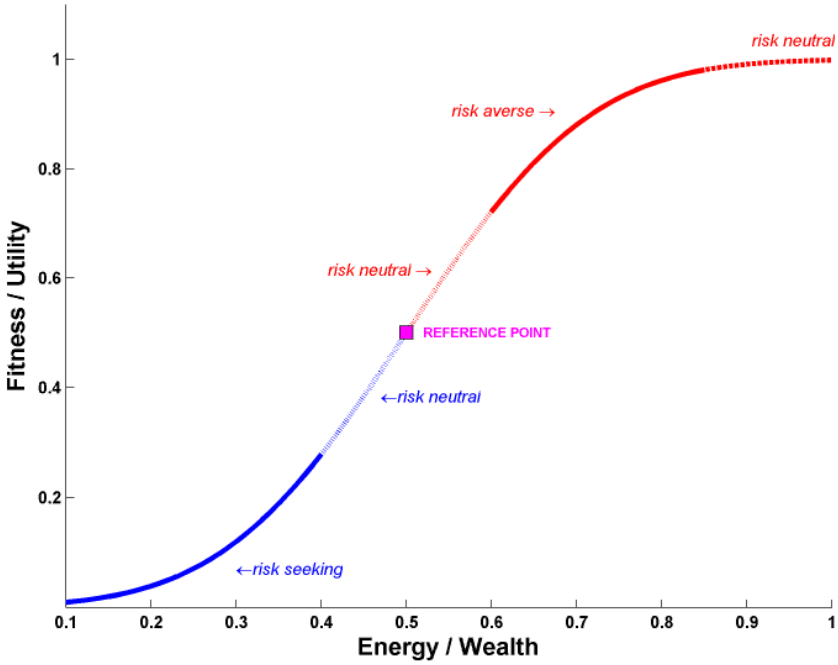

Figure 6.1 Schematic of risk-attitude changes in relation to a reference point (either for money or for food/energy). Risk-attitude equates to the curvature of this relationship. Below reference point, risk-seeking behaviour is seen. Near the reference point, decisions are risk-neutral (insensitive to risk). As energy or wealth increases, increasing risk-aversion is seen. At very high levels (e.g. repletion or satiation), this relation saturates and we again see risk-neutral behaviour.

6.1.4 AIMS AND HYPOTHESES

I tested risky decision-making in healthy men over three sessions, one week apart, using a within-subjects randomised design. I employed a controlled feeding manipulation, and

assayed the same individual's decision-making preferences across different metabolic states; post-14 hr fast, immediately following and one hour post-ingestion of a 2066 kcal meal. I assessed the effect of the feeding paradigm on subjective measures of appetite as well as circulating levels of acyl-ghrelin, with percentage body fat and circulating leptin levels providing an assay of energy reserves.

Leptin is a peptide hormone produced by fat cells, which modulates satiety and indexes adiposity (Seeley and Woods, 2003). Leptin provides negative feedback to hypothalamic centres to help maintain energy homeostasis (Morton et al., 2006), but also has been shown to influence feeding behaviour and food preference (Figlewicz et al., 2007), acting for example on ventral tegmetal area neurons to reduce spiking rate (Fulton et al., 2006).

Prandial suppression of circulating acyl-ghrelin, the primary centrally-acting orexigenic hormone, is a humoral signal of acute nutrient intake highly sensitive to short-term changes in metabolic state, correlating with subjective indices of hunger (Cummings, 2006). Ghrelin is secreted by the stomach, and entrains to a diurnal rhythm, peaking prior to meals (Muller et al., 2002). Post-prandial suppression of plasma ghrelin is proportional to calorific load (Callahan et al., 2004), and also acts as a modulator on hypothalamic and brainstem dopaminergic neurons to enhance firing rate (Palmiter, 2007).

I predicted that individuals making monetary decisions would become more risk-averse after feeding if the meal had a larger impact on metabolic state (i.e. a larger fall in ghrelin). This effect should only occur at the time when ghrelin levels fall, as there is a time-lag before the calorific impact of a meal is registered in terms of changes in plasma hormone concentrations. I hypothesised that there might also be an immediate shift towards risk-neutrality due to satiation (a non-humoural, rapid effect), as ecological models predict a shift towards a risk-neutral attitude with repletion.

6.2 METHODS

6.2.1 PARTICIPANTS

Twenty four, healthy, normal-weight, male volunteers were recruited (mean age: 25±7 years; BMI: 22.6±1.7 kg/m2; **Table 6.1**). Subjects were weight-stable for three months prior to recruitment.

Age (yrs)	BMI (kg/m^2)	Body fat (%)	Glucose (mmol/L)
22	24.5	14.0	4.9
20	22.2	12.5	4.9
22	20.7	10.5	4.5
32	21.2	11.0	5.2
20	24.7	16.5	4.9
20	21.6	12.5	4.5
25	21.2	11.5	4.8
22	22.8	13.0	4.7
22	20.3	8.5	4.8
22	20.4	9.5	4.7
27	25.0	16.0	4.7
22	20.3	10.0	4.9
21	21.9	15.5	4.6
22	23.1	15.0	4.9
23	25.0	14.5	4.5
34	24.8	19.0	4.5
46	23.3	11.5	5.1
20	22.9	12.0	4.8

Table 6.1 Baseline anthropometric and glucose results for included subjects.

One subject was excluded because of baseline fasting hyperglycaemia, another dropped out after the first week, and three excluded because of technical problems. Thus, 19 subjects' data were included in the final behavioural analysis. From these, one subject had haemolysed blood samples for a relevant timepoint, which renders hormonal assay inaccurate, and is excluded from the endocrine analyses.

Baseline measures of reward and food-related behaviour were normal (BIS: 17.3 ± 2.8; BAS drive: 10.0 ± 2.3; BAS reward responsiveness: 16.5 ± 1.4; BAS fun seeking: 11.4 ± 2.3; n = 19). Volunteers provided informed consent and this study was approved by the University College London Research Ethics Committee.

6.2.2 STUDY PROTOCOL

6.2.2.1 *Prior to testing day*

Participants attended a preliminary session, where anthropometric measurements were taken (height with a stadiometer, weight and percentage body fat with Tanita scales (Tanita, Hoofdrrop, Netherlands), and subjects received verbal and written information familiarizing them with the experimental procedure and visual analogue scores (VAS). VAS assessed hunger, fullness, prospective food consumption, sickness and anxiety (Flint et al., 2000; Batterham, 2007), and were 100mm long with positive and negative text ratings anchored at each end. The day before testing sessions, subjects followed a standardization protocol (Chandarana et al., 2009), involving refraining from alcohol and strenuous exercise and consuming an 774 kcal meal between 19:30 and 20:30. Subjects then fasted and drank only water until attending our clinical facility the following morning.

6.2.2.2 *Testing day*

On each study day subjects arrived at 9:00 and an ante-cubital arm vein was cannulated (t= -60 min) for subsequent blood sampling. After relaxing for one hour post-cannulation, baseline blood samples were taken and subjects completed visual analogue scores (VAS) (t=0 min). Blood samples were drawn and subjects completed VAS, every 30 minutes from t=0 until t=210 min. At t=60 min subjects consumed a standardized 2066 kcal meal within 30 mins (**Figure 6.2**).

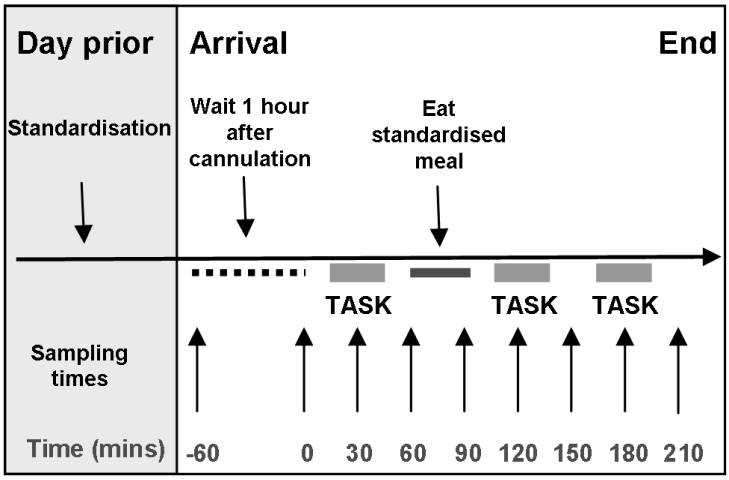

Figure 6.2 Sequence of each experimental session. Testing was performed at fasting (t = 0 to 60 mins), just after a meal (t=90 to t=150 mins), and 1hr after feeding (t=150 to t=210 mins) Hormonal assays and visual analogue scale ratings were taken every 30 mins.

6.2.2.2.1 BLOOD PROCESSING AND ASSAYS

Blood was collected into EDTA tubes containing 5000 kallikrein inhibitor units-per-ml of aprotonin (Bayer, Newbury, Berks, UK). Plasma was separated immediately by centrifugation at 4 °C. Samples for analysis of acyl-ghrelin were acidified by addition of 50µl of 1N hydrochloric acid (HCl) per ml and 4-(2-Aminoethyl)-benzenesulfonyl fluoride hydrochloride (Fluka, UK), 10µl 100mg/ml, was added. Samples were frozen and stored at -80°C until assayed.

For all assays samples were measured in duplicate. Fasting plasma leptin concentrations were measured using a commercially available ELISA (Millipore UK Ltd., Watford, UK). All samples were run on one plate and the sensitivity was 0.125 ng/ml and the intra-assay variation 3.5%. Plasma acyl-ghrelin was measured using commercially available radioimmunoassay (Millipore UK Ltd., Watford, UK). The assay sensitivity was 7.8 pg/ml, the intra- assay variability was 6.6% and the, inter-assay variability was 8.3%.

6.2.2.2.2 BEHAVIOURAL TESTING

Testing was undertaken in three different feeding states: fasted (t=0 to t=60 min), immediately post-meal (t=90 to t=150 min) and 60 minutes post-meal (t=150 to t=210

min). Subjects performed one of three different decision-making tasks within each hour to ensure that cognitive demand was the same throughout the experimental session. Each task was performed once in each week, in randomised order. These comprised a risk-preference elicitation task using paired lotteries, and two additional control tasks. Each task took approximately 30 +/-5 mins to complete. Importantly, behavioural measures were correlated with hormone levels and VAS from the nearest 30 min sampling point, ensuring that assay titres corresponded with an accurate reflection of hormonal status whilst performing the cognitive task.

6.2.3 PARADIGM

6.2.3.1 *Risk preference paradigm*

I employed a multiple paired lottery choice task, presenting a sequence of 200 paired lotteries (**Figure 6.3**; **Appendix B**), with subjects required to select one preferred option per pair (Hey and Orme, 1994). Lotteries were constructed by varying the probabilities over six fixed monetary prizes (£0, £20, £40, £60, £80, £100), represented as four cards with one of these amounts displayed upon each card. Thus, the probability of each prize could be varied in 0.25 increments (0, 0.25, 0.5, 0.75, 1). Each week, subjects were exposed to the same set of lotteries. The left-right on-screen position of the lotteries, and position of the 4 cards within each lottery were randomised, to ensure attention to the task, and to avoid response habituation. On debriefing, no subject reported realising that the lottery sequences were the same across the three weeks. The lottery list was constructed on the assumption that individuals are on average risk-averse – hence most offers were between a safer lottery with lower expected value (EV), and a riskier (higher variance) lottery with higher EV, allowing us to maximise power for discriminating small but consistent state-dependent differences in risk-preference within-subjects while maintaining the same lottery set across subjects. Lotteries were presented on a laptop computer screen, and keypress responses recorded using Cogent 2000 software (Wellcome Trust Centre for Neuroimaging, London).

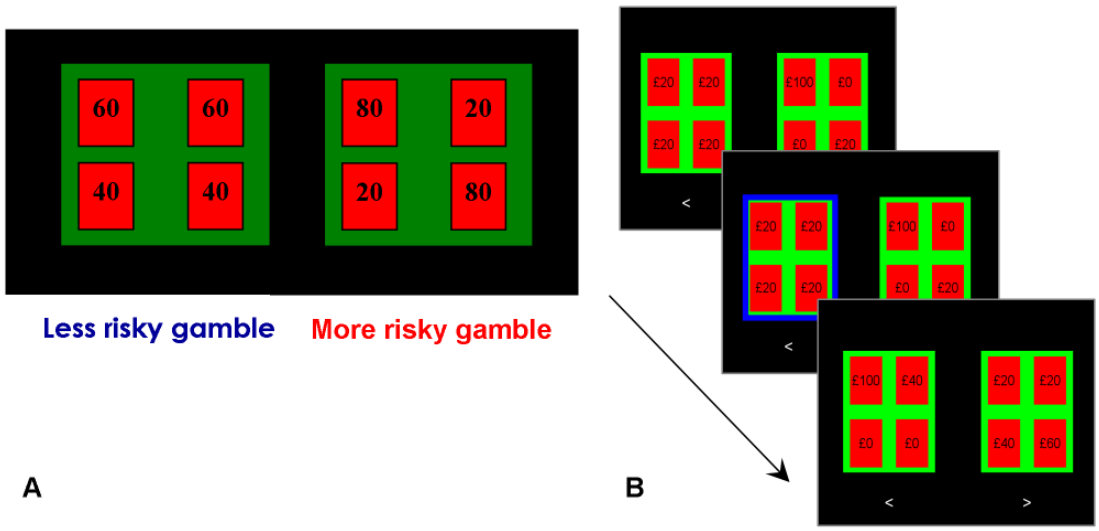

Figure 6.3 Risk preference task. A. On every trial, a choice between two lotteries was presented on-screen, and subjects were required to select their preferred option from each pair. Lotteries were represented as four cards, with a numerical display of one of six fixed monetary prizes (£0, £20, £40, £60, £80, £100). Each card had an equal chance of being picked. B. The same set of 200 sequential paired lotteries were presented on each visit. Subjects had unlimited time to make a button-press response – the selected lottery was then highlighted on screen with a blue border, before the next trial ensued. No feedback was given about lottery outcomes during the task.

6.2.3.2 *Control paradigms*

I used two additional cognitive paradigms in each week, controlling for cognitive load within each session. These comprised an intertemporal choice and a learning task. In the intertemporal choice task, subjects were required to make sequential choices between different amounts of money with different waiting times to payment. Subjects were presented with 200 choice pairs on a computer screen; 180 were between a smaller amount of money sooner and a larger amount of money after a delay, with the remaining 20 trials being the converse. Amounts ranged from £3-£100, and delays from 3 weeks-1 year. In the learning task, subjects had to learn about the likelihood of being rewarded from a set of 8 fractal stimuli, each giving 50p or 0p reward per trial with probability of either 0.8 or 0.2. This was repeated with a new set of fractal stimuli in week 2, and in week 3 subjects were shown paired stimuli from the first two sessions and asked to pick their preferential option,

with additional monetary reward generated according the probabilistic contingencies of their chosen stimuli. All tasks were of approximately the same duration (30+/-5 mins), and in intervening periods subjects were able to rest or read while remaining in the study room.

6.2.3.3 ***Payment***

Payout was determined by a random lottery incentive mechanism, with one choice, selected randomly across all 3 weeks, played out for real to determine winnings. A similar mechanism was used for the intertemporal choice task, with a provision that one of either the risk or the intertemporal choice task would be played out (chosen by random number generation on a computer). Winnings from the risk preference task ranged from £0-80, in addition to a baseline payment of £40/week for participation (generated from the rewards accrued in the cue learning task).

6.2.4 BEHAVIOURAL ANALYSIS

My primary measure was the percentage of riskier vs less risky choices made in each week by every subject. Risk was quantified by the variance of lottery prizes about the mean value (Sharpe, 1964; Rothschild and Stiglitz, 1971). This percentage measure provides an indication of any consistent changes between metabolic states across subjects. As the sets of paired lotteries are identical across subjects and sessions, any differences between states reflect changes in decision criteria. I also implemented a logistic regression model to separately analyse changes in sensitivity to EV and variance across states. This enabled us to describe changes in risk-return tradeoff, estimate absolute risk-preferences, and the degree of choice noisiness. Statistical analysis was implemented in MATLAB (version 6.5, MathWork, Natick, MA), and SPSS (SPSS for Windows, Rel. 12.0.1. 2001. Chicago: SPSS Inc.). For one subject, an extended list of 360 paired lotteries was used for the first two sessions, and the reduced list of 200 lotteries used on session three. I excluded this subject when analysing choice percentages (as these will depend upon the set of choices), but included these data in model based analyses (as model parameter estimation is possible for either choice set).

6.2.5 DECISION-MAKING MODEL

In addition to the summary percentage of risky choice, to obtain an absolute measure of risk-preference, I applied a mean-variance logistic regression model to each subject's choices. This is formulated in an identical fashion to **Chapter 4**, to reiterate:

$$P_{choose\ gamble} = \frac{1}{1 + e^{-\beta \Delta U}} \quad \textbf{(6.1)}$$

where

$$\Delta U = \Delta \mu - \rho \Delta \sigma^2 \quad \textbf{(6.2)}$$

$\Delta\sigma^2$ is the difference in variance of the lotteries, $\Delta\mu$ is the difference in EV of the lotteries, and ρ is a free parameter (risk coefficient) that indicates the EV-risk trade-off for that subject. β is a free parameter indicating choice randomness, or sensitivity to the stimulus dimension (i.e. utility difference, ΔU).

Here the risk coefficient indicates the increase in mean value difference (in pounds sterling) required to offset a one [pound sterling]^2 increment in variance difference of an option. I restricted the analysis to this first order approximation of risk, as here the aim was simply to quantify changes in percentage risky choice in monetary terms. This model partitions choices into riskier/less risky choices and enables separate inferences regarding the noise and risk-return parameters. Model parameters were estimated with maximum-likelihood analysis, again using a non-linear Nelder-Mead simplex search algorithm.

6.3 RESULTS

6.3.1 METABOLIC STATE MEASURES

The paradigm was effective at manipulating subjective ratings of hunger and inducing significant concurrent changes in acyl-ghrelin levels (**Figure 6.4A**).

6.3.1.1 *Hunger*

There was a highly significant change in self-reported visual analogue scores (VAS) for hunger over the eight measured timepoints, before and after the meal, and across subjects (two-way repeated measures ANOVA (week, timepoint), main effect of timepoint: $F(7,126) = 266$, $p<0.001$). This effect was consistent across weeks (main effect of week: $F(2,36) = 0.75$, $p = 0.48$), although there was highly significant heterogeneity in the effect of the meal between subjects ($F(1,18) = 571$, $p<0.001$). Hunger VAS increased from baseline to administration of the meal (increase in hunger VAS from t = 0 to t = 60 min: 8.2 ± 1.4, post-hoc contrast, t = 0 vs t = 60, $F(1,18) = 36.9$, $p <0.001$), then fell immediately post-meal, reaching a nadir at t = 120 min (decrease in hunger VAS from t=0 to t=120 min: 52.0 ± 2.4, post-hoc contrast, t = 0 vs t = 120, $F(1,18) = 462$, $p <0.001$).

6.3.1.2 *Other visual analogue measures*

There was a highly significant concomitant change in prospective food consumption ratings over the course of each session (two-way repeated measures ANOVA (week, timepoint), main effect of timepoint: $F(7,126) = 106$, $p<0.001$; increase in prospective feeding VAS from t = 0 to t = 60 min: 9 ± 1.5, post-hoc contrast, t = 0 vs. t = 60, $F(1,18) = 34.0$, $p <0.01$; decrease in prospective feeding VAS from t = 0 to t = 120 min: 49.4 ± 4.2, post-hoc contrast, t = 0 vs t = 120, $F(1,18) = 137$, $p < 0.001$; average correlation between acyl-ghrelin and prospective food consumption VAS: Pearson's $R = 0.76$).

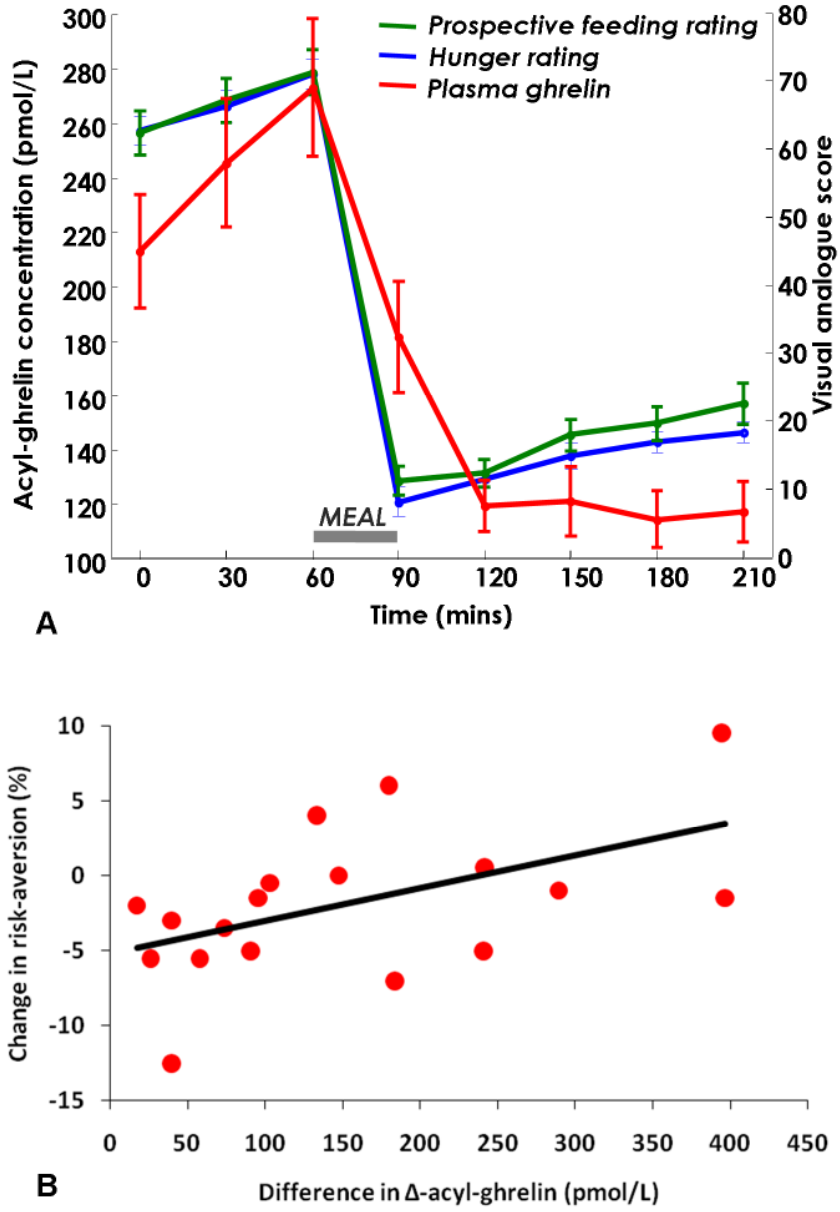

Figure 6.4 Metabolic state and change in risky choice A. Change in hunger VAS (blue), prospective feeding VAS (green), and plasma acyl-ghrelin levels (red) over time-course of session, assayed every 30 mins, averaged across sessions and subjects. There was a significant drop in both hunger ratings and plasma acyl-ghrelin levels ($p<0.001$) after eating; the timecourse of this fall was slower for acyl-ghrelin, showing that this peripheral signal of acute nutrient intake is delayed. Error bars show s.e.m. B. Change in percentage of risky choices significantly correlated with the difference in Δ-ghrelin measurements (within week change in ghrelin from baseline). $p = 0.022$, $r^2 = 0.22$ (N=18).

6.3.1.3 *Acyl-ghrelin changes*

I calculated within-week changes in acyl-ghrelin from the t=0 min timepoint (Δ-ghrelin), which controls for small variations in fasting acyl-ghrelin levels between weeks, for each 30-minute interval throughout a session. Differences in Δ-ghrelin between weeks, calculated from the end of the 30 min interval in which each subject performed the task (t=30/60 min; t=120/150 min; t=180/210 min), indicate the relative difference in orexigenic drive between the three timepoints at which subjects performed the risk task.

Meal consumption caused a significant drop in acyl-ghrelin levels (two-way repeated-measures ANOVA, main effect of timepoint: $F(7,119) = 28.5$, $p < 0.001$), commensurate with the change in hunger ratings (average correlation between mean ghrelin and mean hunger VAS: Pearson's $R = 0.79$, see **Figure 6.4A**), which also peaked just before the meal (increase in plasma acyl-ghrelin from t = 0 to t = 60 min: 63.1 ± 16.9 pmol/L, post-hoc contrast, t = 0 vs t = 60, $F(1,17) = 14.0$, $p = 0.02$), falling to trough level at t = 120 min (decrease in plasma acyl-ghrelin from t=0 to t=120 min: 98.7 ± 16.5 pmol/L, post-hoc contrast, t = 0 vs t = 120, $F(1,17) = 35.9$, $p < 0.001$). There was highly significant variation in the effect of the meal on acyl-ghrelin level changes (between-subjects effect: $F(1,17) = 110.5$, $p<0.001$). However, there was no significant within-subjects difference in hormonal profiles across weeks (main effect of week: $F(34,2) = 0.50$, $p = 0.61$), nor an interaction between week and timepoint ($F(14,238) = 1.17$, $p = 0.30$)

Acyl-ghrelin levels significantly differed from the fasted state across subjects in the specific 30 min window when risk-preference was assessed, (one-way repeated measures ANOVA, $F(2, 34) = 17.7$, $p<0.001$). Pairwise comparisons reveal that this difference only became significant one hour post-prandially (within-subjects contrasts: immediately post-eating vs fasted, $F(1, 17) = 0.228$, $p = 0.64$; one-hour post-eating vs fasted, $F(1,17) = 16.09$, $p = 0.001$).

6.3.2 Effect on risk-sensitive choice

Metabolic state significantly affected choice (one-way repeated-measures ANOVA, $F(2, 34)=3.22$; $p=0.05$ (sphericity assumed, Mauchly's $W=0.86$, $p=0.30$)), with a significant fall in

risk-aversion immediately after eating (baseline fasted percentage risky choice = 37.4%, s.e.m. = 3.0; within-subject increase in risky choice just after meal = 2.8%, s.e.m. = 0.9%; $F(1,17)=9.50$, $p=0.007$; **Figure 6.5 & Figure 6.6A**). This overall difference was no longer significant one hour post-feeding ($F(1,17)=2.48$, $p=0.134$). The difference between fasting and immediate post-meal was highly significant, irrespective of whether the lotteries were classified by variance (as above), standard deviation (paired $t(17)=3.08$, $p=0.007$), coefficient of variation (paired $t(17)=3.04$, $p=0.007$), or variance-to-mean ratio (paired $t(17)=3.00$, $p=0.008$).

6.3.2.1 *Baseline metabolic state measures*

The immediate impact of nutrient intake on risky choice showed a dependence upon baseline indices of body mass index (BMI), percentage body fat and circulating leptin concentrations. Higher baseline leptin correlated with an increase in riskier choices (i.e. a greater fall in risk-aversion) immediately after eating compared to the fasted state ($F(1,17)=4.75$, $p=0.046$, $r^2=0.24$; **Figure 6.6B**). There was also a significant linear relationship between this change in risk attitude and both BMI ($F(1,17)=4.74$, $p=0.046$, $r^2=0.24$), and percentage body fat ($F(1,17)=3.71$, $p=0.073$, $r^2=0.20$).

6.3.2.2 *Change in metabolic state*

The effect of the meal one hour post-feeding (measured by Δ-ghrelin, the within-week change in acyl-ghrelin from t=0 min), significantly correlated with difference in risk attitude compared to baseline ($F(1,17)=6.56$, $p=0.022$, $r^2=0.22$; **Figure 6.4B**). Greater prandial suppression of acyl-ghrelin concentrations, reflecting a larger impact of the meal on reducing a signal of hunger, led to a shift towards less risky choices. By contrast, a small effect correlated with a shift towards more risky choices. Crucially, this effect was only evident an hour after feeding once ghrelin levels had fallen (i.e. once the calorific impact of the meal had registered) (fasting vs just after eating: $F(1,17)=0.17$; $p=0.69$).

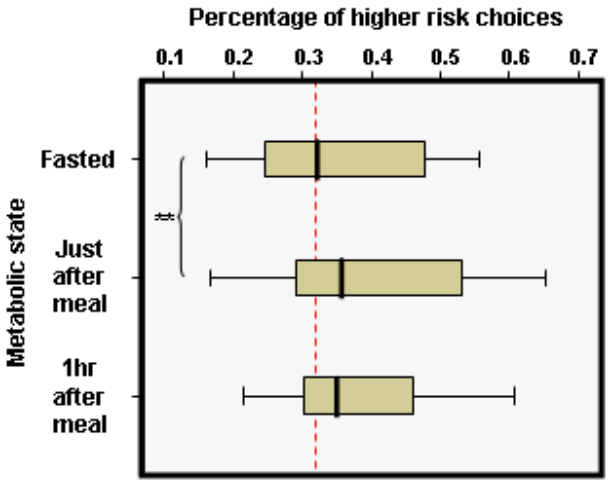

Figure 6.6 Baseline adiposity and change in risky choice A. Bar-plot of change in percentage of risk-averse choices from baseline fasted state. There was a significant decrease in risk-aversion (i.e. increase in risky choices) immediately after feeding (p = 0.007, N = 18). B. Leptin level (x-axis) against change in risk preference for each subject. Best-fitting least-squares estimated linear regression line shown in black (p = 0.046, r^2 = 0.2)

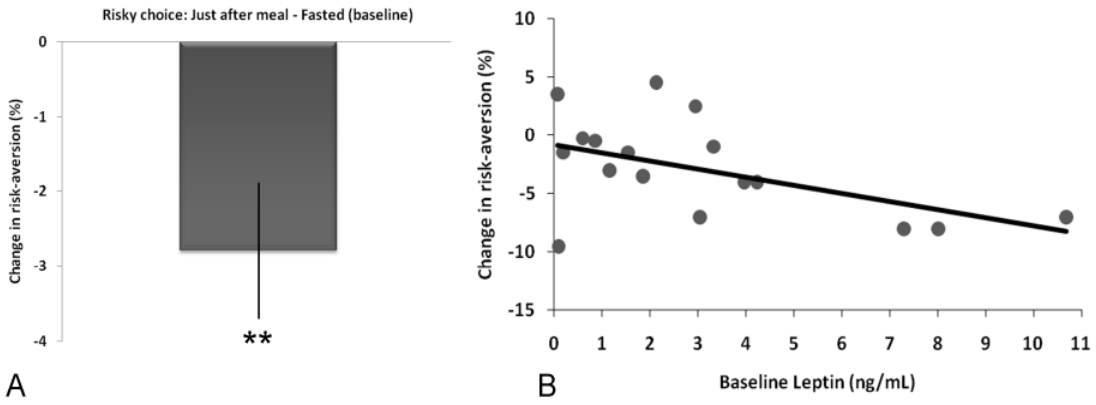

Figure 6.5 Percentage of higher risk choices in each metabolic state. Y-axis shows absolute percentage of trials (total = 200) where the riskier (higher variance) lottery was chosen in preference. Red dotted line indicates average baseline fasting percentage across subjects. Box indicates middle quartiles, bar widths show range.

6.3.2.3 *Further leptin analyses*

As leptin is produced by adipose tissue, one can expect a correlation between body fat and leptin levels, while BMI can be affected additionally by lean (muscle) mass. There was significant positive correlation between circulating plasma leptin concentrations and the body fat percentage measure (Pearson R = 0.55, p = 0.01, one-tailed), and a trend toward a correlation of BMI and leptin levels in the participants (Pearson R = 0.37, p = 0.06, one-tailed). There was also highly significant correlation between BMI and body fat percentage (Pearson R = 0.83, p <0.001). Given this, the addition of BMI to leptin as a predictive variable in a multiple linear regression explained an extra 9% variance in the change in risk attitude, although this was not significant (r2 change = 0.09, p = 0.20), while the addition of body fat percentage did not contribute further due to colinearity (r2 change < 0.01, p = 0.78). There was no correlation between baseline acyl-ghrelin and leptin levels (p = 0.15). Additionally, there was no correlation between leptin, body mass index, or body fat percentage and mean risk attitude across session (p>0.6 for all correlations).

The absence of a significant interaction between the baseline effect of leptin and the effect of an acyl-ghrelin change on risk aversion (2-way categorical ANOVA, leptin x acyl-ghrelin: $F(1,13) = 0.88$, $p = 0.36$), may indicate separate effects at different timescales (immediate vs delayed effect of feeding), although this sample is not powered to detect this interaction given that all the subjects were of normal weight.

6.3.3 DECISION-MAKING MODEL

To quantify changes in risk-sensitivity, and demonstrate a selective effect of metabolic state on risk attitude, I fit individual subject behaviour to an economic decision-making model (see Methods). Risk significantly influenced choice over and above EV, as the full model with mean and variance terms was greatly superior to a reduced model based upon EV alone (likelihood ratio test, mean $\chi^2(1)=58$, $p<0.001$). Subjects were all risk-averse at baseline (mean risk coefficient=1.26×10^{-2}; std=0.96×10^{-2}). The risk coefficient decreased significantly (indicating reduced risk-aversion) between fasting and one hour post-feeding (paired $t(18)=2.15$; $p=0.039$, one-tailed). I saw no difference in choice randomness in any state (fasted vs just fed: paired $t(18)=0.94$, $p=0.35$; fasted vs 1 hr: paired $t(18)=0.18$, $p=0.86$), indicating that feeding does not make choices more 'noisy'. Change in risk coefficient across

states significantly correlated with hormonal indices of baseline metabolic state and the meal-effect on hunger.

Confirming my initial analysis, leptin correlated with reduced risk-aversion immediately after eating compared to the fasted state ($F(1,18)=5.90$, $p=0.027$, $r^2=0.27$). I also observed a significant correlation between this change in risk attitude and percentage body fat ($F(1,18)=4.59$, $p=0.048$, $r^2=0.22$), and a trend in relation to BMI ($F(1,18)=4.23$, $p=0.057$, $r^2=0.21$). Prandial suppression of acyl-ghrelin (t=0 min to one hour post-feeding) correlated with a difference in the risk coefficient compared to baseline ($F(1,18)=6.62$, $p=0.020$, $r^2=0.29$). Translating this effect size into financial terms indicates that, when fasted, subjects are predicted to be indifferent between a 50:50 gamble of winning £30 or £0, and a sure amount of £8.45, giving a risk premium of £15-£8.64=£6.55 . Immediately after eating, for the same gamble, subjects are now indifferent to a sure amount of £9.40, a risk-premium of £5.50. Quantitatively, this indicates a decrease of £0.95 in risk premium for this lottery after feeding.

6.4 DISCUSSION

6.4.1 EFFECTS OF A CHANGE IN METABOLIC STATE ON RISK PREFERENCE

Changes in metabolic state systematically altered economic decision making. Individuals became more risk-averse with a greater post-prandial fall in acyl-ghrelin (i.e. larger signal of nutrient intake). A smaller effect, indicating a lower than anticipated impact of the meal, correlated with greater risk-seeking. This effect was only present an hour after eating, once ghrelin levels changed. This observation of an homeostatic dependence of choice upon metabolic state is consistent with ecological perspectives on risk (McNamara, 1992), however a transfer of effect from the metabolic to the monetary domain has not been demonstrated previously. Importantly, these effects are therefore independent of baseline (economic) risk-attitude.

A direct comparison can be made with Prospect Theory, where changes in wealth below a reference point induce risk-seeking behaviour, while earnings above a reference point lead to risk-aversion behaviour (Pietras and Hackenberg, 2001). Critically, this suggests that changes in acyl-ghrelin signal the effects of a caloric load (i.e. calorie intake rate) that are relative, or adapted to, metabolic requirements. In other words, the degree to which acyl-

ghrelin changes after a meal could act as a hormonal signal for the adequacy of the current rate of calorific intake, and act centrally to modify behaviour. Mechanistically, ghrelin-receptors are expressed in neurons in hypothalamus, ventral tegmental area, and substantia nigra, which project to dopaminoceptive regions implicated in economic decision making under risk in humans (Zigman et al., 2006). These include amygdala and orbitofrontal cortex, regions implicated in reference-dependent valuation of losses and gains and the framing effect (De Martino et al., 2006; De Martino et al., 2009).

6.4.2 IMMEDIATE EFFECTS OF EATING ON RISK PREFERENCE

We also see an immediate effect of a calorific load, with a fall in risk-aversion dependent upon baseline leptin levels. This immediate, rapid impact of the meal cannot be mediated by hormonal changes, and instead must be induced through non-hormonal mechanisms. There are a number of possible explanations, one being that when food becomes available after a period of starvation or hunger, there is a drive to harvest food, which in nature often entails increased risk-taking.

It is also possible to explain the effect directly in terms of reference point effects on risk aversion via changes in the shape of an implicit utility function. The immediate impact of the meal induces satiation, where further calorific intake is assessed to carry mimimal additional value. This in itself induces risk-neutral behaviour. The predicted degree and direction of *change* in risk aversion depends upon baseline energy reserves. At reserve levels close to the reference point there is baseline risk-neutral behaviour (for food). As baseline energy reserves rise above the reference point, the status quo is risk-aversion, because the relationship between fitness and energy is more concave (see **Figure 6.1** for schematic illustration). As observed, there is hardly any change in risk-aversion at lower energy reserves (adiposity), but a fall in risk-aversion if energy reserves are higher. Consistent with previous findings, adiposity is not correlated with baseline risk-attitude for money (Rasmussen et al., 2009). Instead, we find that it predicts change in risk-attitude from the fasted state to immediately after eating.

This effect occurs before the impact of the calorie load is perceived. Once the energetic impact of the meal registers as a change in ghrelin levels, the shift in risk-attitude is linked to endocrine feedback. The magnitude of these effects for an individual will depend upon a number of factors, in particular the precise shape of the relationship between the utility of

food and baseline energy reserves in different metabolic states, which is also likely to be subject to considerable inter-individual variation.

6.4.3 Effects of extreme metabolic states

Prandial ghrelin suppression is reduced in obesity (English et al., 2002). Thus, one predicts greater risk-seeking in obese individuals following feeding, augmented by larger immediate post-prandial effects on risk-taking due to higher baseline adiposity. This mechanism may underpin a component of the aberrant decision-making seen in obese individuals, including impulsivity and reward-seeking behaviour (Nasser et al., 2004; Nederkoorn et al., 2006). One also predicts profound effects on decision-making for individuals operating at very low baseline energy reserves, and note such an explanation has been invoked to explain increased impulsivity in anorexia nervosa (Fessler, 2002). Finally, it is of interest that manipulations affecting hormonal responses to feeding, such as dieting (where circulating acyl-ghrelin increases), or bariatric surgery, may well have cognitive effects, including effects on decision making, beyond the metabolic domain (Cummings et al., 2002).

6.4.4 Conclusion

This demonstration that metabolic state influences human risky economic decisions is predicted by biological models accounting for metabolic reference points, but not by normative economic theory. It is tempting to speculate that maladaptive decision making in aberrant metabolic states may arise out hard-wired imperatives driving strategic decision-making adapted to deal with feeding decisions within a normal biological range. In the context of our study, biology would seem to inform economic theory, not only in providing explanations of psychological phenomena such as loss aversion, but also in highlighting substantive effects of state changes on economic decisions, perhaps reflecting shared evolutionarily conserved neurobiological mechanisms.

Chapter 7

EFFECTS OF DOPAMINE ON DECISION MAKING UNDER RISK

7.1 INTRODUCTION

In **Chapter 4 and 5**, I identified a network of brain regions involved in processing and integrating risk with personal preferences, findings commensurate with previous studies (McCoy and Platt, 2005; Preuschoff et al., 2006; Tobler et al., 2007; Christopoulos et al., 2009). In addition choice, conceived as one's personal trade-off between risk and reward, can be dynamically altered, both by exogenous targets or goals (c.f. **Chapter 5**), or endogenous changes in state (c.f. **Chapter 6**). As discussed in **Chapter 2,** systemic neuromodulatory influences are one potential mechanism mediating preference and changes in preferences.

7.1.1 NEUROMODULATORS AND DECISION MAKING UNDER RISK

Several neuromodulatory transmitters are purported to play a role in risky decision-making, including dopamine, serotonin, and noradrenaline (Rogers et al., 2003; Rogers et al., 2004; Long et al., 2009; Zeeb et al., 2009). Often, several decision-making processes are conflated in these assessments, with risk, impulsivity, learning, and novelty-seeking all potentially being influenced by pharmacological modulation. An economic approach offers a more accurate way of distinguishing pure effects on risk, where risk can be explicitly defined by the summary statistics of a distribution of outcomes. Monetary decision-making tasks where choices are made between actions with different distributions of outcomes thus permit an assessment of risk-reward trade-offs independent of other effects such as delay-discounting or exploration.

7.1.1.1 ***Dopamine***

Several lines of evidence suggest that the dopaminergic system plays a central role in decision-making under risk. A number of neuroimaging studies have found that dopamine rich regions (including striatum, orbitofrontal cortex and anterior insula) are involved in the representation of risk and execution of risk-taking choices (Kuhnen and Knutson, 2005; Abler et al., 2006; Preuschoff et al., 2006; Tobler et al., 2007). Additionally, single-unit recording studies have shown that the tonic firing rates of dopaminergic midbrain neurons scale with uncertainty in risk-based decision-making tasks in primates (Fiorillo et al., 2003), although there is debate about whether this signal in fact represents prediction errors during learning (Fiorillo et al., 2005; Niv et al., 2005), a signal known to be dopaminergically encoded both at the time of reward receipt and following learning at the time of reward-predictive signals (Schultz et al., 1997).

Clinically, Parkinson's disease (PD), where nigro-striatal dopamine pathways are impoverished, can be associated with disrupted decision-making (Cools et al., 2003; Torta et al., 2009). Dopamine agonists, used to treat this disease, can lead to impulse-control disorders and cause pathological gambling behaviour as a psychological side-effect of therapy, a side-effect reported with levodopa monotherapy (Molina et al., 2000; Gallagher et al., 2007), and amplified with both dopamine agonist and levodopa dual therapy (Imamura et al., 2006). Additionally, manipulation of dopamine levels in rats disrupts decision-making under uncertainty in foraging tasks. Administration of amphetamine (which augments dopamine release), D1-, or D2-receptor agonists can increase preference for a risky choice, and the effects of amphetamine can be abolished by dopamine receptor blockade (St Onge and Floresco, 2008). This picture is mixed, with other studies reporting that amphetamine can both increase *and* decrease risky choice in rats dependent on baseline preference (Kaminski and Ator, 2001), with some studies reporting no effect of dopamine augmentation therapy on decision making in PD patients (Czernecki et al., 2002).

However, whether dopamine influences decision-making under risk in healthy humans has not been well established. The majority of studies have used tasks where continual reward feedback is given, either in the context of learning or in gambling tasks where risk is explicit. It is possible that part of dopamine's influence relates to the response to reward feedback rather than risk evaluation itself. Dopamine release is strongly associated with reward feedback and the anticipation of imminent reward (Tobler et al., 2005), with dopamine agonists systematically altering both choice and neural activity following better than average

(i.e. unexpectedly good) rewards (Riba et al., 2008). Furthermore, reported performance impariments by dopaminergic depletion in tasks involving risk assessment, such as the Iowa Gambling Task (IGT) (Sevy et al., 2006), may equally be interpreted in terms of dopamine's role in learning and the integration of evidence, rather than reflecting any objective assessment of the statistical risk inherent in a decision itself. Thus, the IGT recruits numerous processes involved in working memory, learning, set-shifting, attention as well as decision-making, all of which are influenced by dopamine.

More generally, dopamine has been proposed to act as a generic neuromodulatory signal encoding precision or uncertainty (risk) of predictions, in terms of setting the post-synaptic gain of error prediction units (Friston, 2010). Risk is thus an important computational variable in setting a learning rate, which can be construed as an expression of the precision of predictions in hierarchical models, which subjects use to make sequential choices in an uncertain changing environment. There is therefore a direct link between the neuromodulatory effects of dopamine, risk and precision which may transcend reinforcement learning and value learning and may coherently explain the diverse gamut of dopamine's biological roles.

7.1.2 AIMS

Here I aimed to assess the effect of dopamine administration on decision-making under risk in healthy subjects performing two different economic gambling tasks. To test whether dopamine influences the processing of (expected) reward, or of variance (uncertainty or spread of outcomes), or of relative gains and losses (skewness), I used a task where I independently manipulatde both expected value-variance and variance-skewness. Critically, we can distinguish in this paradigm between the effects of dopamine on decision processing from an effect on learning or due to feedback, as all choices are based on explicit presentations of risky gambles (therefore no learning), and no feedback is given during the task. Additionally, we can detect whether dopamine simply makes choices more random (which can often appear as a tendency towards risk-neutrality). By employing a randomised, double blinded, placebo controlled administration of L-dopa (which increases vesicular dopamine release in the central nervous system) (Pothos, 2002), I hypothesized a systematic effect of dopamine augmentation upon individual's risk-reward trade-off.

7.2 METHODS

7.2.1 SETUP

The study was approved by the Institute of Neurology (University College London) Ethics Committee. Forty healthy participants were recruited (14 male, 26 female; mean age 22.7, SD = 3.84 range = 18-33), and attended on two separate occasions one week apart. All subjects gave full informed consent for participation. On each week, subjects received either a 100 mg dose of L-dopa (Madopar - levodopa/benserazide, 100/25mg, Roche) dissolved in fruit squash or an indistinguishable fruit juice placebo, administered 50 minutes before behavioural testing to allow dopamine to reach peak plasma and neural concentration (Crevoisier et al., 1987). Stimuli were presented, and responses recorded, using Cogent presentation software (Wellcome Trust Centre for Neuroimaging, London) written in MATLAB (version 6.5, MathWork, Natick, MA). The task was performed on a standard PC, and choices were indicated using a keyboard. I provided a 5-minute practice tutorial to demonstrate the paradigm. Data were analysed using MATLAB and SPSS (SPSS for Windows, Rel. 12.0.1. 2003. Chicago: SPSS Inc.).

7.2.2 PARADIGMS

To dissociate preferences for different components of risk, in terms of dispersion (variance) and asymmetry of outcomes (skewness), I implemented a very similar decision-making task as used in **Chapter 4,** that controlled the distribution of outcomes to ensure that the expected value, variance and skewness of a set of lotteries could be manipulated independently. Using this task, I then tested whether dopamine administration influenced the impact of average return, uncertainty (spread of outcomes, measured as variance) or relative loss and gain (asymmetry of outcomes, measured as skewness). On each trial, participants were required to choose (5s decision time) between taking a 'sure' (fixed) amount of money or electing to 'gamble' (choosing to play a lottery with a number of potential outcomes). All gambles were represented as 4-segment pie-charts (**Figure 1**). Two separate experiments were conducted, each with 20 subjects. Both were set-up identically, apart from the specific stimulus sets employed.

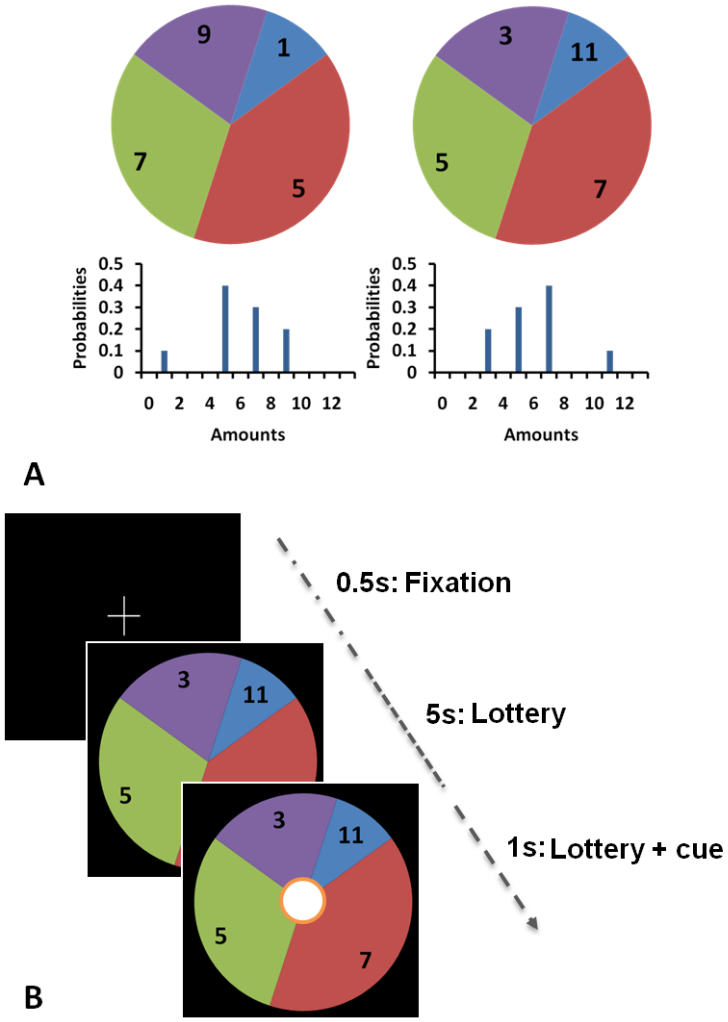

Figure 7.1 Experimental Paradigm. A. The gambles were presented as in Chapter 4, with pie charts divided into different segments showing possible monetary outcomes from the lottery (in pounds sterling) where the angle subtended by each segment indicated the probability of each outcome occurring. A negatively skewed gamble (left) and positively skewed gamble (right) are again shown, with corresponding probability distributions below. Here both example gambles have identical expected value (£6) variance (5£2), but opposite skewness (+/-7.2£3). B. Each task consisted of 252 trials. For each trial, a pie chart was shown, and after 5 seconds, a cue to respond appeared on screen (for 1 second). Subjects indicated by a button press while the cue was on-screen if they wanted to gamble on the lottery, or alternatively select a fixed, sure amount of money (of £4.50 throughout). At the end of the experiment on their second visit, four trials were randomly selected and played out for real. If subjects had elected to gamble, I resolved the lottery by an on-screen graphic of a red ball spinning around the outside of the pie which stopped at a randomly selected position.

7.2.2.1 *Experiment 1: Independent manipulation of expected value and variance*

I constructed a stimulus set of 252 lotteries where expected value and variance were independent and varied over a range (**Appendix C1**). Expected value of the lotteries ranged from £3.25 to £8.00, while variance ranged from 0.47 to 24.05 £^{2}. All stimuli were symmetric (i.e. had zero skewness). Stimuli were constrained to have 4 outcomes (segments of the pie chart), with outcome probabilities varying in minimum 0.1 increments between 0 and 1 to mitigate against probability distortion effects at small probabilities. These restrictions allow the generation of a space of possible lotteries varying in expected value and variance. EV and variance were orthogonal by design (correlation coefficient: $r = 0.07$).

7.2.2.2 *Experiment 2: Independent manipulation of variance and skewness*

Here, I constructed a stimulus set of 252 lotteries where variance and skewness were independent and varied over a range (**Appendix C2**). Expected value of the lotteries was constant (£5.95 - £6.05). Variance ranged from 1.7 to 30.9 £^{2}. Skewness ranged from -38.6 to 38.6 £^{3}. Variance and skewness were orthogonal (correlation coefficient: r <0.01). As in experiment 1, stimuli were constrained to have 4 outcomes (segments of the pie chart), with outcome probabilities varying in minimum 0.1 increments between 0 and 1.

7.2.3 AIMS AND HYPOTHESES

If dopamine solely impacts on the evaluation of anticipated (mean) reward, I would expect to observe a shift in a risk-reward tradeoff in experiment 1 but not in experiment 2 where expected value is constant. Alternatively, if dopamine affects just the evaluation of relative losses and gains in a gamble (which I operationalise here as skewness), then I would expect to observe an effect in experiment 2 alone. If dopamine affects the encoding of uncertainty (variance), I would expect effects in both experiment 1 and in experiment 2. The null hypothesis is that dopamine does not influence risk-return tradeoffs, in which case I would not expect to see a drug-dependent change in systematic tradeoffs between these decision variables.

On each occasion, the participant made decisions about the same set of 252 choices. Using a diverse spread of lotteries enables us to map out responses (choices) to stimuli representing an entire array of risk and value combinations. Consistent tradeoffs between different dimensions of value, variance, and skewness can then be explored and tested by comparing

the performance of different decision-making models where subjects express preferences for each of these components. In addition, utilising a large range of possible gambles is akin to psychophysical methods (Pelli and Farell, 2009), and means that any specific biases engendered by the configuration of a particular gamble will have a minor influence on an overall decision making metric. On each occasion, choices were presented in a randomised order, and the orientation and ordering of pie chart segments was also randomised on each trial. Stimulus sets were constructed and the sure amount alternative was fixed at £4.50, such that participants would choose to gamble approximately 50% of the time on average (based on pilot studies). This meant that the stimulus sets had the greatest power to distinguish subtle effects on changes in EV-variance and variance-skewness tradeoffs.

7.2.4 PAYMENT

To ensure that subjects chose in accordance with their genuine preferences, payment was incentive compatible. Four trials were selected randomly (two from participants' first session and two from their second session) and played out for real at the end of the second visit. For each selected trial, if subjects chose the sure amount, they won £4.50, whereas if they elected to gamble, the lottery was resolved with an animated 'roulette wheel' graphic of a red ball spinning around the pie chart, before coming to rest at a randomly selected position which determined their winnings from that trial. Winnings ranged from £20.00 to £42.50 (mean £32.23), including a baseline participation fee of £12.

7.2.5 PSYCHOLOGICAL QUESTIONNAIRES

Participants completed two questionnaires assessing baseline attitudes to risk on first attendance at the centre. These comprised the revised Domain Specific Risk-Taking scale (DOSPERT) (Weber et al., 2002), which assesses attitudes on two scales of risk-taking and risk-perception in five domains of financial, health and safety, recreational, ethical and social decisions, and the Behavioural Inhibition System and Behavioural Activation System (BIS/BAS) (Carver and White, 1994), assessing individual differences in sensitivities on subscales of drive, reward and fun seeking.

7.2.6 BEHAVIOURAL MODELLING

For a given lottery with 4 potential outcomes *(m_1, m_2,... m_N)*, with probabilities $p = p_1, p_2, \ldots p_n$, I define the raw statistical moments similar to previous chapters, with $EV = \sum_{n=1}^{4} m_n p_n$, $Variance = \sum_{n=1}^{4} (m_n - EV)^2 p_n$, and $Skewness = \sum_{n=1}^{4} (m_n - EV)^3 p_n$.

I analysed choice data by fitting a linear mean-variance-skewness model (**MVS**) where individuals are allowed to express different preferences for variance and skewness. To establish whether individuals are indeed responding to risk, I test this **MVS** model against a series of reduced models, where decisions are based on mean difference (**M**) alone (where subjects only take account of the difference between the sure amount and the expected value of the gamble in selecting actions), a mean-variance model (**MV**), and a mean-skewness (**MS**) model. These utility functions are parameterised identically to those in **Chapter 4**; I refer the reader to this chapter.

I also test a further model able to account for different preferences for positive and negative skewness (**MVS2**), again as previously implemented.

The models again use a logistic choice function, and reported parameters are the maximum likelihood estimates, with an identical optimisation algorithm to previous chapters. Model comparison uses the Bayesian Information Criterion (BIC) (Schwarz, 1978).

7.3 RESULTS

7.3.1 BEHAVIOUR

7.3.1.1 *Experiment 1: Expected value versus variance trade-off*

Subjects distributed their choices between gamble and sure options throughout the course of the experiment, choosing to gamble in on average 43.1% (SD ± 17.23%) of trials on placebo, and 40.6% (SD ± 17.15%) on L-dopa. There was no significant difference between these proportions (paired t-test, $t_{19} = 1.20$, $p = 0.24$) (**Figure 7.2A**). Even accounting for the effect of order in a 2 x 2 repeated measures ANOVA (drug/placebo x drug week 1/drug week 2), there was no overall effect of drug administration ($F_{1,9} = 0.05$, $p = 0.95$), although the order

effect reached trend significance ($F_{1,9}$ = 4.38, p = 0.06), with an average -5.7 +/- 8.0% change in percentage gambling from week 1 to week 2.

7.3.1.2 *Experiment 2: Variance versus skewness trade-off*

Here, subjects also distributed their choices between gamble and sure options throughout the course of this experiment, choosing to gamble in on average 47.8% (SD ± 19.5%) of trials on placebo, and 48.4% (SD ± 19.3%) on L-dopa. There was no significant difference between these proportions (paired t-test, t_{19} = 0.15, p = 0.88) (**Figure 7.2B**). As above, I also entered data into a 2 x 2 repeated measures ANOVA, which confirmed no overall effect of drug administration ($F_{1,9}$ = 0.03, p = 0.87), although the order effect again approached significance ($F_{1,9}$ = 3.83, p = 0.07), with an average -8.1 +/- 17.9% change in percentage gambling from week 1 to week 2.

I further examined for any effects on risk in specific sub-domains (e.g. only for positively skewed gambles with a small chance of high rewards). Choice data were partitioned into 4 domains - high/low variance and positive/negative skewness decisions - and entered into a repeated measures ANOVA. This again revealed no significant effect of drug ($F_{1,9}$ = 0.01, p = 0.91), with no significant interaction between drug and domain ($F_{3,9}$ = 0.11, p = 0.96).

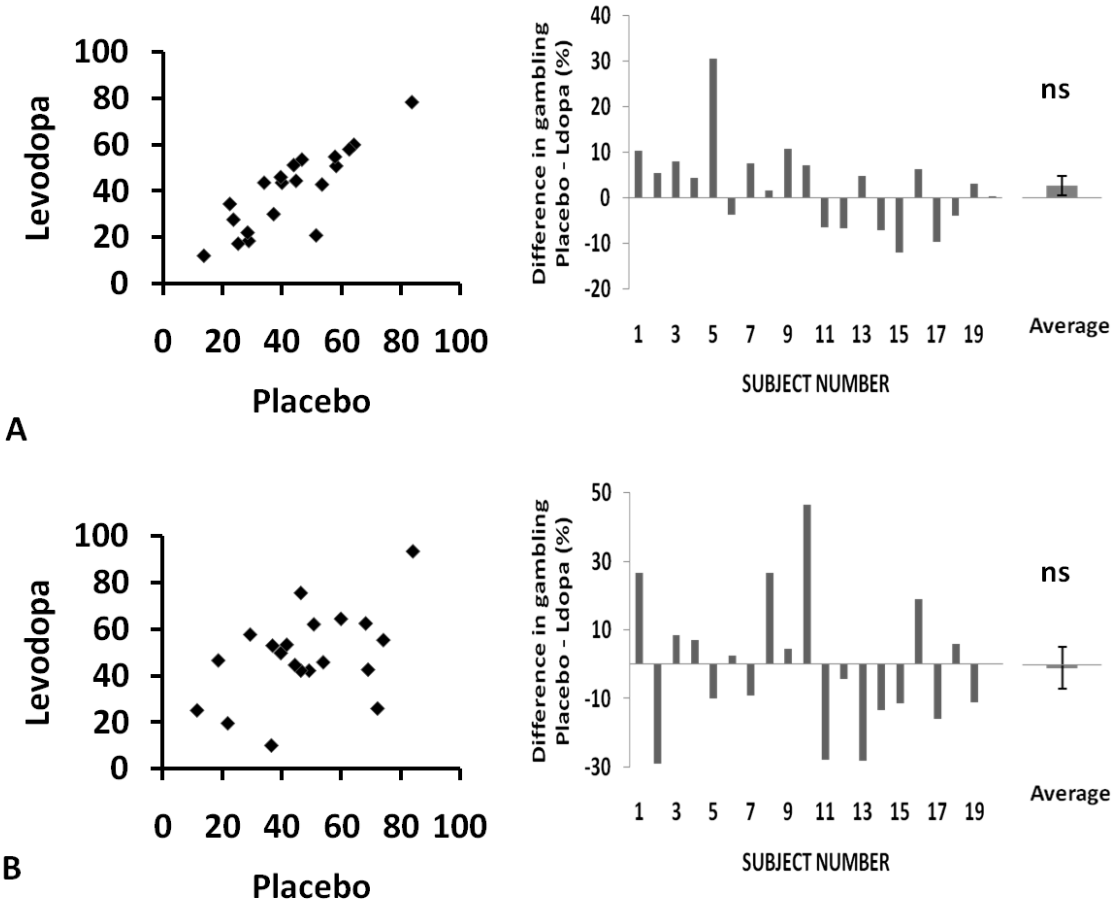

Figure 7.2 Behavioural results. On left, scatterplots of percentage gambling choices on levodopa and placebo (n=20). On right, percentage differences in gambling choice between placebo and levodopa conditions plotted per subject with average effect size (ns = non-significant, error bars show standard error). A. Experiment 1 – Expected value – variance manipulation. B Experiment 2 – Variance – skewness manipulation.

7.3.1.3 *Reaction time*

For analysis, reaction times (RT = time from stimulus presentation to keypress response) were normalised by an inverse transformation (response speed = 1/RT). There was no significant difference in response speed between placebo and L-dopa, either in Experiment 1 (t_{19} = 0.644, p = 0.528), or in Experiment 2 (t_{19} = 1.334, p = 0.198).

7.3.1.4 *Correlation with questionnaire measures of risk attitudes*

Baseline measures of risk-taking were taken from all participants using the Behavioural Inhibition/ Behavioural activation scales (BIS/BAS) and Domain Specific Risk-Taking (DOSPERT) scale. We asked whether sensitivity to drug-induced changes in risk attitude

were dependent on these measures. No significant correlations were found with either of these scores.

7.3.2 BEHAVIOURAL MODELLING

I also performed a model-based analysis of participants' choices, where I estimated parameters for variance- and skewness-aversion from an economic decision model. This model based analysis was designed to test whether subjects' made consistent choices, trading risk and reward in a coherent manner (as opposed to being insensitive to risk). A lack of drug effect could be purely due to a baseline indifference to risk in these subjects. Secondly, parameters estimated from a behavioural model have greater sensitivity to detect small systematic changes in risk-preferences that a simple summary analysis of percentage gambling. Thirdly, I could test specific behavioural hypotheses by comparing the performance of different models in explaining the data. Dopamine may induce a change in risk-preference (i.e. the trade-off between risk and potential reward) or may simply induce a general bias in choice that leads to an increased predilection for gambling, without altering risk-sensitivity. Finally, I can also test whether dopamine significantly changed choice randomness or noise as I explicitly model this as a free parameter that determines the slope of the logistic (softmax) function.

7.3.2.1 *Sensitivity to risk*

I independently manipulated variance and skewness, and predicted that individuals' preferences would be sensitive to both aspects of risk. To test this, I compared a set of models which predict choice on the basis of either the mean value of sure vs lottery options alone (model **M**, risk-insensitive), the mean and lottery variance (model **MV**), and for experiment 2, the mean variance and skewness (model **MVS**).

Risk-sensitive models far outperformed the risk-insensitive model, demonstrating that subjects' choices were significantly influenced by decision risk (**Figure 7.3A**). Moreover, the **MVS** model was superior to the **MV** model in predicting choice in experiment 2 (**Figure 7.3B**), showing that individuals are influenced by both risk dimensions of variance and skewness (experiment 1: $BIC_{\mathbf{M}} = 11827$, $BIC_{\mathbf{MV}} = 5964$, **MV** model posterior probability>0.99 (very strong evidence in favour of **MV** model); experiment 2: $BIC_{\mathbf{M}} = 12999$, $BIC_{\mathbf{MV}} = 8708$,

$BIC_{\mathbf{MVS}}$ = 8352, **MVS** model posterior probability>0.99 (very strong evidence in favour of **MVS** model)).

I estimated parameters corresponding to tastes for these 2 independent risk domains, variance (ρ) and skewness (λ), as well as choice randomness (β), for each subject and each condition (drug/placebo) independently. I entered individually estimated parameters into group-level analysis to test for differences. Participants were on average averse to variance in both experiment 1 ($\rho_{PLACEBO}$ = -0.13, SD +/- 0.08; ρ_{LDOPA} = -0.15, SD +/- 0.10) and experiment 2 ($\rho_{PLACEBO}$ = -0.11, SD +/- 0.07; ρ_{LDOPA} = -0.12, SD +/- 0.10), and preferred positively skewed lotteries ($\lambda_{PLACEBO}$ = 0.0039, SD +/- 0.0253; λ_{LDOPA} = 0.0011, SD +/- 0.0169). While 19/20 subjects here were variance averse, skew preferences were heterogeneous, with 8/20 positive skew-seeking individuals (on placebo). β values were low (experiment 1: $\beta_{PLACEBO}$ = 0.52 SD +/- 0.17, β_{LDOPA} = 0.49 SD +/- 0.13; experiment 2: $\beta_{PLACEBO}$ = 0.53 SD +/- 0.18, β_{LDOPA} = 0.53 SD +/- 0.24), indicating that choices were well partitioned by the behavioural models and that choice noise was low.

7.3.2.2 *Drug-induced changes in preference*

There were no significant differences in ρ, λ, or β parameters between drug and placebo sessions, either in experiment 1 (paired t-tests, ρ: t_{19} = 1.63, p = 0.12; β: t_{19} = 0.35, p = 0.96; **Figure 7.3C**) or in experiment 2 (paired t-tests, ρ: t_{19} = 0.29, p = 0.78; λ: t_{19} = 0.62, p = 0.54; β: t_{19} = 0.01, p = 0.99, **Figure 7.3D**). This indicates that L-dopa had no effect on altering risk-return tradeoffs, either in terms of the impact of uncertainty or spread of outcomes, or on relative losses and gains. Moreover, there was no effect on choice randomness – choices were equally noisy in both sessions.

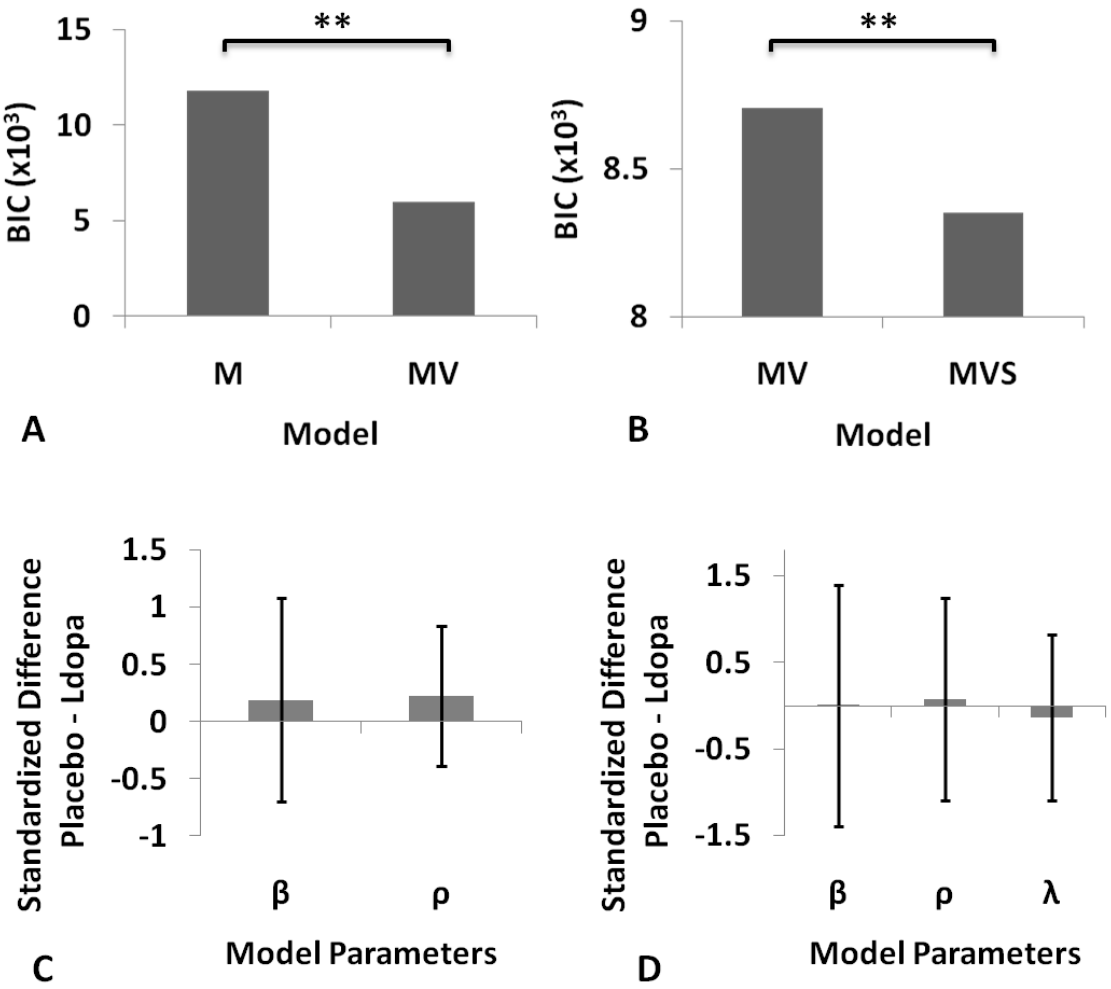

Figure 7.3 Behavioural modelling. A. Experiment 1: Log-evidence, approximated by the Bayesian information criterion (BIC), for mean only (M) and mean-variance (MV) models. Fixed effects analysis of Group Bayes Factors shows MV highly significantly superior to M model (likelihood ratio test: p<10-5). B. Experiment 2: BIC scores for mean-variance (MV) and mean-variance-skewness (MVS) models. MVS highly significantly superior to MV model (likelihood ratio test: p<10-5). BIC=k.ln(n) – 2ln(L), where L is the model likelihood, n is the number of observations and k is the number of free parameters. Lower BIC indicates better model fit. C. Experiment 1: Differences in (standardised) model parameters for choice noise (β) and variance preference (ρ) between placebo and levodopa sessions. Error bars show standard deviation. D. Experiment 2: Differences in (standardised) model parameters for choice noise (β), variance (ρ), and skewness (λ) preference between placebo and levodopa sessions. Error bars show standard deviation.

Finally, I checked for evidence of skewness intransitivity in experiment 2 by fitting a different model (**MVS2**) where subjects can express different sensitivities for positive and negatively skewed lotteries. If individuals prefer or dislike both positive and negative skew, this will not be well captured by the **MVS** model, hence lowering the power to detect drug-induced changes in preference. Indeed, the **MVS2** model was significantly better than the simpler **MVS** model at explaining choice, even accounting for its extra parameter

($BIC_{\mathbf{MVS}}$=8352, $BIC_{\mathbf{MVS2}}$=7914), and revealed that 9/20 participants disliked both positive and negative skew compared to symmetric gambles, while 3/20 preferred both positive and negative skew. However, even in this more sensitive model, I detected no difference in preference (or choice noise) between drug and placebo (average parameter values: $\rho_{PLACEBO}$ = -0.12, SD +/- 0.08, ρ_{LDOPA} = -0.12, SD +/- 0.10; $\lambda^{+}_{PLACEBO}$ = 0.0052, SD +/- 0.0207; λ^{+}_{LDOPA} = 0.0073, SD +/- 0.0246; $\lambda^{-}_{PLACEBO}$ = -0.0027, SD +/- 0.0241; λ^{-}_{LDOPA} = -0.0002, SD +/- 0.0339; $\beta_{PLACEBO}$ = 0.55 SD +/- 0.23, β_{LDOPA} = 0.53 SD +/- 0.23. Paired t-tests, ρ: t_{19} = 0.21, p = 0.84; λ^{+}: t_{19} = 0.50, p = 0.62; λ^{-}: t_{19} = 0.35, p = 0.73; β: t_{19} = 0.30, p = 0.77).

7.4 DISCUSSION

Here, I explored the effect of L-dopa administration on evaluation of different aspects of risk, and the impact on decision making, in healthy humans. To control for possible drug-induced changes in learning and response to reward, the paradigm was specifically designed to isolate effects on risk evaluation. Moreover, by using an economic task and behavioural modelling, I could empirically quantify changes in risk preferences.

7.4.1 RISK SENSITIVITY

All subjects were clearly sensitive to risk, being generally averse to increasing variance (spread of outcomes), and with a range of preferences for skewed gambles (asymmetrical distribution of outcomes). The behavioural modelling revealed the importance of both of these risk dimensions, as simpler models based only on the average anticipated reward (expected value) failed to explain behaviour as well as the **MV** and **MVS** models. Crucially, I find that L-dopa administration does not affect preferences for either variance or for skewness. Moreover, the fact that I observe no changes in experiment 1 means that neither average value, variance, or the trade-off between them is influenced by L-dopa.

This paradigm substantially differs from previous psychopharmacological studies of risk, as here I assess choice preferences for independent statistical features of a distribution of outcomes. This economic quantification of risk preference lends power and precision over previous diverse paradigms that have been used to assess risk-taking (e.g. Cups task (Levin et al., 2007), Game of Dice Task (Brand et al., 2005), Risk Task (Rogers et al., 1999)). In these tasks risk is explicitly described for participants, as opposed to less specific alternatives such as the IGT and Ballon Analogue Risk Task (BART) (Lejuez et al., 2002), where participants

are uncertain about the real probability of rewards. Summary measures of percentage gambling are used to delineate risk-taking, however these measures are specific to the set of stimuli used - stimulus sets in which different features, such as expected value, variance, and skewness, are often correlated. This renders it difficult to quantify precise effects, to map these on to specific psychological or neural processes, and to determine the true effect size of choice shifts.

The paradigm I used was sensitive to small changes in risk preference, as revealed by the systematic decrease in propensity to gamble from week 1 to week 2 across subjects. The 6% choice shift in experiment 1 equates to a difference in model ρ parameters of 0.03. In financial terms this translates to a difference in risk premium of £0.80 for a 50:50 chance of winning £10 or £0 (i.e. this same gamble becomes £0.80 less appealing to an individual from week 1 to week 2). Thus although the paradigm was sensitive to this small, systematic drift in risk attitude over time, I did not detect a drug effect.

It can also be difficult to distinguish between drug induced changes in risk-reward trade-off versus changes in choice noise in previous paradigms. Inattentive or random responding in a binary choice task will shift choice proportions towards 50%, an effect which can often masquerade as a change in risk evaluation, and may account for some previous findings in drug studies (Kaminski and Ator, 2001). Importantly, I can account for non-specific effects of drug administration on the randomness of responses in the behavioural model, which partitions effects into changes in risk preferences, and the independent quantification of choice noise.

7.4.2 Effects of L-dopa

The dose of 100mg L-dopa used here has been previously employed in a range of studies, demonstrating effects on semantic priming (Kischka et al., 1996; Angwin et al., 2004; Copland, 2009), cognitive control (Onur et al., 2011), learning and memory (Knecht et al., 2004; Floel et al., 2005; de Vries et al., 2010), perception (Pleger et al., 2009), and decision-making (Pessiglione et al., 2006; Sharot et al., 2009b). A 100mg dose minimises side effects of nausea or drowsiness, which can significantly impact upon performance. I also ensured a delay between drug administration and task execution such that the task was performed at the time of peak L-dopa concentration (Dethy et al., 1997), making it unlikely that the lack of effect is simply due to low L-dopa levels. The absence of a change in reaction time demonstrates that there was no non-specific slowing as a side-effect of dopamine (Micallef-

Roll et al., 2001). The reported effects of L-dopa on reaction time in healthy individuals are mixed, occasionally speeding responses (Rihet et al., 2002; Hasbroucq et al., 2003), but often with no effect (Kischka et al., 1996; Rakitin et al., 2006), thus I was unsurprised to find this in this study.

7.4.3 RISK VERSUS REWARD LEARNING

Given previous reports of the effects of dopamine manipulation on risk-taking in patients and healthy humans, I address alternative explanations for the lack of effect here. I was careful to design our task to eliminate the effects of learning and reward feedback. Here, our stimuli were explicit, whereas in many previous studies the level of risk associated with a stimulus needs to be learnt over a number of trials. For example, in the IGT where different decks of cards are presented, the quality of the decks needs to be ascertained by repeated sampling (Buelow and Suhr, 2009). Since dopamine has a central role in reward-based learning, and encodes reward-prediction error (Schultz et al., 1997), it is possible that the effect of dopaminergic manipulation could be exerted at this early stage when probabilistic contingencies are being acquired. This is especially the case given dopamine release encodes positive reward prediction errors (better than expected reward), whereas dopaminergic neurons have a limited dynamic range to encode lack of expected reward (Bayer and Glimcher, 2005; Niv et al., 2005). L-dopa augments dopamine release at synapses (Pothos, 2002), therefore could encourage risk-taking by boosting the apparent value of stimuli in the face of unpredictable reward. Moreover, differential effects of dopamine on the response to rewards and punishments (Daw et al., 2002; Frank et al., 2004; Cools et al., 2009) could encourage risk-taking by outweighing previous poor outcomes with recent successful outcomes. This effect cannot be engendered in our paradigm, as all choices were resolved after the end of the experiment, as is standard in experimental economic paradigms (Kagel and Roth, 1995).

Related to this is the distinction between explicit risk, where the probabilities of outcomes are precisely known, and ambiguity, where the outcome distribution is unknown and needs to be learnt through exploration. Ambiguity-aversion is a well-known behavioural bias (Ellsberg, 1961), very different from risk attitude. However the two are frequently conflated in risk-taking tasks such as the BART and IGT, where risks are not explicit. Our finding of a lack of effect of dopamine on risk evaluation is consistent with findings in PD patients of specific deficits in decision making under ambiguity rather than risk (Delazer et al., 2009).

7.4.4 DOPAMINE RECEPTORS

An alternative explanation for the absence of a change in risk-taking with L-dopa might be that any effect is specific to dopamine receptor subtypes. Pathological gambling and other impulse control disorders is a noted side effect of dopamine agonists, but rarely of L-dopa monotherapy in isolation (Gallagher 2007). One possibility is that risk-taking is a specific byproduct of D1-receptor stimulation, an effect that might be opposed by simulataneous D2-receptor stimulation. Contrary to this is the findings that the risk-promoting effects of amphetamine are abolished by both D1- and D2-receptor antagonists (St Onge and Floresco, 2008), and that D1, D2 and D3-specific dopamine agonists all have been reported to induce gambling behaviour (Grosset et al., 2006; Lu et al., 2006), although D3- receptor agonism has also been reported to decrease risky choice in an animal model (St Onge and Floresco, 2008). L-dopa itself also potentiates gambling behaviour in co-administration with dopamine agonists (Imamura et al., 2006). An abnormal baseline in PD patients with depleted nigrostriatal systems may engender disrupted dopamine receptor expression or sensitivity that renders them vulnerable to agonist effects, however these side-effects have also been reported in individuals treated for restless legs syndrome (Tippmann-Peikert et al., 2007). L-dopa promotes the phasic and tonic release of dopamine from synapses in response to afferent depolarisation, while dopamine agonists enhance the tonic stimulation of post- and pre-synaptic receptors in a non-physiological manner (Breitenstein et al., 2006). Thus differential effects of these agents could also be attributed to the distinction between phasic and tonic dopamine, which have been suggested to map onto different computational processes (Niv et al., 2007). An important future avenue for research is to delineate whether effects on gambling behaviour are dopamine-receptor specific, and whether any effects pertain to risk evaluation or other processes such as learning and reward-responsiveness.

7.4.5 GENETIC HETEROGENEITY

Genetic influences may also determine the effects of L-dopa on risk-taking, and a variety of polymorphisms in D1 (Comings et al., 1997; Takahashi et al., 2010), D2 (Comings et al., 1996; Lobo et al., 2010) and D4 (Comings et al., 2001; Dreber et al., 2009) receptors, and the dopamine transporter gene (Comings et al., 2001) have been associated with risky decision making or impulsive behaviour. There may also be pharmacogenetic interactions, with a report of L-dopa increasing risk-taking, in a paradigm with feedback and dynamic risk changes, only for subjects with a specific DRD4 polymorphism (Eisenegger et al., 2010). Dopamine receptor polymorphisms are also suggested to mediate different neuronal

responses to reward during gambling tasks (Forbes et al., 2007; Marco-Pallarés et al., 2009; Camara et al., 2010). Given the constellation of findings, and the fact that individual polymorphisms appear to account for only a small fraction of the tendency to pathological gambling (Comings et al., 2001), the specific effects of each receptor on different elements of the decision making and learning process remains to be fully described.

7.4.6 Role of other neurotransmitters

It is also possible that an alternative neurotransmitter is involved in imbuing risk-preference. Evidence from both neuroimaging and single-unit recording studies have implicated serotonin in reward processing (Tanaka et al., 2007; Nakamura et al., 2008; McCabe et al., 2010), and serotonin augmentation (Tanaka et al., 2009) or depletion (Rogers et al., 2003; Long et al., 2009) alters reward and risk-based decision-making. An effect of serotonin on risk-attitude could also contribute to the effect of satiety and starvation on decision making under risk (Symmonds et al., 2010b). While the rewarding and appetitive effects of food have been attributed to dopaminergic systems (Berridge, 1996), serotonin is also critical in behavioural homeostasis (Leibowitz and Alexander, 1998). Serotonin and dopamine receptor genes may also interact to determine propensity for risk-taking (Ha et al., 2009).

7.4.7 Conclusion

The central finding from this study is that L-dopa administration does not affect risk preference in healthy humans. This contrasts to studies implicating dopamine in risky decision making, and suggests that dopamine exerts an influence through other mechanisms such as modulation of learning or response to reward, rather than the evaluation of risk itself. Our paradigm offers a careful control over different aspects of risk which are often conflated in behavioural studies, and a quantification of risk-preference independent of non-specific effects on choice noise due to attentional changes. Thus, this task could be further adapted to dissociate possible effects of dopamine on reward feedback, and to explore the effects of stimulation of different dopamine receptor subtypes as well as the likely impact of other neuromodulatory agents. Economically inspired paradigms can offer experimental control to selectively manipulate aspects of a decision and sensitively assay pharmacological effects. I will discuss further these future potential avenues of investigation in **Chapter 9**.

Chapter 8

THE CHRONOMETRY OF RISK PROCESSING

8.1 INTRODUCTION

Risk is a potent decision-making variable and risk-return tradeoffs are central to human economic behaviour. In previous chapters I provide evidence for an involvement of specific cortical and subcortical regions in processing dimensions of this decision variable. Extending the extant literature, I identify a network in posterior parietal and prefrontal cortices as expressing scaled parametric responses to statistical risk inherent in a particular stimulus or decision, measured by the variance (dispersion) and skewness (asymmetry) of an outcome distribution respectively (Smith et al., 2009; Xue et al., 2009; Symmonds et al., 2010a; Symmonds et al., 2011). Moreover, I find evidence to support previous findings that regions in anterior insula and inferior frontal gyrus express differential sensitivity depending upon an individual's risk-taking preferences and choices (Christopoulos et al., 2009; Tobler et al., 2009), in other words exhibiting activity that reflects a subjective risk assessment.

While fMRI allows precise regional localisation of risk-sensitive regions its major limitation relates to its poor temporal resolution, being constrained to processes on the timescale of several seconds (Kim et al., 1997). This means that while fMRI data are useful in building up an anatomical picture of a decision-making network, it cannot inform the precise temporal sequence of processing events. However decisions under risk, where different outcomes need to be represented and considered occur rapidly, with individuals able to express clear and consistent preferences within 1-3s (Diederich, 2003; Kuhnen and Knutson, 2005; Huettel et al., 2006; Bollard et al., 2007; Xue et al., 2009). This implies rapid neural processing of salient statistical features of a decision, an integration of this decision information with an individual's subjective preferences or decision strategy, and generation of an appropriate signal to engender a motor response within this time frame. In this study, I utilised the fine-grained data from magnetoencephalography (MEG) to study the temporal evolution of responses to risk within this decision-making network.

As abstraction of information is clearly crucial in informing a decision I hypothesised an early processing of variance and skewness. I expected this to be evident in parietal and prefrontal cortex regions previously implicated in these processes. I also predicted choice-related signals would emerge subsequent in time to risk assessment and evaluation, with an influence of individual risk preference on these choice-related signals in anterior insula. There have been few studies using electrographic or magnetoencephalographic recording of economic decision making (Gehring and Willoughby, 2002; Schutter et al., 2004; Hewig et al., 2007; Hedgcock et al., 2010; Harris et al., 2011; Steffen et al., 2011), but these have focused on evoked responses (event-related potentials (ERPs) or fields (ERFs)), usually to feedback about the outcome of decisions. While the receipt of a reward or loss may reasonably generate synchronised and time-locked event-related signals occurring rapidly following a feedback signal, it is unlikely that the responses associated with risk evaluation occur in such a uniform time-locked manner. The evaluation of risk is likely to occur over a period of tens to hundreds of milliseconds, and indeed start at different times on different trials due to natural within-subject cognitive variability. This variability curtails an easy detection in evoked responses, as signal changes will average out rather than cleanly summate. I therefore focus purely on spectral responses in the time-frequency domain. This enables the detection of changes in trial-by-trial oscillatory power induced by specific components of a decision, without requiring time- or phase-locked signals. Given my a priori knowledge about the regional localisation of a risk evaluation network (Symmonds et al., 2011), I draw inferences in source space and map the temporal profile of responses in posterior parietal, prefrontal and insular cortices.

I required subjects to choose between gambling on a lottery or selecting a sure amount of money on each trial, and similar to my previous paradigms independently manipulated the variance and skewness of a set of individually presented lotteries, recording choices and simultaneous neural responses (i.e. MEG signal changes) as a function of these changing variables. My key question was when and where within my a priori regions of interest are risk signals represented. I again utilised behavioural economic models to measure subjects' subjective preferences for variance and skewness, which enabled me to determine when and where these individual preferences influence neural signals leading to choice, and whether risk-preferences modulate an expected early encoding of variance and skewness in addition to modulating a later choice signal.

8.2 MATERIALS AND METHODS

8.2.1 PARTICIPANTS

The study was approved by the Institute of Neurology (University College London) Ethics Committee. 17 subjects (mean age: 31; age range: 25-50; 5 male) were recruited for the experiment. 1 (female) subject was excluded because of metal artefact due to dental work, and 1 (male) subject excluded because of excessive drowsiness and failure to make button-press responses during the experiment.

8.2.2 TASK

To dissociate different components of risk, in terms of dispersion (variance) and asymmetry of outcomes (skewness), I adapted my previously used decision-making task (Symmonds et al., 2011) that controlled the distribution of outcomes, and ensured that variance and skewness of a set of lotteries were manipulated independently by design. Hence, as variance and skewness of gambles were orthogonal factors, I could test whether neural activity evoked by variance could be distinguished from that evoked by skewness. Participants were required to choose between taking a 'sure' (fixed) amount of money or elect to 'gamble' (choosing to play a lottery with a number of potential outcomes). Gambles were represented as pie-charts, where variance and skewness of outcomes varied over a range, with expected value kept constant (**Figure 8.1 A&B**).

8.2.3 INDEPENDENT MANIPULATION OF VARIANCE AND SKEWNESS

I constructed a stimulus set of 252 lotteries (each presented once) where variance and skewness were independent and varied over a range. For every level of variance (16 levels), I independently varied skewness (16 levels, 8 positively skewed, 8 negatively skewed). Expected value of the lotteries was kept constant (between £5.95 and £6.05), and the sure amount alternative remained constant throughout at £4.50. Stimuli were constrained to have 4 outcomes (segments of the pie chart), with outcome probabilities varying in minimum 0.1 increments between 0 and 1 to mitigate against probability distortion effects at small probabilities. These restrictions allow the generation of a space of possible lotteries varying in skewness and variance (**Figure 8.1 C, Appendix D**). Where 2 possible lotteries were equidistant from the desired array of points, I selected a lottery at random. At the end of the experiment, three trials were randomly selected and played out for real. If subjects had elected to gamble, I resolved the lottery by an on-screen graphic of a red ball spinning

around the outside of the pie until it stopped at a randomly selected position. This procedure was also shown in the practice, to demonstrate the idea that the size of each segment of the pie chart represented the chance of that outcome occurring. Winnings ranged between £13 and £35 (mean £21.17).

8.2.4 BEHAVIOURAL MODELLING

This follows a similar procedure to **Chapter 4**. For a given lottery with 4 potential outcomes *(m_1, m_2, m_3, m_4)*, with probabilities $p = p_1, p_2, p_3, p_4$, Expected Value (EV) = $\sum_{n=1}^{4} m_n p_n$, Variance = $\sum_{n=1}^{4} (m_n - EV)^2 \, p_n$, and Skewness = $\sum_{n=1}^{4} (m_n - EV)^3 \, p_n$.

I analysed choice data by fitting a linear mean-variance-skewness model (**MVS**) where individuals are allowed to express different preferences for variance and skewness. To demonstrate sensitivity to both variables of interest, I compared the behavioural fit of this model to two alternatives; a model based on mean difference (**M**) alone (where subjects only take account of the difference between the sure amount and the expected value of the gamble in selecting actions), and a mean-variance model (**MV**). These were specified as previously.

I again used a logistic/softmax function to allow for noise in action selection.

I estimated best-fitting model parameters using maximum likelihood analysis, with optimisation implemented with a non-linear Nelder-Mead simplex search algorithm in Matlab (Matlab, Natwick, USA). I compared models using the Akaike Information Criterion (AIC), a comparison which penalises model complexity (Akaike, 1974).

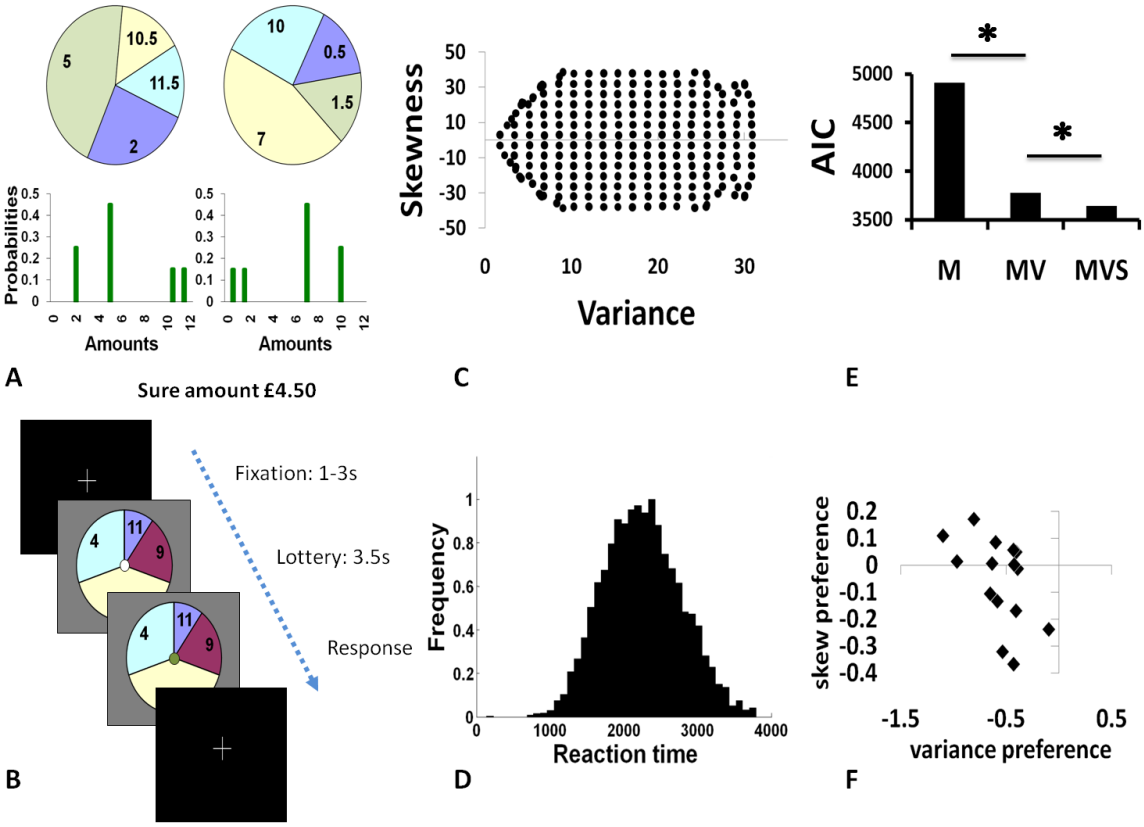

Figure 8.1 Experimental paradigm and behaviour. A. We represented gambles on-screen as pie-charts, divided into four segments showing possible lottery outcomes. Numbers show the monetary value of each outcome (in pounds sterling) and the angle subtended by each segment indicated the probability of each outcome occurring. A positively skewed gamble (left) has a small chance of a better than average outcome (the tail of the distribution is to the right). Conversely, a negatively skewed gamble (right) has a small chance of a worse than average outcome (the tail is to the left). Both examples have identical variance and expected value. B. Each trial was self paced, with subjects first shown a fixation cross, and then pressing a button to commence. Following initial button press, a gamble was presented for 3.5 seconds, during which time the subject was required to make a two-alternative forced choice between opting to gamble, or to take a sure amount of money of £4.50. Subjects selected actions by button press, indicated on screen by a colour change in the central fixation circle. At the end of the experiment, three trials were randomly selected and played out for real. If subjects had elected to gamble, we resolved the lottery by an on-screen graphic of a red ball spinning around the outside of the pie which stopped at a randomly selected position. C. Plot of the stimulus space used in this study, showing 252 gambles independent in variance and skewness. The non-uniformity at the extremes of variance is limited by the restrictions on stimulus generation (a fixed expected value of £5.95-6.05, 4 segment pie charts with a minimum probability of 0.1) D. Reaction times were normally distributed between approximately 1-3s. 99.7% of button press responses occurred after 1s following stimulus presentation. E. Summed AIC scores for 3 models: mean only (M), mean-variance (MV), mean-variance-skewness (MVS). A lower score indicates a better model fit. The MV model was significantly better than the M model ($\chi 2$: $p < 1 \times 10^{-5}$), while the MVS model was significantly better than MV ($\chi 2$: $p < 1 \times 10^{-5}$). F. Parameter estimates from the MVS model reveal a range of preferences for variance (negative coefficent reflects variance aversion), and skewness (coefficient reflects preference for positive versus negative skewness).

8.2.5 MEG

8.2.5.1 *MEG - experimental setup and preprocessing*

MEG was recorded continuously (sample rate: 1200 Hz), using a 274-channel whole-head system (CTF Omega), with participants in a seated position. Stimuli were presented and responses recorded using Cogent presentation software (Wellcome Trust Centre for Neuroimaging, London) written in MATLAB (version 6.5.1, MathWork, Natick, MA). Visual cues were projected onto a screen directly in front of the participant. Choices were indicated by pressing a button box with the right index finger.

Imaging data were analysed using Statistical Parametic Mapping software (routines in the academic freeware package SPM8; Wellcome Trust Centre for Neuroimaging, UK, www.fil.ion.ucl.ac.uk/spm).

MEG data were epoched to obtain 1000ms data segments corresponding to the first second after presentation of the stimulus. This cutoff was chosen as the time window during which stimuli were being evaluated, before button press responses occurred. On 99.7% of trials motor responses occurred only after this point (**Figure 8.1D**). Data were downsampled to 200Hz, bandpass filtered from 1-80Hz, and baseline corrected. 100ms of MEG data prior to presentation of stimulus (when fixation cross was on screen) was sampled as a baseline period. Data were logarithmically rescaled before subsequent analysis.

I performed artefact rejection using an algorithm that rejected all trials where the root mean square (RMS) power was a factor of 10 greater than the average RMS power per trial across subjects.

8.2.5.2 *MEG - Source level analysis*

I source localised induced responses within four predefined time windows (0-250ms, 250-500ms, 500-750ms, 750-1000ms) and four frequency bands theta (4-8Hz), alpha (8-16Hz), beta (16-32 Hz) and gamma (32-64 Hz), using the multiple sparse prior routine within SPM8 (Friston et al., 2008), with group constraints (Litvak and Friston, 2008). This inverse solution performs an iterative Bayesian optimisation to localise potential activation within a tessellated cortical surface template mesh of several hundred patches, where the mesh is a

tessellated template based on the canonical Montreal Neurological Institute (MNI) brain (Mazziotta, 2001). Hence I obtained 16 (4 time x 4 frequency) source images per subject per trial.

Our contrasts of interest pertained to the 3 parameteric variables of variance, skewness and subject's choice (a categorical variable indicating gamble or sure choice) on each trial. For each subjects' data (i.e. within-subjects), these 3 variables were entered into a multiple linear regression (in a GLM) against trial-by-trial source-localised data. All parametric variables were normalised to the range 0-1 and mean-centred. This regression analysis was performed at each of the above time and frequency bins, generating within-subject statistical maps of the regression coefficients corresponding to variance, skewness and choice regressors. To make group (between-subject) inferences I then imported each of these 16 (4 time x 4 frequency) source level statistical images per subject into a two-way repeated measures ANOVA, repeating this process for variance, skewness and choice regressors respectively.

The GLM-estimated coefficients for each parametric variable gave the estimated slope of the best linear fit, where the null hypothesis at each sensor is that activity is insensitive to variance, skewness or choice respectively (i.e. the regression coefficient equals zero). For inference (using a mass univariate statistical approach) *F*-tests were performed to isolate the main effect of time, collapsing across frequency bands. In other words, I ask where source-localised power correlates with variance, skewness or choice at any of the 4 time windows. Subsequent *t*-tests were then used to delineate the effect size within each time-bin in areas expressing a significant main effect.

8.2.5.3 ***Covariate analyses***

I next asked whether neuronal responses correlating with choice (differential activity for gamble versus sure) was modulated by risk preferences (i.e. an interaction between behavioural preference and neural activity coupled with choice), which I hypothesised would reflect an integration of preferences at the stage of action selection. I expected regions sensitive to subjective preferences to express different patterns of choice-related activity dependent upon individual variance or skewness aversion. Secondly, I examined for an interaction of behavioural preference within the regions sensitive to variance and skewness, asking if risk-preferences alter the primary encoding of these decision statistics. I speculated that I might observe an interaction between preference and synchronised activity correlating with risk, for both variance and skewness, which I posited would reflect an integration of

subjective preference with objective decision statistics. I carried out this between-subjects covariate analysis separately for each time window and each of the three regressors, enteringsource-level estimated regression coefficients (beta images) for variance, skewness, and choice for each subject, inputting images for each of the four frequency bands into second-level one-way ANOVAs. For the choice ANOVA, I included both variance and skewness covariates (estimated from behaviour according to the **MVS** model) in the same statistical model. For the variance and skewness ANOVAs, the corresponding behavioural covariate was entered. I then performed contrasts at the second-level to isolate significant effects of preference on choice-related activity (across all frequencies) and similarly measured effects of preference on variance and skew-evoked activity.

8.2.5.4 *Time-frequency analysis within identified regions*

In order to obtain a full time-frequency characterisation I used a psudoinverse to extract regional signals from the areas displaying maximal effects of the parametric regressors. This data extraction was performed in 10mm spheres centred on peak voxel coordinates from the statistical image using a source-extraction routine implemented in SPM. I used a Morlet wavelet time-frequency decomposition with 7 cycles, with a frequency-dependent cycle length as implemented in SPM8 (Kiebel et al., 2005). I performed this on each trial's waveform (i.e. not on an average waveform), thus capturing evoked (phase-locked) and induced (non-phase-locked) oscillatory power. Analysing changes in induced power is critical for this cognitive task, as the neural processes of interest (evaluating the statistics of a decision and making a choice) are unlikely to be either time- or phase-locked to stimulus presentation, given that individuals express variability in their speed of assessment on different trials. This means that a simpler ERF analysis of evoked waveforms in the time domain is likely to be uninformative, given that these (temporally jittered) evoked waveforms will cancel each other out during averaging, rather than summating. I then repeated the above GLM analyses on the source extracted data in continuous frequency and time, performing multiple linear regression at the within-subject level for variance, skewenss and choice regressors, and entering these effect sizes into t-tests (or regressions against covariates) at the group level in the standard hierarchical approach. Significant effects within each region-of-interest could then be displayed as a time-frequency plot.

8.2.5.5 *Statistical reporting and figures*

I report effects within a mask of bilateral posterior parietal cortex, anterior insula, and dorsal prefrontal cortex, given that these areas of prior interest. I report voxel-wise significant results at a $p<0.01$ threshold and clusters of greater than 50 voxels. Brain image figures show second-level SPM-F or SPM-T images, superimposed upon a canonical brain image, thresholded at $p=0.01$. Stereotactic coordinates are reported in MNI space (Mazziotta, 2001). Time-frequency images show second-level equivalent Z-score maps, with corresponding linear time-plots of the significance of effects averaged over our four a-priori frequency bands.

8.3 RESULTS

8.3.1 BEHAVIOUR

8.3.1.1 *Choices*

The stimulus set was designed to ensure that, on average, participants would evenly distribute their choices between gamble and sure amounts. This maximises power for both behavioural fitting and subsequent analysis of oscillatory power corresponding to choice. As planned, our subjects (n = 15), on average, distributed their choices between gamble and sure options throughout the course of the experiment (mean percentage of gamble choices = 55%, std. 17%). There were few error (missed) trials (0.4% of all trials). Variance and skewness were uncorrelated with choice, aided by use of the orthogonal stimulus set. Response times (from stimulus presentation to button press) were 2.26 +/- (SD) 0.53s (**Figure 8.1D**).

8.3.1.2 *Behavioural modelling*

I independently manipulated variance and skewness, expecting that individuals' preferences would be sensitive to both summary statistics. To formally test this, I compared a mean-variance-skewness model (**MVS**) where individuals are allowed to express preferences for both variance and skewness, to a set of alternative decision models. As predicted, a mean-variance-skewness (**MVS**) model provided a significantly better fit to the behavioural data than the alternatives (summed AIC scores: **M**: 4909; **MV**: 3778; **MVS**: 3642); **MVS** model posterior probability>0.99 (very strong evidence in favour of **MVS**) (**Figure 8.1E**).

I then used the winning **MVS** model to provide subject-specific preferences for variance and skewness (**Figure 8.1F**). All subjects were averse to variance (average variance preference: -0.56 +/- SD 0.25), and 7/15 preferred negative to positive skewness (average skewness preference: -0.06 +/- SD 0.16). Beta (temperature) values for the logistic function were low, indicating that choices were well partitioned by the linear model (average beta = 0.13; SD. 0.06).

8.3.2 MEG SOURCE LEVEL ANALYSIS

8.3.2.1 *Parametric responses to variance and skewness*

The primary focus of this study was to make inferences about the temporal processing of risk during decision making in prior regions of interest. Hence, I localised induced power in four pre-specified time windows (0-250ms, 250-500ms, 500-750ms, 750-1000ms) following stimulus presentation, at each of 4 frequency windows (4-8Hz ('theta'), 8-16Hz ('alpha'), 16-32Hz ('beta'), 32-48Hz ('gamma')). Although our regions of interest from fMRI studies are based on areas showing positive correlations with variance and skewness, I am agnostic about the direction of correlation with MEG responses and have no a priori assumptions about the frequency bands in which specific effects will be expressed. I aimed to identify *any* responses showing a significant linear correlation with our variables of interest, irrespective of whether these responses were driven by synchronisation or desynchronisation. Although increased power at high (gamma band) frequencies has been shown to positively correlate with BOLD activity, conversely increases in low-frequency power negatively correlate with the BOLD signal (Logothetis et al., 2001). I thus perform bidirectional F-tests constructed from linear contrasts to identify the main effects of each regressor.

There was a significant effect of variance in left posterior parietal cortex ($F_{3,219}$ = 4.25, p = 0.005; **Figure 8.2A**). This linear modulation of induced power occurred in the initial 0-250ms following lottery presentation ($t_{1,219}$ = 1.95, p = 0.02), and peaked between 250-500ms ($t_{1,219}$ = 2.94, p = 0.002) (**Figure 8.2B**). Time-frequency decomposition within this region revealed the peak effect was driven by synchronised, correlated, beta activity between 250-300ms, preceded by alpha activity (**Figure 8.2C&D)**. For skewness, I observed significant effects in dorsomedial prefrontal cortex, with the peak effect on the right (R DMPFC: $F_{3,219}$ = 4.75, p = 0.003; L DMPFC: $F_{3,219}$ = 4.17, p = 0.007; **Figure 8.2E**), a response present ($t_{1,219}$ = 4.21, p < 0.0001) between the 500-750ms time window (**Figure 8.2E&F**). There was simultaneous greater theta and beta-band synchronisation for positive, more than

negative, skewed gambles at 250-300ms concurrent in time with the parietal response to variance. Subsequently, at 650-700ms, there was greater gamma band synchronisation for negative skewed gambles (**Figure 8.2G&H**). This demonstrates that both components of risk (variance and skewness) induce independent scaled modulations of oscillatory activity at indentical time epochs in parietal and prefrontal cortex, regions previously identified as showing anatomic localisation of such responses, occurring rapidly after stimulus presentation. The temporally delayed response to negatively skewed (vs positively skewed) gambles is notable as it suggests that lotteries with positive tails (a small chance of a large outcome) are registered prior to the mirror image lotteries with occasional poor outcomes

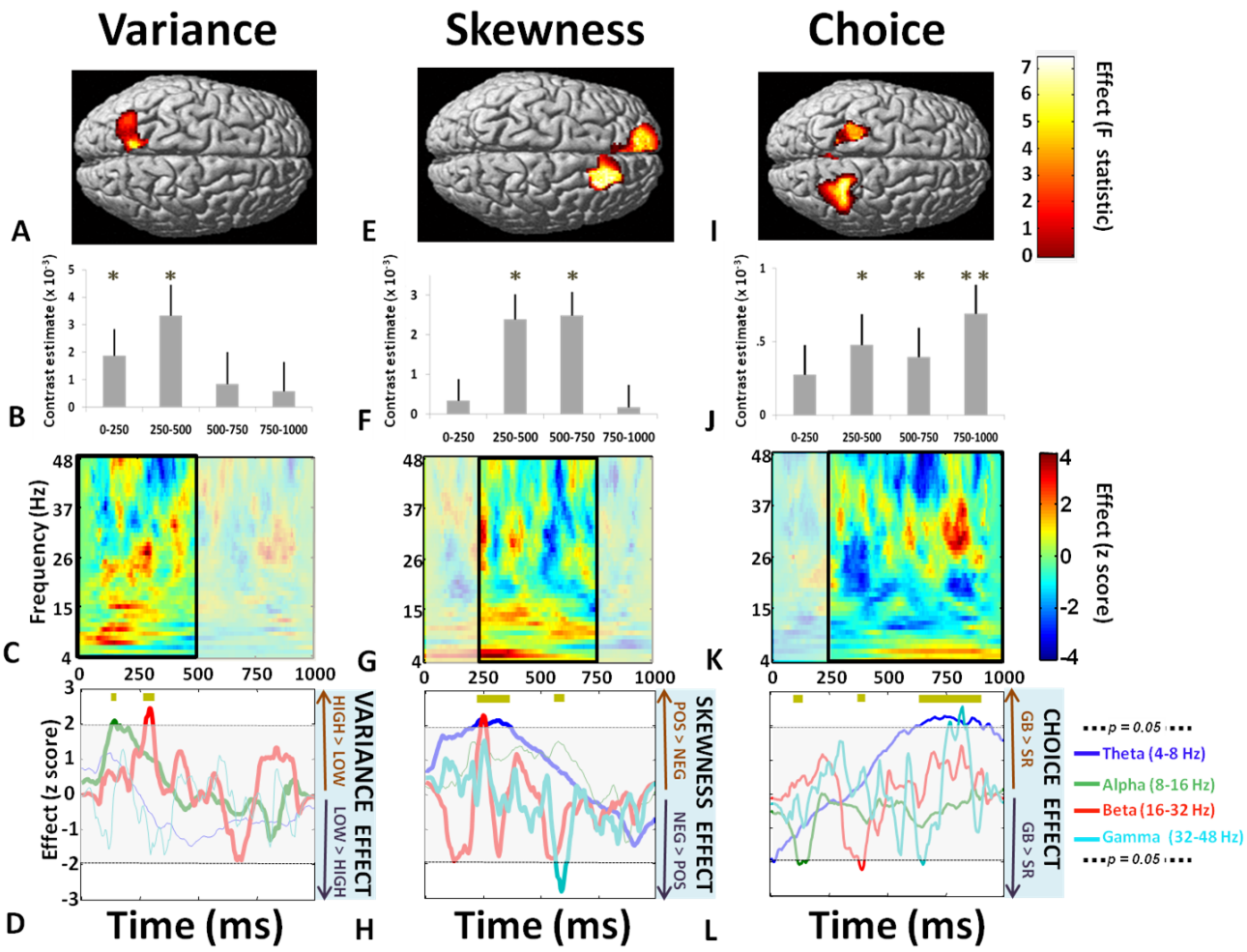

Figure 8.2 Responses to risk and choice. A. Source-reconstructed induced power parametrically correlating with variance in left posterior parietal cortex (all effects across 4 frequency bands: 'theta' (4-8Hz), 'alpha' (8-16Hz), 'beta' (16-32Hz), 'gamma' (32-48Hz)). B. Timecourse of effect, showing significant effects in first 0-250ms window, peaking at 250-500ms (variance peak voxel at -12, -56, 52). C. Time-frequency plot of extracted data. D. Peak effects at 150ms and 260ms in alpha and beta bands respectively. E. Source-reconstructed induced power parametrically correlating with skewness in left and right DMPFC (across all frequencies). F. Timecourses of effects in right DMPFC (skewness peak voxel at 22, 24, 34). G. Time-frequency plot of extracted data. Positive effect indicates greater activity for positive than negatively skewed gambles, while negative effect indicates the opposite pattern. H. Peak positive correlation at 240-300 ms and peak negative correlation at 600 ms in alpha-theta and gamma bands respectively. I. Source-reconstructed induced power correlating with trial-by-trial choices (gamble versus sure, across all frequency bands). The effect is seen bilaterally over the central sulcus. J. Timecourse for peak voxel (at 28, -46, 50) shows effects commencing at 250-500ms, maximal at 750-1000ms after stimulus presentation. K. Time-frequency plot of extracted data. Positive effect indicates greater activity preceding gamble than sure choices, while negative effect indicates the opposite pattern. L. Greater beta activity before sure choices early at 400ms, while greater theta and gamma activity before gamble choices at 620-880ms. Figures show second-level SPM-F image thresholded at p<0.01, superimposed upon a canonical brain (* = p<0.01, ** = p<0.0001; colourbars show F-statistics or z-score). Time-frequency data extracted from 10mm sphere centred on peak voxel. Significant time-windows identified from preceding analysis highlighted. Time-courses (bottom row) are of effect significance, with data averaged by our four a priori frequency bands. Dotted lines show p<0.05 two-tailed significance threshold, with significant timepoints indicated by gold bar.

8.3.2.2 *Modulations of induced activity before gamble or sure choices*

I next ask whether there were choice-specific modulations of induced oscillatory power, which was evident bilaterally over the central sulcus (on right: $F_{3,219}$=7.40; p = 0.0001; on left: $F_{3,219}$ = 5.56, p = 0.001; **Figure 8.2I**), reaching its peak effect in the 750-1000ms time window following stimulus presentation ($t_{1,219}$ = 3.49, p = 0.0003; **Figure 8.2J**). Analysis in continuous time and frequency revealed two temporally separate events – greater early responses preceding sure more than gamble choices, occurring in the beta band at 300-350ms, but conversely greater late responses for gamble than sure choices expressed as concurrent theta and gamma band synchronisation at 600-800ms (**Figure 8.2K&L**). This is consistent with an hypothesis that signals driving a motor response evolve after intitial processing of the gamble stimulus. The novel finding here is that I see neural responses correlating with sure choices arising 250ms prior to those for gamble choices.

8.3.2.3 *Effects of variance and skewness preferences*

I considered two ways in which regional activity could express an integration of the encoded statistics of each lottery with individuals' tastes for risk. Firstly, preferences could exert an effect on an action-selection network where one would expect a correlation between differential activation preceding sure or gamble choices and an individual subjects' risk preference. For example, a more variance-averse individual when presented with a risky decision might generate a stronger signal prior to accepting a gamble, while an individual who is tolerant of variance might express a stronger signal prior to selecting a sure choice.

8.3.2.3.1 EFFECT ON CHOICE-RELATED ACTIVITY

I focused on regions where both variance and skewness preferences influenced choice-related activity. There was a significant correlation between choice activity and both variance and skew preferences in the anterior insula / inferior frontal gyrus region, and in dorsal premotor cortex (Figure 8.3**A**). This between-subjects effect of behavioural preference on neural activity was expressed just prior to decision execution in the 500-1000ms window (conjunction analysis: 500-750ms, $t_{1,54}$ = 2.69, p = 0.005; 750-1000ms, $t_{1,54}$ = 2.75, p = 0.004), but also in the first time window (0-250ms: variance coefficient x choice activity: $t_{1,54}$= 2.70, p = 0.005; Figure 8.3**B**). Time-frequency extraction (Figure 8.3**C**) showed that both variance averse and variance tolerant individuals expressed synchronisation of

oscillatory power in high frequency bands prior to gamble choices at 400ms (predominantly in the beta band for variance tolerant individuals versus gamma band for variance averse individuals). Variance tolerant individuals also show earlier synchronised activity correlating with subsequent gamble or sure choices at 250ms, concurrent with activity seen for primary stimulus encoding of variance and skewness. In the theta band, there is even evidence of emergence of activity coupled with choice at ~100ms. Thus insula activity predictive of choice occurs early, simultaneous with encoding of the variance and skewness of a risky stimulus in parietal and prefrontal cortices. From the very earliest stages of risk encoding we observe an effect of preference, an effect that directs upcoming choice. Moreover this insula activity is differentially expressed depending upon an individual's risk preference, as would be expected from an area having a modulatory influence on risk processing according to subjective tastes for risk.

In addition, variance averse individuals demonstrated significantly greater (beta and gamma band) responses at 850-900ms prior to choosing to gamble versus choosing a sure option, with greater theta band responses for the opposite choices at the same timepoint. This late effect is consistent with an anticipatory response prior to action execution, with heightened activity prior to gamble choices if one is risk averse (and an opposite pattern at the same timepoint if risk-seeking. Splitting subjects by both variance and skewness preferences, a general pattern emerged such that variance averse and positive-skew seeking individuals (disliking uncertainty and driven by the potential of large rewards) expressed late synchronisations across beta and gamma frequencies before choosing to gamble, while individuals with the opposite preference pattern exhibited earlier activity, in particular in the beta band, before choosing to gamble (Figure 8.3**D**). Thus, insula activity predicts *both* gamble and sure choices but exhibits different patterns and timecourses of activity depending upon an individual's specific risk preferences.

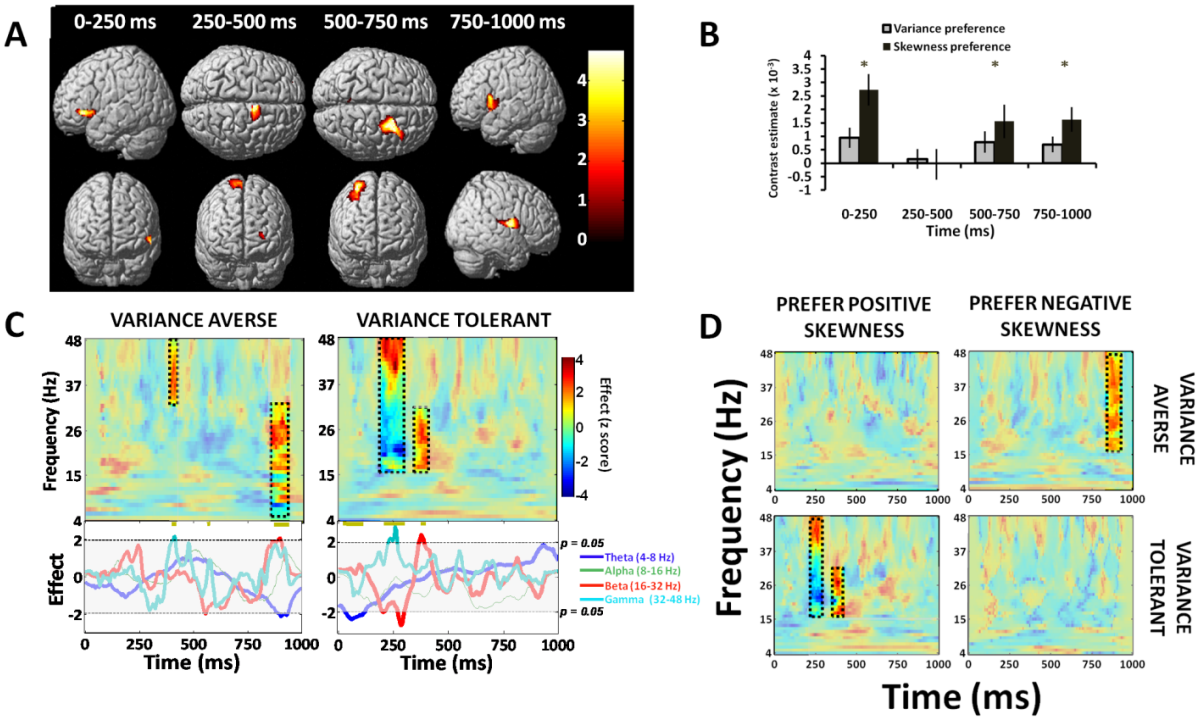

Figure 8.3 Choice-related activity is modulated by risk-preferences. A. Source-reconstructed induced power over 4 time windows showing regions where choice-related activity covaried with both variance and skewness preferences (conjunction analysis - colourbar shows T-statistic). B. The interaction between neural activity and behavioural preference (both for variance and skewness) plotted for left anterior insula (peak voxel -44, -14, -2). Significant effects were observed in the 0-250 ms window and between 500-1000 ms. C. Time-frequency effects in left anterior insula region plotted for variance averse and variance tolerant subjects (median split). The behavioural-neural interaction is driven by late responses at 900ms for variance averse individuals, but early responses around 250ms in variance tolerant individuals. D. Median split of subjects into variance averse/tolerant and positive/negative skew averse individuals. Late increased beta and gamma activity prior to gamble choices most evident in variance and negative skew averse individuals, while early theta and beta activity prior to gamble choices most evident in variance tolerant,

8.3.2.3.2 *EFFECT ON ACTIVITY EVOKED BY LOTTERY STATISTICS*

Preferences could also be expressed intrinsically in regions representing variance or skewness. These areas could themselves express different sensitivities to risk statistics depending upon an individual's risk preferences. Consequently, I next tested for regions expressing a between-subjects correlation between either variance or skewness effects and subjects' variance and skewness preferences respectively. In other words, I looked for an interaction between individual preferences and the parametric, induced, MEG signal response.

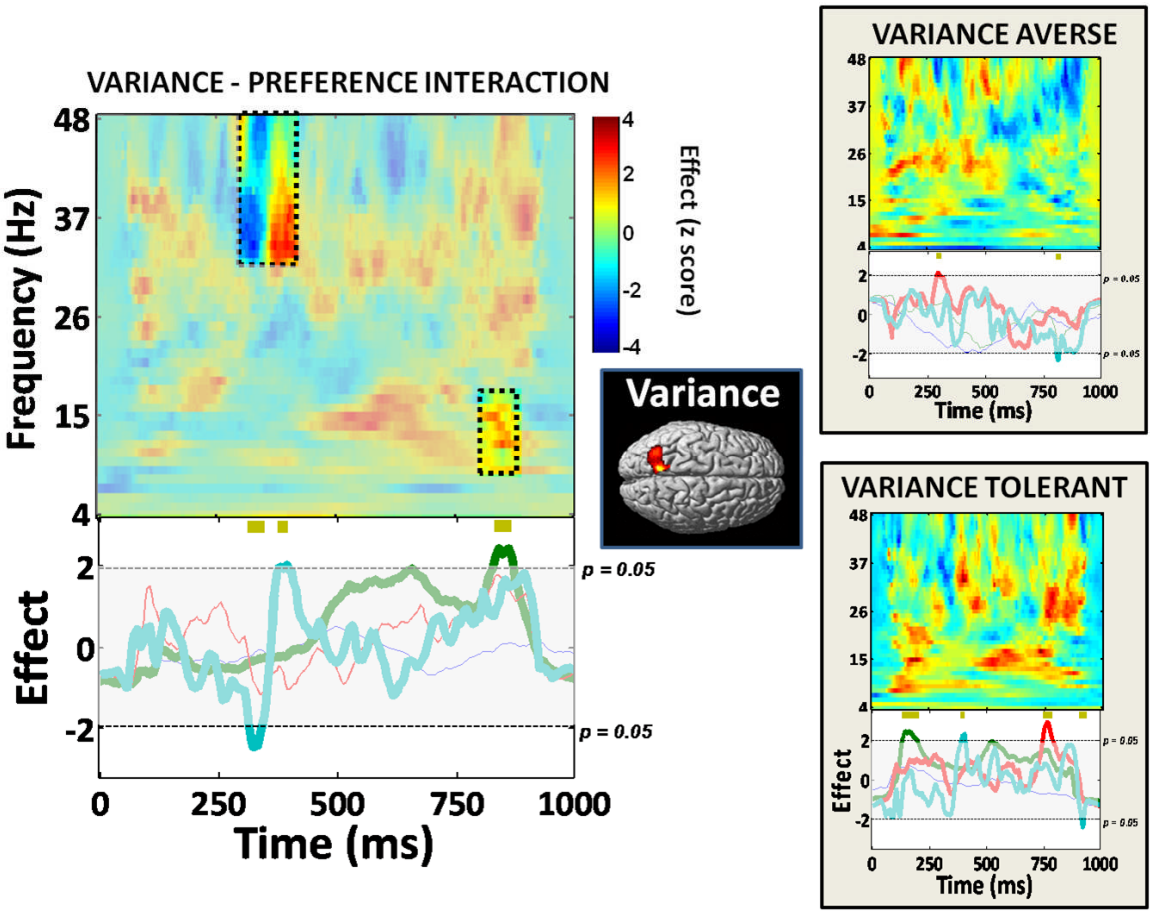

Figure 8.4 Between-subject effect of preference on neural response to variance. Left - source-reconstructed induced power in left posterior parietal variance-sensitive region showing early (300ms) and late (800ms) correlations with variance preferences. Right – subjects (median) split by variance preference. Variance tolerant subjects show a negative correlation in the gamma band at 300ms (i.e. more synchronised activity for low variance) while variance averse subjects show a positive correlation (i.e. more synchronised activity for high variance) in the gamma (and beta) bands at this time. The opposite pattern ensues for the later correlation.

I identified such an effect in variance-sensitive posterior parietal cortex (**Figure 8.4**). Gamma band activity (note a different frequency band than expressing a main effect of variance) showed a biphasic correlation with preference at 300ms. This reflected a positive correlation with increasing variance in variance-averse individuals relative to a negative correlation in variance-tolerant individuals. Furthermore, the main effect of variance (i.e. statistical risk encoding) in this region occurred at different time-points for variance-tolerant and averse individuals respectively. Variance-tolerant individuals show an early (~200ms) correlation of alpha band activity with variance, while variance averse individuals show slightly later beta synchronisation (250-300ms). These early effects are entirely consistent with an hypothesised effect of preference on stimulus encoding. A converse pattern of effects is seen at 750-850ms, with positive correlation with beta and gamma in variance tolerant individuals and the opposite in variance averse. This is concurrent with choice-related insula activity, thus may reflect synchronisation between these regions in a risk-sensitive network prior to action execution.

Similarly, the skew-sensitive DMPFC region also showed an effect of preference (**Figure 8.4**). A correlation with skewness preference was seen concurrent with encoding of skewness at 250ms. or the 200-300ms time period there was enhanced positive correlation with (positive) skewness in individuals disliking positive skewness and preferring negative skew (across frequency bands). In subjects who show converse preferences and prefer positive skew, I observed a negative correlation with skewness (i.e. early increased beta band activity for more negatively skewed gambles).

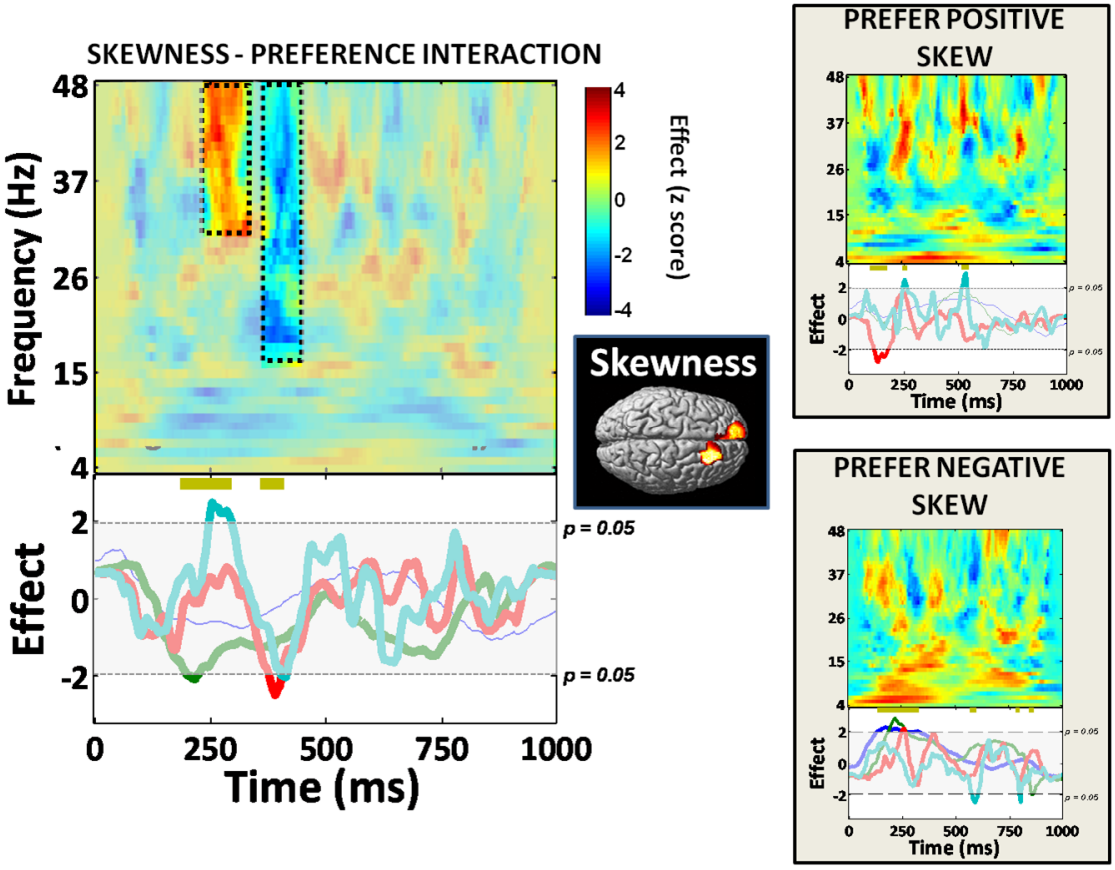

Figure 8.5. Between-subject effect of preference on neural response to skewness. Left - source-reconstructed induced power in right DMPFC skew-sensitive region showing early (200-400 ms) correlation with skewness preferences. Right – subjects (median) split by skewness preference. Subjects averse to negative skew show decreased beta show a negative correlation (i.e. more activity for negative skewness) in the gamma band at 300ms while positive skew averse subjects show a positive correlation (i.e. more activity for positive skewness) in the theta, beta and gamma bands at this time.

8.4 DISCUSSION

The timing of processing in the brain is of fundamental importance. To my knowledge this is the investigation of the temporal evolution of induced responses to risk in a decision making task. I identify specific patterns of activation within previously identified risk-sensitive regions (Huettel et al., 2006; Preuschoff et al., 2006; Platt and Huettel, 2008; Mohr et al., 2010a). I characterise parametric spectral responses, showing induced oscillatory power during the evaluation of lotteries was modulated specifically by the variance and skewness of each gamble on a trial-by-trial basis. A linear response to variance was observed in parietal cortex within the first 250 ms, and to skewness in dorsomedial prefrontal cortex persisting until 750ms following stimulus presentation. These findings again support the assertion,

based on previous behavioural (Coombs and Bowen, 1971; Peiro, 1999) and fMRI (Symmonds et al., 2011; Wu et al., 2011) findings ,that risk is not a unitary phenomenon but is a variable with independent dimensions that are evaluated in discrete neural networks. The posterior parietal cortex is known to accumulate perceptual evidence under uncertainty prior to action selection (Huk and Shadlen, 2005; Kiani et al., 2008), suggesting that this region is specialised for processing statistical decision-related information, and more generally is implicated in numerical and spatial quantification (Hubbard et al., 2005; Piazza et al., 2007). Dorsomedial prefrontal cortex has been reported to encode the probability of loss (Smith et al., 2009; Xue et al., 2010), and is also consistently implicated in risk-processing (Critchley et al., 2001; Tobler et al., 2007; Bach et al., 2009; St Onge and Floresco, 2009; Venkatraman et al., 2009; Mohr et al., 2010b).

The early responses observe match the processing speed during other decision making tasks, for example judging the direction of moving dot stereograms (Bogacz et al., 2006; Heekeren et al., 2006), more complex perceptual discrimination between pictures of faces and houses (Fleming et al., 2010b), or value comparisons (Milosavljevic et al., 2010). I interpret these early stimulus-locked responses as consistent with specialised cortical evaluation of risk. It is interesting to note that skewness-induced responses occur simultaneously with variance-induced responses. Variance is a first order measure of uncertainty, while skewness (mathematically) reflects a second order attribute of the gamble – the relative amount of relative gain versus loss inherent in a gamble. Although one can postulate a natural primacy in temporal processing of these dimensions, recent investigations in trading behaviour under time pressure suggests that skew sensitivity emerges rapidly (Bollard et al., 2007). Indeed, the distributed spatial processing of these risk dimensions corroborates the hypothesis that the dispersion and relative hedonic asymmetry of outcomes are supported by separable, specialised, neural processing.

I found a main effect of choice over the central sulcus, concordant with a motor cortex origin. This response occurred after the stimulus encoding effects seen in parietal and prefrontal cortex although interestingly I observed a different temporal profile prior to gambling than a sure choice option. In the late phase of the 1000ms period after stimulus presentation, gamble-related responses were greatest at ~800ms, contrasting with greater responses prior to sure choice in the same frequency band, but occurring earlier at 300-400ms.

Behaviourally, subjects' choices are sensitive to both the spread (variance) and asymmetry of a distribution of possible outcomes (skewness), but there is heterogeneity in these

preferences, similar to my and others' behavioural findings (Lopes, 1984; Symmonds et al., 2011). I asked where and when these subjective tastes for risk biased choice are expressed. In anterior insula and inferior frontal gyrus, commonly implicated in risk tasks (Preuschoff et al., 2006; Tobler et al., 2007; Christopoulos et al., 2009; Tobler et al., 2009), neural activity predicts subsequent action selection and is modulated by individual tastes for risk (both for variance and skewness), with a similar effect seen in premotor cortex. Intriguingly, the temporal profile of the insula response shows two distinct effects - an early influence of risk preference on choice-activity at 0-250ms after stimulus presentation, and a later effect, just prior to making a decision at 750-1000ms. The early effect occurs concurrently with the encoding of risk dimensions in parietal and prefrontal cortices, indicating an integral role in a risk-processing network.

The anterior insula has been suggested to promote or inhibit gamble selection dependent upon risk-preference in fMRI studies (Paulus et al., 2003a; Christopoulos et al., 2009; Engelmann and Tamir, 2009a; Xue et al., 2010). My findings in **Chapter 4** also supported this theory. The effect I observe here is consistent with this – while both all participants show greater gamma synchronisation before choosing to gamble, beta band activity differentiates variance-tolerant from variance-averse individuals (hence could be antagonising the gamma band activity to promote risk-tolerant choices). Moreover, positive skew seeking, variance tolerant individuals (similar to casino gamblers who accept risk for the chance of high reward show strong early responses directing choice, while more conservative individuals preferring negative skewness and disliking uncertainty (variance) show mainly late responses after choosing to gamble. Moreover, the later response in anterior insula is consistent with an affective response to risk, in particular as it follows choice sensitive premotor activity. Insula activation has also been hypothesises to reflect such an anticipatory or evaluative effect (Kuhnen and Knutson, 2005; Preuschoff et al., 2008). These data illustrate a dual role of the insula, both at the time of risk encoding and also reflecting risk expectancy during entrainment of a motor program for action selection.

I also observed that activity correlating with the encoding of objective risk itself, in both parietal and prefrontal cortex, was modulated by risk preferences. Indeed, in parietal and dorsomedial prefrontal cortex, the response to risk was sensitive to preference from the very earliest time-point, with greater oscillatory activity when gambles were more aversive to the individual which supports an hypothesis of enhanced processing of more (negatively) salient cues in these regions. This preference-dependent effect was seen even before significant main effects of variance and skewness, emerging even before insula activity before a period

of concurrent activation. This strongly indicates that preference is imbued to neural activity from the point of initial risk encoding, furthermore that insula activity communicates with these risk-encoding regions at this time to establish a choice. Interesting, a late decrement in gamma-band variance-related activity is also seen in variance-averse individuals at 750-850ms. This effect, occurring at the same time as the later insula response, may again reflect synchronisation between these regions in a risk-sensitive network, but now an effect anticipating action execution.

MEG is maximally sensitive to cortical effects; hence here I do not explore subcortical risk processing (Knutson et al., 2005; Preuschoff et al., 2006; Mohr et al., 2010a). MEG offers the ability to resolve risk-sensitive processes at a sub-second timescale, and here for the first time I map out the evolution of a decision process, through risk assessment and integration with individually specific traits or predilection to an ultimate choice. Using MEG to measure the temporal precedence of specific processes bypasses the problems of inferring causality from fMRI data (Friston, 2009), and also provides information about parametric changes in steady-state oscillatory power which underlie a range of similar cognitive processes such as sensory perception (Gray and Singer, 1989; Tiitinen et al., 1993; Tallon-Baudry and Bertrand, 1999) a comparison between alternative percepts (Spitzer et al., 2010), and maintenance in working memory (Romo et al., 1999). For example, here I observe both early and late correlations between choice and preference in insula, findings that would be confounded at the temporal resolution of fMRI but which inform my interpretation of the decision process. Additionally, fMRI can be blind to excitatory activity at lower oscillatory frequencies (Goense et al., 2011), here revealed by MEG.

8.5 CONCLUSION

Here, I provide a characterisation of the temporal sequence of decision making under risk. I report evidence supporting an initial rapid processing of salient risk dimensions in parietal cortex followed by dorsomedial prefrontal cortex and highlight a graded parametric variation in oscillatory power that correlates with experimentally manipulated variables specific to the decision at hand. This localisation independently replicates my previous results in **Chapter 4,** with a different imaging modality. Similar modulation has been recently reported in the context of perceptual decision-making (Spitzer et al, 2010), and here I demonstrate a similar pattern of processing for the first time in an economic decision-making experiment. Strikingly, individual preferences have an effect upon neural risk-

sensitive networks at two specific times – early at the time of stimulus risk encoding and later by altering the expression of oscillatory responses selective for action. Simultaneous activation of anterior insula and risk-sensitive parietal and prefrontal cortex in a manner dependent upon individual tastes for risk points to this region supporting processes that modulate risk-responses to influence choice. More broadly, this study demonstrates the powerful potential of MEG as a complimentary tool to directly map out the causal sequence of neuronal activity, and enable a temporal dissection of the cognitive processes engaged in decision-making.

Chapter 9

GENERAL DISCUSSION

9.1 EVIDENCE FOR SUMMARY STATISTIC MODELS

9.1.1 OVERVIEW AND CONTRIBUTIONS

Classical utility theory assumes that each possible state of the world is assigned a value, which is then weighted by a probability (Machina, 2005). In this thesis I provide evidence for an alternative hypothesis, namely that the human brain is adapted to decompose a decision into summary statistics reflecting the dispersion and asymmetry of an outcome distribution.

An important methodological contribution is paradigm design. The paradigms herein substantially differ from previous approaches to risk, as I render more tractable its investigation by independently varying statistical features of a distribution of outcomes. Using multiple, rather than binary outcomes overcomes limitations of previous experiments and gives the ability to flexibly map out a desired stimulus space. This approach of compartmentalizing the independent properties of a stimulus in order to deconstruct the associated neural networks is well established in sensory neuroscience. Such a method enables testing of systematic influences on different aspects of behaviour, as well as allowing independent neural inferences to be drawn.

Similar to processing of component features of complex visual stimuli, I find that contrary to a common assumption, risk is not monolithic but can be decomposed into separate dimensions which have a segregated representation in the brain. While agnostic as to the exact coding of these statistics (e.g. variance, standard deviation and coefficient of variation are all correlated measures of spread), I observed that responses to the dispersion versus the asymmetry of outcomes evoke activity in anatomically separate networks. Strikingly, neural activity during risky choice also reflects individuals' tastes for different features of an

outcome distribution, leading to an evaluation and integration within dissociable neural regions involved in risk processing (Symmonds et al., 2011).

9.1.2 BEHAVIOUR

A consistent behavioural finding throughout these studies is that experimental subjects were on average both variance and positive skew-averse. This means individuals dislike uncertainty (outcome dispersion) and prefer gambles with mostly above average rewards associated with a small chance of low payoffs. Negative skew preferring individuals are tolerant of downside risk, a common feature in everyday scenarios such as property investment or consenting to surgery – generally the outcomes or rewards are good, but there is a small chance of heavy loss. Positive skew preferring individuals on the other hand seek large-but-unlikely rewards, and people with such preferences might take the opportunity of investing in oil exploration or gambling in a casino. Critically, these preferences do not relate to the spread of a distribution, but the relative potential for gains and losses entailed. In contrast with normative theoretical predictions of positive skew preference in variance averse individuals (Scott and Horvath, 1980), I find that individual's behavioural preferences are heterogeneous and uncorrelated.

There have been relatively few experimental investigations where variance and skewness are dissociated. In experiments where preferences for lotteries with different variance and skewness have been systematically examined, individuals exhibit similar heterogeneous behaviour. Several studies have reported predominantly positive skew-seeking behaviour (Coombs and Pruitt, 1960; Alderfer, 1970), or used positive skew preference to explain gambling behaviour (Golec and Tamarkin, 1998; Garrett and Sobel, 1999). Other studies have reported varied preferences, with different participants showing positive or negative skew-seeking as in my studies (Lopes, 1984), or negative skew preference on average (Lichtenstein, 1965). Skewness has also been shown to influence perceived riskiness in different directions (Coombs and Bowen, 1971), and negative skew-seeking behaviour is also reported as common in investors (Tan, 1991; Taleb, 2004).

While there are no clear biological restrictions on the range of preferences individuals are allowed to exhibit in a summary statistic framework, it is nonetheless interesting to speculate on the reasons why different studies report disparate preferences for variance and skewness. Distorted estimates of very small probabilities are likely to have an additional impact on choice, and some previous studies have used extremely unlikely events when

demonstrating skew-preferences. Many previous studies also present mixed gambles (with both possible financial losses and gains), rather than presenting decisions purely in the gain domain as in the current study. This raises the possibility that contextual frame (loss or gain) of the decision could additionally influence predilections for risk.

9.1.3 NEURAL ENCODING OF SUMMARY STATISTICS

There have been a number of recent investigations examining neural responses to components of a risky decision. These studies have highlighted a number of brain regions interested in risk, in particular anterior insula, DMPFC, PPC, and ventral striatum. Whilst many of these studies frame risk in terms of summary statistics (e.g. Fiorillo et al., 2005; Preuschoff et al., 2006; Tobler et al., 2007; Christopoulos et al., 2009; Tobler et al., 2009; Mohr et al., 2010b), others follow the tradition of classical economics and define values by the subjective utility and probability of outcomes (e.g. Hsu et al., 2005; Knutson et al., 2005; Kuhnen and Knutson, 2005; Knutson and Bossaerts, 2007; Tom et al., 2007; Samanez-Larkin et al., 2010). Given that risk is not an explicit variable in classical theory, these are seemingly incommensurable findings (Boorman and Sallet, 2009).

Previously observed non-linear ventral striatum activation for probability (Hsu et al, 2009) could be explained by positive skewness encoding as these variables are correlated when binary outcomes are used. It is also possible that the converse is true, although less likely given that in these studies I employ multiple outcomes. Moreover, and perhaps more tellingly, there is no clear model of how multiple outcomes would be encoded. Indeed one might expect neural representation of both 'win' and 'loss' outcomes assuming separate encoding of amounts and probabilities. Often in neural decision making experiments for binary gambles, only the probability of winning is modelled. While agnostic as to the exact coding of the summary statistics of outcome distributions (e.g. variance, standard deviation and coefficient of variation are correlated measures of spread), critically I find responses to dispersion versus asymmetry of outcomes evokes activity in anatomically separate networks. Moreover, I independently replicate these anatomical findings during single-shot decisions using fMRI and MEG.

Consistent with these data, PPC insula and DMPFC activation were also reported in a study with choices between multiple-outcome lotteries (e.g. Venkatraman et al., 2009), potentially reflecting preferences for different kinds of outcome distribution. Additionally, a recent paper (Wu et al., 2011) has examined skewness, investigating neural responses to

presentation of 4 repeatedly presented mixed gambles (high variance, low variance, positively skewed, negatively skewed) in a passive viewing (no-choice) paradigm. In line with my findings, the authors report greater ventral striatal activity for positive versus negatively skewed gambles and anterior insula sensitivity to skewness. There are several important differences and limitations in the aformentioned study compared to the experiments I present in **Chapters 4 and 8**. Critically, my subjects made active choices allowing a distinction between processes supporting risk quantification and evaluation from choice. I did not present outcomes of gambles on each trial, thus I could outrule feedback-related activity. In addition, I employ an orthogonal parametric design presenting a range of gambles with different variance and skewness, avoiding a potential confound between skewness and high variance. My paradigm is controlled to avoid a priori expectations of high risk stimuli and these design features enabled me to accurately and independently measure behavioural and neural sensitivity to each risk dimension. Moreover, I avoid the limitations of using a small number of stimuli as in a cognitive paradigm. Interestingly, Wu at al., 2011 elicited ratings of arousal, perceived risk and preference for each of the 4 lotteries, and found that these ratings are not commensurate, highlighting a disparity between the gambles that subjects preferred and gambles that evoked an affective response. Despite differences in behavioural preferences between this study and my participants, there is a similarity in neural responses. Here, I report anterior insula activation for positively skewed gambles in negative-skew preferring subjects, whereas anterior insula was most active for skewed versus symmetric gambles in Wu's study where subjects exhibit converse preferences.

9.1.4 CHOICE

Another notable finding from the fMRI studies is that a network of brain regions demonstrates greater activation for a gamble than a sure choice. This has also been reported in several previous studies (Matthews et al., 2004; Weber and Huettel, 2008b; Christopoulos et al., 2009). This indicates that recruitment of brain regions is different when generating gamble versus sure choices. This contrasts with the simplifying assumption portrayed in behavioural models, where the process of choice is modelled as a softmax comparison between equally-weighted utilities for a lottery and sure amount. While I make no assumptions here about the neural processes underlying choice generation, similar differential activation in striatum has been related to the acceptance or rejection of a default action (Yu et al., 2010) and in prefrontal cortex during the selection of 'exploratory' actions (Daw et al., 2006).

I shed light on this activity in **Chapter 8**, showing different temporal processing prior to gamble and sure choices. In other words, in brain regions supporting the formulation of a motor plan (premotor and motor cortex), this choice-related activity is expressed at different times, and by different mechanisms, as dictated by one's taste for risk. In fMRI, one lacks the temporal resolution to distinguish these clearly-seen effects using MEG.

9.1.5 FUTURE DIRECTIONS

Although the evidence here indicates that the brain decomposes risky choices into summary statistics, it is likely that the brain does encode states of the world in specific circumstances. There is a large body of evidence for OFC encoding of stimulus value in decisions without risk (Plassmann et al., 2007a; Rangel et al., 2008a). In risk-free situations, there is an expectation of a single specific outcome. Choosing between options entails a comparison – the action selected is necessarily predicted to lead to the optimal outcome. Uncertainty is irrelevant in completely predictable scenarios, and it is unsurprising that a risk-evaluation network remains quiescent. Binary probabilistic scenarios are very similar – again there is a predicted state (a win), but here there is uncertainty. In situations where the states are the most salient feature, and in particular where outcomes are given following choice (i.e. learning), the OFC appears to be recruited (Chib et al., 2009).

In my single-shot experiments, risky choices comprise multiple potential states of the world, and the salient features are the dispersion and asymmetry of outcomes (which are experimentally manipulated) rather than the average expected value of actions (which are static). These scenarios strongly activate a risk network in insula, parietal and prefrontal cortex.

Although computationally simpler to track summary statistics, at other times it can be easy to track and update all states and probabilities if they are limited in number (D'Acremont and Bossaerts, 2008). Thus an important future direction is to establish whether both processes work in concert – tracking important states (e.g. best or worst outcome), as well as measuring distributional uncertainty. This could underlie biases during decisions with particularly salient states, and also explain why some outcomes might be ignored (i.e. akin to 'editing').

A second important avenue is to delineate which statistics are the most representative approximations of neural activity - variance, coefficient of variation, range, and entropy are

all measures of dispersion; skewness, partial moments, and value-at-risk all measure asymmetry. In practice this is challenging because of the highly correlated nature of these descriptives, however in principle the method I have developed herein could be extended to orthogonalise any given dimensions. For example, one could clearly differentiate between asymmetry versus a state-based encoding of only the best and worst outcomes in an experiment where the extreme outcomes are held constant but the shape of the outcome distribution is altered. This is similar to asking if the kurtosis of a distribution elicits neural activity (i.e. differences in the distribution between the extreme and modal outcome).

Surveying my data, dispersion is unlikely to be encoded as entropy, as this pertains to the *probability* rather than *value* of states, therefore variance is well dissociated when using multiple outcome gambles (though not for binary gambles). In addition, the brain is unlikely to be sensitive to purely single-sided measures of asymmetry such as probability of loss or only to extreme outcomes, as we found sensitivity to relative asymmetry outperformed these type of models in **Chapter 4**.

9.2 TRACKING OF RISK IN SEQUENTIAL DECISION MAKING

9.2.1 OVERVIEW AND CONTRIBUTIONS

Much of the existing literature on neural responses to risk focuses on single-shot choices. This is critical for delineating evaluative, anticipatory and feedback-related activity during individual decisions, but does not answer how risk is tracked during a chain of decisions or choices. I tackled this question in **Chapter 5**, presenting a chain of individually simple decisions which lead to different distributions of potential outcomes when strung together in a sequence. I further manipulated the possible distributions of outcomes by varying a threshold or watermark that participants were required to reach to obtain reward. I highlighted two separate but interlinked questions that needed to be addressed in such an experiment. I thus asked *which* utility model the brain approximates in tracking value and risk through a sequence of decisions, and also asked *how* individuals weigh up all possible alternative outcomes when making such plans.

Methodological contributions here included both the construction and analysis of different models of sequential choice, and also applying the method of simulated moments to fit these models. This study (Symmonds et al., 2010a) is to my knowledge the first example of the use

of this simulation method in a neuroscientificaly motivated decision making experiment. This was essential here as maximum likelihood estimation for such a sequential task, where trials are not independent but rather are conditional on previous responses, is computationally difficult to implement.

The key finding was a similar observation of responses to individual statistical moments of a distribution of outcomes in prototypical valuation and risk-sensitive areas, although there are several key differences from **Chapter 4** which I discuss further below.

9.2.2 CONTINUATION VALUE MODELS OF CHOICE

An important point is that observed responses track the statistics of outcomes predicted several trials into the future in accordance with a specific model (**ACV**) of planned choice. This contrasts with the optimal **OCV** model, which would be consistent with a rational decision maker with full knowledge of the available terminal outcomes (where one fixed best strategy is followed from the outset).

Although using a fixed strategy model is possible in this task, more generally it can fail in situations where an individual errs or if some planned alternatives are no longer available. An **ACV** decision-maker considering all possible future outcomes is myopic (i.e. does not deterministically plan choices in advance). However, such a decision-maker can mitigate future errors or constraints by weighting all possible action-outcome combinations, enabling recovery from error by selecting the best set of remaining choices without needing to assume a fixed strategy. **ACV** can also partly capture decision processes where a proportion of (but not necessarily all) possible outcomes in a decision-tree are considered. A more informed version of the **ACV** model might weight strategies according to the proportion of time that they are expected to be chosen either according to previous experience, or based on a rational expectations model similar to quantal response equilibria models of choice (McKelvey and Palfrey, 1998).

Implicit in behavioural modeling is that one necessarily tests the joint hypothesis that both **MVS** and **ACV** models are true, because the continuation value models are coupled to a valuation model. Thus, while these neural data support **ACV** over **OCV** contingent upon **MVS**, it is possible that this could be bettered by a combination with an alternative utility model. In **Chapter 5**, I cannot draw direct statistical comparisons between utility models (as the models are non-nested with different numbers of parameters), however the other studies

provide good supportive evidence for the **MVS** model. In addition, it is possible that I do not see neural responses corresponding to an **OCV** model even in individuals who actually do follow this strategy purely because there is no requirement for a trial-by-trial tracking of the outcome distribution if you have pre-planned a trajectory of choices. However, the fact that I see responses corresponding to the **ACV** model suggests, that at least in some subjects, these average continuation values are being continuously tracked and re-evaluated.

9.2.3 CHOSEN VERSUS EVALUATED RISK

A second observation in the sequential risk study is that the responses are conditional upon choice - chosen risk rather than a pure stimulus-bound assessment as in **Chapters 4** and **8**. All options apart from the sure-only strategy entail risk, so it is not straightforward to analyse the representation of risk independent of choice. This contingency may partly explain the predominant OFC activity seen. The OFC is commonly reported to reflect chosen value (Padoa-Schioppa and Assad, 2006). My data suggests that chosen value, at least for sequential decisions under risk, is also decomposed into summary statistics of expectation and risk.

More broadly, the prefrontal cortex represents higher order contingencies and maintains representations over extended periods of time (i.e. working memory). This has been explored at both a cellular (Kennerley and Wallis, 2009) and systems (Barbey et al., 2011) level. It is therefore unsurprising that we should observe maintenance of attributes of a plan (i.e. the value of a planned trajectory of actions) in this region. Interestingly, I observe a representation of this value or cost function in terms of the sufficient statistics of an anticipated distribution of contingent outcomes.

9.2.4 TARGET LEVEL

Finally, these statistics are relative or adapted to the current target level, reflecting an integration of risk with an externally imposed constraint. I observed a separate neuronal response correlated with the current target level. This adaptation of signals to an overarching target or goal can help overcome the limited dynamic range of neuronal signalling, as responses can be scaled to the context rather than encoding absolute numerosity. This also implies that responses to expected value are integrated with information about the target in generating action values. This parallels a range of fMRI and

neurophysiological findings of adaptive signaling during decision making (Tobler et al., 2005; Elliott et al., 2008; De Martino et al., 2009; Padoa-Schioppa, 2009), psychological insights about relative valuation (Stewart et al., 2003), and rank-dependent decision theories (Quiggin, 1982).

9.2.5 FUTURE DIRECTIONS

There are a number of important questions arising from this study. Firstly, more refined measures of strategy valuation could be tested against behavioural and neural data, in particular the aforementioned quantal response equilibria models. In addition, the concept of pruning of behavioural options is central to solving complex problems and has been addressed in machine learning (Almuallim, 1996). Whether and how certain types of strategy are downweighted or ignored in goal-directed choice is unknown, although certainly my findings would indicate this.

A second important question is how and when targets are integrated in the decision process. Many real-world situations involve reaching a threshold or goal, and the entire body of work on reference-dependent decision making addresses the behavioural consequences of salient targets or anchors. This study was necessarily simplistic in its manipulation of targets. It is an open question as to whether overarching goals are separately maintained in prefrontal cortex and at what stage these influence action and strategy valuation. The separate timescales required to track trial-by-trial predictions versus longer-term consequences would seem to necessitate distinct neuronal supports, although here I only offer tentative evidence in this direction. Studies using methods with high temporal resolution, such as MEG, could potentially address how these hypothesized separate neuronal pools might interact.

A final issue is that here I focus on the encoding or prediction of outcomes. Mechanistically, it is vital to ask how these predictions then guide or inform choice. The **ACV** model appears optimal under bounded rationality assumptions that individuals might not follow an intended choice trajectory, however it would be important to test this prediction and to examine neural responses consequent on such deviations to fully elucidate this process.

9.3 INTEGRATION OF RISK WITH RISK-PREFERENCE

9.3.1 OVERVIEW AND CONTRIBUTIONS

In **Chapter 2**, I discussed possible neurobiological mechanisms by which individual subjective preference could be imbued to choices. In the first instance, I suggested that the primary encoding of risk itself could be different for risk-averse and risk-seeking people. In other words, risk preference could reflect an intrinsic property of risk-sensitive zones in the brain. An alternative is that risk preference could affect action, or the encoding of a motor program, biasing choice towards or away from a risky option. This type of bias I envisaged to be instantiated after primary stimulus encoding, prior to action execution, an influence perhaps generated by a separate cortical region such as insula. A third hypothesis was that a specialised cortical region such as medial prefrontal / orbitofrontal cortex integrated different aspects of value, and in the process of integration weighted different dimensions of the choice to construct an overall 'utility'.

I find strong evidence in favour of the first two mechanisms in **Chapters 4 and 8**; in the latter I elucidate the precise timing of insula influence on the choice process. I also find some evidence of the third hypothesis in particular in **Chapter 5**, as different components of value are each represented in OFC.

9.3.2 THE EFFECT OF RISK PREFERENCE ON RISK ENCODING

One important finding is that preferences are imbued in the process of decision making from the very outset of stimulus evaluation. Risk, both in terms of variance and skewness of outcomes, is encoded differently depending on one's risk preference in a risk evaluation network. This does not simply appear to be due to the presence of a risk response in risk-sensitive individuals or an absence of response in risk-neutral individuals. Rather, the direction of effect, both seen in **Chapter 4 and 8**, reflects the type of risk-preference that an individual exhibits.

The timing of this risk encoding also seems to be crucial for the formation of preference. I demonstrate in **Chapter 8** that early encoding of variance predicts risk-tolerant choices. One could speculate that risk-tolerant individuals have an improved ability to assess variance, subsequently make more 'rational' choices. The effect is more subtle than this, as both

positive and negative skew-preference are expressed early at the time of stimulus risk encoding (but with different directions of effect).

9.3.3 THE ROLE OF THE INSULA

In **Chapter 4**, I reported an integration of risk information with individual preferences (i.e. a 'risk valuation') in anterior insula and IFG. The insula is suited to perform such integration, with a central role in representing interoceptive states (e.g. arousal or sympathetic outflow) consequent upon the perception and evaluation of risk (Craig, 2002; Critchley et al., 2004; Craig, 2009; Singer et al., 2009). It also influences behavioural output by motoric projections to basal ganglia and pre-motor areas or via regions performing value comparison in orbitofrontal cortex (Augustine, 1996; Plassmann et al., 2007a; FitzGerald et al., 2009a). Here, I decorrelated choice from risk, offering the same gamble against different sure amounts, whereas many previous studies have characterised risk anticipation contingent on choice rather than the process of quantifying decision statistics (Kuhnen and Knutson, 2005; Preuschoff et al., 2006; Christopoulos et al., 2009; Tobler et al., 2009; Xue et al., 2010).

An anticipation of chosen risk could recruit insula activity, explaining consistent reports of (risk-attitude dependent) activity in this region. Thus in **Chapter 5**, where responses to statistical moments are also conditioned on choice, the variance-related activity we see in insula could reflect downstream emotional or physiological responses consequential on detecting increased risk rather than direct risk-assessment itself. However, finding a parametric response to risk in these regions is less easily explained as a simple arousal response unless one invokes a monotonic relationship between risk and arousal. Rather, this pattern supports the idea that anterior insula is combining a statistical assessment of a choice with individual tastes for different aspects of risk to arrive at an integrated measure of value.

These findings are further explored in **Chapter 8**, where I map the chronometry of risk processing. Interestingly, I find evidence for an influence of the insula at two time points, both concurrent with stimulus evaluation and immediately preceding action execution. Specifically, the insula expresses activity that predicts subsequent choice at 250-500 ms after stimulus presentation. Moreover, the earlier that activity in insula predicts choice, the more likely one is to be risk tolerant rather than risk averse. This activity starts slightly after the initial encoding of risk itself, and the synchronicity of this response strongly suggests an interaction between insula, parietal cortex and dorsomedial prefrontal cortex at the time of

stimulus evaluation which then subsequently influences action. Secondly, the insula reactivates strongly at 800-900 ms following stimulus evaluation, maximally for risk averse individuals prior to choosing to gamble. This is entirely consistent with an affective anticipatory response, strongest in those who dislike taking risks. Thus, this tentatively ties together the two dominant theories of insula function in risky choice – not only does the insula express an affective or emotional response prior to risk-taking, but also is centrally involved in the evaluation of risk and its integration with intrinsic preferences.

9.3.4 SEARCHING FOR A HEDONIMETER

My finding that expected value and overall utility correlates with activity in mOFC supports an hypothesis that mOFC integrates overall value (an estimate of mean and risk) given a predicted distribution of outcomes. In **Chapter 5** these variables related to a distribution of outcomes not from a single choice but from a set of serial choices, forecast to the end of each block. This corroborates a suggestion that neural responses to value invoke an integrated, goal-directed, representation of choice (Quintana and Fuster, 1999; Fincham et al., 2002). In **Chapter 4**, I also observe a signal correlating with utility in mOFC, albeit a weaker response.

The fact that these responses are much stronger in a sequential risk taking task, and are commonly observed in experiments where reward feedback is given, hints at one possible role for the mOFC in decision making. As previously discussed, it is not necessary to invoke an integrated area encoding utility to explain choice, rather a distributed network of areas could together causally influence neural activity leading to action in premotor and motor regions. However, encoding the predicted trajectories of events in the world is vital if we are to evaluate the consequences of our actions. Prefrontal cortex, with its central role in maintaining strategy representations over several seconds by sustained delay-period activity, and its' role in working memory maintenance modulated by dopamine (Sawaguchi, 2001), would be suited for making these predictions. Hence OFC activity could reflect expected value (contingent on choice or as a counterfactual response) not because it is the equivalent of an hedonimeter in the brain, directing actions in accordance with an internal utility scale, but rather because it *predicts and anticipates* future outcomes. This concords with a Bayesian brain hypothesis (Knill and Pouget, 2004; Friston, 2010), but interestingly suggests that OFC does not simply encode predicted states of the world, but also the likely hedonic consequence of these states.

9.3.5 FUTURE DIRECTIONS

A critical future line of research is to explore the specific role of the insula in encoding risk preference. I show strong evidence that the insula co-activates with risk-processing regions from an early stage of information processing. Indeed, it appears that insula activates shortly after the PPC and DMPFC, in a way that temporally parallels intrinsic preference. This suggests the insula is receiving information from these more primary regions; what is less clear is if the insula is concurrently modulating the activity within the aforementioned areas in a top-down fashion. This could be addressed in a causal analysis.

Moreover, the late reactivation of the insula which is seen in variance averse individuals in **Chapter 8,** synchronous with motoric responses to choice, indicates a co-activation that potentially anticipates or predicts outcomes. An intriguing hypothesis for further exploration is that insula influences both the perception and anticipation of risk by message-passing between evaluative and executive regions of cortex. There is some evidence that disruptions of insula function affect risk sensitivity and risky choice (Weller et al., 2009) –reversible modulations of insula activity at specific times during a decision process (e.g. with transcranial magnetic stimulation) could determine if and how the insula fulfils these roles.
Finally, there are unanswered questions about the role of the mOFC in risky choice. Comparisons between feedback and no-feedback paradigms, and situations where keeping track of risk between trials is required or superfluous could test the hypotheses about maintenance and tracking of chosen risk in mOFC.

9.4 MODULATING RISK PREFERENCE

9.4.1 OVERVIEW AND CONTRIBUTIONS

In **Chapters 6 & 7**, I investigated how risk preferences are modulated by intrinsic physiological state and extrinsic pharmacological manipulation respectively. I found a significant effect of metabolic state on risk-preference that shifted decisions in a riskier or less risky direction depending upon the impact of a calorific meal. Conversely, I found no systematic effect of dopamine administration on decision making under risk. These findings are novel, and exploit the same theme of systematic experimental manipulations of risk in order to quantify effects on valuation in a controlled manner.

9.4.2 PHYSIOLOGICAL STATE

I demonstrate that metabolic state is an important modulator of risk preference. This is the first quantitative demonstration of an effect of physiological state on economic decision making, and illustrates that biological effects can have systematic, non-trivial influences on financial choices. This counters some of the more heated arguments that neurobiology is irrelevant to economics, as here physiological state is an important predictor variable for behaviour (and one that is amenable to biological influence).

It is interesting to speculate on the mechanism of such an effect in light of my other findings. There are several potential loci for this influence. Hypothalamus projects to both prefrontal and insular cortices, and hence may directly mediate such effects by relaying changes in hormonal state to risk processing areas. Alternatively, cortical neurons may be directly sensitive to ghrelin and leptin levels (as well as other peptide transmitters), as they express relevant receptors (albeit at low concentration) (Zigman et al., 2006).

9.4.3 NEUROMODULATORY INFLUENCES ON RISK

The lack of effect of levodopa on decision making is contrary to some previous assertions that dopamine may quantify risk. I suggest that instead dopamine is important during reward feedback rather than risk evaluation. I utilised my paradigm design to dissociate possible effects on the evaluation of different risk dimensions without feedback or learning. Although there are several caveats in the interpretation of such a null result, this provides some supportive evidence of absence of a neffect and is more specific than previous experimental findings in the literature.

Although a lack of effect could be for pharmacokinetic or pharmacogenetic reasons, the dosage and schedule deliberated paralleled many previous studies using levodopa where effects have been demonstrated. Dopamine is however integral to reward processing, manifesting phasic and tonic responses, with striatal and prefrontal regions receiving nigrostriatal and mesocortical dopaminergic projections respectively. While the morphology of in vivo physiological effects at the cellular level in response to acute levodopa administration is unclear, one might reasonably expect a disruption with consequent behavioural change. However this disruption does not appear to have an influence on the perception of risk or ability to execute appropriate and consistent action. Indeed one might conjecture that dopaminergic transmission is unlikely to be an effective mediator of

(complex) perceptual or cognitive information in itself given the sparsity of cortical and subcortical projection targets. Instead, a modulatory role on action representation in response to environmental changes seems likely in view of dopamine's diverse roles.

9.4.4 FUTURE DIRECTIONS

Other physiological drives have a substantial impact on behaviour – for instance thirst and emotional arousal have both been shown to influence risky choice (Isen and Geva, 1987; Hayden and Platt, 2009). One line of investigation is to explore the impact of these other factors on risky choice in a systematic manner exploiting the same paradigms.

A second important avenue is to map out the influence of other neuromodulatory transmitters on risk perception, and conversely the response to feedback. Alternative transmitters such as acetylcholine are present in higher concentration in sensory and associative cortex, thus realistically may influence the perception of uncertainty. Serotonin is also implicated in (negative) valuation (Daw et al., 2002), and serotonergic neurons from the dorsal raphe nucleus project densely to medial prefrontal cortex. Thus, serotonin is a candidate to influence both skewness representation, and to disrupt the maintenance of anticipated value which we find in this region.

9.5 CONCLUSION

Neurobiological evidence can be used to furnish process theories of choice (i.e. theories that describe choices as the product of a series of distinct computations in functionally or anatomically separable networks), and yield new hypotheses beyond the bounds of traditional economic methodologies. Strong and vociferous arguments have been advanced about the irrelevance of neuroscience in addressing traditional economic questions (Gul and Pesendorfer, 2008, 2009), and from a more positive viewpoint about the scope and limitations of neuroscientific evidence in illuminating economic theory (Harrison, 2008; Bernheim, 2009). However, while economic methodologies provide a clear quantitative framework within which to explore the neurophysiology of decision making (and which I exploit in these studies), I argue that a purely economic lens severely restricts the kind of question asked about the causes of, and influences upon, human behaviours.

For example, the influence of affect or arousal on risky choice can be understood as a modulation of risk integration in neural regions typically reflecting interoceptive processes. Knowledge about attentional or limbic systems can inform out-of-sample predictions about the influence of specific choice configurations on risky decision-making, where notable psychological effects such as framing can be rephrased in neurobiological terms rather than as purely descriptive economic theories (Kahneman and Tversky, 1979). Physiological influences on choice, known from the ecological literature, can be hypothesised to exert a state-dependent generic influence on risk processing at a basic neurophysiological level, leading to the expectation of an effect of metabolic state not only on decisions for food but also for financial decisions **Chapter 6,** (Symmonds et al., 2010b). Effects of damage to specific brain regions on decision making (Clark et al., 2008; Weller et al., 2009) can be interpreted as deficits at specific points in a neural processing pathway, and modulatory pharmacological influences on risk-taking can be quantified (**Chapter 7)**. Such exogenous influences are not within the scope of typical economic endeavour, despite their tangible impact.

Neural data can also help arbitrate between behavioural models, whether these are competing theories of risk (as in **Chapter 4**), or strategy evaluation (as in **Chapter 5**). Even when different hypotheses are indistinguishable by observing choices alone, they can posit very different underlying structural mechanisms, such as the decomposition of predicted outcomes into summary statistics. Moreover, elucidating structural mechanisms can yield new instruments for furnishing models – for example, constraints may be imposed by the temporal processing of different dimensions of risk, and the time-sequence of the integration of statistical information with subjective preference (**Chapter 8**), or by the way in which noise is introduced into decisions.

In conclusion, the studies in this thesis elaborate the neural mechanisms underlying how humans make both single-shot and sequential decisions under risk, central elements in decision-making scenarios ranging from foraging to financial investment. This demonstrates that phylogenetically ancient circuitry subserving valuation and reward decompose choice into their salient statistical features, enabling the sophisticated representation of the future and its alternatives.

Bibliography

Abler B, Walter H, Erk S, Kammerer H, Spitzer M (2006) Prediction error as a linear function of reward probability is coded in human nucleus accumbens. Neuroimage 31:790-795.

Akaike H (1974) A new look at the statistical model identification. IEEE Transactions On Automatic Control 19:716-723.

Alderfer CP (1970) Choices with risk: Beyond the mean and variance. The journal of business 43:341.

Aldrich J (1997) RA Fisher and the making of maximum likelihood 1912-1922. Statistical Science 12:162-176.

Allais M (1953) Le Comportement de l'Homme Rationnel devant le Risque: Critique des Postulats et Axiomes de l'Ecole Americaine. Econometrica 21:503-546.

Almuallim H (1996) An efficient algorithm for optimal pruning of decision trees. Artificial Intelligence 83:347-362.

Andersen R, Cui H (2009) Intention, action planning, and decision making in parietal-frontal circuits. Neuron 63:568-583.

Angwin AJ, Chenery HJ, Copland DA, Arnott WL, Murdoch BE, Silburn PA (2004) Dopamine and semantic activation: an investigation of masked direct and indirect priming. Journal of the International Neuropsychological Society 10:15-25.

Apicella CL, Dreber A, Campbell B, Gray PB, Hoffman M, Little AC (2008) Testosterone and financial risk preferences. Evolution and Human Behavior 29:384-390.

Ariely D, Norton MI (2008) How actions create-not just reveal-preferences. Trends in cognitive sciences 12:13-16.

Aristotle (1998) Aristotle. The Nicomachean Ethics. In: (Ackrill J, Urmson J, eds): Oxford World" s Classics. Translated with an Introduction by David Ross. Revised by JL Ackrill and JO Urmson. Oxford University Press Inc., New York.

Augustine J (1996) Circuitry and functional aspects of the insular lobe in primates including humans. Brain Research Reviews 22:229-244.

Bach D, Seymour B, Dolan R (2009) Neural activity associated with the passive prediction of ambiguity and risk for aversive events. Journal of Neuroscience 29:1648.

Bandettini PA, Wong EC, Hinks RS, Tikofsky RS, Hyde JS (1992) Time course EPI of human brain function during task activation. Magnetic Resonance in Medicine 25:390-397.

Barbey AK, Koenigs M, Grafman J (2011) Orbitofrontal contributions to human working memory. Cerebral Cortex 21:789.

Barnard A, Duck I, Lynn M, Timlake W (1967) The Application of Electromagnetic Theory to Electrocardiology:: II. Numerical Solution of the Integral Equations. Biophysical Journal 7:463-491.

Barnard CJ, Brown CAJ (1985) Risk-Sensitive Foraging in Common Shrews (Sorex araneus L.). Behavioral Ecology and Sociobiology 16:161-164.

Bateson M, Kacelnik A (1997) Starlings' preferences for predictable and unpredictable delays to food. Animal Behaviour 53:1129-1142.

Batterham RL (2007) PYY modulation of cortical and hypothalamic brain areas predicts feeding behaviour in humans. Nature 450:106-109.

Bawa VS (1975) Optimal rules for ordering uncertain prospects. Journal of Financial Economics 2:95-121.

Bayer HM, Glimcher PW (2005) Midbrain dopamine neurons encode a quantitative reward prediction error signal. Neuron 47:129-141.

Bechara A, Damasio H, Damasio AR (2000) Emotion, decision making and the orbitofrontal cortex. Cerebral Cortex 10:295.

Bechara A, Damasio AR, Damasio H, Anderson SW (1994) Insensitivity to future consequences following damage to human prefrontal cortex* 1. Cognition 50:7-15.

Bechara A, Damasio H, Tranel D, Damasio AR (1997) Deciding advantageously before knowing the advantageous strategy. Science 275:1293.

Becker GM, DeGroot MH, Marschak J (1964) Measuring utility by a single-response sequential method. Behavioral Science 9.

Bedford T, Cooke RM (2001) Probabilistic risk analysis: foundations and methods: Cambridge Univ Pr.

Behrens TE, Woolrich MW, Walton ME, Rushworth MF (2007) Learning the value of information in an uncertain world. Nat Neurosci 10:1214-1221.

Behrmann M, Geng J, Shomstein S (2004) Parietal cortex and attention. Current Opinion in Neurobiology 14:212-217.

Bellman RE (2003) Dynamic programming: Dover Pubns.

Bernheim B (2009) On the potential of neuroeconomics: A critical (but hopeful) appraisal. American Economic Journal: Microeconomics 1:1-41.

Berns GS, Laibson D, Loewenstein G (2007) Intertemporal choice-toward an integrative framework. Trends in cognitive sciences 11:482-488.

Berridge KC (1996) Food reward: brain substrates of wanting and liking. Neuroscience & Biobehavioral Reviews 20:1-25.

Birn RM, Saad ZS, Bandettini PA (2001) Spatial heterogeneity of the nonlinear dynamics in the FMRI BOLD response. Neuroimage 14:817-826.

Birn RM, Cox RW, Bandettini PA (2002) Detection versus estimation in event-related fMRI: choosing the optimal stimulus timing. Neuroimage 15:252-264.

Birnbaum MH (2008) New Paradoxes of Risky Decision Making. PSYCHOLOGICAL REVIEW-NEW YORK- 115:463.

Bjork JM, Momenan R, Hommer DW (2009) Delay discounting correlates with proportional lateral frontal cortex volumes. Biological psychiatry 65:710-713.

Blakemore C, Tobin EA (1972) Lateral inhibition between orientation detectors in the cat's visual cortex. Experimental brain research 15:439-440.

Bloch F, Hansen W, Packard M (1946) Nuclear induction. Physical review 70:460-474.

Bluethgen R, Gintschel A, Hackethal A, Müller A (2008) Financial advice and individual investors' portfolios.

Bogacz R, Brown E, Moehlis J, Holmes P, Cohen JD (2006) The physics of optimal decision making: A formal analysis of models of performance in two-alternative forced-choice tasks. Psychological Review 113:700.

Bollard A, Liu R, Nursimulux A, Rangelo A, Bossaertso P (2007) Neurophysiological evidence on perception of reward and risk: Implications for trading under time pressure. In: Working Paper, CalTech.

Boorman ED, Sallet J (2009) Mean–variance or prospect theory? The nature of value representations in the human brain. The Journal of Neuroscience 29:7945.

Boorman ED, Behrens TEJ, Woolrich MW, Rushworth MFS (2009) How green is the grass on the other side? Frontopolar cortex and the evidence in favor of alternative courses of action. Neuron 62:733-743.

Bossaerts P (2010) Risk and risk prediction error signals in anterior insula. Brain Structure and Function:1-9.

Boxerman JL, Hamberg LM, Rosen BR, Weisskoff RM (1995) MR contrast due to intravascular magnetic susceptibility perturbations. Magnetic Resonance in Medicine 34:555-566.

Boynton GM, Engel SA, Glover GH, Heeger DJ (1996) Linear systems analysis of functional magnetic resonance imaging in human V1. The Journal of Neuroscience 16:4207.

Boysen ST, Berntson GG (1995) Responses to quantity: Perceptual versus cognitive mechanisms in chimpanzees (Pan troglodytes). Journal of Experimental Psychology: Animal Behavior Processes 21:82.

Brand M, Fujiwara E, Borsutzky S, Kalbe E, Kessler J, Markowitsch HJ (2005) Decision-making deficits of korsakoff patients in a new gambling task with explicit rules: associations with executive functions. Neuropsychology 19:267.

Breitenstein C, Korsukewitz C, Flöel A, Kretzschmar T, Diederich K, Knecht S (2006) Tonic dopaminergic stimulation impairs associative learning in healthy subjects. Neuropsychopharmacology 31:2552-2564.

Breiter HC, Aharon I, Kahneman D, Dale A, Shizgal P (2001) Functional Imaging of Neural Responses to Expectancy and Experience of Monetary Gains and Losses. Neuron 30:619-639.

Broca P (1865) Sur le siège de la faculté du langage articulé. Bulletins de la Société d'Anthropologie de Paris 6:377-393.

Bruder H, Fischer H, Reinfelder HE, Schmitt F (1992) Image reconstruction for echo planar imaging with nonequidistant k space sampling. Magnetic Resonance in Medicine 23:311-323.

Buchel C, Holmes AP, Rees G, Friston KJ (1998) Characterizing stimulus-response functions using nonlinear regressors in parametric fMRI experiments. Neuroimage 8:140-148.

Buckner RL (1998) Event-related fMRI and the hemodynamic response. Human Brain Mapping 6:373-377.

Budescu DV, Weiss W (1987) Reflection of transitive and intransitive preferences: A test of prospect theory* 1. Organizational Behavior and Human Decision Processes 39:184-202.

Buelow MT, Suhr JA (2009) Construct validity of the Iowa gambling task. Neuropsychology review 19:102-114.

Buonocore MH, Gao L (1997) Ghost artifact reduction for echo planar imaging using image phase correction. Magnetic Resonance in Medicine 38:89-100.

Burock MA, Buckner RL, Woldorff MG, Rosen BR, Dale AM (1998) Randomized event-related experimental designs allow for extremely rapid presentation rates using functional MRI. Neuroreport 9:3735.

Buxton RB, Frank LR (1997) A model for the coupling between cerebral blood flow and oxygen metabolism during neural stimulation. Journal of Cerebral Blood Flow & Metabolism 17:64-72.

Buxton RB, Wong EC, Frank LR (1998) Dynamics of blood flow and oxygenation changes during brain activation: the balloon model. Magnetic Resonance in Medicine 39:855-864.

Buxton RB, Uludag K, Dubowitz DJ, Liu TT (2004) Modeling the hemodynamic response to brain activation. Neuroimage 23:S220-S233.

Callahan HS, Cummings DE, Pepe MS, Breen PA, Matthys CC, Weigle DS (2004) Postprandial suppression of plasma ghrelin level is proportional to ingested caloric load but does not predict intermeal interval in humans. Journal of Clinical Endocrinology & Metabolism 89:1319.

Camara E, Krämer UM, Cunillera T, Marco-Pallarés J, Cucurell D, Nager W, Mestres-Missé A, Bauer P, Schüle R, Schöls L (2010) The Effects of COMT (Val108/158Met) and DRD4 (SNP- 521) Dopamine Genotypes on Brain Activations Related to Valence and Magnitude of Rewards. Cerebral Cortex 20:1985.

Camerer C (2003a) Behavioral game theory: Experiments in strategic interaction: Princeton University Press Princeton, NJ.

Camerer C (2003b) Behavioral game theory: Experiments in strategic interaction: Princeton University Press Princeton, NJ.

Camerer CF (2000) Prospect theory in the wild: Evidence from the field. Advances in behavioral economics.

Cannon CM, Palmiter RD (2003) Reward without dopamine. The Journal of Neuroscience 23:10827.

Caraco T (1981) Energy budgets, risk and foraging preferences in dark-eyed juncos (Junco hyemalis). Behavioral Ecology and Sociobiology 8:213-217.

Caraco T, Blanckenhorn WU, Gregory GM, Newman JA, Recer GM, Zwicker SM (1990) Risk-sensitivity: ambient temperature affects foraging choice. Animal Behaviour 39:338-345.

Carlson SM, Davis AC, Leach JG (2005) Less is more. Psychological Science 16:609.

Carver CS, White TL (1994) Behavioral inhibition, behavioral activation, and affective responses to impending reward and punishment: The BIS/BAS scales. Journal of Personality and Social Psychology 67:319-319.

Cavada C, Goldman-Rakic P (1989) Posterior parietal cortex in rhesus monkey: II. Evidence for segregated corticocortical networks linking sensory and limbic areas with the frontal lobe. The Journal of Comparative Neurology 287:422-445.

Chandarana K, Drew ME, Emmanuel J, Karra E, Gelegen C, Chan P, Cron NJ, Batterham RL (2009) Subject Standardization, Acclimatization, and Sample Processing Affect Gut Hormone Levels and Appetite in Humans. Gastroenterology 136:2115-2126.

Chapman R, Ilmoniemi R, Barbanera S, Romani G (1984) Selective localization of alpha brain activity with neuromagnetic measurements. Electroencephalography and Clinical Neurophysiology 58:569-572.

Chaudhri OB, Salem V, Murphy KG, Bloom SR (2008) Gastrointestinal Satiety Signals. Annual Review of Physiology 70:239-255.

Chib VS, Rangel A, Shimojo S, O'Doherty JP (2009) Evidence for a common representation of decision values for dissimilar goods in human ventromedial prefrontal cortex. The Journal of Neuroscience 29:12315.

Christopoulos G, Tobler P, Bossaerts P, Dolan R, Schultz W (2009) Neural Correlates of Value, Risk, and Risk Aversion Contributing to Decision Making under Risk. Journal of Neuroscience 29:12574.

Churchland PS, Sejnowski TJ (1992) The computational brain: The MIT press.

Clark L, Manes F, Antoun N, Sahakian BJ, Robbins TW (2003) The contributions of lesion laterality and lesion volume to decision-making impairment following frontal lobe damage. Neuropsychologia 41:1474-1483.

Clark L, Bechara A, Damasio H, Aitken M, Sahakian B, Robbins T (2008) Differential effects of insular and ventromedial prefrontal cortex lesions on risky decision-making. Brain 131:1311.

Clower D, Dum R, Strick P (2005) Basal ganglia and cerebellar inputs to'AIP'. Cerebral Cortex 15:913.

Cohen D (1968) Magnetoencephalography: evidence of magnetic fields produced by alpha-rhythm currents. Science 161:784.

Collins DL, Holmes C, Peters TM, Evans AC (1995) Automatic 3 D model based neuroanatomical segmentation. Human Brain Mapping 3:190-208.

Comings D, Gade R, Wu S, Chiu C, Dietz G, Muhleman D, Saucier G, Ferry L, Rosenthal R, Lesieur H (1997) Studies of the potential role of the dopamine D1 receptor gene in addictive behaviors. Molecular Psychiatry 2:44.

Comings D, Gade Andavolu R, Gonzalez N, Wu S, Muhleman D, Chen C, Koh P, Farwell K, Blake H, Dietz G (2001) The additive effect of neurotransmitter genes in pathological gambling. Clinical Genetics 60:107-116.

Comings DE, Rosenthal RJ, Lesieur HR, Rugle LJ, Muhleman D, Chiu C, Dietz G, Gade R (1996) A study of the dopamine D2 receptor gene in pathological gambling. Pharmacogenetics and Genomics 6:223.

Cools R, Barker RA, Sahakian BJ, Robbins TW (2003) L-Dopa medication remediates cognitive inflexibility, but increases impulsivity in patients with Parkinson's disease. Neuropsychologia 41:1431-1441.

Cools R, Frank MJ, Gibbs SE, Miyakawa A, Jagust W, D'Esposito M (2009) Striatal dopamine predicts outcome-specific reversal learning and its sensitivity to dopaminergic drug administration. The Journal of Neuroscience 29:1538.

Coombs C, Huang L (1970) Tests of a portfolio theory of risk preference. Journal of Experimental Psychology 85:23-29.

Coombs C, Bowen J (1971) A test of VE-theories of risk and the effect of the central limit theorem. Acta Psychologica 35:15-28.

Coombs CH (1960) Components of risk in decision making: Probability and variance preferences. Journal of Experimental Psychology 60:265.

Coombs CH, Pruitt DG (1960) Components of risk in decision making: Probability and variance preferences. Journal of Experimental Psychology 60:265-277.

Copland DA (2009) Dopaminergic neuromodulation of semantic processing: A 4-T fMRI study with levodopa. Cerebral Cortex 19:2651.

Coricelli G, Critchley HD, Joffily M, O'Doherty JP, Sirigu A, Dolan RJ (2005) Regret and its avoidance: a neuroimaging study of choice behavior. Nature Neuroscience 8:1255-1262.

Corrado G, Doya K (2007) Understanding neural coding through the model-based analysis of decision making. J Neurosci 27:8178-8180.

Courtney SM, Ungerleider LG (1997) What fMRI has taught us about human vision. Current Opinion in Neurobiology 7:554-561.

Craig A (2002) How do you feel? Interoception: the sense of the physiological condition of the body. Nature Reviews Neuroscience 3:655-666.

Craig A (2009) How do you feel--now? The anterior insula and human awareness. Nature reviews Neuroscience 10:59.

Crevoisier C, Hoevels B, Zürcher G, Da Prada M (1987) Bioavailability of L-dopa after Madopar HBS administration in healthy volunteers. European neurology 27:36-46.

Critchley H, Wiens S, Rotshtein P, Öhman A, Dolan R (2004) Neural systems supporting interoceptive awareness. Nature Neuroscience 7:189-195.

Critchley HD, Mathias CJ, Dolan RJ (2001) Neural activity in the human brain relating to uncertainty and arousal during anticipation. Neuron 29:537-545.

Croxson P, Johansen-Berg H, Behrens T, Robson M, Pinsk M, Gross C, Richter W, Richter M, Kastner S, Rushworth M (2005) Quantitative investigation of connections of the prefrontal cortex in the human and macaque using probabilistic diffusion tractography. Journal of Neuroscience 25:8854.

Croy MI, Hughes RN (1991) Effects of food supply, hunger, danger and competition on choice of foraging location by the fifteen-spined stickleback, Spinachia spinachia L. Animal Behaviour 42:131-139.

Cummings DE (2006) Ghrelin and the short-and long-term regulation of appetite and body weight. Physiology & behavior 89:71-84.

Cummings DE, Weigle DS, Frayo RS, Breen PA, Ma MK, Dellinger EP, Purnell JQ (2002) Plasma Ghrelin Levels after Diet-Induced Weight Loss or Gastric Bypass Surgery. N Engl J Med 346:1623-1630.

Cunnington R, Windischberger C, Deecke L, Moser E (2002) The preparation and execution of self-initiated and externally-triggered movement: a study of event-related fMRI. Neuroimage 15:373-385.

Czernecki V, Pillon B, Houeto J, Pochon J, Levy R, Dubois B (2002) Motivation, reward, and Parkinson's disease: influence of dopatherapy. Neuropsychologia 40:2257-2267.

D'Acremont M, Bossaerts P (2008) Neurobiological studies of risk assessment: A comparison of expected utility and mean-variance approaches. Cognitive, Affective & Behavioral Neuroscience 8:363.

Damasio AR, Everitt B, Bishop D (1996) The somatic marker hypothesis and the possible functions of the prefrontal cortex [and discussion]. Philosophical transactions: Biological sciences 351:1413-1420.

Daw ND, Kakade S, Dayan P (2002) Opponent interactions between serotonin and dopamine. Neural Networks 15:603-616.

Daw ND, O'Doherty JP, Dayan P, Seymour B, Dolan RJ (2006) Cortical substrates for exploratory decisions in humans. Nature 441:876-879.

De Martino B, Kumaran D, Seymour B, Dolan RJ (2006) Frames, biases, and rational decision-making in the human brain. Science 313:684-687.

De Martino B, Kumaran D, Holt B, Dolan RJ (2009) The neurobiology of reference-dependent value computation. J Neurosci 29:3833-3842.

de Vries MH, Ulte C, Zwitserlood P, Szymanski B, Knecht S (2010) Increasing dopamine levels in the brain improves feedback-based procedural learning in healthy participants: an artificial-grammar-learning experiment. Neuropsychologia 48:3193-3197.

Deichmann R, Gottfried J, Hutton C, Turner R (2003) Optimized EPI for fMRI studies of the orbitofrontal cortex. Neuroimage 19:430-441.

Dekel E, Lipman BL, Rustichini A (1998) Standard state-space models preclude unawareness. Econometrica:159-173.

Delazer M, Sinz H, Zamarian L, Stockner H, Seppi K, Wenning G, Benke T, Poewe W (2009) Decision making under risk and under ambiguity in Parkinson's disease. Neuropsychologia 47:1901-1908.

Delgado MR, Nystrom LE, Fissell C, Noll D, Fiez JA (2000) Tracking the hemodynamic responses to reward and punishment in the striatum. Journal of neurophysiology 84:3072.

Denk F, Walton M, Jennings K, Sharp T, Rushworth M, Bannerman D (2005) Differential involvement of serotonin and dopamine systems in cost-benefit decisions about delay or effort. Psychopharmacology 179:587-596.

Dethy S, Laute MA, Van Blercom N, Damhaut P, Goldman S, Hildebrand J (1997) Microdialysis-HPLC for plasma levodopa and metabolites monitoring in parkinsonian patients. Clinical chemistry 43:740.

Diederich A (2003) Decision making under conflict: Decision time as a measure of conflict strength. Psychonomic bulletin & review 10:167-176.

Doya K (2008) Modulators of decision making. Nat Neurosci 11:410-416.

Dreber A, Apicella CL, Eisenberg DTA, Garcia JR, Zamore RS, Lum JK, Campbell B (2009) The 7R polymorphism in the dopamine receptor D4 gene (DRD4) is associated with financial risk taking in men. Evolution and Human Behavior 30:85-92.

Dreher JC, Kohn P, Berman KF (2006) Neural Coding of Distinct Statistical Properties of Reward Information in Humans. Cerebral Cortex 16:561-573.

Duyn JH, Moonen CTW, van Yperen GH, de Boer RW, Luyten PR (1994) Inflow versus deoxyhemoglobin effects in BOLD functional MRI using gradient echoes at 1.5 T. NMR in Biomedicine 7:83-88.

Ebstein R (2006) The molecular genetic architecture of human personality: beyond self-report questionnaires. Molecular Psychiatry 11:427-445.

Edgeworth FY (1881) Mathematical psychics. History of Economic Thought Books.

Edwards W (1961) Behavioral decision theory. Annual review of psychology 12:473-498.

Eisenegger C, Knoch D, Ebstein RP, Gianotti LRR, Sándor PS, Fehr E (2010) Dopamine receptor D4 polymorphism predicts the effect of L-DOPA on gambling behavior. Biological psychiatry 67:702-706.

Elliott R, Friston KJ, Dolan RJ (2000) Dissociable neural responses in human reward systems. The Journal of Neuroscience 20:6159.

Elliott R, Agnew Z, Deakin JF (2008) Medial orbitofrontal cortex codes relative rather than absolute value of financial rewards in humans. Eur J Neurosci 27:2213-2218.

Elliott R, Newman JL, Longe OA, Deakin J (2003) Differential response patterns in the striatum and orbitofrontal cortex to financial reward in humans: a parametric functional magnetic resonance imaging study. The Journal of Neuroscience 23:303.

Ellsberg D (1961) Risk, ambiguity, and the Savage axioms. The Quarterly Journal of Economics 75:643-669.

Engelmann J, Tamir D (2009a) Individual differences in risk preference predict neural responses during financial decision-making. Brain Research 1290:28-51.

Engelmann JB, Tamir D (2009b) Individual differences in risk preference predict neural responses during financial decision-making. Brain research 1290:28-51.

English PJ, Ghatei MA, Malik IA, Bloom SR, Wilding JPH (2002) Food Fails to Suppress Ghrelin Levels in Obese Humans. J Clin Endocrinol Metab 87:2984-2987.

Epstein LG, Schneider M (2003) Recursive multiple-priors. Journal of Economic Theory 113:1-31.

Eysenck HJ (1990) Genetic and environmental contributions to individual differences: The three major dimensions of personality. Journal of Personality 58:245-261.

Fagley N (1993) A note concerning reflection effects versus framing effects.

Faisal AA, Selen LPJ, Wolpert DM (2008) Noise in the nervous system. Nature Reviews Neuroscience 9:292-303.

Fecteau S, Knoch D, Fregni F, Sultani N, Boggio P, Pascual-Leone A (2007) Diminishing risk-taking behavior by modulating activity in the prefrontal cortex: a direct current stimulation study. The Journal of Neuroscience 27:12500.

Fehr E, Schmidt KM (1999) A theory of fairness, competition, and cooperation*. Quarterly journal of Economics 114:817-868.

Fellows L, Boutelle M, Fillenz M (1993) Physiological stimulation increases nonoxidative glucose metabolism in the brain of the freely moving rat. Journal of Neurochemistry 60:1258-1263.

Felsted JA, Ren X, Chouinard-Decorte F, Small DM (2010) Genetically determined differences in brain response to a primary food reward. The Journal of Neuroscience 30:2428.

Ferguson AS, Stroink G (1997) Factors affecting the accuracy of the boundary element method in the forward problem. I. Calculating surface potentials. Biomedical Engineering, IEEE Transactions on 44:1139-1155.

Fessler CMT (2002) Pseudoparadoxical impulsivity in restrictive anorexia nervosa: A consequence of the logic of scarcity. The international journal of eating disorders 31:376-388.

Figlewicz DP, Naleid AMD, Sipols AJ (2007) Modulation of food reward by adiposity signals. Physiology & behavior 91:473-478.

Fincham JM, Carter CS, van Veen V, Stenger VA, Anderson JR (2002) Neural mechanisms of planning: a computational analysis using event-related fMRI. Proc Natl Acad Sci U S A 99:3346-3351.

Fiorillo CD, Tobler PN, Schultz W (2003) Discrete coding of reward probability and uncertainty by dopamine neurons. Science 299:1898-1902.

Fiorillo CD, Tobler PN, Schultz W (2005) Evidence that the delay-period activity of dopamine neurons corresponds to reward uncertainty rather than backpropagating TD errors. Behav Brain Funct 1:7.

Fishburn PC (1984) Foundations of Risk Measurement. I. Risk As Probable Loss. Management Science 30:396-406.

FitzGerald T, Seymour B, Dolan R (2009a) The role of human orbitofrontal cortex in value comparison for incommensurable objects. Journal of Neuroscience 29:8388.

FitzGerald THB, Seymour B, Dolan RJ (2009b) The role of human orbitofrontal cortex in value comparison for incommensurable objects. The Journal of Neuroscience 29:8388.

Fleming SM, Thomas CL, Dolan RJ (2010a) Overcoming status quo bias in the human brain. Proceedings of the National Academy of Sciences 107:6005.

Fleming SM, Whiteley L, Hulme OJ, Sahani M, Dolan RJ (2010b) Effects of category-specific costs on neural systems for perceptual decision-making. Journal of neurophysiology 103:3238.

Flint A, Raben A, Blundell JE, Astrup A (2000) Reproducibility, power and validity of visual analogue scales in assessment of appetite sensations in single test meal studies. International journal of obesity and related metabolic disorders: journal of the International Association for the Study of Obesity 24:38-48.

Floel A, Hummel F, Breitenstein C, Knecht S, Cohen L (2005) Dopaminergic effects on encoding of a motor memory in chronic stroke. Neurology 65:472.

Floresco SB, Tse MTL, Ghods-Sharifi S (2007) Dopaminergic and glutamatergic regulation of effort-and delay-based decision making. Neuropsychopharmacology 33:1966-1979.

Forbes E, Brown S, Kimak M, Ferrell R, Manuck S, Hariri A (2007) Genetic variation in components of dopamine neurotransmission impacts ventral striatal reactivity associated with impulsivity. Molecular Psychiatry 14:60-70.

Fox PT, Raichle ME (1986) Focal physiological uncoupling of cerebral blood flow and oxidative metabolism during somatosensory stimulation in human subjects. Proceedings of the National Academy of Sciences of the United States of America 83:1140.

Frank MJ, Seeberger LC, O'Reilly RC (2004) By carrot or by stick: cognitive reinforcement learning in parkinsonism. Science 306:1940.

Friston K (2004) Experimental design and statistical parametric mapping.

Friston K (2009) Causal modelling and brain connectivity in functional magnetic resonance imaging. PLoS biology 7:e1000033.

Friston K (2010) The free-energy principle: a unified brain theory? Nature Reviews Neuroscience 11:127-138.

Friston K, Holmes A, Poline J, Price C, Frith C (1996) Detecting activations in PET and fMRI: levels of inference and power. Neuroimage 4:223-235.

Friston K, Fletcher P, Josephs O, Holmes A, Rugg M, Turner R (1998a) Event-Related fMRI: Characterizing Differential Responses* 1. Neuroimage 7:30-40.

Friston K, Harrison L, Daunizeau J, Kiebel S, Phillips C, Trujillo-Barreto N, Henson R, Flandin G, Mattout J (2008) Multiple sparse priors for the M/EEG inverse problem. Neuroimage 39:1104-1120.

Friston KJ, Ashburner J, Frith CD, Poline JB, Heather JD, Frackowiak RSJ (1995a) Spatial registration and normalization of images. Human Brain Mapping 3:165-189.

Friston KJ, Holmes AP, Worsley KJ, Poline JB, Frith CD, Frackowiak RSJ (1995b) Statistical parametric maps in functional imaging: a general linear approach. Human Brain Mapping 2:189-210.

Friston KJ, Fletcher P, Josephs O, Holmes A, Rugg MD, Turner R (1998b) Event-Related fMRI: Characterizing Differential Responses. Neuroimage 7:30-40.

Fulton S, Pissios P, Manchon RP, Stiles L, Frank L, Pothos EN, Maratos-Flier E, Flier JS (2006) Leptin regulation of the mesoaccumbens dopamine pathway. Neuron 51:811-822.

Gall FJ, Spurzheim G (1818) Anatomie et physiologie du système nerveux en général, et du cerveau en particulier: avec des observations sur la possibilité de reconnoître plusieurs dispositions intellectuelles et morales de l'homme et des animaux par la configuration de leurs têtes: F. Schoell.

Gallagher DA, O'Sullivan SS, Evans AH, Lees AJ, Schrag A (2007) Pathological gambling in Parkinson's disease: risk factors and differences from dopamine dysregulation. An analysis of published case series. Movement Disorders 22:1757-1763.

Garrett TA, Sobel RS (1999) Gamblers favor skewness, not risk: Further evidence from United States' lottery games. Economics Letters 63:85-90.

Gehring WJ, Willoughby AR (2002) The medial frontal cortex and the rapid processing of monetary gains and losses. Science 295:2279.

Gianotti LRR, Knoch D, Faber PL, Lehmann D, Pascual-Marqui RD, Diezi C, Schoch C, Eisenegger C, Fehr E (2009) Tonic activity level in the right prefrontal cortex predicts individuals' risk taking. Psychological Science 20:33.

Gigerenzer G, Goldstein DG (1996) Reasoning the fast and frugal way: models of bounded rationality. Psychological Review 103:650.

Gläscher J (2009) Visualization of group inference data in functional neuroimaging. Neuroinformatics 7:73-82.

Glimcher PW, Rustichini A (2004) Neuroeconomics: the consilience of brain and decision. Science 306:447-452.

Glover GH, Lemieux SK, Drangova M, Pauly JM (1996) Decomposition of inflow and blood oxygen level dependent (BOLD) effects with dual echo spiral gradient recalled echo (GRE) fMRI. Magnetic Resonance in Medicine 35:299-308.

Goense J, Whittingstall K, Logothetis NK (2011) Neural and BOLD responses across the brain. Wiley Interdisciplinary Reviews: Cognitive Science.

Gold JI, Shadlen MN (2007) The Neural Basis of Decision Making. Annual Review of Neuroscience 30:535-574.

Golec J, Tamarkin M (1998) Bettors Love Skewness, Not Risk, at the Horse Track. Journal of Political Economy 106:205-225.

Gonzalez C, Dana J, Koshino H, Just M (2005) The framing effect and risky decisions: Examining cognitive functions with fMRI. Journal of Economic Psychology 26:1-20.

Gonzalez R, Wu G (1999) On the shape of the probability weighting function. Cognitive Psychology 38:129-166.

Gottfried JA, O'Doherty J, Dolan RJ (2003) Encoding predictive reward value in human amygdala and orbitofrontal cortex. Science 301:1104.

Gray CM, Singer W (1989) Stimulus-specific neuronal oscillations in orientation columns of cat visual cortex. Proceedings of the National Academy of Sciences of the United States of America 86:1698.

Green DM, Swets JA (1974) Signal detection theory and psychophysics: Robert E. Krieger.

Grefkes C, Ritzl A, Zilles K, Fink G (2004) Human medial intraparietal cortex subserves visuomotor coordinate transformation. Neuroimage 23:1494-1506.

Grill HJ, Kaplan JM (2002) The neuroanatomical axis for control of energy balance. Frontiers in Neuroendocrinology 23:2-40.

Grootoonk S, Hutton C, Ashburner J, Howseman A, Josephs O, Rees G, Friston K, Turner R (2000) Characterization and correction of interpolation effects in the realignment of fMRI time series. Neuroimage 11:49-57.

Grosset KA, Macphee G, Pal G, Stewart D, Watt A, Davie J, Grosset D (2006) Problematic gambling on dopamine agonists: not such a rarity. Movement Disorders 21:2206-2208.

Gul F, Pesendorfer W (2008) The case for mindless economics. Foundations of positive and normative economics.

Gul F, Pesendorfer W (2009) A Comment on Bernheim's Appraisal of Neuroeconomics. American Economic Journal: Microeconomics 1:42-47.

Guldin W, Markowitsch H (1983) Cortical and thalamic afferent connections of the insular and adjacent cortex of the rat. The Journal of Comparative Neurology 215:135-153.

Ha RY, Namkoong K, Kang JI, Kim YT, Kim SJ (2009) Interaction between serotonin transporter promoter and dopamine receptor D4 polymorphisms on decision making. Progress in Neuro-Psychopharmacology and Biological Psychiatry 33:1217-1222.

Haber S (2003) The primate basal ganglia: parallel and integrative networks. Journal of Chemical Neuroanatomy 26:317-330.

Hämäläinen M, Hari R, Ilmoniemi RJ, Knuutila J, Lounasmaa OV (1993) Magnetoencephalography—theory, instrumentation, and applications to noninvasive studies of the working human brain. Reviews of modern Physics 65:413.

Hansen LP (1982) Large sample properties of generalized method of moments estimators. Econometrica: Journal of the Econometric Society:1029-1054.

Hare TA, Camerer CF, Rangel A (2009) Self-control in decision-making involves modulation of the vmPFC valuation system. Science 324:646.

Harel N, Lee SP, Nagaoka T, Kim DS, Kim SG (2002) Origin of negative blood oxygenation level–dependent fMRI signals. Journal of Cerebral Blood Flow & Metabolism 22:908-917.

Hariri AR, Mattay VS, Tessitore A, Kolachana B, Fera F, Goldman D, Egan MF, Weinberger DR (2002) Serotonin transporter genetic variation and the response of the human amygdala. Science 297:400.

Harless DW, Camerer CF (1994) The predictive utility of generalized expected utility theories. Econometrica 62:1251-1289.

Harris A, Adolphs R, Camerer C, Rangel A (2011) Dynamic Construction of Stimulus Values in the Ventromedial Prefrontal Cortex. PLoS ONE 6:e21074.

Harrison G (2008) Neuroeconomics: A critical reconsideration. Economics and Philosophy 24:303-344.

Harrison GW, Rutström EE (2008) Risk aversion in the laboratory. Risk aversion in experiments.

Harrison GW, Rutström EE (2009) Expected utility theory and prospect theory: One wedding and a decent funeral. Experimental Economics 12:133-158.

Harvey CR, Siddique A (2000) Conditional Skewness in Asset Pricing Tests. The Journal of Finance 55:1263-1295.

Hasbroucq T, Tandonnet C, Micallef-Roll J, Blin O, Possamaï CA (2003) An electromyographic analysis of the effect of levodopa on the response time of healthy subjects. Psychopharmacology 165:313-316.

Hayden BY, Platt ML (2009) Gambling for Gatorade: risk-sensitive decision making for fluid rewards in humans. Animal cognition 12:201-207.

Head H (1920) Aphasia and kindred disorders of speech. Brain 43:87.

Hedgcock W, Crowe D, Leuthold A, Georgopoulos A (2010) A magnetoencephalography study of choice bias. Experimental brain research 202:121-127.

Heeger DJ, Ress D (2002) What does fMRI tell us about neuronal activity? Nature Reviews Neuroscience 3:142-151.

Heeger DJ, Huk AC, Geisler WS, Albrecht DG (2000) Spikes versus BOLD: what does neuroimaging tell us about neuronal activity? Nature Neuroscience 3:631-632.

Heekeren HR, Marrett S, Ruff DA, Bandettini P, Ungerleider LG (2006) Involvement of human left dorsolateral prefrontal cortex in perceptual decision making is independent of response modality. Proceedings of the National Academy of Sciences 103:10023.

Henson R (2007) Efficient experimental design for fMRI. Statistical parametric mapping The analysis of functional brain images:193–210.

Herrnstein RJ (1974) Formal properties of the matching law. Journal of the Experimental Analysis of Behavior 21:159.

Hershberger WA (1986) An approach through the looking-glass. Learning & behavior 14:443-451.

Hershey JC, Schoemaker PJH (1980) Prospect theory's reflection hypothesis: A critical examination. Organizational Behavior and Human Performance 25:395-418.

Hewig J, Trippe R, Hecht H, Coles MGH, Holroyd CB, Miltner WHR (2007) Decision-making in blackjack: an electrophysiological analysis. Cerebral Cortex 17:865.

Hey JD, Orme C (1994) Investigating generalizations of expected utility theory using experimental data. Econometrica: Journal of the Econometric Society 62:1291-1326.

Hoge RD, Atkinson J, Gill B, Crelier GR, Marrett S, Pike GB (1999) Linear coupling between cerebral blood flow and oxygen consumption in activated human cortex. Proceedings of the National Academy of Sciences of the United States of America 96:9403.

Hogg S (1996) A review of the validity and variability of the elevated plus-maze as an animal model of anxiety. Pharmacology Biochemistry and Behavior 54:21-30.

Holt CA, Laury SK (2002) Risk aversion and incentive effects. American Economic Review:1644-1655.

Hommel JD, Trinko R, Sears RM, Georgescu D, Liu ZW, Gao XB, Thurmon JJ, Marinelli M, DiLeone RJ (2006) Leptin receptor signaling in midbrain dopamine neurons regulates feeding. Neuron 51:801 - 810.

Houk JC, Wise SP (1995) Distributed modular architectures linking basal ganglia, cerebellum, and cerebral cortex: Their role in planning and controlling action. Cerebral Cortex.

Houston A, Clark C, McNamara J, Mangel M (1988) Dynamic models in behavioural and evolutionary ecology. Nature 332:29-34.

Houston AI, McNamara JM (1982) A sequential approach to risk-taking. Animal Behaviour 30:61.

Houston AI, McNamara JM (1999) Models of adaptive behaviour: an approach based on state. Cambridge, UK: Cambridge University Press.

Houston AI, McNamara JM (2001) Models of Adaptive Behaviour. Ecology 38:491-495.

Hsu M, Anen C, Quartz SR (2008) The right and the good: distributive justice and neural encoding of equity and efficiency. Science 320:1092.

Hsu M, Krajbich I, Zhao C, Camerer C (2009) Neural response to reward anticipation under risk is nonlinear in probabilities. Journal of Neuroscience 29:2231.

Hsu M, Bhatt M, Adolphs R, Tranel D, Camerer CF (2005) Neural systems responding to degrees of uncertainty in human decision-making. Science 310:1680.

Hubbard E, Piazza M, Pinel P, Dehaene S (2005) Interactions between number and space in parietal cortex. Nature Reviews Neuroscience 6:435-448.

Huettel SA, Song AW, McCarthy G (2005) Decisions under Uncertainty: Probabilistic Context Influences Activation of Prefrontal and Parietal Cortices. Journal of Neuroscience 25:3304-3311.

Huettel SA, Stowe CJ, Gordon EM, Warner BT, Platt ML (2006) Neural signatures of economic preferences for risk and ambiguity. Neuron 49:765-775.

Huk AC, Shadlen MN (2005) Neural activity in macaque parietal cortex reflects temporal integration of visual motion signals during perceptual decision making. The Journal of Neuroscience 25:10420.

Hutton C, Bork A, Josephs O, Deichmann R, Ashburner J, Turner R (2002) Image Distortion Correction in fMRI: A Quantitative Evaluation. Neuroimage 16:217-240.

Imamura A, Uitti RJ, Wszolek ZK (2006) Dopamine agonist therapy for Parkinson disease and pathological gambling. Parkinsonism & Related Disorders 12:506-508.

Isen A, Patrick R (1983) The effect of positive feelings on risk taking: When the chips are down. Organizational Behavior and Human Performance 31:194-202.

Isen A, Geva N (1987) The influence of positive affect on acceptable level of risk: The person with a large canoe has a large worry. Organizational Behavior and Human Decision Processes 39:145-154.

Iyer A, Lindner A, Kagan I, Andersen RA (2010) Motor preparatory activity in posterior parietal cortex is modulated by subjective absolute value. PLoS Biol 8:e1000444.

Jackson JH (1873) ON THE ANATOMICAL & PHYSIOLOGICAL LOCALISATION OF MOVEMENTS IN THE BRAIN. The Lancet 101:84-85.

Josephson BD (1962) Possible new effects in superconductive tunnelling. Physics Letters 1:251-253.

Jullien B, Salanie B (2000) Estimating preferences under risk: The case of racetrack bettors. Journal of Political Economy 108:503-530.

Kable JW, Glimcher PW (2007) The neural correlates of subjective value during intertemporal choice. Nat Neurosci 10:1625-1633.

Kacelnik A, Bateson M (1996) Risky Theories--The Effects of Variance on Foraging Decisions. Amer Zool 36:402-434.

Kagel JH, Roth AE (1995) The handbook of experimental economics. Princeton, NJ.

Kahneman D, Tversky A (1979) Prospect Theory: An Analysis of Decision under Risk. Econometrica 47:263-291.

Kahneman D, Tversky A (1984) Choices, values, and frames. American psychologist 39:341.

Kaminski BJ, Ator NA (2001) Behavioral and pharmacological variables affecting risky choice in rats. Journal of the Experimental Analysis of Behavior 75:275.

Karni E, Schmeidler D, Vind K (1983) On state dependent preferences and subjective probabilities. Econometrica: Journal of the Econometric Society:1021-1031.

Kass RE, Raftery AE (1995) Bayes Factors. Journal of the American Statistical Association 90:773-795.

Kennerley SW, Wallis JD (2009) Encoding of reward and space during a working memory task in the orbitofrontal cortex and anterior cingulate sulcus. Journal of neurophysiology 102:3352.

Kennerley SW, Dahmubed AF, Lara AH, Wallis JD (2009) Neurons in the frontal lobe encode the value of multiple decision variables. Journal of cognitive neuroscience 21:1162-1178.

Kennerley SW, Walton ME, Behrens TEJ, Buckley MJ, Rushworth MFS (2006) Optimal decision making and the anterior cingulate cortex. Nature Neuroscience 9:940-947.

Kenning P, Plassmann H (2005) Neuroeconomics: an overview from an economic perspective. Brain Res Bull 67:343-354.

Kheramin S, Body S, Ho MY, Velazquez-Martinez D, Bradshaw C, Szabadi E, Deakin J, Anderson I (2004) Effects of orbital prefrontal cortex dopamine depletion on inter-temporal choice: a quantitative analysis. Psychopharmacology 175:206-214.

Kiani R, Hanks TD, Shadlen MN (2008) Bounded integration in parietal cortex underlies decisions even when viewing duration is dictated by the environment. The Journal of Neuroscience 28:3017.

Kiebel SJ, Tallon Baudry C, Friston KJ (2005) Parametric analysis of oscillatory activity as measured with EEG/MEG. Human Brain Mapping 26:170-177.

Kim SG, Richter W, U urbil K (1997) Limitations of temporal resolution in functional MRI. Magnetic Resonance in Medicine 37:631-636.

Kischka U, Kammer TH, Maier S, Weisbrod M, Thimm M, Spitzer M (1996) Dopaminergic modulation of semantic network activation. Neuropsychologia 34:1107-1113.

Klein A, Andersson J, Ardekani BA, Ashburner J, Avants B, Chiang MC, Christensen GE, Collins DL, Gee J, Hellier P (2009) Evaluation of 14 nonlinear deformation algorithms applied to human brain MRI registration. Neuroimage 46:786-802.

Knecht S, Breitenstein C, Bushuven S, Wailke S, Kamping S, Flöel A, Zwitserlood P, Ringelstein EB (2004) Levodopa: faster and better word learning in normal humans. Annals of neurology 56:20-26.

Knill DC, Pouget A (2004) The Bayesian brain: the role of uncertainty in neural coding and computation. TRENDS in Neurosciences 27:712-719.

Knoch D, Pascual-Leone A, Meyer K, Treyer V, Fehr E (2006a) Diminishing reciprocal fairness by disrupting the right prefrontal cortex. Science 314:829.

Knoch D, Gianotti LRR, Pascual-Leone A, Treyer V, Regard M, Hohmann M, Brugger P (2006b) Disruption of right prefrontal cortex by low-frequency repetitive transcranial magnetic stimulation induces risk-taking behavior. The Journal of Neuroscience 26:6469.

Knutson B, Bossaerts P (2007) Neural antecedents of financial decisions. Journal of Neuroscience 27:8174.

Knutson B, Taylor J, Kaufman M, Peterson R, Glover G (2005) Distributed neural representation of expected value. Journal of Neuroscience 25:4806-4812.

Kobayashi S, de Carvalho P (2010) Adaptation of Reward Sensitivity in Orbitofrontal Neurons. Journal of Neuroscience 30:534.

Koenigs M, Young L, Adolphs R, Tranel D, Cushman F, Hauser M, Damasio A (2007) Damage to the prefrontal cortex increases utilitarian moral judgements. Nature 446:908-911.

Korn H, Bausela F, Charpier S, Faber DS (1993) Synaptic noise and multiquantal release at dendritic synapses. Journal of neurophysiology 70:1249.

Korotkova TM, Sergeeva OA, Eriksson KS, Haas HL, Brown RE (2003) Excitation of ventral tegmental area dopaminergic and nondopaminergic neurons by orexins/hypocretins. The Journal of Neuroscience 23:7.

Kosfeld M, Heinrichs M, Zak PJ, Fischbacher U, Fehr E (2005) Oxytocin increases trust in humans. Nature 435:673-676.

Koszegi B, Rabin M (2007) Mistakes in choice-based welfare analysis. The American economic review 97:477-481.

Köszegi B, Rabin M (2006) A Model of Reference-Dependent Preferences*. The Quarterly Journal of Economics 121:1133-1165.

Kreek MJ, Nielsen DA, Butelman ER, LaForge KS (2005) Genetic influences on impulsivity, risk taking, stress responsivity and vulnerability to drug abuse and addiction. Nature Neuroscience 8:1450-1457.

Krügel U, Schraft T, Kittner H, Kiess W, Illes P (2003) Basal and feeding-evoked dopamine release in the rat nucleus accumbens is depressed by leptin. European journal of pharmacology 482:185-187.

Kuhnen CM, Knutson B (2005) The neural basis of financial risk taking. Neuron 47:763-770.

Lauterbur PC (1973) Image formation by induced local interactions: examples employing nuclear magnetic resonance. Nature 242:190-191.

Lauwereyns J, Watanabe K, Coe B, Hikosaka O (2002) A neural correlate of response bias in monkey caudate nucleus. Nature 418:413-417.

Lee D (2005) Neuroeconomics: making risky choices in the brain. Nat Neurosci 8:1129-1130.

Leibowitz SF, Alexander JT (1998) Hypothalamic serotonin in control of eating behavior, meal size, and body weight. Biological psychiatry 44:851-864.

Lejuez C, Read JP, Kahler CW, Richards JB, Ramsey SE, Stuart GL, Strong DR, Brown RA (2002) Evaluation of a behavioral measure of risk taking: The Balloon Analogue Risk Task (BART). Journal of Experimental Psychology: Applied 8:75.

Lenard NR, Berthoud HR (2008) Central and peripheral regulation of food intake and physical activity: pathways and genes. Obesity 16:S11-S22.

Levin IP, Weller JA, Pederson AA, Harshman LA (2007) Age-related differences in adaptive decision making: Sensitivity to expected value in risky choice. Judgment and Decision Making 2:225-233.

Levitt SD, Dubner SJ (2006) Freakonomics: A rogue economist explores the hidden side of everything: HarperCollins.

Li J, Delgado MR, Phelps EA (2011) How instructed knowledge modulates the neural systems of reward learning. Proceedings of the National Academy of Sciences 108:55.

Lichtenstein S (1965) Bases for preferences among three-outcome bets. Journal of Experimental Psychology 69:162-169.

Litvak V, Friston K (2008) Electromagnetic source reconstruction for group studies. Neuroimage 42:1490-1498.

Lobo DSS, Souza RP, Tong RP, Casey DM, Hodgins DC, Smith GJ, Williams RJ, Schopflocher DP, Wood RT, el-Guebaly N (2010) Association of functional variants in the dopamine D2-like receptors with risk for gambling behaviour in healthy Caucasian subjects. Biological psychology 85:33-37.

Loewenstein CF (2001) Risk as feelings. Psychological bulletin 127:267.

Logothetis NK (2008) What we can do and what we cannot do with fMRI. Nature 453:869-878.

Logothetis NK, Pauls J, Augath M, Trinath T, Oeltermann A (2001) Neurophysiological investigation of the basis of the fMRI signal. Nature 412:150-157.

Lohrenz T, McCabe K, Camerer CF, Montague PR (2007) Neural signature of fictive learning signals in a sequential investment task. Proc Natl Acad Sci U S A 104:9493-9498.

Long AB, Kuhn CM, Platt ML (2009) Serotonin shapes risky decision making in monkeys. Social Cognitive and Affective Neuroscience 4:346-356.

Loomes G, Sugden R (1982) Regret theory: An alternative theory of rational choice under uncertainty. Economic Journal 92:805-824.

Loomes G, Sugden R (1995) Incorporating a stochastic element into decision theories. European Economic Review 39:641-648.

Lopes L (1984) Risk and distributional inequality. Journal of Experimental Psychology: Human Perception and Performance 10:465-485.

Lopes LL, Oden GC (1999) The role of aspiration level in risky choice: A comparison of cumulative prospect theory and SP/A theory. Journal of Mathematical Psychology 43:286-313.

Lu C, Bharmal A, Suchowersky O (2006) Gambling and Parkinson disease. Archives of neurology 63:298.

Machina MJ (2005) 'Expected Utility / Subjective Probability' Analysis without the Sure-Thing Principle or Probabilistic Sophistication. Economic Theory 26:1-62.

MacKay D (2003) Information theory, inference, and learning algorithms: Cambridge Univ Pr.

MacKillop J, Menges DP, McGeary JE, Lisman SA (2007) Effects of craving and DRD4 VNTR genotype on the relative value of alcohol: an initial human laboratory study. Behav Brain Funct 3.

MacPherson CB (1968) Thomas Hobbes, Leviathan. In: London: Penguin Books.

Maimon G, Assad JA (2009) Beyond Poisson: increased spike-time regularity across primate parietal cortex. Neuron 62:426-440.

Mansfield P (1977) Multi-planar image formation using NMR spin echoes. Journal of Physics C: Solid State Physics 10:L55.

Marco-Pallarés J, Cucurell D, Cunillera T, Krämer UM, C mara E, Nager W, Bauer P, Schüle R, Schöls L, Münte TF (2009) Genetic variability in the dopamine system (dopamine receptor D4, catechol-O-methyltransferase) modulates neurophysiological responses to gains and losses. Biological psychiatry 66:154-161.

Markowitz H (1952) Portfolio Selection. The Journal of Finance 7:77-91.

Marr D (1982) Vision. . In: New York: WH Freeman.

Marsh B, Kacelnik A (2002) Framing effects and risky decisions in starlings. Proceedings of the National Academy of Sciences 99:3352.

Mathiesen C, Caesar K, Akgören N, Lauritzen M (1998) Modification of activity dependent increases of cerebral blood flow by excitatory synaptic activity and spikes in rat cerebellar cortex. The Journal of physiology 512:555-566.

Matsumoto M, Hikosaka O (2007) Lateral habenula as a source of negative reward signals in dopamine neurons. Nature 447:1111-1115.

Matthews SC, Simmons AN, Lane SD, Paulus MP (2004) Selective activation of the nucleus accumbens during risk-taking decision making. Neuroreport 15:2123.

Mazziotta J (2001) A probabilistic atlas and reference system for the human brain: International Consortium for Brain Mapping (ICBM). Philosophical Transactions of the Royal Society B: Biological Sciences 356:1293-1322.

McCabe C, Mishor Z, Cowen PJ, Harmer CJ (2010) Diminished neural processing of aversive and rewarding stimuli during selective serotonin reuptake inhibitor treatment. Biological psychiatry 67:439-445.

McClure SM, Laibson DI, Loewenstein G, Cohen JD (2004) Separate neural systems value immediate and delayed monetary rewards. Science 306:503.

McCoy AN, Platt ML (2005) Risk-sensitive neurons in macaque posterior cingulate cortex. Nat Neurosci 8:1220-1227.

McFadden D (1989) A Method of Simulated Moments for Estimation of Discrete Response Models without Numerical Integration. Econometrica 57:995-1026.

McKelvey RD, Palfrey TR (1998) Quantal response equilibria for extensive form games. Experimental Economics 1:9-41.

McNamara CM (1992) Risk-sensitive foraging: A a review of the theory. Bulletin of mathematical biology 54:355-378.

Micallef-Roll J, Rihet P, Hasbroucq T, Possamaï C, Blin O (2001) Levodopa-induced drowsiness in healthy volunteers: results of a choice reaction time test combined with a subjective evaluation of sedation. Clinical neuropharmacology 24:91.

Milosavljevic M, Malmaud J, Huth A, Koch C, Rangel A (2010) The Drift Diffusion Model can account for the accuracy and reaction time of value-based choices under high and low time pressure. Judgment and Decision Making 5:437-449.

Mink JW (2003) The basal ganglia and involuntary movements: impaired inhibition of competing motor patterns. Archives of neurology 60:1365.

Mischel W, Shoda Y, Rodriguez M (1989) Delay of gratification in children. Science 244:933.

Mohr P, Biele G, Heekeren H (2010a) Neural Processing of Risk. Journal of Neuroscience 30:6613.

Mohr P, Biele G, Krugel L, Li S, Heekeren H (2010b) Neural foundations of risk-return trade-off in investment decisions. Neuroimage 49:2556-2563.

Molina JA, Sáinz Artiga MJ, Fraile A, Jiménez Jiménez FJ, Villanueva C, Ortí Pareja M, Bermejo P F (2000) Pathologic gambling in Parkinson's disease: A behavioral manifestation of pharmacologic treatment? Movement Disorders 15:869-872.

Morlet J, Arens G, Fourgeau E, Giard D (1982) Wave propagation and sampling theory; Part II, Sampling theory and complex waves. Geophysics 47:222.

Morton G, Cummings D, Baskin D, Barsh G, Schwartz M (2006) Central nervous system control of food intake and body weight. Nature 443:289-295.

Mosher JC, Lewis PS, Leahy RM (1992) Multiple dipole modeling and localization from spatio-temporal MEG data. Biomedical Engineering, IEEE Transactions on 39:541-557.

Muller AF, Lamberts S, Janssen JA, Hofland LJ, Koetsveld PV, Bidlingmaier M, Strasburger CJ, Ghigo E, Van der Lely AJ (2002) Ghrelin drives GH secretion during fasting in man. European Journal of Endocrinology 146:203.

Müller SM, Machina MJ (1987) Moment preferences and polynomial utility. Economics Letters 23:349-353.

Munafo MR, Clark TG, Moore LR, Payne E, Walton R, Flint J (2003) Genetic polymorphisms and personality in healthy adults: a systematic review and meta-analysis. Molecular Psychiatry 8:471-484.

Myung IJ (2003) Tutorial on maximum likelihood estimation. Journal of Mathematical Psychology 47:90-100.

Nakamura K, Matsumoto M, Hikosaka O (2008) Reward-dependent modulation of neuronal activity in the primate dorsal raphe nucleus. The Journal of Neuroscience 28:5331.

Nasser JA, Gluck ME, Geliebter A (2004) Impulsivity and test meal intake in obese binge eating women. Appetite 43:303-307.

Nederkoorn C, Braet C, Van Eijs Y, Tanghe A, Jansen A (2006) Why obese children cannot resist food: The role of impulsivity. Eating Behaviors 7:315-322.

Nelder JA, Wedderburn RWM (1972) Generalized linear models. Journal of the Royal Statistical Society Series A (General) 135:370-384.

Nicolle A, Symmonds M, Dolan R (2011) Optimistic biases in observational learning of value. Cognition.

Nienborg H, Cumming BG (2009) Decision-related activity in sensory neurons reflects more than a neuron's causal effect. Nature 459:89-92.

Niv Y, Duff MO, Dayan P (2005) Dopamine, uncertainty and TD learning. Behavioral and Brain Functions 1:1–9.

Niv Y, Daw ND, Joel D, Dayan P (2007) Tonic dopamine: opportunity costs and the control of response vigor. Psychopharmacology 191:507-520.

O'Doherty J, Hampton A, Kim H (2007) Model-based fMRI and its application to reward learning and decision making. Annals of the New York Academy of Sciences 1104:35-53.

O'Doherty J, Rolls E, Francis S, Bowtell R, McGlone F (2001a) Representation of pleasant and aversive taste in the human brain. Journal of neurophysiology 85:1315.

O'Doherty J, Kringelbach ML, Rolls ET, Hornak J, Andrews C (2001b) Abstract reward and punishment representations in the human orbitofrontal cortex. Nature Neuroscience 4:95-102.

O'Doherty J, Dayan P, Schultz J, Deichmann R, Friston K, Dolan RJ (2004) Dissociable roles of ventral and dorsal striatum in instrumental conditioning. Science 304:452-454.

Ogawa S, Lee T, Kay A, Tank D (1990) Brain magnetic resonance imaging with contrast dependent on blood oxygenation. Proceedings of the National Academy of Sciences 87:9868.

Ogawa S, Tank DW, Menon R, Ellermann JM, Kim SG, Merkle H, Ugurbil K (1992) Intrinsic signal changes accompanying sensory stimulation: functional brain mapping with magnetic resonance imaging. Proceedings of the National Academy of Sciences of the United States of America 89:5951.

Ojemann GA (1978) Organization of short-term verbal memory in language areas of human cortex: Evidence from electrical stimulation* 1. Brain and Language 5:331-340.

Olds J, Milner P (1954) Positive reinforcement produced by electrical stimulation of septal area and other regions of rat brain. Journal of comparative and physiological psychology 47:419.

Onur OA, Piefke M, Lie C-H, Thiel CM, Fink GR (2011) Modulatory Effects of Levodopa on Cognitive Control in Young, but not in Older Subjects: A Pharmacological fMRI Study. Journal of cognitive neuroscience:1-14.

Oullier O, Kelso JAS (2006) Neuroeconomics and the metastable brain. Trends in cognitive sciences 10:353-353.

Padoa-Schioppa C (2009) Range-adapting representation of economic value in the orbitofrontal cortex. Journal of Neuroscience 29:14004.

Padoa-Schioppa C, Assad JA (2006) Neurons in the orbitofrontal cortex encode economic value. Nature 441:223-226.

Padoa-Schioppa C, Assad JA (2008) The representation of economic value in the orbitofrontal cortex is invariant for changes of menu. Nature Neuroscience 11:95.

Palmiter RD (2007) Is dopamine a physiologically relevant mediator of feeding behavior? TRENDS in Neurosciences 30:375-381.

Panageas S, Westerfield MM (2009) High-Water Marks: High Risk Appetites ? Convex Compensation, Long Horizons, and Portfolio Choice. Journal of Finance 64:1-36.

Parker A, Newsome W (1998) Sense and the single neuron: probing the physiology of perception. Annual Review of Neuroscience 21:227-277.

Parzen E (1962) On estimation of a probability density function and mode. The annals of mathematical statistics 33:1065-1076.

Pauling L, Coryell CD (1936) The magnetic properties and structure of hemoglobin, oxyhemoglobin and carbonmonoxyhemoglobin. Proceedings of the National Academy of Sciences of the United States of America 22:210.

Paulus M, Rogalsky C, Simmons A, Feinstein J, Stein M (2003a) Increased activation in the right insula during risk-taking decision making is related to harm avoidance and neuroticism. Neuroimage 19:1439-1448.

Paulus MP, Rogalsky C, Simmons A, Feinstein JS, Stein MB (2003b) Increased activation in the right insula during risk-taking decision making is related to harm avoidance and neuroticism. Neuroimage 19:1439-1448.

Peiro A (1999) Skewness in financial returns. Journal of Banking and Finance 23:847-862.

Pelli DG, Farell B (2009) Psychophysical methods. Handbook of Optics: Vision and vision optics.

Penfield W, Boldrey E (1937) Somatic motor and sensory representation in the cerebral cortex of man as studied by electrical stimulation. Brain 60:389.

Penny W, Holmes A, Friston K (2003) Random effects analysis. Human brain function:843-850.

Penny W, Stephan K, Mechelli A, Friston K (2004a) Comparing dynamic causal models. Neuroimage 22:1157-1172.

Penny W, Stephan K, Mechelli A, Friston K (2004b) Modelling functional integration: a comparison of structural equation and dynamic causal models. Neuroimage 23:S264-S274.

Pessiglione M, Seymour B, Flandin G, Dolan RJ, Frith CD (2006) Dopamine-dependent prediction errors underpin reward-seeking behaviour in humans. Nature 442:1042-1045.

Peters J, Buchel C (2009) Overlapping and Distinct Neural Systems Code for Subjective Value during Intertemporal and Risky Decision Making. Journal of Neuroscience 29:15727.

Phillips PEM, Walton ME, Jhou TC (2007) Calculating utility: preclinical evidence for cost–benefit analysis by mesolimbic dopamine. Psychopharmacology 191:483-495.

Piazza M, Pinel P, Le Bihan D, Dehaene S (2007) A magnitude code common to numerosities and number symbols in human intraparietal cortex. Neuron 53:293-305.

Pietras CJ, Hackenberg TD (2001) Risk-sensitive choice in humans as a function of an earnings budget. Journal of the Experimental Analysis of Behavior 76:1-19.

Pietras CJ, Searcy GD, Huitema BE, Brandt AE (2008) Effects of monetary reserves and rate of gain on human risky choice under budget constraints. Behavioural Processes 78:358-373.

Pine A, Shiner T, Seymour B, Dolan RJ (2010) Dopamine, time, and impulsivity in humans. The Journal of Neuroscience 30:8888.

Pine A, Seymour B, Roiser JP, Bossaerts P, Friston KJ, Curran HV, Dolan RJ (2009) Encoding of marginal utility across time in the human brain. The Journal of Neuroscience 29:9575.

Plassmann H, O'Doherty J, Rangel A (2007a) Orbitofrontal cortex encodes willingness to pay in everyday economic transactions. The Journal of Neuroscience 27:9984.

Plassmann H, O'Doherty J, Rangel A (2007b) Orbitofrontal cortex encodes willingness to pay in everyday economic transactions. Journal of Neuroscience 27:9984-9988.

Plassmann H, O'Doherty J, Shiv B, Rangel A (2008) Marketing actions can modulate neural representations of experienced pleasantness. Proc Natl Acad Sci U S A 105:4.

Platt ML, Glimcher PW (1999) Neural correlates of decision variables in parietal cortex. Nature 400:233-238.

Platt ML, Huettel SA (2008) Risky business: the neuroeconomics of decision making under uncertainty. Nat Neurosci 11:398-403.

Pleger B, Blankenburg F, Ruff CC, Driver J, Dolan RJ (2008) Reward facilitates tactile judgments and modulates hemodynamic responses in human primary somatosensory cortex. The Journal of Neuroscience 28:8161.

Pleger B, Ruff CC, Blankenburg F, Kloppel S, Driver J, Dolan RJ (2009) Influence of dopaminergically mediated reward on somatosensory decision-making. PLoS Biol 7:e1000164.

Poldrack RA, Mumford JA (2009) Independence in ROI analysis: where is the voodoo? Social Cognitive and Affective Neuroscience 4:208.

Pothos EN (2002) Regulation of dopamine quantal size in midbrain and hippocampal neurons. Behavioural brain research 130:203-207.

Pratt J (1964) Risk Aversion in the Small and in the Large. Econometrica: Journal of the Econometric Society:122-136.

Prelec D (1998) The probability weighting function. Econometrica 66:497-527.

Preuschoff K, Bossaerts P, Quartz SR (2006) Neural differentiation of expected reward and risk in human subcortical structures. Neuron 51:381-390.

Preuschoff K, Quartz SR, Bossaerts P (2008) Human insula activation reflects risk prediction errors as well as risk. J Neurosci 28:2745-2752.

Procyk E, Tanaka Y, Joseph JP (2000) Anterior cingulate activity during routine and non-routine sequential behaviors in macaques. Nature Neuroscience 3:502-508.

Quiggin J (1982) A theory of anticipated utility. Journal of Economic Behavior & Organization 3:323-343.

Quintana J, Fuster JM (1999) From perception to action: temporal integrative functions of prefrontal and parietal neurons. Cereb Cortex 9:213-221.

Rabin M (2000) Risk Aversion and Expected-Utility Theory: A Calibration Theorem. University of California at Berkeley, Economics Working Papers: E00 279.

Raftery AE (1995) Bayesian Model Selection in Social Research. Sociological Methodology 25:111-163.

Ragozzino ME (2007) The contribution of the medial prefrontal cortex, orbitofrontal cortex, and dorsomedial striatum to behavioral flexibility. Annals of the New York Academy of sciences 1121:355-375.

Rakitin BC, Scarmeas N, Li T, Malapani C, Stern Y (2006) Single-dose levodopa administration and aging independently disrupt time production. Journal of cognitive neuroscience 18:376-387.

Rangel A, Camerer C, Montague PR (2008a) A framework for studying the neurobiology of value-based decision making. Nat Rev Neurosci 9:545-556.

Rangel A, Camerer C, Montague PR (2008b) A framework for studying the neurobiology of value-based decision making. Nature Reviews Neuroscience 9:545-556.

Rasmussen EB, Lawyer SR, Reilly W (2009) Percent body fat is related to delay and probability discounting for food in humans. Behavioural Processes 83:23-30.

Real L, Ott J, Silverfine E (1982) On the Tradeoff Between the Mean and the Variance in Foraging: Effect of Spatial Distribution and Color Preference. Ecology 63:1617-1623.

Resulaj A, Kiani R, Wolpert DM, Shadlen MN (2009) Changes of mind in decision-making. Nature 461:263-266.

Riba J, Krämer UM, Heldmann M, Richter S, Münte TF (2008) Dopamine agonist increases risk taking but blunts reward-related brain activity. PLoS ONE 3:e2479.

Rihet P, Possamaï CA, Micallef-Roll J, Blin O, Hasbroucq T (2002) Dopamine and human information processing: a reaction-time analysis of the effect of levodopa in healthy subjects. Psychopharmacology 163:62.

Roe RM, Busemeyer JR, Townsend JT (2001) Multialternative decision field theory: A dynamic connectionst model of decision making. Psychological Review 108:370.

Roesch MR, Calu DJ, Schoenbaum G (2007) Dopamine neurons encode the better option in rats deciding between differently delayed or sized rewards. Nature Neuroscience 10:1615-1624.

Rogers RD, Lancaster M, Wakeley J, Bhagwagar Z (2004) Effects of beta-adrenoceptor blockade on components of human decision-making. Psychopharmacology 172:157-164.

Rogers RD, Tunbridge EM, Bhagwagar Z, Drevets WC, Sahakian BJ, Carter CS (2003) Tryptophan depletion alters the decision-making of healthy volunteers through altered processing of reward cues. Neuropsychopharmacology.

Rogers RD, Owen AM, Middleton HC, Williams EJ, Pickard JD, Sahakian BJ, Robbins TW (1999) Choosing between small, likely rewards and large, unlikely rewards activates inferior and orbital prefrontal cortex. The Journal of Neuroscience 19:9029.

Romani GL, Williamson SJ, Kaufman L (1982) Biomagnetic instrumentation. Review of Scientific Instruments 53:1815-1845.

Romo R, Brody CD, Hernández A, Lemus L (1999) Neuronal correlates of parametric working memory in the prefrontal cortex. Nature 399:470-473.

Rothschild M, Stiglitz JE (1971) Increasing risk II: Its economic consequences. Journal of Economic Theory 3:66-84.

Rudebeck PH, Walton ME, Smyth AN, Bannerman DM, Rushworth MFS (2006) Separate neural pathways process different decision costs. Nature Neuroscience 9:1161-1168.

Rushworth M, Behrens T, Rudebeck P, Walton M (2007) Contrasting roles for cingulate and orbitofrontal cortex in decisions and social behaviour. Trends in cognitive sciences 11:168-176.

Salamone JD, Correa M, Farrar A, Mingote SM (2007) Effort-related functions of nucleus accumbens dopamine and associated forebrain circuits. Psychopharmacology 191:461-482.

Salzman CD, Britten KH, Newsome WT (1990) Cortical microstimulation influences perceptual judgements of motion direction. Nature 346:174-177.

Samanez-Larkin GR, Kuhnen CM, Yoo DJ, Knutson B (2010) Variability in Nucleus Accumbens Activity Mediates Age-Related Suboptimal Financial Risk Taking. J Neurosci 30:1426-1434.

Samejima K, Ueda Y, Doya K, Kimura M (2005) Representation of action-specific reward values in the striatum. Science 310:1337-1340.

Samuelson PA (1938) A Note on the Pure Theory of Consumer's Behaviour. Economica 5:61-71.

Samuelson PA (1969) Lifetime Portfolio Selection by Dynamic Stochastic Programming. Review of Economics and Statistics 51:239-246.

Samuelson W, Zeckhauser R (1988) Status quo bias in decision making. Journal of Risk and uncertainty 1:7-59.

Sanfey AG, Loewenstein G, McClure SM, Cohen JD (2006) Neuroeconomics: cross-currents in research on decision-making. Trends Cogn Sci 10:108-116.

Savage LJ (1951) The theory of statistical decision. Journal of the American Statistical Association 46:55-67.

Sawaguchi T (2001) The effects of dopamine and its antagonists on directional delay-period activity of prefrontal neurons in monkeys during an oculomotor delayed-response task. Neuroscience Research 41:115-128.

Scherg M (1990) Fundamentals of dipole source potential analysis. Auditory evoked magnetic fields and potentials 6:40–69.

Schinka J, Letsch E, Crawford F (2002) DRD4 and novelty seeking: Results of meta analyses. American Journal of Medical Genetics 114:643-648.

Schmitt V, Fischer J (2011) Representational format determines numerical competence in monkeys. Nature Communications 2:257.

Schneider SL (1992) Framing and conflict: Aspiration level contingency, the status quo, and current theories of risky choice. Journal of Experimental Psychology: Learning, Memory, and Cognition 18:1040.

Schneider SL, Lopes LL (1986) Reflection in preferences under risk: Who and when may suggest why. Journal of Experimental Psychology: Human Perception and Performance 12:535.

Schridde U, Khubchandani M, Motelow JE, Sanganahalli BG, Hyder F, Blumenfeld H (2008) Negative BOLD with large increases in neuronal activity. Cerebral Cortex 18:1814.

Schultz DP, Schultz SE (2007) A history of modern psychology: Wadsworth Pub Co.

Schultz W, Dayan P, Montague PR (1997) A neural substrate of prediction and reward. Science 275:1593-1599.

Schultz W, Preuschoff K, Camerer C, Hsu M, Fiorillo CD, Tobler PN, Bossaerts P (2008) Explicit neural signals reflecting reward uncertainty. Philos Trans R Soc Lond B Biol Sci 363:3801-3811.

Schutter DJLG, de Haan EHF, van Honk J (2004) Anterior asymmetrical alpha activity predicts Iowa gambling performance: Distinctly but reversed. Neuropsychologia 42:939-943.

Schwarz G (1978) Estimating the dimension of a model. The Annals of Statistics 6:461-464.

Schweimer J, Hauber W (2006) Dopamine D1 receptors in the anterior cingulate cortex regulate effort-based decision making. Learning & Memory 13:777.

Scott R, Horvath P (1980) On the direction of preference for moments of higher order than the variance. Journal of Finance 35:915-919.

Scoville WB, Milner B (1957) Loss of recent memory after bilateral hippocampal lesions. Journal of Neurology, Neurosurgery & Psychiatry 20:11.

Seeley RJ, Woods SC (2003) Monitoring of stored and available fuel by the CNS: implications for obesity. Nature Reviews Neuroscience 4:901-909.

Sesack S, Deutch A, Roth R, Bunney B (1989) Topographical organization of the efferent projections of the medial prefrontal cortex in the rat: an anterograde tract-tracing study with Phaseolus vulgaris leucoagglutinin. The Journal of Comparative Neurology 290:213-242.

Sevy S, Hassoun Y, Bechara A, Yechiam E, Napolitano B, Burdick K, Delman H, Malhotra A (2006) Emotion-based decision-making in healthy subjects: short-term effects of reducing dopamine levels. Psychopharmacology 188:228-235.

Shadlen MN, Newsome WT (1996) Motion perception: seeing and deciding. Proceedings of the National Academy of Sciences of the United States of America 93:628.

Shadlen MN, Newsome WT (1998) The variable discharge of cortical neurons: implications for connectivity, computation, and information coding. The Journal of Neuroscience 18:3870.

Shallice T, Burgess P (1991) DEFICITS IN STRATEGY APPLICATION FOLLOWING FRONTAL LOBE DAMAGE IN MAN. Brain 114:727-741.

Sharot T, De Martino B, Dolan RJ (2009a) How choice reveals and shapes expected hedonic outcome. The Journal of Neuroscience 29:3760.

Sharot T, Shiner T, Brown AC, Fan J, Dolan RJ (2009b) Dopamine enhances expectation of pleasure in humans. Current Biology 19:2077-2080.

Sharpe WF (1964) Capital Asset Prices: A Theory of Market Equilibrium under Conditions of Risk. Journal of Finance 19:425-442.

Shi C, Cassell M (1998) Cortical, thalamic, and amygdaloid connections of the anterior and posterior insular cortices. The Journal of Comparative Neurology 399:440-468.

Shipton HW (1975) EEG analysis: A history and a prospectus. Annual review of biophysics and bioengineering 4:1-13.

Shiv B, Loewenstein G, Bechara A, Damasio H, Damasio AR (2005) Investment behavior and the negative side of emotion. Psychological Science 16:435.

Shmuel A, Augath M, Oeltermann A, Logothetis NK (2006) Negative functional MRI response correlates with decreases in neuronal activity in monkey visual area V1. Nature Neuroscience 9:569-577.

Siegmund DO, Worsley KJ (1995) Testing for a signal with unknown location and scale in a stationary Gaussian random field. The annals of statistics 23:608-639.

Siesjo BK (1978) Brain energy metabolism.

Simon HA (1982) Models of bounded rationality.

Singer T, Critchley H, Preuschoff K (2009) A common role of insula in feelings, empathy and uncertainty. Trends in Cognitive Sciences 13:334-340.

Slovic P, Fischhoff B, Lichtenstein S (1977) Behavioral Decision Theory. Annual review of psychology 28:1-39.

Small DM, Zatorre RJ, Dagher A, Evans AC, Jones-Gotman M (2001) Changes in brain activity related to eating chocolate. Brain 124:1720.

Smith B, Mitchell D, Hardin M, Jazbec S, Fridberg D, Blair R, Ernst M (2009) Neural substrates of reward magnitude, probability, and risk during a wheel of fortune decision-making task. Neuroimage 44:600-609.

Sokoloff L (1977) Relation between physiological function and energy metabolism in the central nervous system. Journal of Neurochemistry 29:13-26.

Spitzer B, Wacker E, Blankenburg F (2010) Oscillatory correlates of vibrotactile frequency processing in human working memory. The Journal of Neuroscience 30:4496.

Sporns O, Tononi G, Edelman GM (2000) Connectivity and complexity: the relationship between neuroanatomy and brain dynamics. Neural Networks 13:909-922.

St Onge J, Floresco S (2009) Prefrontal cortical contribution to risk-based decision making. Cerebral Cortex 20:12.

St Onge JR, Floresco SB (2008) Dopaminergic Modulation of Risk-Based Decision Making. Neuropsychopharmacology 34:681-697.

Steffen A, Rockstroh B, Wienbruch C, Miller GA (2011) Distinct cognitive mechanisms in a gambling task share neural mechanisms. Psychophysiology.

Stehling MK, Turner R, Mansfield P (1991) Echo-planar imaging: magnetic resonance imaging in a fraction of a second. Science 254:43.

Stephens DW (1981) The logic of risk-sensitive foraging preferences. Animal Behaviour 29:628-629.

Stephens DW, Brown JS, Ydenberg RC (2007) Foraging : behavior and ecology. Chicago: University of Chicago Press.

Stewart N, Chater N, Stott HP, Reimers S (2003) Prospect relativity: How choice options influence decision under risk. Journal of Experimental Psychology: General 132:23.

Sutton RS, Barto AG (1998a) Reinforcement learning : an introduction. Cambridge, Mass.: MIT Press.

Sutton RS, Barto AG (1998b) Reinforcement learning : an introduction. Cambridge, Mass.: MIT Press.

Symmonds M, Dolan R (2011) The Neurobiology of Preferences. In: The Neuroscience of Preference and Choice (Elsevier, ed).

Symmonds M, Bossaerts P, Dolan R (2010a) A behavioural and neural evaluation of prospective decision-making under risk. Journal of Neuroscience in press.

Symmonds M, Wright N, Bach D, Dolan R (2011) Deconstructing risk: separable encoding of variance and skewness in the brain. Neuroimage in press.

Symmonds M, Emmanuel J, Drew M, Batterham R, Dolan R (2010b) Metabolic state alters economic decision making under risk in humans. PLoS ONE 5:e11090.

Takahashi H, Matsui H, Camerer C, Takano H, Kodaka F, Ideno T, Okubo S, Takemura K, Arakawa R, Eguchi Y (2010) Dopamine D1 Receptors and Nonlinear Probability Weighting in Risky Choice. The Journal of Neuroscience 30:16567.

Taleb N (2004) Bleed or Blowup? Why Do We Prefer Asymmetric Payoffs? Journal of Behavioral Finance 5:2-7.

Tallon-Baudry C, Bertrand O (1999) Oscillatory gamma activity in humans and its role in object representation. Trends Cogn Sci 3:151-162.

Tan K (1991) Risk return and the three-moment capital asset pricing model: Another look. Journal of Banking & Finance 15:449-460.

Tanaka SC, Shishida K, Schweighofer N, Okamoto Y, Yamawaki S, Doya K (2009) Serotonin affects association of aversive outcomes to past actions. The Journal of Neuroscience 29:15669.

Tanaka SC, Schweighofer N, Asahi S, Shishida K, Okamoto Y, Yamawaki S, Doya K (2007) Serotonin differentially regulates short-and long-term prediction of rewards in the ventral and dorsal striatum. PLoS ONE 2:e1333.

Tanne-Gariepy J, Rouiller E, Boussaoud D (2002) Parietal inputs to dorsal versus ventral premotor areas in the macaque monkey: evidence for largely segregated visuomotor pathways. Experimental Brain Research 145:91-103.

Tesauro G (1992) Practical issues in temporal difference learning. Machine learning 8:257-277.

Thaler R, Sunstein C (2008a) Nudge: Improving decisions about health, wealth, and happiness: Yale Univ Pr.

Thaler RH, Sunstein CR (2008b) Nudge: Improving decisions about health, wealth, and happiness: Yale Univ Pr.

Thulborn KR, Waterton JC, Matthews PM, Radda GK (1982) Oxygenation dependence of the transverse relaxation time of water protons in whole blood at high field. Biochimica et Biophysica Acta (BBA)-General Subjects 714:265-270.

Thut G, Schultz W, Roelcke U, Nienhusmeier M, Missimer J, Maguire RP, Leenders KL (1997) Activation of the human brain by monetary reward. Neuroreport 8:1225.

Tiitinen H, Sinkkonen J, Reinikainen K, Alho K, Lavikainen J, Näätänen R (1993) Selective attention enhances the auditory 40-Hz transient response in humans.

Tindell AJ, Smith KS, Berridge KC, Aldridge JW (2009) Dynamic Computation of Incentive Salience:"Wanting" What Was Never "Liked". The Journal of Neuroscience 29:12220.

Tippmann-Peikert M, Park J, Boeve B, Shepard J, Silber M (2007) Pathologic gambling in patients with restless legs syndrome treated with dopaminergic agonists. Neurology 68:301.

Tobler P, Christopoulos G, O'Doherty J, Dolan R, Schultz W (2009) Risk-dependent reward value signal in human prefrontal cortex. Proceedings of the National Academy of Sciences 106:7185.

Tobler PN, Fiorillo CD, Schultz W (2005) Adaptive coding of reward value by dopamine neurons. Science 307:1642-1645.

Tobler PN, O'Doherty JP, Dolan RJ, Schultz W (2007) Reward value coding distinct from risk attitude-related uncertainty coding in human reward systems. J Neurophysiol 97:1621-1632.

Todorov E (2006) Optimal control theory. Bayesian brain: probabilistic approaches to neural coding:269–298.

Tolhurst D, Movshon J, Dean A (1983) The statistical reliability of signals in single neurons in cat and monkey visual cortex. Vision Research 23:775-785.

Tom SM, Fox CR, Trepel C, Poldrack RA (2007) The neural basis of loss aversion in decision-making under risk. Science 315:515.

Torta DME, Castelli L, Zibetti M, Lopiano L, Geminiani G (2009) On the role of dopamine replacement therapy in decision-making, working memory, and reward in Parkinson's disease: Does the therapy-dose matter? Brain and Cognition 71:84-91.

Tremblay L, Schultz W (1999) Relative reward preference in primate orbitofrontal cortex. Nature 398:704-708.

Tuomisto T, Hari R, Katila T, Poutanen T, Varpula T (1983) Studies of auditory evoked magnetic and electric responses: Modality specificity and modelling. Il Nuovo Cimento D 2:471-483.

Tversky A, Kahneman D (1974) Judgment under uncertainty: Heuristics and biases. Science 185:1124.

Tversky A, Kahneman D (1991) Loss aversion in riskless choice: A reference-dependent model. The Quarterly Journal of Economics 106:1039.

Tversky A, Kahneman D (1992) Advances in prospect theory: Cumulative representation of uncertainty. Journal of Risk and uncertainty 5:297-323.

Ullsperger M, Von Cramon DY (2003) Error monitoring using external feedback: specific roles of the habenular complex, the reward system, and the cingulate motor area revealed by functional magnetic resonance imaging. The Journal of Neuroscience 23:4308.

Ursu S, Carter CS (2005) Outcome representations, counterfactual comparisons and the human orbitofrontal cortex: implications for neuroimaging studies of decision-making. Brain Res Cogn Brain Res 23:51-60.

Vanzetta I, Hildesheim R, Grinvald A (2005) Compartment-resolved imaging of activity-dependent dynamics of cortical blood volume and oximetry. The Journal of Neuroscience 25:2233.

Venkatraman V, Payne J, Bettman J, Luce M, Huettel S (2009) Separate neural mechanisms underlie choices and strategic preferences in risky decision making. Neuron 62:593-602.

Volkow ND, Wang GJ, Telang F, Fowler JS, Logan J, Childress AR, Jayne M, Ma Y, Wong C (2008) Dopamine increases in striatum do not elicit craving in cocaine abusers unless they are coupled with cocaine cues. Neuroimage 39:1266-1273.

Von Neumann J, Morgenstern O (1944) Theory of games and economic behavior. Princeton: Princeton University Press.

Voon V, Gao J, Brezing C, Symmonds M, Ekanayake V, Fernandez H, Dolan RJ, Hallett M (2011) Dopamine agonists and risk: impulse control disorders in Parkinson's; disease. Brain 134:1438-1446.

Vul E, Harris C, Winkielman P, Pashler H (2009) Puzzlingly high correlations in fMRI studies of emotion, personality, and social cognition. Perspectives on Psychological Science 4:274.

Wade TR, de Wit H, Richards JB (2000) Effects of dopaminergic drugs on delayed reward as a measure of impulsive behavior in rats. Psychopharmacology.

Wakabayashi KT, Fields HL, Nicola SM (2004) Dissociation of the role of nucleus accumbens dopamine in responding to reward-predictive cues and waiting for reward. Behavioural brain research 154:19-30.

Wald A (1950) Statistical decision functions. New York 660.

Walton ME, Bannerman DM, Alterescu K, Rushworth MFS (2003) Functional specialization within medial frontal cortex of the anterior cingulate for evaluating effort-related decisions. The Journal of Neuroscience 23:6475.

Wang J-H, Tzeng LY, Tien J (2006) Willingness to pay and the demand for lotto. Applied Economics 38:1207-1216.

Weber B, Huettel S (2008a) The neural substrates of probabilistic and intertemporal decision making. Brain Research 1234:104-115.

Weber BJ, Huettel SA (2008b) The neural substrates of probabilistic and intertemporal decision making. Brain research 1234:104-115.

Weber E, Johnson E, eds (2008) Decisions under uncertainty: Psychological, economic, and neuroeconomic explanations of risk preference.

Weber EU, Blais AR, Betz NE (2002) A domain-specific risk-attitude scale: Measuring risk perceptions and risk behaviors. Journal of Behavioral Decision Making 15:263-290.

Weil RS, Furl N, Ruff CC, Symmonds M, Flandin G, Dolan RJ, Driver J, Rees G (2010) Rewarding feedback after correct visual discriminations has both general and specific influences on visual cortex. Journal of neurophysiology 104:1746.

Weiskopf N, Hutton C, Josephs O, Turner R, Deichmann R (2007) Optimized EPI for fMRI studies of the orbitofrontal cortex: compensation of susceptibility-induced gradients in the readout direction. Magnetic Resonance Materials in Physics, Biology and Medicine 20:39-49.

Weller J, Levin I, Shiv B, Bechara A (2009) The effects of insula damage on decision-making for risky gains and losses. Social neuroscience 4:347-358.

Wise RA, Rompré PP (1989) Brain dopamine and reward. Annual review of psychology 40:191-225.

Wood G, Nuerk HC, Sturm D, Willmes K (2008) Using parametric regressors to disentangle properties of multi-feature processes. Behav Brain Funct 4:38.

Woolrich MW, Ripley BD, Brady M, Smith SM (2001) Temporal autocorrelation in univariate linear modeling of FMRI data. Neuroimage 14:1370-1386.

Worsley KJ, Marrett S, Neelin P, Vandal AC, Friston KJ, Evans AC (1996) A unified statistical approach for determining significant signals in images of cerebral activation. Human Brain Mapping 4:58-73.

Wright ND, Symmonds M, Fleming SM, Dolan RJ (2011) Neural Segregation of Objective and Contextual Aspects of Fairness. The Journal of Neuroscience 31:5244.

Wu CC, Bossaerts P, Knutson B, Ben-Jacob E (2011) The Affective Impact of Financial Skewness on Neural Activity and Choice. PLoS ONE 6:130-168.

Wunderle JM, Jr., Castro MS, Fetcher N (1987) Risk-Averse Foraging by Bananaquits on Negative Energy Budgets. Behavioral Ecology and Sociobiology 21:249-255.

Xue G, Lu Z, Levin I, Bechara A (2010) The impact of prior risk experiences on subsequent risky decision-making: The role of the insula. Neuroimage.

Xue G, Lu Z, Levin I, Weller J, Li X, Bechara A (2009) Functional dissociations of risk and reward processing in the medial prefrontal cortex. Cerebral Cortex 19:1019.

Yacubian J, Glascher J, Schroeder K, Sommer T, Braus DF, Buchel C (2006) Dissociable systems for gain- and loss-related value predictions and errors of prediction in the human brain. J Neurosci 26:9530-9537.

Yacubian J, Sommer T, Schroeder K, Gläscher J, Braus D, Büchel C (2007) Subregions of the ventral striatum show preferential coding of reward magnitude and probability. Neuroimage 38:557-563.

Yokel RA, Wise RA (1978) Amphetamine-type reinforcement by dopaminergic agonists in the rat. Psychopharmacology 58:289-296.

Yu R, Mobbs D, Seymour B, Calder AJ (2010) Insula and Striatum Mediate the Default Bias. The Journal of Neuroscience 30:14702.

Zeeb FD, Robbins TW, Winstanley CA (2009) Serotonergic and dopaminergic modulation of gambling behavior as assessed using a novel rat gambling task. Neuropsychopharmacology 34:2329-2343.

Zhang K, Guo JZ, Peng Y, Xi W, Guo A (2007) Dopamine-mushroom body circuit regulates saliency-based decision-making in Drosophila. Science 316:1901.

Zigman JM, Jones JE, Lee CE, Saper CB, Elmquist JK (2006) Expression of ghrelin receptor mRNA in the rat and the mouse brain. Journal of Comparative Neurology 494:528-548.

Appendix A

	Amounts (p)																
Lottery	**0**	**20**	**40**	**60**	**80**	**100**	**120**	**140**	**160**	**180**	**200**	**220**	**240**	**260**	**Expected value**	**Variance**	**Skewness**
1	0	0	0	0.1	0	0.2	0.1	0.2	0.4	0	0	0	0	0	130	0.11	-0.83
2	0	0	0	0.1	0	0.1	0.2	0.4	0	0.2	0	0	0	0	132	0.11	-0.49
3	0	0	0	0	0.2	0.1	0.2	0.1	0.3	0.1	0	0	0	0	130	0.11	-0.19
4	0	0	0	0	0.1	0.3	0.1	0.2	0.1	0.2	0	0	0	0	130	0.11	0.19
5	0	0	0	0	0.2	0	0.4	0.2	0.1	0	0.1	0	0	0	128	0.11	0.49
6	0	0	0	0	0.1	0.1	0.5	0.1	0	0.1	0.1	0	0	0	130	0.11	0.81
7	0	0	0.1	0	0.2	0	0.1	0.1	0.5	0	0	0	0	0	126	0.18	-0.85
8	0	0	0	0.1	0.2	0	0.1	0.1	0.3	0.2	0	0	0	0	132	0.18	-0.49
9	0	0	0.1	0	0	0.1	0.1	0.6	0	0	0	0.1	0	0	132	0.18	-0.17
10	0	0	0.1	0	0	0	0.6	0.1	0.1	0	0	0.1	0	0	128	0.18	0.17
11	0	0	0	0.1	0.1	0.1	0.2	0.3	0.1	0	0	0.1	0	0	128	0.18	0.49
12	0	0	0	0.1	0	0.1	0.6	0	0	0.1	0	0.1	0	0	128	0.17	0.83
13	0	0.1	0	0	0.2	0	0.1	0.2	0.2	0.2	0	0	0	0	126	0.24	-0.84
14	0	0	0.1	0.1	0	0	0.3	0.1	0.1	0.2	0.1	0	0	0	132	0.24	-0.50
15	0	0	0.1	0	0.1	0.2	0	0.1	0.4	0	0	0.1	0	0	132	0.24	-0.18
16	0	0	0	0.2	0	0.2	0.2	0.1	0	0.1	0.2	0	0	0	128	0.24	0.18
17	0	0	0.1	0	0.1	0.1	0.1	0.5	0	0	0	0	0.1	0	128	0.24	0.50
18	0	0	0	0	0.2	0.4	0.1	0	0	0.1	0.1	0.1	0	0	128	0.24	0.83
19	0	0.1	0	0.1	0.1	0	0	0.1	0.4	0.1	0.1	0	0	0	132	0.31	-0.83
20	0	0	0.2	0	0.1	0.1	0	0	0.4	0.1	0.1	0	0	0	128	0.31	-0.50
21	0	0.1	0	0	0.1	0.1	0.4	0	0	0	0.3	0	0	0	128	0.31	-0.16
22	0	0	0.1	0	0.3	0	0.2	0.1	0	0	0.3	0	0	0	126	0.30	0.17
23	0	0	0	0.1	0.1	0.4	0	0	0.1	0.1	0	0.2	0	0	132	0.31	0.50
24	0	0	0	0	0.4	0.2	0.1	0	0	0.1	0	0.2	0	0	126	0.30	0.83
25	0.1	0	0.1	0	0	0	0.2	0.1	0.4	0	0	0.1	0	0	128	0.37	-0.83
26	0	0	0.3	0	0	0	0.2	0	0	0.5	0	0	0	0	126	0.37	-0.50
27	0	0	0.2	0.1	0	0	0.1	0.3	0	0.1	0.1	0.1	0	0	128	0.37	-0.17
28	0	0	0.1	0	0.3	0	0.2	0	0	0.2	0	0.2	0	0	132	0.37	0.17
29	0	0.1	0	0	0	0.3	0.2	0.2	0	0	0.1	0	0	0.1	130	0.37	0.50
30	0	0	0.1	0	0.2	0.2	0.2	0	0	0.2	0	0	0	0.1	126	0.37	0.83
31	0.1	0	0.1	0.1	0	0	0.1	0	0.1	0.5	0	0	0	0	128	0.43	-0.83
32	0.1	0	0.1	0	0.1	0	0.2	0.1	0	0.3	0	0.1	0	0	126	0.43	-0.50
33	0	0	0.2	0.2	0	0	0	0.2	0	0.1	0.3	0	0	0	126	0.43	-0.16
34	0	0.1	0	0.1	0	0.1	0.2	0.2	0.1	0	0	0	0.2	0	134	0.43	0.16
35	0	0	0.2	0	0	0.2	0.3	0	0.1	0	0	0	0.2	0	128	0.43	0.50
36	0	0	0	0.3	0	0.3	0	0.1	0.1	0	0	0.1	0	0.1	126	0.43	0.83
37	0.2	0	0	0	0	0	0.2	0.1	0.3	0	0.1	0.1	0	0	128	0.50	-0.84
38	0	0.2	0.1	0	0	0	0.2	0	0	0.3	0.2	0	0	0	126	0.50	-0.50
39	0	0.1	0.1	0.2	0	0	0	0	0.4	0	0	0.2	0	0	126	0.50	-0.17
40	0	0.1	0	0.1	0.1	0.1	0.1	0.2	0	0	0.1	0	0.2	0	134	0.50	0.17
41	0	0	0.1	0.2	0.1	0	0.3	0	0	0	0.1	0	0.2	0	128	0.50	0.50
42	0	0	0.1	0.1	0	0.3	0.1	0.2	0	0	0	0	0	0.2	132	0.50	0.84
43	0.2	0	0	0	0	0.2	0	0	0.1	0.2	0.3	0	0	0	132	0.56	-0.83
44	0.1	0	0.2	0	0.1	0	0	0	0	0.5	0	0.1	0	0	128	0.56	-0.50
45	0.1	0	0.1	0	0.2	0.1	0	0	0.1	0.1	0.2	0	0.1	0	128	0.56	-0.17
46	0	0	0.2	0.2	0	0	0	0.2	0	0.2	0	0.1	0	0.1	132	0.56	0.17
47	0	0	0.1	0	0.5	0	0	0	0	0.1	0	0.2	0	0.1	132	0.56	0.50
48	0	0	0.1	0.2	0.1	0.1	0.2	0	0.1	0	0	0	0	0.2	126	0.56	0.84
49	0.1	0.2	0	0	0	0	0	0	0.1	0.4	0.2	0	0	0	132	0.62	-0.83
50	0.1	0.2	0	0	0	0	0.1	0	0.3	0.1	0	0.2	0	0	126	0.62	-0.50
51	0.1	0.1	0.1	0	0	0	0.1	0.2	0.1	0.1	0.1	0	0	0.1	126	0.62	-0.16
52	0	0.1	0.1	0.2	0.1	0	0	0	0.1	0.2	0	0	0.2	0	126	0.62	0.17
53	0	0.1	0.1	0	0.1	0.4	0	0	0	0	0	0	0.3	0	126	0.62	0.50
54	0	0	0	0.2	0.4	0	0.1	0	0	0	0	0.1	0	0.2	130	0.62	0.81
55	0.2	0.1	0	0	0	0	0	0	0.1	0.3	0.3	0	0	0	132	0.69	-0.82
56	0.1	0.2	0	0	0	0	0	0.2	0.1	0	0.3	0	0.1	0	132	0.69	-0.50
57	0.2	0	0	0	0.2	0.1	0	0	0	0.3	0.1	0	0	0.1	126	0.69	-0.16
58	0	0.1	0.1	0.2	0	0	0.2	0	0	0.1	0	0	0.3	0	132	0.69	0.17
59	0	0	0.1	0.2	0.3	0	0	0	0	0	0.2	0	0	0.2	132	0.69	0.50
60	0	0	0	0.3	0.3	0.1	0	0	0	0	0	0	0.1	0.2	128	0.69	0.82

Appendix B

Lottery A				*Lottery B*				*Expected value*	
Card 1	**Card 2**	**Card 3**	**Card 4**	**Card 1**	**Card 2**	**Card 3**	**Card 4**	*difference*	*Risk difference*
20	20	20	20	0	0	20	100	10	2266.67
40	40	40	40	0	60	60	60	5	900.00
60	60	60	60	40	60	100	100	15	900.00
20	20	40	60	0	0	40	100	0	1866.67
0	20	20	40	0	0	0	80	0	1333.33
40	40	40	80	0	0	100	100	0	2933.33
20	40	60	80	0	20	40	100	-10	1200.00
0	20	20	20	0	0	20	60	5	700.00
20	20	20	40	0	20	80	100	25	2166.67
60	60	60	60	20	60	60	100	0	1066.67
40	40	40	80	0	0	0	100	-25	2100.00
60	60	60	60	0	20	20	100	-25	1966.67
80	80	80	80	60	100	100	100	10	400.00
0	20	40	60	20	20	100	100	30	1466.67
0	0	80	80	20	20	40	100	5	-700.00
20	20	20	20	0	60	60	80	30	1200.00
0	20	40	60	0	0	60	100	10	1733.33
0	0	0	60	0	40	40	100	30	800.00
20	40	40	100	0	40	60	100	0	533.33
20	40	80	80	0	0	0	100	-30	1600.00
40	40	40	80	0	80	80	80	10	1200.00
60	80	80	80	0	40	60	100	-25	1633.33
60	60	60	60	0	0	0	80	-40	1600.00
40	40	40	40	0	40	60	60	0	800.00
20	20	20	20	0	0	60	100	20	2400.00
0	20	40	40	20	20	40	100	20	1066.67
20	40	80	80	0	60	80	100	5	966.67
60	80	100	100	40	100	100	100	0	533.33
20	40	40	40	20	20	60	100	15	1366.67
40	40	100	100	20	60	100	100	0	266.67
20	20	20	20	0	40	40	40	10	400.00
0	0	40	40	20	40	60	100	35	633.33
20	40	60	80	0	0	60	100	-10	1733.33
20	60	60	100	0	0	80	100	-15	1700.00
0	0	40	40	20	20	80	100	35	1166.67
20	20	20	20	0	100	100	100	55	2500.00
0	20	20	40	0	0	0	60	-5	633.33
40	40	40	40	0	20	60	80	0	1333.33
20	20	20	40	0	0	60	80	10	1600.00
20	20	20	20	0	60	100	100	45	2233.33
60	60	60	60	40	40	40	80	-10	400.00
20	20	20	60	0	80	100	100	40	1866.67
0	60	60	60	20	40	40	100	5	300.00
20	40	40	60	0	60	80	100	20	1600.00
20	20	20	60	0	0	40	60	-5	500.00
0	0	20	20	0	0	0	60	5	766.67
80	80	80	80	40	40	100	100	-10	1200.00
80	80	80	80	20	20	80	100	-25	1700.00
80	80	80	80	40	60	100	100	-5	900.00
40	40	40	40	0	0	20	60	-20	800.00
80	80	80	80	0	0	20	100	-50	2266.67
0	60	60	60	40	60	60	80	15	-633.33
40	40	40	40	20	40	40	40	-5	100.00
0	0	20	40	0	0	0	80	5	1233.33
60	80	80	80	0	100	100	100	0	2400.00
0	0	0	60	20	40	40	40	20	-800.00
20	20	40	40	0	20	100	100	25	2633.33
40	40	40	40	20	40	80	80	15	900.00
0	20	40	40	0	0	20	80	0	1066.67
0	0	40	40	0	0	20	100	10	1733.33
20	20	40	60	0	40	40	80	5	700.00
0	40	40	40	20	40	60	80	20	266.67
60	60	60	60	40	40	80	100	5	900.00
0	0	60	60	0	20	40	100	10	666.67
0	20	20	60	0	0	60	80	10	1066.67
0	40	40	40	0	0	60	60	0	800.00
20	20	40	40	0	80	80	100	35	1833.33
20	20	20	20	0	20	80	80	25	1700.00
20	40	80	80	20	20	80	100	0	800.00
0	0	80	80	40	40	40	100	15	-1233.33

0	40	40	40	20	60	60	100	30	666.67
60	60	60	60	40	40	80	80	0	533.33
0	20	40	40	20	20	80	100	30	1333.33
20	20	20	40	0	0	100	100	25	3233.33
0	0	40	60	0	20	40	60	5	-233.33
60	60	60	60	20	80	100	100	15	1433.33
20	20	20	20	0	0	0	60	-5	900.00
20	20	20	20	0	60	60	60	25	900.00
0	60	60	60	0	40	40	80	-5	166.67
20	20	40	60	0	20	20	80	-5	833.33
20	20	20	40	0	0	60	60	5	1100.00
0	0	0	60	40	40	100	100	55	300.00
0	0	40	40	20	60	80	80	40	266.67
0	20	20	60	0	0	80	100	20	2133.33
20	40	40	60	20	20	40	100	5	1166.67
0	60	60	60	20	20	80	80	5	300.00
20	40	80	80	0	0	80	100	-10	1866.67
0	20	20	20	0	0	60	80	20	1600.00
20	40	40	40	0	40	40	60	0	533.33
0	20	20	40	0	0	80	100	25	2500.00
60	80	80	80	20	60	80	100	-10	1066.67
60	60	60	60	0	0	0	100	-35	2500.00
20	40	80	80	40	60	60	100	10	-266.67
0	20	20	20	0	0	0	60	0	800.00
0	0	40	60	0	0	80	100	20	1866.67
20	20	20	40	0	0	0	60	-10	800.00
0	0	0	60	0	0	20	80	10	533.33
60	60	80	80	0	80	100	100	0	2133.33
0	0	20	20	0	20	20	60	15	500.00
20	20	40	40	0	0	40	80	0	1333.33
20	40	40	60	0	20	80	100	10	2000.00
0	0	40	40	20	40	60	60	25	-166.67
0	0	0	60	40	80	100	100	65	-100.00
20	40	40	40	0	80	80	80	25	1500.00
20	20	20	40	0	0	20	80	0	1333.33
20	20	20	60	0	0	0	100	-5	2100.00
0	40	40	40	20	20	60	60	10	133.33
0	20	40	40	0	0	80	80	15	1766.67
20	40	40	40	0	0	40	60	-10	800.00
60	60	80	80	20	100	100	100	10	1466.67
0	20	40	60	20	20	40	60	5	-300.00
0	40	40	40	20	40	40	100	20	800.00
60	60	60	60	40	60	80	80	5	366.67
20	20	20	60	0	40	40	60	5	233.33
0	0	0	60	20	20	80	100	40	800.00
20	40	60	80	0	40	60	100	0	1066.67
20	20	40	40	0	0	20	60	-10	666.67
0	20	40	60	20	20	80	100	25	1033.33
0	0	0	40	20	20	100	100	50	1733.33
0	0	20	20	0	0	20	60	10	666.67
60	60	60	60	0	0	60	80	-25	1700.00
40	40	40	80	0	80	80	100	15	1566.67
40	40	40	80	20	20	80	100	5	1300.00
0	20	20	20	0	0	60	100	25	2300.00
20	40	40	40	0	0	60	80	0	1600.00
0	60	60	60	20	20	80	100	10	800.00
60	60	60	60	0	40	60	80	-15	1166.67
0	0	80	80	40	60	100	100	35	-1233.33
20	20	20	60	0	0	80	100	15	2366.67
20	40	40	100	0	60	100	100	15	1033.33
20	40	40	60	0	100	100	100	35	2233.33
20	20	40	40	0	0	0	100	-5	2366.67
20	20	40	40	20	20	20	100	10	1466.67
40	40	40	40	20	60	80	80	20	800.00
20	20	20	40	0	40	80	80	25	1366.67
60	60	80	80	20	40	40	100	-20	1066.67
0	0	40	60	0	0	20	100	5	1366.67
20	20	20	40	0	60	80	100	35	1766.67
0	20	40	40	0	0	0	60	-10	533.33
60	60	60	60	40	100	100	100	25	900.00
0	60	60	60	0	0	20	100	-15	1366.67
0	0	80	80	40	100	100	100	45	-1233.33
20	40	40	40	0	20	60	60	0	800.00
0	20	40	40	20	20	60	100	25	1100.00
60	60	80	80	0	0	80	100	-25	2633.33
20	40	40	40	0	20	20	60	-10	533.33
0	0	40	40	0	0	20	80	5	900.00
60	80	80	80	0	80	80	100	-10	1866.67
0	0	80	80	40	80	100	100	40	-1333.33
0	60	60	60	0	20	20	80	-15	300.00

0	40	40	40	20	20	20	80	5	500.00
60	60	80	80	0	40	80	100	-15	1833.33
40	40	40	40	0	20	60	60	-5	900.00
20	20	20	20	0	20	40	40	5	366.67
0	60	60	60	40	40	40	80	5	-500.00
0	20	20	40	0	0	40	100	15	1966.67
20	20	20	60	0	20	80	80	15	1300.00
0	20	20	20	0	0	20	40	0	266.67
20	20	40	60	0	0	60	100	5	2033.33
0	0	40	60	0	0	0	80	-5	700.00
20	40	40	60	0	20	40	80	-5	900.00
0	20	20	20	0	0	100	100	35	3233.33
0	20	40	60	0	0	60	80	5	1033.33
20	40	40	40	0	40	60	80	10	1066.67
80	80	80	80	40	40	80	100	-15	900.00
20	20	20	20	0	80	80	80	40	1600.00
20	20	40	40	0	20	20	100	5	1833.33
0	20	20	20	0	0	60	60	15	1100.00
20	20	40	40	0	60	80	80	25	1300.00
0	0	40	40	0	0	0	60	-5	366.67
20	20	20	40	0	0	0	100	0	2400.00
0	40	40	40	0	20	80	80	15	1300.00
0	60	60	60	0	20	60	100	0	1066.67
20	60	60	100	20	20	80	100	-5	633.33
20	20	20	40	0	60	60	60	20	800.00
20	20	40	40	0	0	0	60	-15	766.67
0	20	40	40	20	20	100	100	35	1766.67
80	80	80	80	0	40	60	100	-30	1733.33
20	20	40	60	0	0	0	100	-10	2133.33
40	40	40	40	20	20	20	60	-10	400.00
20	40	40	40	0	0	0	100	-10	2400.00
0	20	20	20	0	0	0	40	-5	300.00
60	80	80	80	60	80	100	100	10	266.67
20	20	20	20	0	0	60	80	15	1700.00
40	40	40	40	0	40	40	80	0	1066.67
20	20	40	40	0	0	60	80	5	1566.67
80	80	80	80	60	80	80	100	0	266.67
20	20	20	20	0	0	60	60	10	1200.00
20	20	20	20	0	0	40	40	0	533.33
20	20	20	40	0	0	40	40	-5	433.33
0	60	60	60	40	80	80	80	25	-500.00
20	20	20	20	0	0	20	60	0	800.00
0	0	20	20	0	0	0	40	0	266.67
20	40	40	40	0	0	80	80	5	2033.33
0	60	60	60	0	0	0	80	-25	700.00
20	20	40	60	0	40	100	100	25	2033.33
20	40	40	40	0	60	60	100	20	1600.00
0	0	0	60	40	40	40	100	40	0.00
20	40	40	60	0	20	20	80	-10	933.33
80	80	100	100	20	100	100	100	-10	1466.67

Appendix C1

	Probabilities				Amounts (£)					
Trial	**p1**	**p2**	**p3**	**p4**	**m1**	**m2**	**m3**	**m4**	**EV**	**Var**
1	0.4	0.1	0.1	0.4	3	1.5	5	3.5	3.25	0.66
2	0.1	0.4	0.1	0.4	5.5	2	1	4.5	3.25	2.26
3	0.35	0.15	0.35	0.15	1	4.5	5.5	2	3.25	4.01
4	0.3	0.3	0.2	0.2	6	0.5	5	1.5	3.25	5.76
5	0.2	0.3	0.3	0.2	5	6.5	0	1.5	3.25	7.56
6	0.3	0.2	0.2	0.3	6.5	0.5	6	0	3.25	9.36
7	0.2	0.2	0.3	0.3	6.5	0.5	7	0	3.5	10.95
8	0.4	0.1	0.1	0.4	0	0.5	6.5	7	3.5	11.60
9	0.15	0.35	0.15	0.35	5	4	2.5	3.5	3.75	0.51
10	0.1	0.4	0.4	0.1	6	2.5	5	1.5	3.75	2.26
11	0.35	0.35	0.15	0.15	1.5	6	5	2.5	3.75	4.01
12	0.3	0.3	0.2	0.2	6.5	1	2	5.5	3.75	5.76
13	0.2	0.3	0.2	0.3	7.5	5.5	0	2	3.75	7.46
14	0.3	0.2	0.3	0.2	7	1	0.5	6.5	3.75	9.36
15	0.25	0.25	0.25	0.25	0	6.5	7.5	1	3.75	10.81
16	0.4	0.4	0.1	0.1	0	7.5	1	6.5	3.75	12.76
17	0.15	0.35	0.35	0.15	0.5	7.5	0	7	3.75	13.01
18	0.4	0.1	0.4	0.1	0	7	7.5	0.5	3.75	13.36
19	0.15	0.15	0.35	0.35	3	5	3.5	4.5	4	0.48
20	0.25	0.15	0.1	0.5	2.5	6.5	1.5	4.5	4	2.25
21	0.1	0.4	0.4	0.1	0	5	3	8	4	4.00
22	0.2	0.2	0.3	0.3	3	5	1	7	4	5.80
23	0.2	0.1	0.3	0.4	0	5.5	7.5	3	4	7.50
24	0.25	0.25	0.25	0.25	0.5	1.5	7.5	6.5	4	9.25
25	0.2	0.2	0.3	0.3	1	7	7.5	0.5	4	10.95
26	0.1	0.4	0.1	0.4	3.5	8	4.5	0	4	12.85
27	0.2	0.2	0.3	0.3	0.5	7.5	8	0	4	14.50
28	0.1	0.4	0.4	0.1	7	0	8	1	4	14.60
29	0.35	0.15	0.15	0.35	0	0.5	7.5	8	4	14.88
30	0.1	0.1	0.4	0.4	0.5	7.5	0	8	4	15.25
31	0.35	0.15	0.15	0.35	4.5	5.5	3	4	4.25	0.51
32	0.1	0.4	0.4	0.1	2	3	5.5	6.5	4.25	2.26
33	0.35	0.35	0.15	0.15	6.5	2	5.5	3	4.25	4.01
34	0.3	0.2	0.2	0.3	1.5	2.5	6	7	4.25	5.76
35	0.3	0.3	0.2	0.2	2.5	6	8	0.5	4.25	7.46
36	0.25	0.25	0.25	0.25	3.5	5	0	8.5	4.25	9.31
37	0.2	0.3	0.2	0.3	5	0	3.5	8.5	4.25	11.06
38	0.1	0.4	0.4	0.1	1.5	8	0.5	7	4.25	12.76
39	0.4	0.1	0.4	0.1	8.5	4	0	4.5	4.25	14.46
40	0.25	0.25	0.25	0.25	0	0.5	8.5	8	4.25	16.06

41	0.2	0.3	0.2	0.3	0.5	0	8	8.5	4.25	16.46
42	0.1	0.4	0.1	0.4	7.5	8.5	1	0	4.25	16.56
43	0.15	0.35	0.15	0.35	8	0	0.5	8.5	4.25	16.86
44	0.4	0.1	0.1	0.4	0	8	0.5	8.5	4.25	17.26
45	0.35	0.35	0.15	0.15	5	4	5.5	3.5	4.5	0.48
46	0.1	0.15	0.5	0.25	2	7	5	3	4.5	2.25
47	0.4	0.1	0.4	0.1	3.5	8.5	5.5	0.5	4.5	4.00
48	0.2	0.3	0.2	0.3	3.5	1.5	5.5	7.5	4.5	5.80
49	0.2	0.1	0.4	0.3	0.5	6	3.5	8	4.5	7.50
50	0.25	0.25	0.25	0.25	2	7	8	1	4.5	9.25
51	0.3	0.2	0.2	0.3	8	7.5	1.5	1	4.5	10.95
52	0.1	0.1	0.4	0.4	5	4	0.5	8.5	4.5	12.85
53	0.2	0.2	0.3	0.3	8	1	0.5	8.5	4.5	14.50
54	0.25	0.25	0.25	0.25	9	1	8	0	4.5	16.25
55	0.15	0.15	0.35	0.35	8	1	0	9	4.5	17.85
56	0.1	0.1	0.4	0.4	1.5	7.5	0	9	4.5	18.00
57	0.25	0.25	0.25	0.25	0	9	0.5	8.5	4.5	18.13
58	0.3	0.2	0.3	0.2	9	0.5	0	8.5	4.5	18.55
59	0.4	0.1	0.4	0.1	9	1	0	8	4.5	18.65
60	0.35	0.15	0.35	0.15	9	8.5	0	0.5	4.5	18.98
61	0.4	0.4	0.1	0.1	9	0	8.5	0.5	4.5	19.40
62	0.15	0.15	0.35	0.35	3.5	6	4.5	5	4.75	0.51
63	0.4	0.1	0.4	0.1	6	7	3.5	2.5	4.75	2.26
64	0.15	0.15	0.35	0.35	3.5	6	2.5	7	4.75	4.01
65	0.1	0.1	0.4	0.4	9.5	0	6	3.5	4.75	5.76
66	0.2	0.2	0.3	0.3	8.5	1	3	6.5	4.75	7.46
67	0.25	0.25	0.25	0.25	5.5	4	9	0.5	4.75	9.31
68	0.3	0.2	0.3	0.2	9	5.5	0.5	4	4.75	11.06
69	0.1	0.1	0.4	0.4	2	7.5	8.5	1	4.75	12.76
70	0.1	0.4	0.4	0.1	5	0.5	9	4.5	4.75	14.46
71	0.15	0.15	0.35	0.35	3.5	6	9.5	0	4.75	16.26
72	0.35	0.15	0.35	0.15	9.5	7.5	0	2	4.75	18.06
73	0.2	0.3	0.2	0.3	0	0.5	9.5	9	4.75	19.86
74	0.15	0.35	0.15	0.35	8.5	9.5	1	0	4.75	20.01
75	0.1	0.4	0.4	0.1	8	0	9.5	1.5	4.75	20.16
76	0.25	0.25	0.25	0.25	9	0.5	9.5	0	4.75	20.31
77	0.2	0.3	0.3	0.2	0.5	9.5	0	9	4.75	20.76
78	0.1	0.4	0.4	0.1	1	9.5	0	8.5	4.75	20.86
79	0.15	0.15	0.35	0.35	0.5	9	9.5	0	4.75	21.21
80	0.4	0.4	0.1	0.1	0	9.5	9	0.5	4.75	21.66
81	0.15	0.35	0.35	0.15	4	4.5	5.5	6	5	0.48
82	0.5	0.15	0.1	0.25	5.5	7.5	2.5	3.5	5	2.25
83	0.1	0.1	0.4	0.4	9	1	4	6	5	4.00
84	0.1	0.4	0.1	0.4	10	6	0	4	5	5.80
85	0.3	0.2	0.1	0.4	8.5	1	6.5	4	5	7.50
86	0.25	0.25	0.25	0.25	7.5	8.5	1.5	2.5	5	9.25
87	0.15	0.35	0.4	0.1	10	2	7	0	5	11.00

88	0.4	0.4	0.1	0.1	9	1	5.5	4.5	5	12.85
89	0.25	0.25	0.25	0.25	3	0	10	7	5	14.50
90	0.25	0.25	0.25	0.25	0.5	9.5	8.5	1.5	5	16.25
91	0.4	0.1	0.1	0.4	0.5	8	2	9.5	5	18.00
92	0.3	0.2	0.3	0.2	9	10	1	0	5	19.60
93	0.3	0.2	0.3	0.2	10	9	0	1	5	21.40
94	0.25	0.25	0.25	0.25	0.5	0	10	9.5	5	22.63
95	0.3	0.3	0.2	0.2	10	0	9.5	0.5	5	23.10
96	0.4	0.1	0.1	0.4	10	1	9	0	5	23.20
97	0.35	0.35	0.15	0.15	0	10	9.5	0.5	5	23.58
98	0.4	0.1	0.1	0.4	0	0.5	9.5	10	5	24.05
99	0.15	0.35	0.15	0.35	4	5.5	6.5	5	5.25	0.51
100	0.4	0.1	0.4	0.1	4	7.5	6.5	3	5.25	2.26
101	0.15	0.15	0.35	0.35	6.5	4	3	7.5	5.25	4.01
102	0.1	0.1	0.4	0.4	0.5	10	6.5	4	5.25	5.76
103	0.3	0.2	0.3	0.2	3.5	1.5	7	9	5.25	7.46
104	0.25	0.25	0.25	0.25	4.5	1	9.5	6	5.25	9.31
105	0.3	0.2	0.2	0.3	5.5	0	10.5	5	5.25	11.06
106	0.1	0.4	0.4	0.1	8	9	1.5	2.5	5.25	12.76
107	0.4	0.1	0.1	0.4	9.5	5	5.5	1	5.25	14.46
108	0.35	0.15	0.15	0.35	10	4	6.5	0.5	5.25	16.26
109	0.15	0.35	0.15	0.35	8	10	2.5	0.5	5.25	18.06
110	0.35	0.15	0.35	0.15	10.5	4	0	6.5	5.25	19.76
111	0.35	0.15	0.35	0.15	10.5	2.5	0	8	5.25	21.56
112	0.1	0.4	0.1	0.4	3	10.5	7.5	0	5.25	23.06
113	0.1	0.1	0.4	0.4	7	4	5	6	5.5	0.65
114	0.5	0.25	0.15	0.1	6	4	8	3	5.5	2.25
115	0.4	0.1	0.1	0.4	4.5	9.5	1.5	6.5	5.5	4.00
116	0.1	0.4	0.1	0.4	10.5	6.5	0.5	4.5	5.5	5.80
117	0.2	0.4	0.3	0.1	1.5	4.5	9	7	5.5	7.50
118	0.4	0.1	0.4	0.1	7.5	11	3.5	0	5.5	9.25
119	0.35	0.15	0.4	0.1	2.5	10.5	7.5	0.5	5.5	11.00
120	0.3	0.3	0.2	0.2	6.5	4.5	0	11	5.5	12.70
121	0.2	0.3	0.2	0.3	0	7.5	11	3.5	5.5	14.50
122	0.25	0.25	0.25	0.25	4	11	7	0	5.5	16.25
123	0.4	0.1	0.1	0.4	10	2.5	8.5	1	5.5	18.00
124	0.2	0.3	0.3	0.2	7.5	11	0	3.5	5.5	19.75
125	0.15	0.15	0.35	0.35	4.5	6.5	11	0	5.5	21.48
126	0.15	0.15	0.35	0.35	11	0	10	1	5.5	23.25
127	0.4	0.4	0.1	0.1	6	5.5	7.5	4	5.75	0.66
128	0.1	0.4	0.4	0.1	8	4.5	7	3.5	5.75	2.26
129	0.35	0.15	0.35	0.15	3.5	7	8	4.5	5.75	4.01
130	0.4	0.1	0.1	0.4	7	10.5	1	4.5	5.75	5.76
131	0.2	0.2	0.3	0.3	2	9.5	4	7.5	5.75	7.46
132	0.25	0.25	0.25	0.25	1.5	10	6.5	5	5.75	9.31
133	0.15	0.15	0.35	0.35	11.5	0	7	4.5	5.75	11.01
134	0.4	0.4	0.1	0.1	2	9.5	3	8.5	5.75	12.76

135	0.1	0.1	0.4	0.4	5.5	6	10	1.5	5.75	14.46
136	0.2	0.3	0.2	0.3	11.5	8	0	3.5	5.75	16.26
137	0.25	0.25	0.25	0.25	4	0	11.5	7.5	5.75	18.06
138	0.15	0.35	0.35	0.15	0	9.5	2	11.5	5.75	19.76
139	0.15	0.35	0.35	0.15	3	11	0.5	8.5	5.75	21.56
140	0.35	0.15	0.35	0.15	0	5	11.5	6.5	5.75	23.31
141	0.4	0.1	0.1	0.4	6.5	4	8	5.5	6	1.00
142	0.25	0.5	0.15	0.1	4.5	6.5	8.5	3.5	6	2.25
143	0.1	0.4	0.1	0.4	10	5	2	7	6	4.00
144	0.4	0.1	0.4	0.1	7	1	5	11	6	5.80
145	0.1	0.3	0.4	0.2	7.5	9.5	5	2	6	7.50
146	0.1	0.4	0.1	0.4	0.5	8	11.5	4	6	9.25
147	0.15	0.1	0.4	0.35	11	1	8	3	6	11.00
148	0.3	0.2	0.3	0.2	5	0.5	7	11.5	6	12.70
149	0.2	0.2	0.3	0.3	0.5	11.5	8	4	6	14.50
150	0.25	0.25	0.25	0.25	0.5	11.5	4.5	7.5	6	16.25
151	0.4	0.1	0.1	0.4	10.5	3	9	1.5	6	18.00
152	0.2	0.3	0.2	0.3	4	0.5	8	11.5	6	19.75
153	0.35	0.15	0.15	0.35	11.5	7	5	0.5	6	21.48
154	0.15	0.35	0.35	0.15	0.5	1.5	10.5	11.5	6	23.25
155	0.4	0.1	0.4	0.1	6	4	6.5	8.5	6.25	1.06
156	0.1	0.1	0.4	0.4	8.5	4	7.5	5	6.25	2.26
157	0.35	0.15	0.35	0.15	4	7.5	8.5	5	6.25	4.01
158	0.4	0.4	0.1	0.1	7.5	5	1.5	11	6.25	5.76
159	0.3	0.3	0.2	0.2	4.5	8	2.5	10	6.25	7.46
160	0.25	0.25	0.25	0.25	7	2	5.5	10.5	6.25	9.31
161	0.35	0.35	0.15	0.15	5	7.5	12	0.5	6.25	11.01
162	0.1	0.4	0.1	0.4	9	10	3.5	2.5	6.25	12.76
163	0.4	0.1	0.1	0.4	2	6	6.5	10.5	6.25	14.46
164	0.3	0.2	0.2	0.3	4	12	0.5	8.5	6.25	16.26
165	0.25	0.25	0.25	0.25	4.5	8	12	0.5	6.25	18.06
166	0.15	0.35	0.15	0.35	12	2.5	0.5	10	6.25	19.76
167	0.35	0.15	0.15	0.35	1	3.5	9	11.5	6.25	21.56
168	0.35	0.15	0.35	0.15	12	7	0.5	5.5	6.25	23.31
169	0.4	0.1	0.1	0.4	7	4	9	6	6.5	1.45
170	0.1	0.25	0.15	0.5	4	5	9	7	6.5	2.25
171	0.4	0.1	0.4	0.1	7.5	10.5	5.5	2.5	6.5	4.00
172	0.4	0.1	0.4	0.1	5.5	1.5	7.5	11.5	6.5	5.80
173	0.4	0.1	0.3	0.2	5.5	8	10	2.5	6.5	7.50
174	0.1	0.4	0.1	0.4	12	4.5	1	8.5	6.5	9.25
175	0.4	0.35	0.1	0.15	8.5	3.5	1.5	11.5	6.5	11.00
176	0.3	0.2	0.2	0.3	7.5	1	12	5.5	6.5	12.70
177	0.25	0.15	0.1	0.5	12	0	7.5	5.5	6.5	14.50
178	0.25	0.25	0.25	0.25	12	1	5	8	6.5	16.25
179	0.4	0.1	0.1	0.4	11	3.5	9.5	2	6.5	18.00
180	0.3	0.2	0.2	0.3	1	8.5	4.5	12	6.5	19.75
181	0.15	0.15	0.35	0.35	5.5	7.5	12	1	6.5	21.48

182	0.15	0.15	0.35	0.35	1	12	11	2	6.5	23.25
183	0.4	0.1	0.1	0.4	6.5	9.5	4	7	6.75	1.56
184	0.35	0.15	0.35	0.15	6.5	4	7	9.5	6.75	2.31
185	0.4	0.1	0.1	0.4	5	4	9.5	8.5	6.75	3.96
186	0.4	0.4	0.1	0.1	5.5	8	2	11.5	6.75	5.76
187	0.3	0.2	0.2	0.3	8.5	10.5	3	5	6.75	7.46
188	0.25	0.25	0.25	0.25	2.5	6	11	7.5	6.75	9.31
189	0.3	0.3	0.2	0.2	7	6.5	12	1.5	6.75	11.06
190	0.1	0.1	0.4	0.4	9.5	4	3	10.5	6.75	12.76
191	0.1	0.4	0.4	0.1	6.5	2.5	11	7	6.75	14.46
192	0.35	0.35	0.15	0.15	2	11.5	5.5	8	6.75	16.26
193	0.35	0.15	0.15	0.35	11.5	9.5	4	2	6.75	18.06
194	0.35	0.15	0.35	0.15	12	8	1.5	5.5	6.75	19.76
195	0.15	0.15	0.35	0.35	4	9.5	1.5	12	6.75	21.56
196	0.4	0.1	0.4	0.1	1.5	9	12	4.5	6.75	23.06
197	0.4	0.4	0.1	0.1	6.5	7.5	4	10	7	2.00
198	0.1	0.4	0.1	0.4	10	6	4	8	7	2.60
199	0.1	0.1	0.4	0.4	3	11	8	6	7	4.00
200	0.4	0.4	0.1	0.1	6	8	12	2	7	5.80
201	0.4	0.1	0.3	0.2	6	8.5	10.5	3	7	7.50
202	0.25	0.25	0.25	0.25	10.5	9.5	3.5	4.5	7	9.25
203	0.1	0.4	0.15	0.35	2	9	12	4	7	11.00
204	0.4	0.1	0.4	0.1	11	6.5	3	7.5	7	12.85
205	0.25	0.25	0.25	0.25	5	2	9	12	7	14.50
206	0.25	0.25	0.25	0.25	11.5	2.5	10.5	3.5	7	16.25
207	0.4	0.1	0.4	0.1	2.5	10	11.5	4	7	18.00
208	0.2	0.3	0.3	0.2	2	3	11	12	7	19.60
209	0.2	0.2	0.3	0.3	11	3	12	2	7	21.40
210	0.2	0.3	0.3	0.2	2.5	2	12	11.5	7	23.10
211	0.4	0.1	0.1	0.4	2	3	11	12	7	23.20
212	0.4	0.1	0.4	0.1	7.5	4	7	10.5	7.25	2.16
213	0.4	0.1	0.4	0.1	8	4	6.5	10.5	7.25	2.56
214	0.1	0.4	0.4	0.1	3	6.5	8	11.5	7.25	4.06
215	0.1	0.4	0.4	0.1	2.5	6	8.5	12	7.25	5.76
216	0.3	0.3	0.2	0.2	5.5	9	11	3.5	7.25	7.46
217	0.25	0.25	0.25	0.25	8	6.5	3	11.5	7.25	9.31
218	0.2	0.3	0.3	0.2	6.5	3	11.5	8	7.25	11.06
219	0.4	0.1	0.1	0.4	3.5	10	4.5	11	7.25	12.76
220	0.1	0.1	0.4	0.4	7.5	7	11.5	3	7.25	14.46
221	0.15	0.35	0.15	0.35	8.5	12	6	2.5	7.25	16.26
222	0.35	0.15	0.15	0.35	2.5	4.5	10	12	7.25	18.06
223	0.3	0.2	0.2	0.3	3	2.5	12	11.5	7.25	19.86
224	0.25	0.25	0.25	0.25	12	2.5	11.5	3	7.25	20.31
225	0.3	0.2	0.3	0.2	2.5	3	12	11.5	7.25	20.76
226	0.1	0.4	0.4	0.1	11	2.5	12	3.5	7.25	20.86
227	0.35	0.35	0.15	0.15	2.5	12	11.5	3	7.25	21.21
228	0.4	0.4	0.1	0.1	2.5	12	11.5	3	7.25	21.66

229	0.1	0.4	0.4	0.1	4	7	8	11	7.5	2.65
230	0.1	0.4	0.1	0.4	11	8.5	4	6.5	7.5	3.25
231	0.1	0.1	0.4	0.4	11.5	3.5	8.5	6.5	7.5	4.00
232	0.4	0.1	0.4	0.1	9	12	6	3	7.5	5.85
233	0.2	0.4	0.3	0.1	3.5	6.5	11	9	7.5	7.50
234	0.25	0.25	0.25	0.25	11	4	5	10	7.5	9.25
235	0.3	0.3	0.2	0.2	11	4	10.5	4.5	7.5	10.95
236	0.1	0.1	0.4	0.4	8	7	11.5	3.5	7.5	12.85
237	0.2	0.3	0.3	0.2	11	3.5	11.5	4	7.5	14.50
238	0.25	0.25	0.25	0.25	11	4	12	3	7.5	16.25
239	0.4	0.1	0.4	0.1	12	10.5	3	4.5	7.5	18.00
240	0.35	0.35	0.15	0.15	12	3	3.5	11.5	7.5	18.98
241	0.4	0.1	0.4	0.1	12	3.5	3	11.5	7.5	19.40
242	0.4	0.4	0.1	0.1	7.5	8	4	11.5	7.75	2.86
243	0.1	0.1	0.4	0.4	11.5	4	7	8.5	7.75	3.26
244	0.25	0.25	0.25	0.25	4	3.5	12	11.5	7.75	16.06
245	0.1	0.4	0.4	0.1	4	12	3.5	11.5	7.75	17.26
246	0.1	0.4	0.4	0.1	12	7	9	4	8	4.00
247	0.3	0.1	0.4	0.2	7	3	8	12	8	6.00
248	0.1	0.2	0.4	0.3	9.5	4	7	11.5	8	7.50
249	0.35	0.15	0.35	0.15	5.5	4	10.5	12	8	9.18
250	0.15	0.15	0.35	0.35	12	4	5	11	8	11.10
251	0.1	0.1	0.4	0.4	8.5	7.5	4	12	8	12.85
252	0.3	0.3	0.2	0.2	4	12	11.5	4.5	8	14.50

Appendix C2

	Probabilities				Amounts						
Trial	**p1**	**p2**	**p3**	**p4**	**m1**	**m2**	**m3**	**m4**	**EV**	**Var**	**Skew**
1	0.3	0.2	0.4	0.1	6.5	3.5	7	6	6.05	1.72	-2.95
2	0.7	0.1	0.1	0.1	6	9.5	5	4	6.05	1.72	3.13
3	0.6	0.1	0.2	0.1	6.5	7	6	1.5	5.95	2.27	-8.60
4	0.55	0.1	0.1	0.25	5.5	10.5	4	6	5.975	2.56	8.44
5	0.5	0.1	0.1	0.3	6.5	6	1	7	6.05	2.92	-12.58
6	0.1	0.1	0.1	0.7	11	4	6	5.5	5.95	3.07	12.07
7	0.15	0.1	0.55	0.2	2	8	7	5.5	6.05	3.40	-8.78
8	0.55	0.1	0.15	0.2	5	4	10	6.5	5.95	3.40	8.78
9	0.35	0.15	0.3	0.2	6.5	4.5	8	3	5.95	3.42	-2.95
10	0.2	0.35	0.15	0.3	9	5.5	7.5	4	6.05	3.42	2.95
11	0.4	0.1	0.4	0.1	6.5	6	7	0.5	6.05	3.52	-16.72
12	0.2	0.1	0.1	0.6	6	0.5	8	6.5	5.95	3.57	-15.23
13	0.1	0.1	0.2	0.6	4	11.5	6	5.5	6.05	3.57	15.23
14	0.1	0.1	0.5	0.3	6	0	6.5	7	5.95	4.02	-20.63
15	0.3	0.1	0.1	0.5	6.5	0	6	7	6.05	4.17	-21.69
16	0.1	0.1	0.6	0.2	0	7.5	6.5	7	6.05	4.17	-21.61
17	0.1	0.1	0.1	0.7	4	12	6	5.5	6.05	4.17	20.09
18	0.2	0.1	0.55	0.15	6.5	0	7	6	6.05	4.20	-21.65
19	0.1	0.1	0.7	0.1	5	4	5.5	12	5.95	4.27	21.25
20	0.1	0.45	0.1	0.35	4	5	12	6	5.95	4.45	21.02
21	0.1	0.1	0.2	0.6	3.5	12	7	5	5.95	5.02	20.39
22	0.25	0.1	0.55	0.1	5	6.5	7.5	0	6.025	5.11	-20.36
23	0.15	0.4	0.1	0.35	7	8	0.5	5	6.05	5.12	-14.41
24	0.6	0.1	0.2	0.1	7	5	2	9.5	6.05	5.12	-8.78
25	0.6	0.2	0.1	0.1	5	10	7	2.5	5.95	5.12	8.78
26	0.1	0.15	0.35	0.4	11.5	5	7	4	5.95	5.12	14.41
27	0.2	0.15	0.4	0.25	2.5	5	8.5	5.5	6.025	5.16	-2.89
28	0.2	0.15	0.4	0.25	9.5	7	3.5	6.5	5.975	5.16	2.89
29	0.15	0.1	0.6	0.15	7.5	6.5	7	0.5	6.05	5.50	-24.66
30	0.55	0.2	0.15	0.1	5	5.5	11.5	4	5.975	5.54	24.00
31	0.1	0.15	0.15	0.6	4	11.5	5.5	5	5.95	5.57	24.37
32	0.1	0.1	0.65	0.15	7.5	6.5	7	0	5.95	6.30	-30.46
33	0.15	0.6	0.15	0.1	7.5	7	0	6.5	5.975	6.36	-30.80
34	0.55	0.1	0.2	0.15	5	4	5.5	12	6.05	6.40	30.07
35	0.15	0.1	0.6	0.15	12	4	5	5.5	6.025	6.44	30.50
36	0.15	0.1	0.65	0.1	12	5.5	5	4	6	6.48	30.94
37	0.25	0.5	0.15	0.1	7.5	7	0	6.5	6.025	6.49	-31.53
38	0.45	0.15	0.3	0.1	7	0	7.5	6.5	6.05	6.55	-31.91
39	0.35	0.35	0.15	0.15	7	7.5	6.5	0	6.05	6.57	-31.84
40	0.55	0.15	0.15	0.15	5	5.5	12	4	5.975	6.59	31.13
41	0.1	0.15	0.15	0.6	5.5	4	12	5	5.95	6.62	31.58
42	0.65	0.15	0.1	0.1	5	12	3.5	5.5	5.95	6.70	31.18

43	0.15	0.2	0.2	0.45	12	4	5.5	5	5.95	6.70	31.33
44	0.55	0.1	0.1	0.25	5	12	10	4	5.95	6.75	26.46
45	0.5	0.1	0.25	0.15	7.5	5.5	7	0	6.05	6.80	-31.49
46	0.2	0.35	0.15	0.3	7.5	8	7	2	5.95	6.80	-14.56
47	0.3	0.2	0.35	0.15	10	4.5	4	5	6.05	6.80	14.56
48	0.1	0.4	0.1	0.4	1	7	0.5	7.5	5.95	6.82	-26.36
49	0.2	0.1	0.4	0.3	1	7.5	8	6	5.95	6.82	-20.44
50	0.3	0.2	0.4	0.1	6	11	4	4.5	6.05	6.82	20.44
51	0.2	0.4	0.25	0.15	5	8.5	2	7	5.95	6.85	-8.77
52	0.2	0.15	0.4	0.25	7	5	3.5	10	6.05	6.85	8.77
53	0.25	0.25	0.25	0.25	4.5	8	9	2.5	6	6.88	-2.81
54	0.25	0.25	0.25	0.25	4	3	9.5	7.5	6	6.88	2.81
55	0.1	0.1	0.1	0.7	0	7	0.5	7.5	6	8.30	-35.78
56	0.1	0.2	0.2	0.5	0	6	3	8.5	6.05	8.52	-20.47
57	0.3	0.35	0.2	0.15	8.5	2	7.5	8	5.95	8.52	-14.56
58	0.15	0.3	0.35	0.2	4	3.5	10	4.5	6.05	8.52	14.56
59	0.1	0.5	0.2	0.2	12	3.5	6	9	5.95	8.52	20.47
60	0.1	0.15	0.5	0.25	3	0	8	7	6.05	8.55	-32.13
61	0.25	0.5	0.15	0.1	5	4	12	9	5.95	8.55	32.13
62	0.25	0.15	0.4	0.2	9	7	6.5	0.5	6	8.55	-26.33
63	0.4	0.2	0.25	0.15	5.5	11.5	3	5	6	8.55	26.33
64	0.6	0.1	0.1	0.2	6.5	11.5	8	1	6.05	8.57	-8.77
65	0.2	0.15	0.3	0.35	8.5	4.5	9	2.5	5.95	8.57	-3.00
66	0.2	0.3	0.35	0.15	3.5	3	9.5	7.5	6.05	8.57	3.00
67	0.1	0.6	0.1	0.2	4	5.5	0.5	11	5.95	8.57	8.77
68	0.1	0.1	0.4	0.4	12	11.5	5	4	5.95	8.62	35.93
69	0.2	0.1	0.4	0.3	0	8.5	7.5	7	5.95	9.02	-38.63
70	0.2	0.3	0.4	0.1	12	5	4.5	3.5	6.05	9.02	38.63
71	0.2	0.2	0.15	0.45	7.5	0.5	3.5	8.5	5.95	10.25	-26.38
72	0.2	0.45	0.2	0.15	11.5	3.5	4.5	8.5	6.05	10.25	26.38
73	0.15	0.2	0.4	0.25	10	0	6.5	7.5	5.975	10.26	-31.94
74	0.15	0.1	0.6	0.15	0.5	3.5	8.5	3	5.975	10.26	-20.42
75	0.1	0.5	0.25	0.15	4.5	9	4	0.5	6.025	10.26	-14.56
76	0.45	0.25	0.15	0.15	2.5	8	9	10	5.975	10.26	-2.87
77	0.45	0.25	0.15	0.15	9.5	4	2	3	6.025	10.26	2.87
78	0.25	0.1	0.5	0.15	8	7.5	3	11.5	5.975	10.26	14.56
79	0.6	0.15	0.1	0.15	3.5	11.5	8.5	9	6.025	10.26	20.42
80	0.2	0.4	0.25	0.15	12	5.5	4.5	2	6.025	10.26	31.94
81	0.5	0.2	0.15	0.15	8	0	5	8.5	6.025	10.29	-37.78
82	0.1	0.35	0.2	0.35	1	8.5	9.5	3	6.025	10.29	-8.68
83	0.35	0.1	0.35	0.2	3.5	11	9	2.5	5.975	10.29	8.68
84	0.5	0.2	0.15	0.15	4	12	3.5	7	5.975	10.29	37.78
85	0.15	0.4	0.1	0.35	9.5	9	3	2	6.025	11.94	-8.76
86	0.4	0.35	0.15	0.1	3	10	2.5	9	5.975	11.94	8.76
87	0.4	0.25	0.1	0.25	9	7.5	4.5	0.5	6.05	11.95	-32.08
88	0.1	0.15	0.3	0.45	8	6	1	9	6.05	11.95	-26.34
89	0.3	0.15	0.1	0.45	11	6	4	3	5.95	11.95	26.34
90	0.1	0.4	0.25	0.25	7.5	3	11.5	4.5	5.95	11.95	32.08
91	0.25	0.25	0.1	0.4	2	6.5	0.5	9.5	5.975	11.99	-14.56

92	0.25	0.2	0.25	0.3	4	10.5	1.5	8.5	6.025	11.99	-2.77
93	0.25	0.2	0.25	0.3	10.5	1.5	8	3.5	5.975	11.99	2.77
94	0.25	0.4	0.1	0.25	10	2.5	11.5	5.5	6.025	11.99	14.56
95	0.1	0.15	0.2	0.55	2.5	7	0	8.5	5.975	12.01	-37.84
96	0.15	0.55	0.2	0.1	5	3.5	12	9.5	6.025	12.01	37.84
97	0.15	0.25	0.15	0.45	0.5	10	1.5	7	5.95	12.02	-20.37
98	0.25	0.45	0.15	0.15	2	5	11.5	10.5	6.05	12.02	20.37
99	0.15	0.45	0.25	0.15	10.5	2	9.5	7.5	5.975	13.64	-2.88
100	0.25	0.45	0.15	0.15	2.5	10	1.5	4.5	6.025	13.64	2.88
101	0.4	0.2	0.1	0.3	6	0	4	10.5	5.95	13.67	-14.61
102	0.3	0.2	0.4	0.1	1.5	12	6	8	6.05	13.67	14.61
103	0.25	0.2	0.35	0.2	9.5	0	8.5	3.5	6.05	13.70	-32.19
104	0.35	0.15	0.2	0.3	9	0	9.5	3	5.95	13.70	-20.42
105	0.2	0.15	0.3	0.35	2.5	12	9	3	6.05	13.70	20.42
106	0.2	0.2	0.35	0.25	12	8.5	3.5	2.5	5.95	13.70	32.19
107	0.15	0.15	0.25	0.45	10	3.5	0.5	8.5	5.975	13.71	-26.28
108	0.35	0.2	0.35	0.1	10	8	2.5	0.5	6.025	13.71	-8.67
109	0.2	0.1	0.35	0.35	4	11.5	2	9.5	5.975	13.71	8.67
110	0.45	0.15	0.25	0.15	3.5	2	11.5	8.5	6.025	13.71	26.28
111	0.25	0.3	0.3	0.15	9.5	0.5	7.5	8.5	6.05	13.75	-37.90
112	0.3	0.15	0.3	0.25	11.5	3.5	4.5	2.5	5.95	13.75	37.90
113	0.2	0.2	0.45	0.15	7	0	9.5	2	5.975	15.31	-32.16
114	0.2	0.2	0.15	0.45	5	12	10	2.5	6.025	15.31	32.16
115	0.2	0.2	0.5	0.1	0.5	2	9	10	6	15.35	-26.18
116	0.1	0.2	0.2	0.5	2	10	11.5	3	6	15.35	26.18
117	0.1	0.15	0.2	0.55	8.5	1	0.5	9	6.05	15.37	-37.92
118	0.55	0.2	0.15	0.1	3	11.5	11	3.5	5.95	15.37	37.92
119	0.2	0.3	0.25	0.25	11.5	6.5	0	7	6	15.38	-20.44
120	0.2	0.25	0.25	0.3	0.5	5	12	5.5	6	15.38	20.44
121	0.3	0.1	0.25	0.35	10.5	6	7.5	1	5.975	15.39	-14.41
122	0.3	0.35	0.1	0.25	1.5	11	6	4.5	6.025	15.39	14.41
123	0.25	0.35	0.2	0.2	1.5	8.5	11	2	5.95	15.45	-2.80
124	0.35	0.2	0.2	0.25	3.5	10	1	10.5	6.05	15.45	2.80
125	0.4	0.1	0.2	0.3	1.5	5	9.5	10	6	15.45	-8.78
126	0.3	0.2	0.1	0.4	2	2.5	7	10.5	6	15.45	8.78
127	0.15	0.1	0.4	0.35	9.5	10.5	1	9	6.025	17.01	-26.28
128	0.15	0.1	0.35	0.4	2.5	1.5	3	11	5.975	17.01	26.28
129	0.15	0.25	0.2	0.4	3	0	9	9.5	6.05	17.05	-38.06
130	0.4	0.2	0.15	0.25	2.5	3	9	12	5.95	17.05	38.06
131	0.5	0.15	0.2	0.15	10	0.5	4	1	6.025	17.09	-14.59
132	0.2	0.5	0.15	0.15	8	2	11.5	11	5.975	17.09	14.59
133	0.1	0.4	0.2	0.3	10.5	10	1	2.5	6	17.10	-3.15
134	0.2	0.3	0.4	0.1	11	9.5	2	1.5	6	17.10	3.15
135	0.1	0.15	0.4	0.35	11.5	8.5	1	9	5.975	17.11	-20.29
136	0.15	0.15	0.35	0.35	4.5	8.5	1	10.5	5.975	17.11	-8.74
137	0.35	0.15	0.35	0.15	11	7.5	1.5	3.5	6.025	17.11	8.74
138	0.35	0.15	0.4	0.1	3	3.5	11	0.5	6.025	17.11	20.29
139	0.4	0.1	0.35	0.15	9.5	10	0.5	6.5	5.95	17.12	-32.09
140	0.1	0.15	0.4	0.35	2	5.5	2.5	11.5	6.05	17.12	32.09

141	0.25	0.4	0.2	0.15	1.5	10.5	1	8	5.975	18.76	-8.72
142	0.25	0.2	0.4	0.15	10.5	11	1.5	4	6.025	18.76	8.72
143	0.3	0.3	0.25	0.15	0	9.5	10	4.5	6.025	18.81	-37.85
144	0.1	0.25	0.2	0.45	11	0	3	9.5	5.975	18.81	-26.20
145	0.25	0.1	0.45	0.2	12	1	2.5	9	6.025	18.81	26.20
146	0.3	0.3	0.25	0.15	2.5	12	2	7.5	5.975	18.81	37.85
147	0.2	0.1	0.3	0.4	7	0.5	1	10.5	5.95	18.82	-14.66
148	0.1	0.4	0.3	0.2	11.5	1.5	11	5	6.05	18.82	14.66
149	0.3	0.35	0.15	0.2	0	7.5	6.5	12	6	18.83	-20.40
150	0.15	0.3	0.4	0.15	1	1.5	9	12	6	18.83	-2.89
151	0.15	0.4	0.15	0.3	11	3	0	10.5	6	18.83	2.89
152	0.3	0.15	0.2	0.35	12	5.5	0	4.5	6	18.83	20.40
153	0.25	0.35	0.2	0.2	9	10	1	0.5	6.05	18.90	-31.96
154	0.2	0.25	0.35	0.2	11.5	3	2	11	5.95	18.90	31.96
155	0.5	0.1	0.2	0.2	10.5	1	0.5	3	6.05	20.47	-8.68
156	0.2	0.1	0.2	0.5	11.5	11	9	1.5	5.95	20.47	8.68
157	0.35	0.15	0.4	0.1	11	9	1	4	6	20.50	-3.00
158	0.4	0.35	0.1	0.15	11	1	8	3	6	20.50	3.00
159	0.45	0.1	0.2	0.25	1	11.5	10	9.5	5.975	20.54	-14.55
160	0.25	0.1	0.45	0.2	2.5	0.5	11	2	6.025	20.54	14.55
161	0.2	0.2	0.35	0.25	8.5	7.5	0	11	5.95	20.55	-37.47
162	0.35	0.2	0.2	0.25	12	3.5	4.5	1	6.05	20.55	37.47
163	0.2	0.2	0.45	0.15	0.5	6	10.5	0	6.025	20.56	-26.21
164	0.2	0.45	0.25	0.1	2.5	9.5	0	12	5.975	20.56	-20.14
165	0.45	0.1	0.2	0.25	2.5	0	9.5	12	6.025	20.56	20.14
166	0.45	0.2	0.2	0.15	1.5	11.5	6	12	5.975	20.56	26.21
167	0.4	0.15	0.35	0.1	0.5	11	9	10	6	20.60	-31.95
168	0.35	0.4	0.1	0.15	3	11.5	2	1	6	20.60	31.95
169	0.4	0.35	0.1	0.15	11	0.5	2.5	7.5	5.95	22.15	-8.69
170	0.4	0.1	0.15	0.35	1	9.5	4.5	11.5	6.05	22.15	8.69
171	0.2	0.1	0.4	0.3	8.5	1.5	10.5	0	6.05	22.17	-37.66
172	0.4	0.3	0.2	0.1	1.5	12	3.5	10.5	5.95	22.17	37.66
173	0.3	0.1	0.2	0.4	11.5	7.5	8	0.5	6	22.20	-14.70
174	0.15	0.15	0.45	0.25	3	4	11	0	6	22.20	-3.00
175	0.15	0.45	0.25	0.15	8	1	12	9	6	22.20	3.00
176	0.3	0.1	0.2	0.4	0.5	4.5	4	11.5	6	22.20	14.70
177	0.1	0.15	0.4	0.35	4.5	11.5	9.5	0	5.975	22.26	-32.16
178	0.25	0.15	0.25	0.35	6.5	11.5	10.5	0	5.975	22.26	-26.16
179	0.1	0.25	0.15	0.5	5	0	1.5	10.5	5.975	22.26	-20.54
180	0.5	0.15	0.25	0.1	1.5	10.5	12	7	6.025	22.26	20.54
181	0.15	0.25	0.25	0.35	0.5	5.5	1.5	12	6.025	22.26	26.16
182	0.4	0.35	0.15	0.1	2.5	12	0.5	7.5	6.025	22.26	32.16
183	0.1	0.3	0.3	0.3	2	7.5	0	12	6.05	23.87	-8.97
184	0.15	0.4	0.3	0.15	8.5	0.5	12	6.5	6.05	23.87	-2.97
185	0.15	0.4	0.3	0.15	3.5	11.5	0	5.5	5.95	23.87	2.97
186	0.3	0.3	0.1	0.3	0	4.5	10	12	5.95	23.87	8.97
187	0.15	0.15	0.35	0.35	5	8	11.5	0	5.975	23.94	-14.52
188	0.15	0.35	0.35	0.15	4	12	0.5	7	6.025	23.94	14.52
189	0.5	0.3	0.1	0.1	10.5	0	0.5	6.5	5.95	23.97	-32.27

190	0.1	0.3	0.5	0.1	5.5	12	1.5	11.5	6.05	23.97	32.27
191	0.25	0.2	0.15	0.4	0	7.5	0.5	11	5.975	23.99	-26.48
192	0.4	0.15	0.2	0.25	1	11.5	4.5	12	6.025	23.99	26.48
193	0.1	0.15	0.35	0.4	1	11.5	0.5	10	6	24.03	-20.18
194	0.15	0.35	0.4	0.1	0.5	11.5	2	11	6	24.03	20.18
195	0.1	0.25	0.25	0.4	12	9	10	0	5.95	24.25	-38.41
196	0.4	0.25	0.25	0.1	12	2	3	0	6.05	24.25	38.41
197	0.1	0.4	0.2	0.3	7	0	11	10.5	6.05	25.57	-37.80
198	0.2	0.1	0.3	0.4	1	5	1.5	12	5.95	25.57	37.80
199	0.45	0.2	0.15	0.2	0.5	11	11.5	9.5	6.05	25.60	-20.18
200	0.2	0.2	0.45	0.15	1	2.5	11.5	0.5	5.95	25.60	20.18
201	0.4	0.35	0.15	0.1	0	11	10	7	6.05	25.65	-36.80
202	0.5	0.15	0.25	0.1	11	1	0	4	6.05	25.65	-14.90
203	0.1	0.5	0.15	0.25	8	1	11	12	5.95	25.65	14.90
204	0.1	0.4	0.15	0.35	5	12	2	1	5.95	25.65	36.80
205	0.1	0.4	0.4	0.1	9.5	11	0	6.5	6	25.65	-32.10
206	0.4	0.1	0.4	0.1	1	5.5	12	2.5	6	25.65	32.10
207	0.1	0.25	0.45	0.2	8.5	12	0.5	9.5	5.975	25.69	-8.80
208	0.25	0.45	0.2	0.1	0	11.5	2.5	3.5	6.025	25.69	8.80
209	0.35	0.1	0.45	0.1	0	2.5	11	8.5	6.05	25.70	-25.93
210	0.15	0.1	0.25	0.5	0.5	0	1.5	11	5.95	25.70	-2.98
211	0.25	0.1	0.5	0.15	10.5	12	1	11.5	6.05	25.70	2.98
212	0.1	0.35	0.45	0.1	3.5	12	1	9.5	5.95	25.70	25.93
213	0.3	0.1	0.25	0.35	10.5	1.5	11	0	6.05	26.95	-30.17
214	0.35	0.3	0.25	0.1	12	1.5	1	10.5	5.95	26.95	30.17
215	0.35	0.3	0.1	0.25	0	12	2	9	6.05	27.25	-14.54
216	0.1	0.35	0.25	0.3	10	12	3	0	5.95	27.25	14.54
217	0.4	0.35	0.1	0.15	11.5	0	9.5	3	6	27.28	-8.81
218	0.35	0.4	0.15	0.1	12	0.5	9	2.5	6	27.28	8.81
219	0.25	0.1	0.25	0.4	10	5.5	12	0	6.05	27.42	-20.53
220	0.1	0.4	0.25	0.25	6.5	12	2	0	5.95	27.42	20.53
221	0.1	0.35	0.45	0.1	5.5	0	11.5	2.5	5.975	27.46	-2.97
222	0.1	0.1	0.35	0.45	9.5	6.5	12	0.5	6.025	27.46	2.97
223	0.1	0.2	0.25	0.45	12	0	0.5	10.5	6.05	27.47	-26.31
224	0.25	0.1	0.2	0.45	11.5	0	12	1.5	5.95	27.47	26.31
225	0.4	0.15	0.15	0.3	11.5	0.5	9	0	6.025	28.79	-21.32
226	0.3	0.15	0.15	0.4	12	3	11.5	0.5	5.975	28.79	21.32
227	0.45	0.1	0.35	0.1	11	0.5	0	10.5	6.05	28.90	-31.21
228	0.45	0.1	0.35	0.1	1	1.5	12	11.5	5.95	28.90	31.21
229	0.25	0.25	0.1	0.4	12	10.5	3.5	0	5.975	29.09	-9.00
230	0.25	0.4	0.1	0.25	0	12	8.5	1.5	6.025	29.09	9.00
231	0.15	0.4	0.3	0.15	5	0	12	11	6	29.10	-3.00
232	0.15	0.15	0.3	0.4	7	1	0	12	6	29.10	3.00
233	0.45	0.15	0.1	0.3	11.5	0.5	7.5	0	6	29.18	-14.55
234	0.15	0.1	0.3	0.45	11.5	4.5	12	0.5	6	29.18	14.55
235	0.15	0.1	0.3	0.45	12	10	10.5	0	5.95	29.27	-26.67
236	0.15	0.1	0.45	0.3	0	2	12	1.5	6.05	29.27	26.67
237	0.1	0.35	0.45	0.1	10.5	11	0	11.5	6.05	30.00	-32.20
238	0.1	0.45	0.1	0.35	0.5	12	1.5	1	5.95	30.00	32.20

239	0.15	0.25	0.45	0.15	11.5	11	0	10.5	6.05	30.02	-31.83
240	0.45	0.25	0.15	0.15	12	1	0.5	1.5	5.95	30.02	31.83
241	0.2	0.15	0.2	0.45	11.5	11	10.5	0	6.05	30.05	-31.46
242	0.2	0.15	0.45	0.2	1.5	1	12	0.5	5.95	30.05	31.46
243	0.2	0.1	0.45	0.25	12	11.5	0	10	6.05	30.42	-25.93
244	0.25	0.1	0.45	0.2	2	0.5	12	0	5.95	30.42	25.93
245	0.35	0.1	0.1	0.45	12	8	10	0	6	30.80	-14.40
246	0.35	0.45	0.1	0.1	0	12	4	2	6	30.80	14.40
247	0.1	0.45	0.15	0.3	11	0	9	12	6.05	30.85	-20.48
248	0.3	0.15	0.1	0.45	12	11	7	0	5.95	30.85	-8.92
249	0.45	0.15	0.1	0.3	12	1	5	0	6.05	30.85	8.92
250	0.3	0.15	0.45	0.1	0	3	12	1	5.95	30.85	20.48
251	0.4	0.4	0.1	0.1	12	0	3	9.5	6.05	30.92	-3.05
252	0.1	0.1	0.4	0.4	2.5	9	0	12	5.95	30.92	3.05

Appendix D

Trial	P1	P2	P3	P4	A1	A2	A3	A4	EV	Variance	Skew
1	0.1	0.1	0.1	0.7	4	5	9.5	6	6.05	1.72	3.13
2	0.3	0.4	0.2	0.1	6.5	7	3.5	6	6.05	1.72	-2.95
3	0.2	0.6	0.1	0.1	6	6.5	1.5	7	5.95	2.27	-8.60
4	0.25	0.1	0.55	0.1	6	4	5.5	10.5	5.98	2.56	8.44
5	0.1	0.3	0.5	0.1	1	7	6.5	6	6.05	2.92	-12.58
6	0.1	0.7	0.1	0.1	4	5.5	11	6	5.95	3.07	12.07
7	0.15	0.2	0.1	0.55	10	6.5	4	5	5.95	3.40	8.78
8	0.55	0.2	0.15	0.1	7	5.5	2	8	6.05	3.40	-8.78
9	0.15	0.2	0.3	0.35	4.5	3	8	6.5	5.95	3.42	-2.95
10	0.35	0.15	0.3	0.2	5.5	7.5	4	9	6.05	3.42	2.95
11	0.1	0.4	0.1	0.4	6	6.5	0.5	7	6.05	3.52	-16.72
12	0.6	0.1	0.2	0.1	6.5	0.5	6	8	5.95	3.57	-15.23
13	0.2	0.1	0.1	0.6	6	11.5	4	5.5	6.05	3.57	15.23
14	0.1	0.3	0.1	0.5	0	7	6	6.5	5.95	4.02	-20.63
15	0.1	0.1	0.7	0.1	4	6	5.5	12	6.05	4.17	20.09
16	0.2	0.6	0.1	0.1	7	6.5	7.5	0	6.05	4.17	-21.61
17	0.1	0.1	0.3	0.5	0	6	6.5	7	6.05	4.17	-21.69
18	0.1	0.55	0.2	0.15	0	7	6.5	6	6.05	4.20	-21.65
19	0.7	0.1	0.1	0.1	5.5	4	12	5	5.95	4.27	21.25
20	0.45	0.1	0.35	0.1	5	4	6	12	5.95	4.45	21.02
21	0.1	0.6	0.2	0.1	12	5	7	3.5	5.95	5.02	20.39
22	0.1	0.55	0.25	0.1	6.5	7.5	5	0	6.03	5.11	-20.36
23	0.4	0.1	0.15	0.35	8	0.5	7	5	6.05	5.12	-14.41
24	0.2	0.1	0.1	0.6	10	7	2.5	5	5.95	5.12	8.78
25	0.35	0.15	0.4	0.1	7	5	4	11.5	5.95	5.12	14.41
26	0.2	0.1	0.1	0.6	2	5	9.5	7	6.05	5.12	-8.78
27	0.25	0.2	0.15	0.4	6.5	9.5	7	3.5	5.98	5.16	2.89
28	0.25	0.15	0.2	0.4	5.5	5	2.5	8.5	6.03	5.16	-2.89
29	0.15	0.1	0.6	0.15	7.5	6.5	7	0.5	6.05	5.50	-24.66
30	0.55	0.1	0.15	0.2	5	4	11.5	5.5	5.98	5.54	24.00
31	0.15	0.15	0.6	0.1	11.5	5.5	5	4	5.95	5.57	24.37
32	0.15	0.1	0.65	0.1	0	6.5	7	7.5	5.95	6.30	-30.46
33	0.15	0.6	0.1	0.15	7.5	7	6.5	0	5.98	6.36	-30.80
34	0.55	0.2	0.15	0.1	5	5.5	12	4	6.05	6.40	30.07
35	0.1	0.15	0.6	0.15	4	12	5	5.5	6.03	6.44	30.50
36	0.15	0.1	0.1	0.65	12	5.5	4	5	6.00	6.48	30.94
37	0.15	0.25	0.1	0.5	0	7.5	6.5	7	6.03	6.49	-31.53
38	0.3	0.1	0.45	0.15	7.5	6.5	7	0	6.05	6.55	-31.91
39	0.35	0.15	0.15	0.35	7.5	0	6.5	7	6.05	6.57	-31.84
40	0.15	0.15	0.55	0.15	12	5.5	5	4	5.98	6.59	31.13
41	0.1	0.6	0.15	0.15	5.5	5	4	12	5.95	6.62	31.58
42	0.2	0.2	0.15	0.45	5.5	4	12	5	5.95	6.70	31.33
43	0.1	0.1	0.15	0.65	5.5	3.5	12	5	5.95	6.70	31.18

44	0.25	0.1	0.55	0.1	4	10	5	12	5.95	6.75	26.46
45	0.3	0.2	0.15	0.35	2	7.5	7	8	5.95	6.80	-14.56
46	0.5	0.15	0.25	0.1	7.5	0	7	5.5	6.05	6.80	-31.49
47	0.2	0.35	0.15	0.3	4.5	4	5	10	6.05	6.80	14.56
48	0.3	0.4	0.1	0.2	6	4	4.5	11	6.05	6.82	20.44
49	0.2	0.4	0.1	0.3	1	8	7.5	6	5.95	6.82	-20.44
50	0.1	0.1	0.4	0.4	1	0.5	7.5	7	5.95	6.82	-26.36
51	0.15	0.25	0.2	0.4	7	2	5	8.5	5.95	6.85	-8.77
52	0.4	0.15	0.2	0.25	3.5	5	7	10	6.05	6.85	8.77
53	0.25	0.25	0.25	0.25	9	4.5	2.5	8	6.00	6.88	-2.81
54	0.25	0.25	0.25	0.25	3	9.5	7.5	4	6.00	6.88	2.81
55	0.7	0.1	0.1	0.1	7.5	7	0	0.5	6.00	8.30	-35.78
56	0.35	0.3	0.2	0.15	2	8.5	7.5	8	5.95	8.52	-14.56
57	0.2	0.3	0.35	0.15	4.5	3.5	10	4	6.05	8.52	14.56
58	0.5	0.1	0.2	0.2	3.5	12	6	9	5.95	8.52	20.47
59	0.2	0.2	0.5	0.1	6	3	8.5	0	6.05	8.52	-20.47
60	0.15	0.1	0.5	0.25	12	9	4	5	5.95	8.55	32.13
61	0.5	0.15	0.1	0.25	8	0	3	7	6.05	8.55	-32.13
62	0.4	0.25	0.15	0.2	6.5	9	7	0.5	6.00	8.55	-26.33
63	0.2	0.4	0.15	0.25	11.5	5.5	5	3	6.00	8.55	26.33
64	0.2	0.15	0.3	0.35	8.5	4.5	9	2.5	5.95	8.57	-3.00
65	0.15	0.3	0.35	0.2	7.5	3	9.5	3.5	6.05	8.57	3.00
66	0.2	0.1	0.1	0.6	1	11.5	8	6.5	6.05	8.57	-8.77
67	0.2	0.1	0.6	0.1	11	4	5.5	0.5	5.95	8.57	8.77
68	0.4	0.1	0.1	0.4	4	12	11.5	5	5.95	8.62	35.93
69	0.1	0.3	0.4	0.2	3.5	5	4.5	12	6.05	9.02	38.63
70	0.2	0.3	0.1	0.4	0	7	8.5	7.5	5.95	9.02	-38.63
71	0.2	0.2	0.15	0.45	4.5	11.5	8.5	3.5	6.05	10.25	26.38
72	0.2	0.2	0.45	0.15	7.5	0.5	8.5	3.5	5.95	10.25	-26.38
73	0.45	0.15	0.25	0.15	2.5	9	8	10	5.98	10.26	-2.87
74	0.15	0.5	0.1	0.25	11.5	3	7.5	8	5.98	10.26	14.56
75	0.6	0.15	0.1	0.15	3.5	11.5	8.5	9	6.03	10.26	20.42
76	0.4	0.2	0.15	0.25	5.5	12	2	4.5	6.03	10.26	31.94
77	0.15	0.1	0.15	0.6	3	3.5	0.5	8.5	5.98	10.26	-20.42
78	0.15	0.25	0.15	0.45	3	4	2	9.5	6.03	10.26	2.87
79	0.15	0.4	0.25	0.2	10	6.5	7.5	0	5.98	10.26	-31.94
80	0.25	0.15	0.5	0.1	4	0.5	9	4.5	6.03	10.26	-14.56
81	0.35	0.1	0.35	0.2	9	11	3.5	2.5	5.98	10.29	8.68
82	0.2	0.1	0.35	0.35	9.5	1	8.5	3	6.03	10.29	-8.68
83	0.2	0.15	0.5	0.15	0	5	8	8.5	6.03	10.29	-37.78
84	0.15	0.2	0.5	0.15	7	12	4	3.5	5.98	10.29	37.78
85	0.35	0.15	0.1	0.4	2	9.5	3	9	6.03	11.94	-8.76
86	0.35	0.4	0.1	0.15	10	3	9	2.5	5.98	11.94	8.76
87	0.3	0.1	0.45	0.15	11	4	3	6	5.95	11.95	26.34
88	0.15	0.3	0.45	0.1	6	1	9	8	6.05	11.95	-26.34
89	0.25	0.25	0.4	0.1	11.5	4.5	3	7.5	5.95	11.95	32.08
90	0.25	0.1	0.25	0.4	7.5	4.5	0.5	9	6.05	11.95	-32.08
91	0.4	0.25	0.25	0.1	2.5	10	5.5	11.5	6.03	11.99	14.56
92	0.2	0.25	0.25	0.3	1.5	8	10.5	3.5	5.98	11.99	2.77

93	0.1	0.25	0.4	0.25	0.5	2	9.5	6.5	5.98	11.99	-14.56
94	0.25	0.25	0.3	0.2	1.5	4	8.5	10.5	6.03	11.99	-2.77
95	0.15	0.2	0.1	0.55	5	12	9.5	3.5	6.03	12.01	37.84
96	0.1	0.55	0.15	0.2	2.5	8.5	7	0	5.98	12.01	-37.84
97	0.15	0.45	0.25	0.15	11.5	5	2	10.5	6.05	12.02	20.37
98	0.45	0.25	0.15	0.15	7	10	1.5	0.5	5.95	12.02	-20.37
99	0.45	0.15	0.25	0.15	10	4.5	2.5	1.5	6.03	13.64	2.88
100	0.45	0.25	0.15	0.15	2	9.5	7.5	10.5	5.98	13.64	-2.88
101	0.3	0.1	0.2	0.4	1.5	8	12	6	6.05	13.67	14.61
102	0.2	0.3	0.4	0.1	0	10.5	6	4	5.95	13.67	-14.61
103	0.35	0.15	0.3	0.2	3	12	9	2.5	6.05	13.70	20.42
104	0.2	0.15	0.3	0.35	9.5	0	3	9	5.95	13.70	-20.42
105	0.35	0.2	0.2	0.25	3.5	12	8.5	2.5	5.95	13.70	32.19
106	0.25	0.2	0.35	0.2	9.5	3.5	8.5	0	6.05	13.70	-32.19
107	0.1	0.2	0.35	0.35	0.5	8	2.5	10	6.03	13.71	-8.67
108	0.15	0.25	0.45	0.15	8.5	11.5	3.5	2	6.03	13.71	26.28
109	0.15	0.25	0.45	0.15	3.5	0.5	8.5	10	5.98	13.71	-26.28
110	0.35	0.1	0.2	0.35	2	11.5	4	9.5	5.98	13.71	8.67
111	0.25	0.3	0.3	0.15	2.5	4.5	11.5	3.5	5.95	13.75	37.90
112	0.3	0.15	0.3	0.25	7.5	8.5	0.5	9.5	6.05	13.75	-37.90
113	0.15	0.45	0.2	0.2	10	2.5	12	5	6.03	15.31	32.16
114	0.2	0.45	0.2	0.15	7	9.5	0	2	5.98	15.31	-32.16
115	0.5	0.2	0.1	0.2	3	11.5	2	10	6.00	15.35	26.18
116	0.1	0.2	0.2	0.5	10	2	0.5	9	6.00	15.35	-26.18
117	0.2	0.1	0.15	0.55	0.5	8.5	1	9	6.05	15.37	-37.92
118	0.55	0.1	0.2	0.15	3	3.5	11.5	11	5.95	15.37	37.92
119	0.25	0.2	0.3	0.25	12	0.5	5.5	5	6.00	15.38	20.44
120	0.3	0.2	0.25	0.25	6.5	11.5	0	7	6.00	15.38	-20.44
121	0.25	0.1	0.35	0.3	4.5	6	11	1.5	6.03	15.39	14.41
122	0.35	0.3	0.25	0.1	1	10.5	7.5	6	5.98	15.39	-14.41
123	0.2	0.25	0.35	0.2	1	10.5	3.5	10	6.05	15.45	2.80
124	0.2	0.35	0.25	0.2	2	8.5	1.5	11	5.95	15.45	-2.80
125	0.1	0.2	0.4	0.3	7	2.5	10.5	2	6.00	15.45	8.78
126	0.2	0.1	0.4	0.3	9.5	5	1.5	10	6.00	15.45	-8.78
127	0.15	0.35	0.4	0.1	9.5	9	1	10.5	6.03	17.01	-26.28
128	0.15	0.1	0.4	0.35	2.5	1.5	11	3	5.98	17.01	26.28
129	0.2	0.15	0.4	0.25	9	3	9.5	0	6.05	17.05	-38.06
130	0.15	0.4	0.25	0.2	9	2.5	12	3	5.95	17.05	38.06
131	0.2	0.15	0.15	0.5	8	11	11.5	2	5.98	17.09	14.59
132	0.2	0.15	0.5	0.15	4	1	10	0.5	6.03	17.09	-14.59
133	0.2	0.4	0.3	0.1	11	2	9.5	1.5	6.00	17.10	3.15
134	0.3	0.1	0.4	0.2	2.5	10.5	10	1	6.00	17.10	-3.15
135	0.15	0.35	0.15	0.35	4.5	10.5	8.5	1	5.98	17.11	-8.74
136	0.15	0.35	0.35	0.15	3.5	1.5	11	7.5	6.03	17.11	8.74
137	0.15	0.35	0.4	0.1	3.5	3	11	0.5	6.03	17.11	20.29
138	0.1	0.15	0.35	0.4	11.5	8.5	9	1	5.98	17.11	-20.29
139	0.4	0.1	0.15	0.35	2.5	2	5.5	11.5	6.05	17.12	32.09
140	0.4	0.15	0.1	0.35	9.5	6.5	10	0.5	5.95	17.12	-32.09
141	0.2	0.4	0.25	0.15	1	10.5	1.5	8	5.98	18.76	-8.72

142	0.15	0.25	0.2	0.4	4	10.5	11	1.5	6.03	18.76	8.72
143	0.25	0.3	0.15	0.3	10	9.5	4.5	0	6.03	18.81	-37.85
144	0.45	0.1	0.2	0.25	2.5	1	9	12	6.03	18.81	26.20
145	0.1	0.45	0.25	0.2	11	9.5	0	3	5.98	18.81	-26.20
146	0.25	0.15	0.3	0.3	2	7.5	2.5	12	5.98	18.81	37.85
147	0.1	0.3	0.4	0.2	0.5	1	10.5	7	5.95	18.82	-14.66
148	0.3	0.2	0.1	0.4	11	5	11.5	1.5	6.05	18.82	14.66
149	0.3	0.15	0.4	0.15	1.5	1	9	12	6.00	18.83	-2.89
150	0.35	0.3	0.15	0.2	4.5	12	5.5	0	6.00	18.83	20.40
151	0.35	0.2	0.15	0.3	7.5	12	6.5	0	6.00	18.83	-20.40
152	0.3	0.15	0.4	0.15	10.5	0	3	11	6.00	18.83	2.89
153	0.25	0.35	0.2	0.2	3	2	11.5	11	5.95	18.90	31.96
154	0.35	0.2	0.2	0.25	10	0.5	1	9	6.05	18.90	-31.96
155	0.2	0.1	0.2	0.5	9	11	11.5	1.5	5.95	20.47	8.68
156	0.5	0.2	0.1	0.2	10.5	0.5	1	3	6.05	20.47	-8.68
157	0.15	0.4	0.35	0.1	9	1	11	4	6.00	20.50	-3.00
158	0.35	0.15	0.1	0.4	1	3	8	11	6.00	20.50	3.00
159	0.1	0.45	0.2	0.25	11.5	1	10	9.5	5.98	20.54	-14.55
160	0.1	0.45	0.2	0.25	0.5	11	2	2.5	6.03	20.54	14.55
161	0.35	0.2	0.2	0.25	12	3.5	4.5	1	6.05	20.55	37.47
162	0.2	0.35	0.2	0.25	7.5	0	8.5	11	5.95	20.55	-37.47
163	0.2	0.45	0.25	0.1	9.5	2.5	12	0	6.03	20.56	20.14
164	0.2	0.2	0.15	0.45	6	11.5	12	1.5	5.98	20.56	26.21
165	0.15	0.2	0.45	0.2	0	6	10.5	0.5	6.03	20.56	-26.21
166	0.25	0.1	0.2	0.45	0	12	2.5	9.5	5.98	20.56	-20.14
167	0.1	0.35	0.15	0.4	10	9	11	0.5	6.00	20.60	-31.95
168	0.4	0.1	0.15	0.35	11.5	2	1	3	6.00	20.60	31.95
169	0.4	0.15	0.35	0.1	11	7.5	0.5	2.5	5.95	22.15	-8.69
170	0.1	0.4	0.35	0.15	9.5	1	11.5	4.5	6.05	22.15	8.69
171	0.4	0.2	0.3	0.1	10.5	8.5	0	1.5	6.05	22.17	-37.66
172	0.1	0.4	0.3	0.2	10.5	1.5	12	3.5	5.95	22.17	37.66
173	0.15	0.25	0.15	0.45	8	12	9	1	6.00	22.20	3.00
174	0.15	0.25	0.45	0.15	3	0	11	4	6.00	22.20	-3.00
175	0.1	0.3	0.2	0.4	4.5	0.5	4	11.5	6.00	22.20	14.70
176	0.4	0.1	0.2	0.3	0.5	7.5	8	11.5	6.00	22.20	-14.70
177	0.25	0.15	0.25	0.35	10.5	11.5	6.5	0	5.98	22.26	-26.16
178	0.1	0.15	0.5	0.25	7	10.5	1.5	12	6.03	22.26	20.54
179	0.4	0.35	0.15	0.1	9.5	0	11.5	4.5	5.98	22.26	-32.16
180	0.35	0.15	0.25	0.25	12	0.5	5.5	1.5	6.03	22.26	26.16
181	0.5	0.25	0.1	0.15	10.5	0	5	1.5	5.98	22.26	-20.54
182	0.35	0.4	0.1	0.15	12	2.5	7.5	0.5	6.03	22.26	32.16
183	0.1	0.3	0.3	0.3	2	7.5	0	12	6.05	23.87	-8.97
184	0.3	0.3	0.3	0.1	0	4.5	12	10	5.95	23.87	8.97
185	0.15	0.15	0.3	0.4	5.5	3.5	0	11.5	5.95	23.87	2.97
186	0.3	0.15	0.15	0.4	12	6.5	8.5	0.5	6.05	23.87	-2.97
187	0.35	0.35	0.15	0.15	11.5	0	5	8	5.98	23.94	-14.52
188	0.15	0.15	0.35	0.35	4	7	0.5	12	6.03	23.94	14.52
189	0.1	0.5	0.1	0.3	0.5	10.5	6.5	0	5.95	23.97	-32.27
190	0.1	0.3	0.1	0.5	11.5	12	5.5	1.5	6.05	23.97	32.27

191	0.25	0.15	0.2	0.4	12	11.5	4.5	1	6.03	23.99	26.48
192	0.15	0.25	0.4	0.2	0.5	0	11	7.5	5.98	23.99	-26.48
193	0.15	0.4	0.1	0.35	0.5	2	11	11.5	6.00	24.03	20.18
194	0.4	0.35	0.1	0.15	10	0.5	1	11.5	6.00	24.03	-20.17
195	0.4	0.1	0.25	0.25	12	0	3	2	6.05	24.25	38.41
196	0.1	0.25	0.25	0.4	12	9	10	0	5.95	24.25	-38.41
197	0.1	0.3	0.2	0.4	5	1.5	1	12	5.95	25.57	37.80
198	0.4	0.3	0.1	0.2	0	10.5	7	11	6.05	25.57	-37.80
199	0.15	0.2	0.2	0.45	11.5	11	9.5	0.5	6.05	25.60	-20.18
200	0.2	0.2	0.15	0.45	1	2.5	0.5	11.5	5.95	25.60	20.18
201	0.15	0.25	0.1	0.5	11	12	8	1	5.95	25.65	14.90
202	0.15	0.4	0.1	0.35	10	0	7	11	6.05	25.65	-36.80
203	0.15	0.4	0.35	0.1	2	12	1	5	5.95	25.65	36.80
204	0.5	0.15	0.1	0.25	11	1	4	0	6.05	25.65	-14.90
205	0.1	0.4	0.4	0.1	2.5	1	12	5.5	6.00	25.65	32.10
206	0.4	0.1	0.1	0.4	11	9.5	6.5	0	6.00	25.65	-32.10
207	0.2	0.45	0.1	0.25	2.5	11.5	3.5	0	6.03	25.69	8.80
208	0.1	0.2	0.25	0.45	8.5	9.5	12	0.5	5.98	25.69	-8.80
209	0.1	0.15	0.25	0.5	12	11.5	10.5	1	6.05	25.70	2.98
210	0.1	0.35	0.45	0.1	3.5	12	1	9.5	5.95	25.70	25.93
211	0.45	0.1	0.35	0.1	11	8.5	0	2.5	6.05	25.70	-25.93
212	0.1	0.5	0.25	0.15	0	11	1.5	0.5	5.95	25.70	-2.98
213	0.25	0.1	0.3	0.35	1	10.5	1.5	12	5.95	26.95	30.17
214	0.1	0.3	0.35	0.25	1.5	10.5	0	11	6.05	26.95	-30.17
215	0.1	0.25	0.3	0.35	10	3	0	12	5.95	27.25	14.54
216	0.35	0.1	0.25	0.3	0	2	9	12	6.05	27.25	-14.54
217	0.35	0.15	0.1	0.4	12	9	2.5	0.5	6.00	27.28	8.81
218	0.35	0.1	0.4	0.15	0	9.5	11.5	3	6.00	27.28	-8.81
219	0.1	0.25	0.4	0.25	6.5	0	12	2	5.95	27.42	20.53
220	0.25	0.4	0.25	0.1	12	0	10	5.5	6.05	27.42	-20.53
221	0.35	0.1	0.1	0.45	12	9.5	6.5	0.5	6.03	27.46	2.97
222	0.35	0.1	0.45	0.1	0	5.5	11.5	2.5	5.98	27.46	-2.97
223	0.1	0.45	0.2	0.25	12	10.5	0	0.5	6.05	27.47	-26.31
224	0.1	0.2	0.25	0.45	0	12	11.5	1.5	5.95	27.47	26.31
225	0.15	0.4	0.3	0.15	9	11.5	0	0.5	6.03	28.79	-21.32
226	0.15	0.15	0.3	0.4	3	11.5	12	0.5	5.98	28.79	21.32
227	0.1	0.1	0.35	0.45	0.5	10.5	0	11	6.05	28.90	-31.21
228	0.1	0.1	0.35	0.45	1.5	11.5	12	1	5.95	28.90	31.21
229	0.25	0.25	0.4	0.1	1.5	0	12	8.5	6.03	29.09	9.00
230	0.25	0.1	0.4	0.25	12	3.5	0	10.5	5.98	29.09	-9.00
231	0.15	0.3	0.4	0.15	1	0	12	7	6.00	29.10	3.00
232	0.3	0.15	0.15	0.4	12	11	5	0	6.00	29.10	-3.00
233	0.15	0.1	0.3	0.45	0.5	7.5	0	11.5	6.00	29.18	-14.55
234	0.45	0.1	0.3	0.15	0.5	4.5	12	11.5	6.00	29.18	14.55
235	0.1	0.45	0.3	0.15	2	12	1.5	0	6.05	29.27	26.67
236	0.15	0.1	0.3	0.45	12	10	10.5	0	5.95	29.27	-26.67
237	0.45	0.1	0.35	0.1	12	0.5	1	1.5	5.95	30.00	32.20
238	0.45	0.35	0.1	0.1	0	11	11.5	10.5	6.05	30.00	-32.20
239	0.15	0.15	0.25	0.45	1.5	0.5	1	12	5.95	30.02	31.83

240	0.45	0.25	0.15	0.15	0	11	11.5	10.5	6.05	30.02	-31.83
241	0.45	0.2	0.15	0.2	12	1.5	1	0.5	5.95	30.05	31.46
242	0.2	0.2	0.45	0.15	11.5	10.5	0	11	6.05	30.05	-31.46
243	0.1	0.45	0.2	0.25	11.5	0	12	10	6.05	30.42	-25.93
244	0.2	0.45	0.25	0.1	0	12	2	0.5	5.95	30.42	25.93
245	0.1	0.45	0.1	0.35	2	12	4	0	6.00	30.80	14.40
246	0.45	0.1	0.1	0.35	0	10	8	12	6.00	30.80	-14.40
247	0.15	0.1	0.45	0.3	11	7	0	12	5.95	30.85	-8.92
248	0.3	0.45	0.1	0.15	0	12	5	1	6.05	30.85	8.92
249	0.1	0.15	0.3	0.45	11	9	12	0	6.05	30.85	-20.48
250	0.1	0.3	0.15	0.45	1	0	3	12	5.95	30.85	20.48
251	0.1	0.4	0.4	0.1	3	12	0	9.5	6.05	30.92	-3.05
252	0.4	0.4	0.1	0.1	12	0	2.5	9	5.95	30.92	3.05